ISSN 1949-8470 (online)

World Journal of *Radiology*

World J Radiol 2014 April 28; 6(4): 62-129

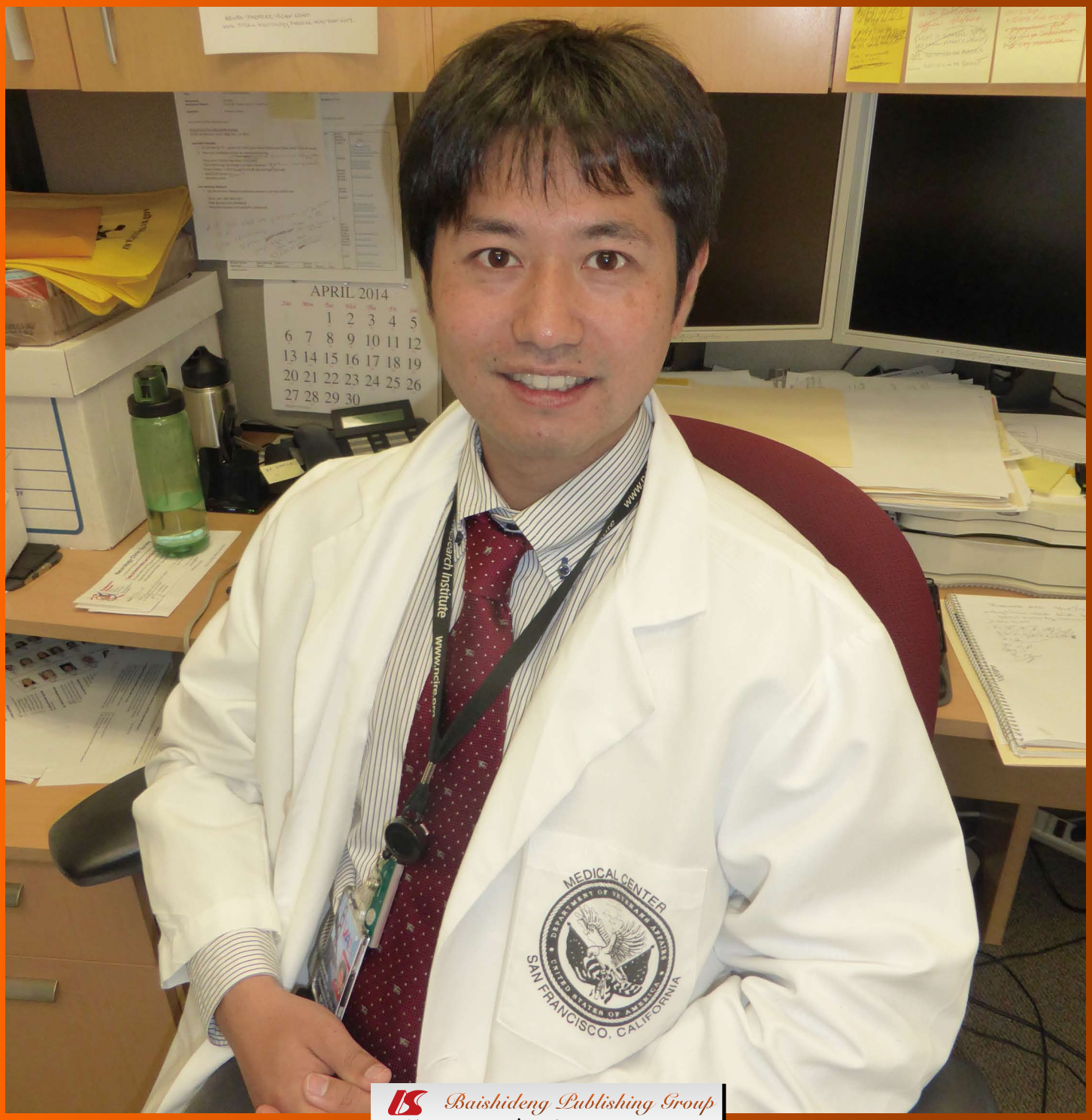

Baishideng Publishing Group
www.wjgnet.com

WJR World Journal of Radiology

A peer-reviewed, online, open-access journal of Radiology

Editorial Board

2014-2017

The *World Journal of Radiology* Editorial Board consists of 365 members, representing a team of worldwide experts in radiology. They are from 36 countries, including Afghanistan (1), Argentina (2), Australia (5), Austria (7), Belgium (2), Brazil (8), Canada (6), Chile (1), China (43), Croatia (1), Denmark (4), Egypt (6), France (5), Germany (22), Greece (10), India (12), Iran (6), Ireland (2), Israel (3), Italy (47), Japan (13), Netherlands (1), New Zealand (1), Pakistan (1), Poland (2), Portugal (1), Serbia (1), Singapore (3), Slovakia (1), South Korea (18), Spain (4), Sweden (2), Switzerland (4), Thailand (1), Turkey (26), United Kingdom (11), and United States (82).

Yue-Qi Zhu, *Shanghai*

Croatia

Goran Kusec, *Osijek*

Denmark

Poul E Andersen, *Odense*
Lars J Petersen, *Aalborg*
Thomas Z Ramsoy, *Frederiksberg*
Morten Ziebell, *Copenhagen*

Egypt

Mohamed F Bazeed, *Mansoura*
Mohamed Abou El-Ghar, *Mansoura*
Reem HA Mohamed, *Cairo*
Mohamed R Nouh, *Alexandria*
Ahmed AKA Razek, *Mansoura*
Ashraf A Zytoon, *Shebin El-Koom*

France

Sabine F Bensamoun, *Compiègne*
Romaric Loffroy, *Dijon*
Stephanie Nougaret, *Montpellier*
Hassane Oudadesse, *Rennes*
Vincent Vinh-Hung, *Fort-de-France*

Germany

Henryk Barthel, *Leipzig*
Peter Bannas, *Hamburg*
Martin Beeres, *Frankfurt*
Ilja F Ciernik, *Dessau*
A Dimitrakopoulou-Strauss, *Heidelberg*
Peter A Fasching, *Erlanegn*
Andreas G Schreyer, *Regensburg*
Philipp Heusch, *Duesseldorf*
Sonja M Kirchhoff, *Munich*
Sebastian Ley, *Munich*
Adel Maataoui, *Frankfurt am Main*
Stephan M Meckel, *Freiburg*
Hans W Muller, *Duesseldorf*
Kay Raum, *Berlin*
Dirk Rades, *Luebeck*
Marc-Ulrich Regier, *Hamburg*
Alexey Surov, *Halle*
Martin Walter, *Magdeburg*
Axel Wetter, *Essen*
Christoph Zilkens, *Düsseldorf*

Greece

Panagiotis Antoniou, *Thessaloniki*
Nikos Efthimiou, *Athens*
Dimitris Karnabatidis, *Patras*
George Latsios, *Athens*
Stylianos Megremis, *Iraklion*
Alexander D Rapidis, *Athens*
Kiki Theodorou, *Larissa*
Ioannis A Tsalafoutas, *Athens*
Evanthia E Tripoliti, *Ioannina*
Athina C Tsili, *Ioannina*

India

Ritesh Agarwal, *Chandigarh*
Chandan J Das, *New Delhi*
Prathamesh V Joshi, *Mumbai*
Naveen Kalra, *Chandigarh*
Chandrasekharan Kesavadas, *Trivandrum*
Jyoti Kumar, *New Delhi*
Atin Kumar, *New Delhi*
Kaushala P Mishra, *Allahabad*
Daya N Sharma, *New Delhi*
Binit Sureka, *New Delhi*
Sanjay Sharma, *New Delhi*
Raja R Yadav, *Allahabad*

Iran

Majid Assadi, *Bushehr*
SeyedReza Najafizadeh, *Tehran*
Mohammad Ali Oghabian, *Tehran*
Amir Reza Radmard, *Tehran*
Ramin Sadeghi, *Mashhad*
Hadi Rokni Yazdi, *Tehran*

Ireland

Tadhg Gleeson, *Wexford*
Frederik JAI Vernimmen, *Cork*

Israel

Dafna Ben Bashat, *Tel Aviv*
Amit Gefen, *Tel Aviv*
Tamar Sella, *Jerusalem*

Italy

Adriano Alippi, *Rome*
Dante Amelio, *Trento*
Michele Anzidei, *Rome*
Filippo F Angileri, *Messinas*
Stefano Arcangeli, *Rome*
Roberto Azzoni, *San Donato milanese*
Tommaso V Bartolotta, *Palermo*
Tommaso Bartalena, *Imola*
Livia Bernardin, *San Bonifacio*
Federico Boschi, *Verona*
Sergio Casciaro, *Lecce*
Emanuele Casciani, *Rome*
Musa M Can, *Napoli*
Alberto Cuocolo, *Napoli*
Michele Ferrara, *Coppito*
Mauro Feola, *Fossano*
Giampiero Francica, *Castel Volturno*
Luigi De Gennaro, *Rome*
Giulio Giovannetti, *Pisa*
Francesca Iacobellis, *Napoli*
Formato Invernizzi, *Monza Brianza*
Francesco Lassandro, *Naples*
Lorenzo Livi, *Florence*
Pier P Mainenti, *Napoli*
Laura Marzetti, *Chieti*
Giuseppe Malinverni, *Crescentino*
Enrica Milanesi, *Turin*
Giovanni Morana, *Treviso*
Lorenzo Monti, *Milan*
Silvia D Morbelli, *Genoa*
Barbara Palumbo, *Perugia*
Cecilia Parazzini, *Milan*
Stefano Pergolizzi, *Messina*
Antonio Pinto, *Naples*
Camillo Porcaro, *Rome*
Carlo C Quattrocchi, *Rome*
Alberto Rebonato, *Perugia*
Giuseppe Rizzo, *Rome*
Roberto De Rosa, *Naples*
Domenico Rubello, *Rovigo*
Andrea Salvati, *Bari*
Sergio Sartori, *Ferrara*
Luca M Sconfienza, *Milano*
Giovanni Storto, *Rionero*
Nicola Sverzellati, *Parma*
Alberto S Tagliafico, *Genova*
Nicola Troisi, *Florence*

Japan

Yasuhiko Hori, *Chiba*
Hidetoshi Ikeda, *Koriyama*
Masahito Kawabori, *Sapporo*
Tamotsu Kamishima, *Sapporo*
Hiro Kiyosue, *Yufu*
Yasunori Minami, *Osaka-sayama*
Yasuhiro Morimoto, *Kitakyushu*
Satoru Murata, *Tokyo*
Shigeki Nagamachi, *Miyazaki*
Hiroshi Onishi, *Yamanashi*
Morio Sato, *Wakayama Shi*
Yoshito Tsushima, *Maebashi*
Masahiro Yanagawa, *Suita*

Netherlands

Willem Jan van Rooij, *Tilburg*

New Zealand

W Howell Round, *Hamilton*

Pakistan

Wazir Muhammad, *Abbottabad*

Poland

Maciej S Baglaj, *Wroclaw*

Piotr Czauderna, *Gdansk*

Portugal

Joao Manuel RS Tavares, *Porto*

Serbia

Olivera Ciraj-Bjelac, *Belgrade*

Singapore

Gopinathan Anil, *Singapore*
Terence KB Teo, *Singapore*
Cher Heng Tan, *Singapore*

Slovakia

Stefan Sivak, *Martin*

South Korea

Ki Seok Choo, *Busan*
Seung Hong Choi, *Seoul*
Dae-Seob Choi, *Jinju*
Hong-Seok Jang, *Seoul*
Yong Jeong, *Daejeon*
Chan Kyo Kim, *Seoul*
Se Hyung Kim, *Seoul*
Joong-Seok Kim, *Seoul*
Sang Eun Kim, *Seongnam*
Sung Joon Kwon, *Seoul*
Jeong Min Lee, *Seoul*
In Sook Lee, *Busan*
Noh Park, *Goyang*
Chang Min Park, *Seoul*
Sung Bin Park, *Seoul*
Deuk Jae Sung, *Seoul*
Choongsoo Shin, *Seoul*
Kwon-Ha Yoon, *Iksan*

Spain

Miguel A De Gregorio, *Zaragoza*
Antonio Luna, *Jaén*
Enrique Marco de Lucas, *Santander*
Fernando Ruiz Santiago, *Granada*

Sweden

Dmitry Grishenkov, *Stockholm*
Tie-Qiang Li, *Stockholm*

Switzerland

Nicolau Beckmann, *Basel*
Christian Boy, *Bern*
Giorgio Treglia, *Bellinzona*
Stephan Ulmer, *Kiel*

Thailand

Sirianong Namwongprom, *Chiang Mai*

Turkey

Kubilay Aydin, *Istanbul*
Ramazan Akdemir, *Sakarya*
Serhat Avcu, *Ankara*
Ayse Aralasmak, *Istanbul*
Oktay Algin, *Ankara*
Nevbahar Akcar, *Meselik*
Bilal Battal, *Ankara*
Zulkif Bozgeyik, *Elazig*
Nazan Ciledag, Aakara
Fuldem Y Donmez, *Ankara*
Gulgun Engin, *Istanbul*
Ahmet Y Goktay, *Izmir*
Oguzhan G Gumustas, *Bursa*
Kaan Gunduz, *Ankara*
Pelin Ozcan Kara, *Mersin*
Kivanc Kamburoglu, *Ankara*
Ozgur Kilickesmez, *Istanbul*
Furuzan Numan, *Istanbul*
Cem Onal, *Adana*
Ozgur Oztekin, *Izmir*
Seda Ozbek (Boruban), *Konya*
Selda Sarikaya, *Zonguldak*
Figen Taser, *Kutahya*
Baran Tokar, *Eskisehir*
Ender Uysal, *Istanbul*
Ensar Yekeler, *Istanbul*

United Kingdom

Indran Davagnanam, *London*
M DC Valdés Hernández, *Edinburgh*
Alan Jackson, *Manchester*
Suneil Jain, *Belfast*
Long R Jiao, *London*
Miltiadis Krokidis, *Cambridge*
Pradesh Kumar, *Liverpool*
Peter D Kuzmich, *Derby*
Georgios Plataniotis, *Brighton*
Vanessa Sluming, *Liverpool*

United States

Garima Agrawal, *Saint Louis*
James R Brasic, *Baltimore*
Rajendra D Badgaiyan, *Buffalo*
Ulas Bagci, *Bethesda*
Anat Biegon, *Stony Brook*
Ramon Casanova, *Winston Salem*
Wenli Cai, *Boston*
Zheng Chang, *Durham*
Corey J Chakarun, *Long Beach*
Kai Chen, *Los Angeles*
Hyun-Soon Chong, *Chicago*
Marco Cura, *Dallas*
Ravi R Desai, *Bensalem*
Delia DeBuc, *Miami*
Carlo N De Cecco, *Charleston*
Timm-Michael L Dickfeld, *Baltimore*
Subba R Digumarthy, *Boston*
Huy M Do, *Stanford*
Todd A Faasse, *Grand Rapids*
Salomao Faintuch, *Boston*
Girish M Fatterpekar, *New York*
Dhakshinamoorthy Ganeshan, *Houston*
Robert J Griffin, *Little Rock*
Andrew J Gunn, *Boston*
Sandeep S Hedgire, *Boston*
Timothy J Hoffman, *Columbia*
Mai-Lan Ho, *San Francisco*
Juebin Huang, *Jackson*
Abid Irshad, *Charleston*
Matilde Inglese, *New York*
El-Sayed H Ibrahim, *Jacksonville*
Paul R Julsrud, *Rochester*
Pamela T Johnson, *Baltimore*
Ming-Hung Kao, *Tempe*
Sunil Krishnan, *Houston*
Richard A Komoroski, *Cincinnati*
Sandi A Kwee, *Honolulu*
King Kim, *Ft. Lauderdale*
Guozheng Liu, *Worcester*
Yiyan Liu, *Newark*
Venkatesh Mani, *New York*
Lian-Sheng Ma, *Pleasanton*
Rachna Madan, *Boston*
Zeyad A Metwalli, *Houston*
Yilong Ma, *Manhasset*
Hui Mao, *Atlanta*
Feroze B Mohamed, *Philadelphia*
Gul Moonis, *Boston*
John L Nosher, *New Brunswick*
Rahmi Oklu, *Boston*
Aytekin Oto, *Chicago*
Bishnuhari Paudyal, *Philadelphia*
Rajul Pandya, *Youngstown*
Chong-Xian Pan, *Sacramento*
Jay J Pillai, *Baltimore*
Neal Prakash, *Duarte*
Reza Rahbar, *Boston*
Ali S Raja, *Boston*
Gustavo J Rodriguez, *El Paso*
David J Sahn, *Portlsand*
Steven Schild, *Scottsdale*
Ali R Sepahdari, *Los Angeles*
Li Shen, *Indianapolis*
JP Sheehan, *Charlottesville*
Atul B Shinagare, *Boston*
Sarabjeet Singh, *Boston*
Charles J Smith, *Columbia*
Kenji Suzuki, *Chicago*
Monvadi Srichai-Parsia, *Washington*
Sree H Tirumani, *Boston*
Hebert A Vargas, *New York*
Sachit Verma, *Philadelphia*
Yoichi Watanabe, *Minneapolis*
Li Wang, *Chapel Hill*
Carol C Wu, *Boston*
Shoujun Xu, *Houston*
Min Yao, *Cleveland*
Xiaofeng Yang, *Atlanta*
Qingbao Yu, *Albuquerque*
Aifeng Zhang, *Chicago*
Chao Zhou, *Bethlehem*
Hongming Zhuang, *Philadelphia*

WJR World Journal of Radiology

Contents

Monthly Volume 6 Number 4 April 28, 2014

AIM AND SCOPE

World Journal of Radiology (*World J Radiol*, *WJR*, online ISSN 1949-8470, DOI: 10.4329) is a peer-reviewed open access academic journal that aims to guide clinical practice and improve diagnostic and therapeutic skills of clinicians.

WJR covers topics concerning diagnostic radiology, radiation oncology, radiologic physics, neuroradiology, nuclear radiology, pediatric radiology, vascular/interventional radiology, medical imaging achieved by various modalities and related methods analysis. The current columns of *WJR* include editorial, frontier, diagnostic advances, therapeutics advances, field of vision, mini-reviews, review, topic highlight, medical ethics, original articles, case report, clinical case conference (clinicopathological conference), and autobiography.

We encourage authors to submit their manuscripts to *WJR*. We will give priority to manuscripts that are supported by major national and international foundations and those that are of great basic and clinical significance.

INDEXING/ABSTRACTING

World Journal of Radiology is now indexed in PubMed Central, PubMed, Digital Object Identifier, and Directory of Open Access Journals.

NAME OF JOURNAL
World Journal of Radiology

ISSN
ISSN 1949-8470 (online)

LAUNCH DATE
December 31, 2009

FREQUENCY
Monthly

EDITORIAL OFFICE
Jin-Lei Wang, Director
Xiu-Xia Song, Vice Director
World Journal of Radiology
Room 903, Building D, Ocean International Center,
No. 62 Dongsihuan Zhonglu, Chaoyang District,
Beijing 100025, China
Telephone: +86-10-85381891
Fax: +86-10-85381893
E-mail: bpgoffice@wjgnet.com
http://www.wjgnet.com

PUBLISHER
Baishideng Publishing Group Co., Limited
Flat C, 23/F., Lucky Plaza, 315-321 Lockhart Road,
Wanchai, Hong Kong, China
Fax: +852-65557188
Telephone: +852-31779906
E-mail: bpgoffice@wjgnet.com
http://www.wjgnet.com

PUBLICATION DATE
April 28, 2014

INSTRUCTIONS TO AUTHORS
Full instructions are available online at http://www.wjgnet.com/1949-8470/g_info_20100316162358.htm.

ONLINE SUBMISSION
http://www.wjgnet.com/esps/

World Journal of Radiology

Online Submissions: http://www.wjgnet.com/esps/
bpgoffice@wjgnet.com
doi:10.4329/wjr.v6.i4.62

World J Radiol 2014 April 28; 6(4): 62-71
ISSN 1949-8470 (online)

EDITORIAL

Liver volumetry: Is imaging reliable? Personal experience and review of the literature

Mirko D'Onofrio, Riccardo De Robertis, Emanuele Demozzi, Stefano Crosara, Stefano Canestrini, Roberto Pozzi Mucelli

Mirko D'Onofrio, Riccardo De Robertis, Emanuele Demozzi, Stefano Crosara, Stefano Canestrini, Roberto Pozzi Mucelli, Department of Radiology, G.B. Rossi Hospital, University of Verona, 37134 Verona, Italy

Author contributions: All authors equally contributed to this paper. D'Onofrio M and Pozzi Mucelli R designed the research and gave their final approval for submission; Demozzi E, Crosara S and Canestrini S performed the research and revised the paper; De Robertis R performed the research, wrote and revised the paper.

Correspondence to: Riccardo De Robertis, MD, Department of Radiology, G.B. Rossi Hospital, University of Verona, Piazzale L.A. Scuro 10, 37134 Verona, Italy. riccardo.derobertis@hotmail.it
Telephone: +39-45-8124301 Fax: +39-45-8027490
Received: October 9, 2013 Revised: January 11, 2014
Accepted: March 13, 2014
Published online: April 28, 2014

Abstract

The amount of the future liver remnant volume is fundamental for hepato-biliary surgery, representing an important potential risk-factor for the development of post-hepatectomy liver failure. Despite this, there is no uniform consensus about the amount of hepatic parenchyma that can be safely resected, nor about the modality that should be chosen for this evaluation. The pre-operative evaluation of hepatic volume, along with a precise identification of vascular and biliar anatomy and variants, are therefore necessary to reduce surgical complications, especially for extensive resections. Some studies have tried to validate imaging methods [ultrasound, computed tomography (CT), magnetic resonance imaging] for the assessment of liver volume, but there is no clear evidence about the most accurate method for this evaluation. Furthermore, this volumetric evaluation seems to have a certain degree of error, tending to overestimate the actual hepatic volume, therefore some conversion factors, which should give a more reliable evaluation of liver volume, have been proposed. It is widespread among non-radiologists the use of independent software for an off-site volumetric analysis, performed on digital imaging and communications in medicine images with their own personal computer, but very few studies have provided a validation of these methods. Moreover, while the pre-transplantation volumetric assessment is fundamental, it remains unclear whether it should be routinely performed in all patients undergoing liver resection. In this editorial the role of imaging in the estimation of liver volume is discussed, providing a review of the most recent literature and a brief personal series of correlations between liver volumes and resection specimens' weight, in order to assess the precision of the volumetric CT evaluation.

Key words: Liver; Hepatectomy; Ultrasound; Computed tomography; Magnetic resonance imaging

Core tip: Imaging plays a fundamental role in the pre-operative volumetric evaluation of patients undergoing liver resection or transplantation. It seems that computed tomography and magnetic resonance imaging are reliable and substantially equivalent for this evaluation. Automatic or semi-automatic methods are efficient and less time-consuming than manual tracing methods. Further studies are needed to definitely evaluate the accuracy of commercially available software for liver volumetry.

D'Onofrio M, De Robertis R, Demozzi E, Crosara S, Canestrini S, Pozzi Mucelli R. Liver volumetry: Is imaging reliable? Personal experience and review of the literature. *World J Radiol* 2014; 6(4): 62-71 Available from: URL: http://www.wjgnet.com/1949-8470/full/v6/i4/62.htm DOI: http://dx.doi.org/10.4329/wjr.v6.i4.62

INTRODUCTION

The increased knowledge of anatomical structures and liver function, the development of new surgical techniques, the improvements in chemotherapy and anesthesiological management made possible during recent years has increased the successful performance of liver resections, with mortality decreased to less than 5%; even more extensive hepatic resections are nowadays routinely successfully performed[1,2]. The pre-operative hepatic volumetry has become fundamental for hepato-biliary surgery[3-5]; it is widely accepted that the future liver remnant volume (FLRV) is an important potential risk-factor for the development of post-hepatectomy liver failure (PHLF), which is associated with an increase of post-operative complications and with a longer hospitalization. PHLF is the standardized term to define the post-surgical acquired deterioration of the synthetics, excretory and detoxifying functions of the liver; this syndrome is characterized by an increase of the international normalized ratio values and of serum bilirubin levels from the fifth post-operative day[6]. This syndrome has a reported incidence of 1.2%-32%[7-9]. As mentioned above, the post-hepatectomy mortality reported in recent years varies between 0% and 5% and the onset of PHLF remains the main cause[10-12]. Factors that contribute to the onset of PHLF can be divided into three groups: patient-related factors (age, diabetes, obesity)[13,14]; parenchyma-related factors (cirrhosis, cholestasis, steatosis, chemotherapy effects)[15-17]; surgery-related factors (bleeding, ischemia-reperfusion damage, sepsis, insufficient FLRV)[18-21]. With hepatic resection an amount of liver parenchyma is lost, and in the remnant hepatocytes arise both regeneration and necrosis. The remnant liver must therefore be able to overcome the necrosis, preserving or recovering an adequate synthetic ability[22]; as a consequence, there must be an adequate and functional FLRV to avoid PHLF[23]. Despite this, there is no uniform consensus among hepatic surgeons on the amount of liver volume that can be safely resected, with a wide range of reported values[24,25]. Guglielmi *et al*[24] reported that in patients with "healthy" liver (absence of hepatic diffuse disease, normal functionality tests) the limit of FLRV% for a safe resection varies between 20% and 30%, while in patients with underlying hepatic disease (cirrhosis, cholestasis, steatosis) the critical FLRV% value rise up to 30%-40%.

IMAGING: WHICH MODALITY SHOULD BE CHOSEN?

Many studies have tried to validate different imaging techniques for liver volumetry, but there is no clear evidence about the most accurate method for this evaluation. Kitajima *et al*[26] reported the possibility of performing liver volumetry by means of conventional ultrasound, with good correlation with the volume of the actual specimen; Xu *et al*[27] reported the usefulness of the three-dimensional ultrasound (3DUS) volumetric evaluation: the measured volumes all significantly correlated with the true volumes, with significant intraobserver and interobserver reproducibility. Despite the relative widespread availability of 3DUS probes and a considerable refinement of this technique in recent years, ultrasound has not universally proven to be successful for 3D evaluation of the liver, because of well-known limits, both physical and related to a variable reproducibility of the exam, which mainly depends on the skill of the examiner[28-30]. The use of more objective methods as computed tomography (CT) or magnetic resonance imaging (MRI) seems therefore fundamental, especially for the planning of more extensive resections, such as liver transplants or major hepatectomies. These two imaging techniques in fact showed a very good accuracy in the estimation of the graft dimensions before transplant[31] and in providing a precise quantification of the pre-operative liver volumes[32-34]. Itoh *et al*[35] stated that the meticulous pre-operative evaluation based on volumetric analysis of 3D CT images, together with improved surgical techniques, were fundamental to achieve "zero mortality" and minimized intraoperative blood loss in this 300 hepatic resections series. Regarding liver transplantation, Ringe *et al*[36] emphasized the role of CT, reporting that this method of imaging of the liver, in combination with dedicated software, plays a key role in the evaluation of candidates for liver donor transplantation: based on the results of liver CT volumetry, 31% of the candidates of this series were excluded as donors. Lee *et al*[37] reported the usefulness of semi automated liver MR volumetry using hepatobiliary phase gadoxetic acid-enhanced images with the quadratic MR image division to measure liver volume in potential living liver donors; the average volume measurement error of the semi automated MR volumetry was 2.35% ± 1.22%. Zappa *et al*[38] applied CT volumetry to the evaluation of total and segmental liver regeneration after hepatectomy: CT was able to identify even segmental regeneration, reporting a 64% increase in liver volume from the future remnant 7 d after hepatectomy. CT imaging can be useful also to evaluate volumetric modifications after the induction of liver hypertrophy prior to surgery: Ulla *et al*[39] reported that CT volumetry, being able to calculate the mean absolute future-liver-remnant (FLR) and FLR/total liver volume (TLV) ratio before and after surgery, plays a key role in decision-making, monitoring and predicting liver hypertrophy pre- and post-operatively; in particular, if the enlargement of the FLR is as expected 6 d after surgery on CT examination, a second-step surgery can be safely performed. It has been reported by Vienne *et al*[40] that CT volumetry is also important prior to endoscopic biliary drainage, in order to estimate the volume of liver to drain: the main factor associated with drainage effectiveness was a liver volume drained of more than 50%. Kalkmann *et al*[41] has proposed the use of CT-based liver volumetry as a parameter to assess therapy response in patients with advanced liver metastasis, reporting that progressive disease led to larger median liver volume variations than partial remission or

stable disease. Literature seems to provide a substantial equivalence between CT and MRI for liver volume estimation, but it must be otherwise noted that there is a bias related to a higher amount of published papers regarding CT-based volumetry. For example, Aoyama *et al*[34] proposed a manual segmentation technique that requires the tracing of 4 images, which showed a high linear correlation with the conventional manual tracing technique (r = 0.98; slope 0.97; $P < 0.001$), and does not depend on imaging modalities, so both MRI and CT images can be used. Kianmanesh *et al*[42] described a technique based on CT measurements of liver angles (the so-called angulometry) that can be used to predict liver ratios on both CT and MRI slices. Angulometry was described as simple and accurate (mean ± SD percentages of the TLV in angulometry and volumetry: 25% ± 4% and 20% ± 3%, respectively, with $P < 0.05$; mean ± SD overestimation of the percentage of the TLV in angulometry: 2.7% ± 7.0%). Numminen *et al*[43] stated that 3D liver models, which can be reconstructed both from modified discrete cosine transform and MRI data, improve the surgeon's knowledge of liver anatomy and made even more complicated liver resections safe. Despite the reported accuracy, the volumetric evaluation performed both with CT and MRI seems to have a certain degree of error, tending to overestimate the actual hepatic volume in respect to the intra-operative volumetric evaluation, probably due to intra-operative loss of blood, as proposed by Niehues *et al*[44]: median liver density in his series was 1.07 g/mL. Regression analysis showed a high correlation between CT volumetry and water displacement (r = 0.985), but CT volumetry was found to be 13% higher than water displacement volumetry ($P < 0.0001$): the only relevant factor leading to this difference seemed to be blood perfusion. For these reasons, some authors have proposed the use of conversion factors and formulas, which should standardize imaging volumetry, providing a more realistic evaluation of liver volume[45,46]. Tongyoo *et al*[47], for example, proposed a formula that combined sonographic portal vein diameters measurement and CT liver volumetry, providing a precise donor screening for graft size adequacy. Sakei *et al*[48] proposed another formula to calculate the standard liver volume of children undergoing liver transplantation (standard liver volume = 689.9 × body surface area - 24.7), using CT images as a reference. Li *et al*[49] proposed the use of an equation (intraoperative weight = 0.844 × preoperative CT volume + 5.271) that can be useful to predict the actual graft weight (r = 0.885). Ribero *et al*[50] reported that the use of an estimated TLV, measured on the basis of correlation existing with body surface area (-794.41 + 1267.28 × body surface area), can identify about 11% of patients in whom liver volumetry directly calculated by CT images underestimates the risk of hepatic insufficiency. Chun *et al*[51] assessed the usefulness of future liver remnant calculation by means of CT standardized to body weight or body surface area, reporting a strong correlation for both measurements (r = 0.98). Vauthey[52] stated that the CT-based calculation of future liver remnant to TLV ratio by using a formula based on body surface area (liver volume = 706 × body surface area + 2.4) can provide a precise assessment of the future remnant before resection, and this is also useful in evaluating response to portal vein embolization. Müller *et al*[53] tested different measurement algorithms to predict TLV and reported that the analysis of 3D CT volumetry showed good correlation between the actual and the calculated liver volume in all tested algorithms; the Heidelberg algorithm reduced the measuring error with deviations of only 1.2%. Kayashima *et al*[54] created an age-adjusted formula using regression analysis retrospectively in 167 donors: 70.767 + (0.703 × graft volume estimated with 3D CT volumetry) + (1.298 × donor age). The mean reported error ratio for the age-adjusted formula (9.6%) was significantly lower than that from 3D CT (14%).

IMAGING: HOW TO CALCULATE LIVER VOLUME?

Various methods have been developed to calculate hepatic volume using CT or MR images. The first proposed method was the manual tracing of the entire liver, but despite a relative precision it was a very time-consuming technique[55-57]. More recently, automatic or semiautomatic segmentation techniques, for example using mathematical models based on histogram cluster analysis, were introduced[58]. Suzuki *et al*[59] developed an automated liver extraction scheme for measuring volumes at CT and compared the automated volumetric assessment based on this scheme with the findings at interactive volumetry performed with commercially available assist software and with manual volumetry, considered as the reference standard. The values obtained with automated and interactive CT liver volumetry agreed with the values obtained with manual volumetry (intra-class correlation coefficient = 0.94 and 0.96); automated volumetry required substantially less user time (less than 1 min/case) than manual volumetry (approximately 40 min/case) and interactive volumetry (approximately 30 min/case). With reference to liver transplantation, Radtke *et al*[60] described and validated a modus 3D volumetry based on unenhanced CT images, which accurately accounted for intrahepatic vascular volumes and offered a precise virtual model of individualized operative conditions for each potential live liver donor. Nakayama *et al*[61] proposed an automated method to obtain liver volumetry on CT images with good correlation with *in vivo* measured volumes (r = 0.792) in patients awaiting living related liver transplantation. Soyer *et al*[62] reported that there is a significant correlation (r = 0.767, $P < 0.001$) between hepatic height and hepatic volume, thus suggesting that hepatic height can be used to quickly predict hepatic volume, thus avoiding time-consuming evaluations as the manual segmentation. Kim *et al*[63] reported that the automated measurement of blood-free volume must be performed at automated CT volumetry in live liver donors; this parameter is more ac-

curate than the ratio between blood-filled volume/1.22 in estimation of hepatic weight. From a technical point of view, it seems fundamental to use thin-section images, as reported by Hori *et al*[64]: liver volumes calculated from 2.5-mm-thick or thicker images resulted significantly smaller than liver volumes calculated from 3D images. If a maximum error of 5% in the calculated graft volume will not have a significant clinical impact, 5-mm-thick images are acceptable for CT volumetry, but if the impact is significant, 3D images could be essential. Luciani *et al*[65] reported that both manual and automated multiphase CT-based volume measurements were strongly correlated to liver volume (r = 0.87 and 0.90, respectively), but automated segmentation was significantly more rapid than manual segmentation (mean time: 16 ± 5 and 86 ± 3 s, respectively). Suzuki *et al*[66] developed a general framework for liver segmentation in both CT and MRI, using an anisotropic diffusion filter to reduce noise, a scale-specific gradient magnitude filter to enhance liver boundaries, a fast-marching algorithm to roughly determine liver boundaries, and a geodesic-active-contour model coupled with a level-set algorithm to refine the initial boundaries. The comparison of this computer volumetry with "gold standard" manual volumetry reported an excellent agreement (intra-class correlation coefficient = 0.94 and 0.98, respectively), with smaller average user time for computer volumetry. The usefulness of geodesic active contour segmentation was already reported[67]: in this series, the computer-estimated liver volumetrics agreed excellently with the gold-standard manual volumetrics (intraclass correlation coefficient = 0.95) with no statistically significant difference. The average accuracy, sensitivity, specificity, and percent volume error were 98.4%, 91.1%, 99.1%, and 7.2%, respectively. Zhou *et al*[68] tested three semiautomatic algorithms: 2D region growing with knowledge-based constraints, 2D voxel classification with propagational learning and Bayesian rule-based 3D region growing, reporting a promising overall performance of the first two methods. The use of independent software for an off-site volumetric analysis is also widespread, mainly among non-radiologists, performed on digital imaging and communications in medicine images with their own personal computer, but very few studies provided a validation of these evaluation methods, comparing, for example, their results to the volumetric analysis performed by the radiologist who performed imaging[69,70]. For example, Dello *et al*[69] compared ImageJ (http://rsb.info.nih.gov/ij/download.html) and OsiriX (http://www.osirix-viewer.com) in performing prospective CT volumetric analysis of the liver on a personal computer in patients undergoing major liver resection, reporting a significant correlation between the measured weights of resection specimens and the volumes calculated prospectively with ImageJ and OsiriX (r = 0.89 and r = 0.83, respectively) and a significant correlation between the volumes measured with radiological software and the volumes measured with ImageJ and OsiriX (r = 0.93 and r = 0.95, respectively). van der Vorst *et al*[70] assessed the accuracy of OsiriX (http://www.osirix-viewer.com) CT volumetry for predicting liver resection volume (RV) and FLVR in patients undergoing partial hepatectomy, and found significant correlations between these data and the weight and volume of the resected specimens (r = 0.95). Lu *et al*[71] reported that the hepatic volume calculation obtained with graphic software was reliable, despite the significant disadvantage in digitalization of CT films and manually copying pixel values.

PERSONAL EXPERIENCE

Materials and methods

A radiologist (M.D.) with 10 years of experience in abdominal imaging, blinded to the actual type of resection and to the final diagnosis, retrospectively reviewed the preoperative CT of all patients with primary liver malignancy (hepatocellular carcinoma or cholangiocarcinoma) that underwent resection of two or more liver segments in the last two years in our liver surgery unit. After reviewing CT, an on-site volumetric analysis was performed, using the post-processing application of our CT workstation (Liver Analysis; Extended Brilliance Workstation, Philips, Eindhoven, The Netherlands). The volumetric data were compared with those obtained at an off-site analysis by the hepatic surgeon (A.R.), with ten years of experience in liver surgery, with an independent off-site post-processing software (OsiriX, www.osirix-viewer.com) on his personal computer; to assess the reliability of the two methods, the RVs obtained with the two analysis methods were then compared with the actual weights of surgical specimen. The patients that underwent surgical resection for liver metastases, as well as those with benign liver tumors, were excluded from the study, because of the possibility of performing atypical resections, whose margins and whose extent cannot be accurately reproduced. Other exclusion criteria were: a pre-operative CT performed in another hospital, to avoid bias deriving from the use of a different scan protocol; the absence of weight data of the surgical specimens. Using these criteria, 14 patients were excluded from the study, 6/14 for a pre-operative CT scan performed in another hospital, 8/14 for the absence of weight data of the surgical specimens. Twenty-two patients were included in this study, 10/22 (45.5%) with hepatocellular carcinoma and 12/22 (54.5%) with cholangiocarcinoma (8/12 hilar cholangiocarcinoma; 4/12 peripheral cholangiocarcinoma).

All exams were performed with a multidetector CT scanner (Brilliance 64, Philips, Eindhoven, The Netherlands), before and after intravenous administration of a iodine contrast medium at a concentration of 370 mg/L (Ultravist 370, BayerScheringPharma AG, Berlin, Germany) through an antecubital vein of the arm, using an automatic double-syringe injector (Stellant, MedRad, Indianola, PA, United States) at a flow rate of 3-4 mL/s, followed by a bolus of 50 mL of saline at the same flow rate; the contrast medium amount was tailored to the patient's weight, injecting 15 mL/kg of contrast medium. Positive oral contrast-medium was never administered. In all cases a quadriphasic examination was performed,

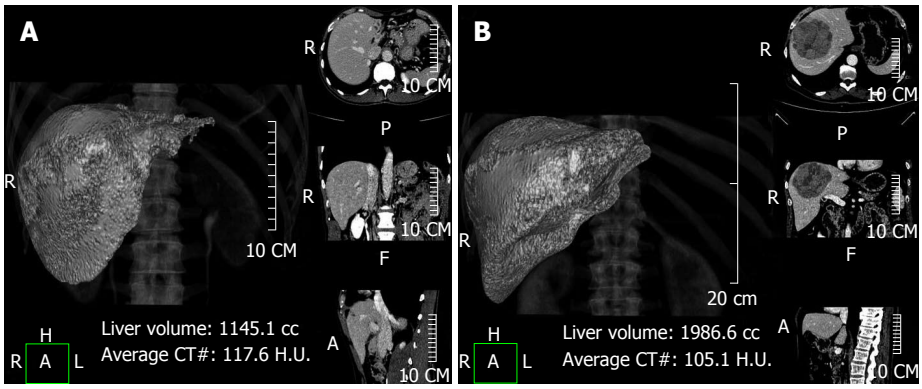

Figure 1 Using a semi-automatic method liver analysis application provides a 3D and a multi-planar reconstruction of the liver. A case of hilar cholangiocarcinoma involving the left hepatic duct, with marked hypotrophy of the left lobe (type IIIb according to the Bismuth-Corlette classification) (A) and a case of hepatocarcinoma in segments 4-5-8 (B) are shown.

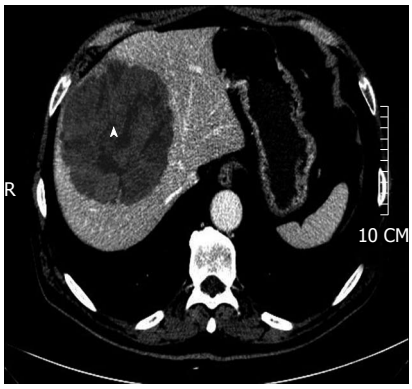

Figure 2 For intra-hepatic masses the manual segmentation of the lesion is needed. A huge hepatocarcinoma (arrowhead) in segments 4-8-5 is shown.

using a bolus tracking technique: a pre-contrastographic scan of the upper abdomen; an arterial phase scan of the upper abdomen, performed 15 s after the reach of the aortic enhancement threshold (120 HU); a portal/venous phase scan of the entire abdomen, performed 70 s after the administration of the contrast media; and a delayed phase scan of the upper abdomen, performed 180 s after the administration of contrast media; an additional 10-min delayed acquisition was performed in patients with cholangiocarcinoma. The following parameters were used: thickness 2 mm; increment 11 mm; tube voltage 120 kV; collimation 64 × 0.625; pitch 0.891 for the pre-contrastographic, venous and delayed phase scan, 0.5 for the arterial phase scan; rotation time 0.75 s. For the on-site analysis, liver volumes were calculated with Liver Analysis application software, which uses the density differences in portal/venous scan images to obtain a semi-automatic liver segmentation. The gallbladder and the main vessels, such as the retro-hepatic inferior cava vein, were manually excluded from segmentation volume. A volumetric reconstruction of the liver and the quantification of TLV were obtained (Figure 1); the lesion was then manually segmented, obtaining the tumor volume (TV) (Figure 2). Then, a virtual hepatectomy was performed (Figure 3), obtaining RV values and FLRV values. The FLRV value was calculated both as an absolute value expressed in cubic centimeters, both as a percentage (FLRV%): for extra-hepatic lesions (*i.e.*, hilar cholangiocarcinoma; the FLRV% was directly calculated as the ratio between FLRV and TLV), while for intra-hepatic lesions the FLRV% was indirectly calculated, first obtaining the actual TLV (ATLV) value, calculated as the difference between TLV and TV, because intra-hepatic lesions represent a non-functioning hepatic portion, which must not be included in the FLRV% value. The surgical specimen's weight was used as the reference standard for the RV measurement, assuming that 1 g of parenchyma was equal to 1 cc; despite some authors[72] having reported that CT overestimates hepatic volume in comparison with the immersion of the surgical specimen in water, used for the *ex vivo* intraoperative volume measurement according to Archimedes' principle. This approximation is acceptable because we considered it as the same for the two analysis methods. The Bland-Altman method was used to test the difference (delta) between the values obtained with the two methods against their average. The Pearson's correlation test was used to assess the correlation between the estimated RV and the weight of surgical specimens. The statistical analysis was performed with GraphPad Prism 5.03.

Results

The following resections were performed: left hepatectomy (resection of segments 2, 3 and 4 in 1 hilar cholangiocarcinoma), right hepatectomy (resection of segments 5, 6, 7 and 8 for 7 hepatocellular carcinomas and 2 cholangiocarcinomas); right hepatectomy and resection of caudate lobe (resection of segments 1, 4, 5, 6, 7 and 8 for 5 hilar cholangiocarcinomas); left hepatectomy and resection of caudate lobe (resection of segments 1, 2, 3, 4, 5 and 8 in 1 hilar cholangiocarcinoma); mesohepatectomy (resection of segments 4, 5 and 8 for 1 hepatocellular carcinoma); bisegmentectomy (1 cholangiocarcinoma, 2 hepatocellular carcinomas).

The average and delta values (difference between the values) of TLV, TV, ATLV, RV, and FLRV obtained with

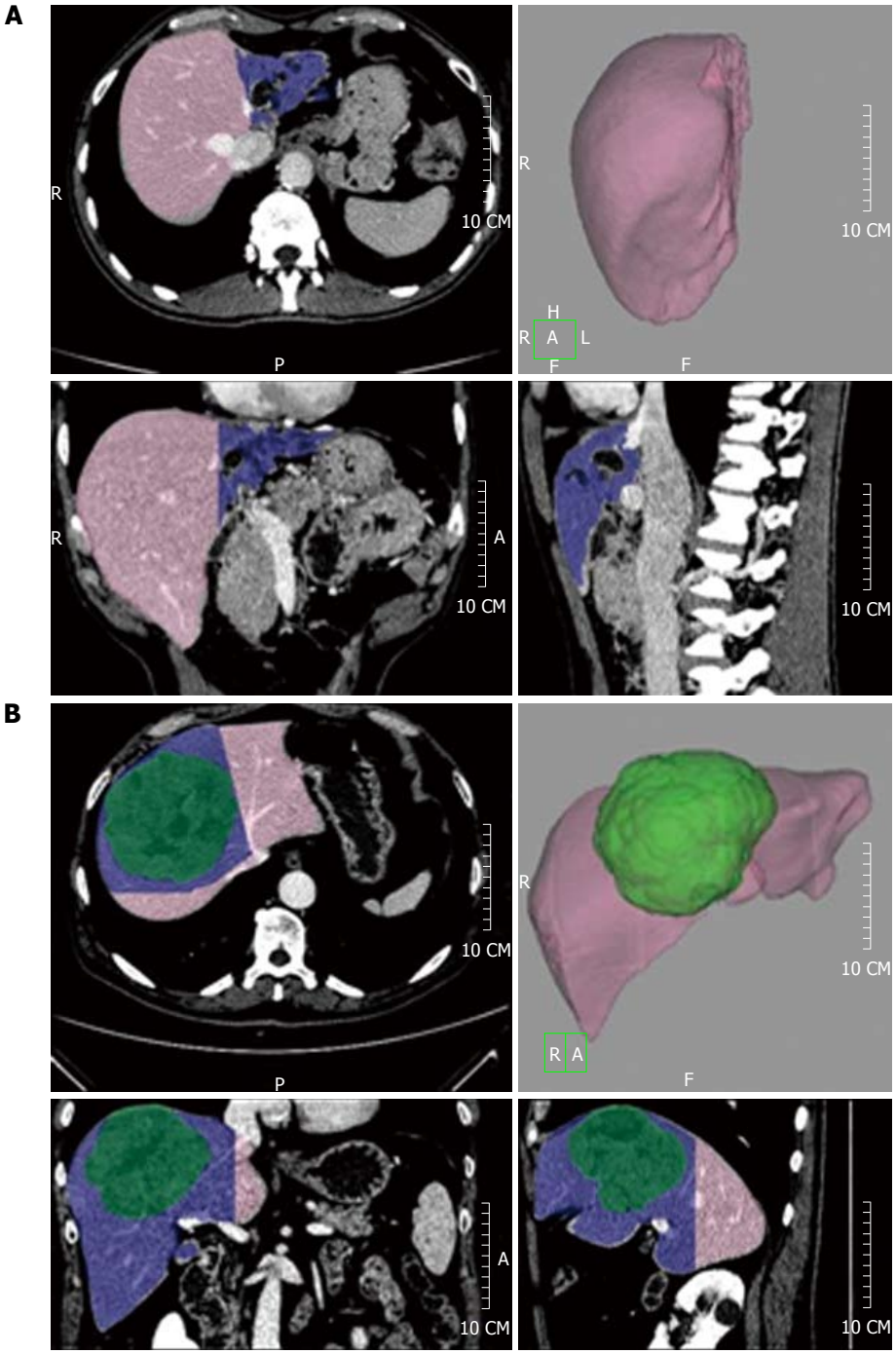

Figure 3 The future liver remnant volume is shown in pink, while the resection volume is shown in blue. A left hepatectomy for a hilar cholangiocarcinoma involving the left hepatic duct (A) and a mesohepatectomy (resection of liver segments 4-8-5) for a hepatocarcinoma (shown in green, B) are shown.

the two analysis methods are shown in Table 1.

Discussion

All patients included in this series had undergone resection of two or more liver segments; in these cases it seems important to perform a pre-operative liver volumetry to assess the FLRV; mean FLRV% obtained with on-site and off-site analysis were equivalent (50% and 49%, respectively). No patient developed PHLF.

The accuracy of the on-site analysis for the prediction of resection type was 100%, because in all cases the virtual resection correctly predicted the actual surgical resection.

The Bland-Altman comparison between the results of the two analysis methods is shown in Figure 4: the overall comparison between the mean values of the volumetric data obtained with on-site analysis and off-site analysis showed good correlation, with bias value of 26.24 (SD = 10.17, 95% limits of agreement from 6.301 to 46.18), thus configuring a substantial equivalence between the two analysis methods. The regression analysis did not show significant differences between the slope of the two regression curves ($F = 0.09$, $P = 0.76$, pooled slope = 0.88).

The RV values obtained with the on-site analysis and

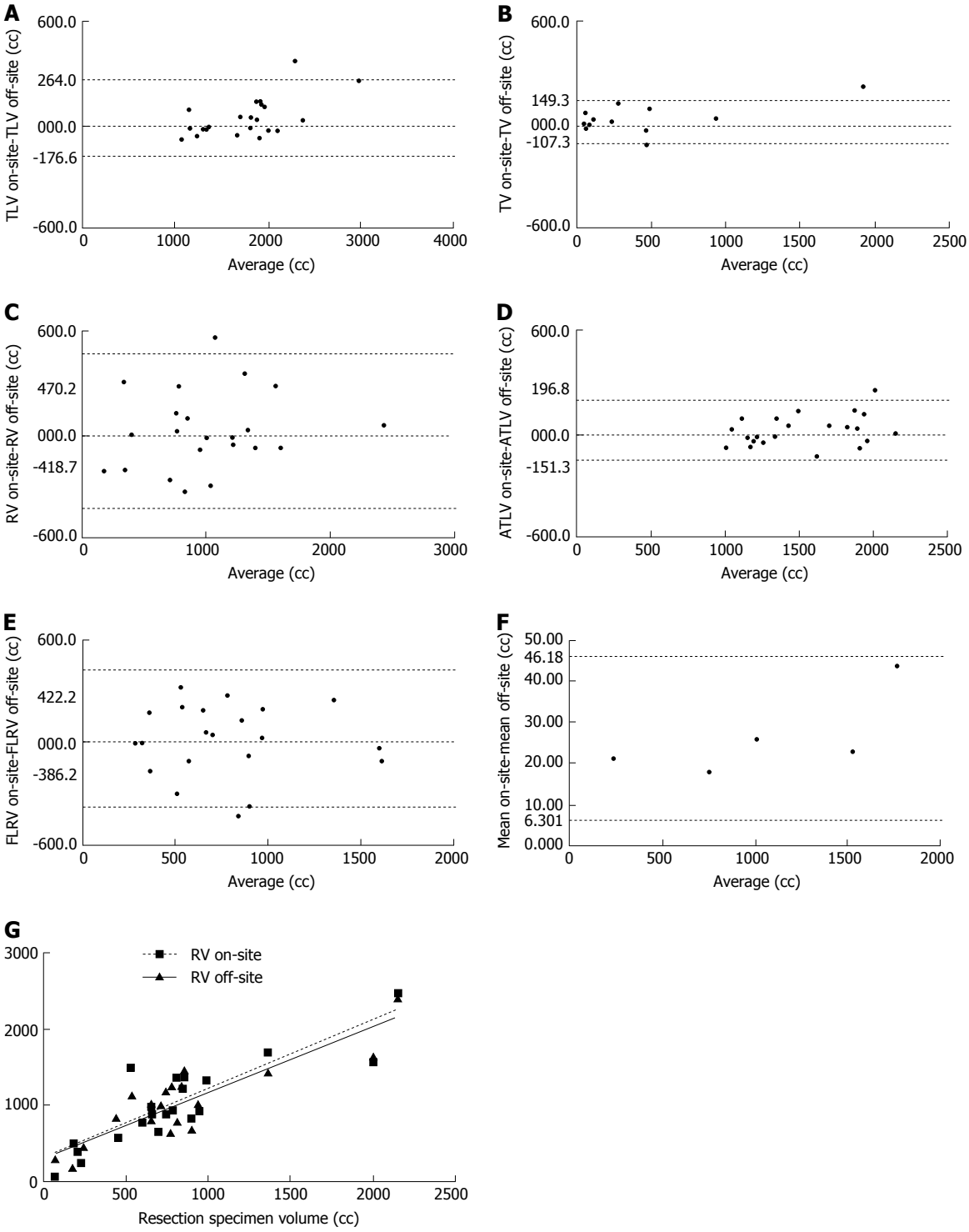

Figure 4 Bland-Altman graphs plotting the mean against the difference for total liver volume (A), tumor volume (B), resection volume (C), actual total liver volume (D), future liver remnant volume (E), and overall mean (F) with the two measurement methods; the correlation lines for the comparison between the resection volume and the actual volume of the resection specimens obtained with Pearson's correlation test are shown in (G). TLV: Total liver volume; TV: Tumor volume; RV: Resection volume; ATLV: Actual total liver volume; FLRV: Future liver remnant volume.

the off-site analysis showed high correlation with the actual surgical specimen's volume, with R values equal to 0.86 (95% confidence interval 0.69 to 0.94, $P < 0.0001$) and 0.88 for the off-site analysis (95% confidence interval 0.73 to 0.95, $P < 0.0001$).

Conclusion

The volumetric analysis obtained with on-site and with off-site analysis methods seems comparable and reliable. Further studies including a larger population are required.

CONCLUSION

The role of imaging in the pre-operative volumetric evaluation of patients undergoing liver resection or transplantation is fundamental. It seems that CT and MRI are

Table 1 Mean values of total liver volume, tumor volume, actual total liver volume, resection volume, future liver remnant volume, their mean and difference

Variable	On-site	Off-site	Mean	Difference
TLV	1787.31	1743.58	1765.48	43.73
TV	248.67	227.68	238.18	20.99
RV	1021.23	995.48	1008.36	25.75
ATLV	1538.65	1515.89	1527.27	22.76
FLRV	766.08	748.10	757.09	17.98

Values in cubic centimeters. TLV: Total liver volume; TV: Tumor volume; RV: Resection volume; ATLV: Actual total liver volume; FLRV: Future liver remnant volume.

substantially equivalent in this evaluation. Automatic or semi-automatic volumetry are efficient and less time-consuming than manual segmentation. Further studies are needed to evaluate the accuracy of commercially available software for liver volumetry.

REFERENCES

1 **Scheele J**, Stangl R, Altendorf-Hofmann A. Hepatic metastases from colorectal carcinoma: impact of surgical resection on the natural history. *Br J Surg* 1990; **77**: 1241-1246 [PMID: 2253003 DOI: 10.1002/bjs.1800771115]
2 **Scheele J**. [Vasculature based segmental resection of the liver]. *Langenbecks Arch Chir* 1990; **375**: 308-317 [PMID: 2259266]
3 **Okamoto E**, Kyo A, Yamanaka N, Tanaka N, Kuwata K. Prediction of the safe limits of hepatectomy by combined volumetric and functional measurements in patients with impaired hepatic function. *Surgery* 1984; **95**: 586-592 [PMID: 6324403]
4 **Cohnert TU**, Rau HG, Buttler E, Hernandez-Richter T, Sauter G, Reuter C, Schildberg FW. Preoperative risk assessment of hepatic resection for malignant disease. *World J Surg* 1997; **21**: 396-400; discussion 401 [PMID: 9143571 DOI: 10.1007/PL00012260]
5 **Rau HG**, Schauer R, Helmberger T, Holzknecht N, von Rückmann B, Meyer L, Buttler E, Kessler M, Zahlmann G, Schuhmann D, Schildberg FW. Impact of virtual reality imaging on hepatic liver tumor resection: calculation of risk. *Langenbecks Arch Surg* 2000; **385**: 162-170 [PMID: 10857486 DOI: 10.1007/s004230050260]
6 **Rahbari NN**, Garden OJ, Padbury R, Brooke-Smith M, Crawford M, Adam R, Koch M, Makuuchi M, Dematteo RP, Christophi C, Banting S, Usatoff V, Nagino M, Maddern G, Hugh TJ, Vauthey JN, Greig P, Rees M, Yokoyama Y, Fan ST, Nimura Y, Figueras J, Capussotti L, Büchler MW, Weitz J. Posthepatectomy liver failure: a definition and grading by the International Study Group of Liver Surgery (ISGLS). *Surgery* 2011; **149**: 713-724 [PMID: 21236455 DOI: 10.1016/j.surg.2010.10.001]
7 **Farges O**, Malassagne B, Flejou JF, Balzan S, Sauvanet A, Belghiti J. Risk of major liver resection in patients with underlying chronic liver disease: a reappraisal. *Ann Surg* 1999; **229**: 210-215 [PMID: 10024102]
8 **Cucchetti A**, Ercolani G, Vivarelli M, Cescon M, Ravaioli M, La Barba G, Zanello M, Grazi GL, Pinna AD. Impact of model for end-stage liver disease (MELD) score on prognosis after hepatectomy for hepatocellular carcinoma on cirrhosis. *Liver Transpl* 2006; **12**: 966-971 [PMID: 16598792]
9 **Mullen JT**, Ribero D, Reddy SK, Donadon M, Zorzi D, Gautam S, Abdalla EK, Curley SA, Capussotti L, Clary BM, Vauthey JN. Hepatic insufficiency and mortality in 1,059 noncirrhotic patients undergoing major hepatectomy. *J Am Coll Surg* 2007; **204**: 854-862; discussion 862-864 [PMID: 17481498]
10 **Poon RT**, Fan ST, Lo CM, Liu CL, Lam CM, Yuen WK, Yeung C, Wong J. Improving perioperative outcome expands the role of hepatectomy in management of benign and malignant hepatobiliary diseases: analysis of 1222 consecutive patients from a prospective database. *Ann Surg* 2004; **240**: 698-708; discussion 708-710 [PMID: 15383797]
11 **Kamiyama T**, Nakanishi K, Yokoo H, Kamachi H, Tahara M, Yamashita K, Taniguchi M, Shimamura T, Matsushita M, Todo S. Perioperative management of hepatic resection toward zero mortality and morbidity: analysis of 793 consecutive cases in a single institution. *J Am Coll Surg* 2010; **211**: 443-449 [PMID: 20822741 DOI: 10.1016/j.jamcollsurg.2010.06.005]
12 **Simmonds PC**, Primrose JN, Colquitt JL, Garden OJ, Poston GJ, Rees M. Surgical resection of hepatic metastases from colorectal cancer: a systematic review of published studies. *Br J Cancer* 2006; **94**: 982-999 [PMID: 16538219]
13 **Nanashima A**, Abo T, Nonaka T, Fukuoka H, Hidaka S, Takeshita H, Ichikawa T, Sawai T, Yasutake T, Nakao K, Nagayasu T. Prognosis of patients with hepatocellular carcinoma after hepatic resection: are elderly patients suitable for surgery? *J Surg Oncol* 2011; **104**: 284-291 [PMID: 21462192 DOI: 10.1002/jso.21932]
14 **Balzan S**, Nagarajan G, Farges O, Galleano CZ, Dokmak S, Paugam C, Belghiti J. Safety of liver resections in obese and overweight patients. *World J Surg* 2010; **34**: 2960-2968 [PMID: 20711580 DOI: 10.1007/s00268-010-0756-1]
15 **Khuntikeo N**, Pugkhem A, Bhudhisawasdi V, Uttaravichien T. Major hepatic resection for hilar cholangiocarcinoma without preoperative biliary drainage. *Asian Pac J Cancer Prev* 2008; **9**: 83-85 [PMID: 18439081]
16 **Takenaka K**, Kanematsu T, Fukuzawa K, Sugimachi K. Can hepatic failure after surgery for hepatocellular carcinoma in cirrhotic patients be prevented? *World J Surg* 1990; **14**: 123-127 [PMID: 2154902]
17 **Selzner M**, Clavien PA. Failure of regeneration of the steatotic rat liver: disruption at two different levels in the regeneration pathway. *Hepatology* 2000; **31**: 35-42 [PMID: 10613725]
18 **Silva MA**, Muralidharan V, Mirza DF. The management of coagulopathy and blood loss in liver surgery. *Semin Hematol* 2004; **41**: 132-139 [PMID: 14872434]
19 **Peralta C**, Prats N, Xaus C, Gelpí E, Roselló-Catafau J. Protective effect of liver ischemic preconditioning on liver and lung injury induced by hepatic ischemia-reperfusion in the rat. *Hepatology* 1999; **30**: 1481-1489 [PMID: 10573528]
20 **Hessheimer AJ**, Fondevila C, Taurá P, Muñoz J, Sánchez O, Fuster J, Rimola A, García-Valdecasas JC. Decompression of the portal bed and twice-baseline portal inflow are necessary for the functional recovery of a "small-for-size" graft. *Ann Surg* 2011; **253**: 1201-1210 [PMID: 21587116 DOI: 10.1097/SLA.0b013e3181ffb2d7]
21 **Gross K**, Katz S, Dunn SP, Cikrit D, Rosenthal R, Grosfeld JL. Bacterial clearance in the intact and regenerating liver. *J Pediatr Surg* 1985; **20**: 320-323 [PMID: 3900325]
22 **Michalopoulos GK**, DeFrances MC. Liver regeneration. *Science* 1997; **276**: 60-66 [PMID: 9082986]
23 **Shoup M**, Gonen M, D'Angelica M, Jarnagin WR, DeMatteo RP, Schwartz LH, Tuorto S, Blumgart LH, Fong Y. Volumetric analysis predicts hepatic dysfunction in patients undergoing major liver resection. *J Gastrointest Surg* 2003; **7**: 325-330 [PMID: 12654556]
24 **Guglielmi A**, Ruzzenente A, Conci S, Valdegamberi A, Iacono C. How much remnant is enough in liver resection? *Dig Surg* 2012; **29**: 6-17 [PMID: 22441614]
25 **Hiroshige S**, Shimada M, Harada N, Shiotani S, Ninomiya M, Minagawa R, Soejima Y, Suehiro T, Honda H, Hashizume M, Sugimachi K. Accurate preoperative estimation of liver-graft volumetry using three-dimensional computed tomography.

Transplantation 2003; **75**: 1561-1564 [PMID: 12792515]
26 **Kitajima K**, Taboury J, Boleslawski E, Savier E, Vaillant JC, Hannoun L. Sonographic preoperative assessment of liver volume before major liver resection. *Gastroenterol Clin Biol* 2008; **32**: 382-389 [PMID: 18403156 DOI: 10.1016/j.gcb.2008.02.007]
27 **Xu HX**, Yin XY, Lu MD, Liu GJ, Xu ZF. Estimation of liver tumor volume using a three-dimensional ultrasound volumetric system. *Ultrasound Med Biol* 2003; **29**: 839-846 [PMID: 12837499]
28 **Oldhafer KJ**, Högemann D, Stamm G, Raab R, Peitgen HO, Galanski M. [3-dimensional (3-D) visualization of the liver for planning extensive liver resections]. *Chirurg* 1999; **70**: 233-238 [PMID: 10230533]
29 **Lang H**, Wolf GK, Prokop M, Weimann A, Pichlmayr R, Zoller WG. [Volumetry of circumscribed liver changes with 3-D ultrasound in comparison with 3-D computerized tomography]. *Langenbecks Arch Chir Suppl Kongressbd* 1998; **115**: 1478-1480 [PMID: 9931917]
30 **Marescaux J**, Clément JM, Tassetti V, Koehl C, Cotin S, Russier Y, Mutter D, Delingette H, Ayache N. Virtual reality applied to hepatic surgery simulation: the next revolution. *Ann Surg* 1998; **228**: 627-634 [PMID: 9833800]
31 **Lang H**, Radtke A, Liu C, Sotiropoulos GC, Hindennach M, Schroeder T, Peitgen HO, Broelsch CE. Improved assessment of functional resectability in repeated hepatectomy by computer-assisted operation planning. *Hepatogastroenterology* 2005; **52**: 1645-1648 [PMID: 16334748]
32 **Tu R**, Xia LP, Yu AL, Wu L. Assessment of hepatic functional reserve by cirrhosis grading and liver volume measurement using CT. *World J Gastroenterol* 2007; **13**: 3956-3961 [PMID: 17663509]
33 **Torzilli G**, Montorsi M, Del Fabbro D, Palmisano A, Donadon M, Makuuchi M. Ultrasonographically guided surgical approach to liver tumours involving the hepatic veins close to the caval confluence. *Br J Surg* 2006; **93**: 1238-1246 [PMID: 16953487]
34 **Aoyama M**, Nakayama Y, Awai K, Inomata Y, Yamashita Y. A simple method for accurate liver volume estimation by use of curve-fitting: a pilot study. *Radiol Phys Technol* 2013; **6**: 180-186 [PMID: 23143712 DOI: 10.1007/s12194-012-0186-x]
35 **Itoh S**, Shirabe K, Taketomi A, Morita K, Harimoto N, Tsujita E, Sugimachi K, Yamashita Y, Gion T, Maehara Y. Zero mortality in more than 300 hepatic resections: validity of preoperative volumetric analysis. *Surg Today* 2012; **42**: 435-440 [PMID: 22200757 DOI: 10.1007/s00595-011-0108-2]
36 **Ringe KI**, Ringe BP, von Falck C, Shin HO, Becker T, Pfister ED, Wacker F, Ringe B. Evaluation of living liver donors using contrast enhanced multidetector CT - The radiologists impact on donor selection. *BMC Med Imaging* 2012; **12**: 21 [PMID: 22828359 DOI: 10.1186/1471-2342-12-21]
37 **Lee J**, Won Kim K, Yeon Kim S, Kim B, Lee SJ, Jung Kim H, Seok Lee J, Gyu Lee M, Song GW, Hwang S, Lee SG. Feasibility of semiautomated MR volumetry using gadoxetic acid-enhanced MRI at hepatobiliary phase for living liver donors. *Magn Reson Med* 2013; Epub ahead of print [PMID: 24151218 DOI: 10.1002/mrm.24964]
38 **Zappa M**, Dondero F, Sibert A, Vullierme MP, Belghiti J, Vilgrain V. Liver regeneration at day 7 after right hepatectomy: global and segmental volumetric analysis by using CT. *Radiology* 2009; **252**: 426-432 [PMID: 19703882 DOI: 10.1148/radiol.2522080922]
39 **Ulla M**, Ardiles V, Levy-Yeyati E, Alvarez FA, Spina JC, Garcia-Mónaco RD, De Santibañes E. New surgical strategy to induce liver hypertrophy: role of MDCT-volumetry to monitor and predict liver growth. *Hepatogastroenterology* 2013; **60**: 337-342 [PMID: 23169065]
40 **Vienne A**, Hobeika E, Gouya H, Lapidus N, Fritsch J, Choury AD, Chryssostalis A, Gaudric M, Pelletier G, Buffet C, Chaussade S, Prat F. Prediction of drainage effectiveness during endoscopic stenting of malignant hilar strictures: the role of liver volume assessment. *Gastrointest Endosc* 2010; **72**: 728-735 [PMID: 20883850 DOI: 10.1016/j.gie.2010.06.040]
41 **Kalkmann J**, Forsting M, Stattaus J. Liver volume variations as a parameter to assess therapy response in advanced metastatic liver disease. *Onkologie* 2011; **34**: 30-34 [PMID: 21346382 DOI: 10.1159/000323373]
42 **Kianmanesh R**, Piardi T, Tamby E, Parvanescu A, Bruno O, Palladino E, Bouché O, Msika S, Sommacale D. Liver angulometry: a simple method to estimate liver volume and ratios. *HPB* (Oxford) 2013; **15**: 976-984 [PMID: 23472855 DOI: 10.1111/hpb.12079]
43 **Numminen K**, Sipilä O, Mäkisalo H. Preoperative hepatic 3D models: virtual liver resection using three-dimensional imaging technique. *Eur J Radiol* 2005; **56**: 179-184 [PMID: 15890482]
44 **Niehues SM**, Unger JK, Malinowski M, Neymeyer J, Hamm B, Stockmann M. Liver volume measurement: reason of the difference between in vivo CT-volumetry and intraoperative ex vivo determination and how to cope it. *Eur J Med Res* 2010; **15**: 345-350 [PMID: 20947471]
45 **Karlo C**, Reiner CS, Stolzmann P, Breitenstein S, Marincek B, Weishaupt D, Frauenfelder T. CT- and MRI-based volumetry of resected liver specimen: comparison to intraoperative volume and weight measurements and calculation of conversion factors. *Eur J Radiol* 2010; **75**: e107-e111 [PMID: 19782490 DOI: 10.1016/j.ejrad.2009.09.005]
46 **Lemke AJ**, Brinkmann MJ, Schott T, Niehues SM, Settmacher U, Neuhaus P, Felix R. Living donor right liver lobes: preoperative CT volumetric measurement for calculation of intraoperative weight and volume. *Radiology* 2006; **240**: 736-742 [PMID: 16868277]
47 **Tongyoo A**, Pomfret EA, Pomposelli JJ. Accurate estimation of living donor right hemi-liver volume from portal vein diameter measurement and standard liver volume calculation. *Am J Transplant* 2012; **12**: 1229-1239 [PMID: 22221803 DOI: 10.1111/j.1600-6143.2011.03909.x]
48 **Saeki I**, Tokunaga S, Matsuura T, Hayashida M, Yanagi Y, Taguchi T. A formula for determining the standard liver volume in children: a special reference for neonates and infants. *Pediatr Transplant* 2012; **16**: 244-249 [PMID: 22151603 DOI: 10.1111/j.1399-3046.2011.01624.x]
49 **Li YC**, Hu Y, Zhang MM, Jin XQ, Fan X, Pu CL, Guo CB, Kang Q, Dai XK, Deng YH. Usage of 64-detector-row spiral computed tomography volumetry in preoperative volume prediction in living donor liver transplantation in children. *Pediatr Surg Int* 2011; **27**: 445-449 [PMID: 21258936 DOI: 10.1007/s00383-010-2830-z]
50 **Ribero D**, Amisano M, Bertuzzo F, Langella S, Lo Tesoriere R, Ferrero A, Regge D, Capussotti L. Measured versus estimated total liver volume to preoperatively assess the adequacy of the future liver remnant: which method should we use? *Ann Surg* 2013; **258**: 801-806; discussion 806-807 [PMID: 24045451 DOI: 10.1097/SLA.0000000000000213]
51 **Chun YS**, Ribero D, Abdalla EK, Madoff DC, Mortenson MM, Wei SH, Vauthey JN. Comparison of two methods of future liver remnant volume measurement. *J Gastrointest Surg* 2008; **12**: 123-128 [PMID: 17924174]
52 **Vauthey JN**, Chaoui A, Do KA, Bilimoria MM, Fenstermacher MJ, Charnsangavej C, Hicks M, Alsfasser G, Lauwers G, Hawkins IF, Caridi J. Standardized measurement of the future liver remnant prior to extended liver resection: methodology and clinical associations. *Surgery* 2000; **127**: 512-519 [PMID: 10819059]
53 **Müller SA**, Bläuer K, Kremer M, Thorn M, Mehrabi A, Meinzer HP, Hinz U, Metzger J, Büchler MW, Schmied BM. Exact CT-based liver volume calculation including nonmetabolic liver tissue in three-dimensional liver reconstruction. *J Surg Res* 2010; **160**: 236-243 [PMID: 19765736 DOI: 10.1016/j.jss.2009.04.050]
54 **Kayashima H**, Taketomi A, Yonemura Y, Ijichi H, Harada N,

Yoshizumi T, Soejima Y, Yoshimitsu K, Maehara Y. Accuracy of an age-adjusted formula in assessing the graft volume in living donor liver transplantation. *Liver Transpl* 2008; **14**: 1366-1371 [PMID: 18756495 DOI: 10.1002/lt.21547]

55 **Soyer P**, Roche A, Elias D, Levesque M. Hepatic metastases from colorectal cancer: influence of hepatic volumetric analysis on surgical decision making. *Radiology* 1992; **184**: 695-697 [PMID: 1509051]

56 **Henderson JM**, Heymsfield SB, Horowitz J, Kutner MH. Measurement of liver and spleen volume by computed tomography. Assessment of reproducibility and changes found following a selective distal splenorenal shunt. *Radiology* 1981; **141**: 525-527 [PMID: 6974875]

57 **Sandrasegaran K**, Kwo PW, DiGirolamo D, Stockberger SM, Cummings OW, Kopecky KK. Measurement of liver volume using spiral CT and the curved line and cubic spline algorithms: reproducibility and interobserver variation. *Abdom Imaging* 1999; **24**: 61-65 [PMID: 9933675]

58 **Gao L**, Heath DG, Kuszyk BS, Fishman EK. Automatic liver segmentation technique for three-dimensional visualization of CT data. *Radiology* 1996; **201**: 359-364 [PMID: 8888223]

59 **Suzuki K**, Epstein ML, Kohlbrenner R, Garg S, Hori M, Oto A, Baron RL. Quantitative radiology: automated CT liver volumetry compared with interactive volumetry and manual volumetry. *AJR Am J Roentgenol* 2011; **197**: W706-W712 [PMID: 21940543 DOI: 10.2214/AJR.10.5958]

60 **Radtke A**, Sotiropoulos GC, Nadalin S, Molmenti EP, Schroeder T, Saner FH, Sgourakis G, Cicinnati VR, Valentin-Gamazo C, Broelsch CE, Malago M, Lang H. Preoperative volume prediction in adult live donor liver transplantation: 3-D CT volumetry approach to prevent miscalculations. *Eur J Med Res* 2008; **13**: 319-326 [PMID: 18700188]

61 **Nakayama Y**, Li Q, Katsuragawa S, Ikeda R, Hiai Y, Awai K, Kusunoki S, Yamashita Y, Okajima H, Inomata Y, Doi K. Automated hepatic volumetry for living related liver transplantation at multisection CT. *Radiology* 2006; **240**: 743-748 [PMID: 16857979]

62 **Soyer P**, Sirol M, Dohan A, Gayat E, Placé V, Hristova L, Hamzi L, Boudiaf M. Hepatic height on coronal computed tomography images predicts total liver volume in European adults without liver disease. *Dig Dis Sci* 2012; **57**: 1692-1697 [PMID: 22314346 DOI: 10.1007/s10620-012-2077-8]

63 **Kim KW**, Lee J, Lee H, Jeong WK, Won HJ, Shin YM, Jung DH, Park JI, Song GW, Ha TY, Moon DB, Kim KH, Ahn CS, Hwang S, Lee SG. Right lobe estimated blood-free weight for living donor liver transplantation: accuracy of automated blood-free CT volumetry--preliminary results. *Radiology* 2010; **256**: 433-440 [PMID: 20551185 DOI: 10.1148/radiol.10091897]

64 **Hori M**, Suzuki K, Epstein ML, Baron RL. Computed tomography liver volumetry using 3-dimensional image data in living donor liver transplantation: effects of the slice thickness on the volume calculation. *Liver Transpl* 2011; **17**: 1427-1436 [PMID: 21850689 DOI: 10.1002/lt.22419]

65 **Luciani A**, Rusko L, Baranes L, Pichon E, Loze B, Deux JF, Laurent A, Tran-Van-Nhieu J, Rahmouni A. Automated liver volumetry in orthotopic liver transplantation using multiphase acquisitions on MDCT. *AJR Am J Roentgenol* 2012; **198**: W568-W574 [PMID: 22623572 DOI: 10.2214/AJR.11.7468]

66 **Suzuki K**, Huynh HT, Liu Y, Calabrese D, Zhou K, Oto A, Hori M. Computerized segmentation of liver in hepatic CT and MRI by means of level-set geodesic active contouring. *Conf Proc IEEE Eng Med Biol Soc* 2013; **2013**: 2984-2987 [PMID: 24110354 DOI: 10.1109/EMBC.2013.6610167]

67 **Suzuki K**, Kohlbrenner R, Epstein ML, Obajuluwa AM, Xu J, Hori M. Computer-aided measurement of liver volumes in CT by means of geodesic active contour segmentation coupled with level-set algorithms. *Med Phys* 2010; **37**: 2159-2166 [PMID: 20527550]

68 **Zhou JY**, Wong DW, Ding F, Venkatesh SK, Tian Q, Qi YY, Xiong W, Liu JJ, Leow WK. Liver tumour segmentation using contrast-enhanced multi-detector CT data: performance benchmarking of three semiautomated methods. *Eur Radiol* 2010; **20**: 1738-1748 [PMID: 20157817 DOI: 10.1007/s00330-010-1712-z]

69 **Dello SA**, Stoot JH, van Stiphout RS, Bloemen JG, Wigmore SJ, Dejong CH, van Dam RM. Prospective volumetric assessment of the liver on a personal computer by nonradiologists prior to partial hepatectomy. *World J Surg* 2011; **35**: 386-392 [PMID: 21136056 DOI: 10.1007/s00268-010-0877-6]

70 **van der Vorst JR**, van Dam RM, van Stiphout RS, van den Broek MA, Hollander IH, Kessels AG, Dejong CH. Virtual liver resection and volumetric analysis of the future liver remnant using open source image processing software. *World J Surg* 2010; **34**: 2426-2433 [PMID: 20652701 DOI: 10.1007/s00268-010-0663-5]

71 **Lu Y**, Wu Z, Liu C, Wang HH. Hepatic volumetry with PhotoShop in personal computer. *Hepatobiliary Pancreat Dis Int* 2004; **3**: 82-85 [PMID: 14969844]

72 **Van Thiel DH**, Hagler NG, Schade RR, Skolnick ML, Heyl AP, Rosenblum E, Gavaler JS, Penkrot RJ. In vivo hepatic volume determination using sonography and computed tomography. Validation and a comparison of the two techniques. *Gastroenterology* 1985; **88**: 1812-1817 [PMID: 3888769]

P- Reviewers: Henninger B, Li JJ **S- Editor**: Wen LL
L- Editor: O'Neill M **E- Editor**: Liu SQ

World Journal of Radiology

Online Submissions: http://www.wjgnet.com/esps/
bpgoffice@wjgnet.com
doi:10.4329/wjr.v6.i4.72

World J Radiol 2014 April 28; 6(4): 72-81
ISSN 1949-8470 (online)

TOPIC HIGHLIGHT

WJR 6th Anniversary Special Issues (8): fMRI

Clinical decision support systems for brain tumor characterization using advanced magnetic resonance imaging techniques

Evangelia Tsolaki, Evanthia Kousi, Patricia Svolos, Efthychia Kapsalaki, Kyriaki Theodorou, Constastine Kappas, Ioannis Tsougos

Evangelia Tsolaki, Evanthia Kousi, Patricia Svolos, Kyriaki Theodorou, Constastine Kappas, Ioannis Tsougos, Medical Physics Department, University of Thessaly, Biopolis, 41110 Larissa, Greece
Efthychia Kapsalaki, Department of Radiology, University Hospital of Larissa, Biopolis, 41110 Larissa, Greece
Author contributions: Tsolaki E and Tsougos I designed the research; Tsolaki E, Kousi E and Svolos P performed the research; Tsolaki E, Kousi E and Tsougos I wrote the paper; Kapsalaki E, Theodorou K and Kappas C performed a critical review and data analysis.
Correspondence to: Ioannis Tsougos, MSc, PhD, Assistant Professor in Medical Physics Department, University of Thessaly, Panepistimiou 2, Biopolis, 41110 Larissa, Greece. tsougos@med.uth.gr
Telephone: +30-241-3501863 Fax: +30-241-3501863
Received: November 12, 2013 Revised: January 23, 2014
Accepted: March 17, 2014
Published online: April 28, 2014

Abstract

In recent years, advanced magnetic resonance imaging (MRI) techniques, such as magnetic resonance spectroscopy, diffusion weighted imaging, diffusion tensor imaging and perfusion weighted imaging have been used in order to resolve demanding diagnostic problems such as brain tumor characterization and grading, as these techniques offer a more detailed and non-invasive evaluation of the area under study. In the last decade a great effort has been made to import and utilize intelligent systems in the so-called clinical decision support systems (CDSS) for automatic processing, classification, evaluation and representation of MRI data in order for advanced MRI techniques to become a part of the clinical routine, since the amount of data from the aforementioned techniques has gradually increased. Hence, the purpose of the current review article is two-fold. The first is to review and evaluate the progress that has been made towards the utilization of CDSS based on data from advanced MRI techniques. The second is to analyze and propose the future work that has to be done, based on the existing problems and challenges, especially taking into account the new imaging techniques and parameters that can be introduced into intelligent systems to significantly improve their diagnostic specificity and clinical application.

Key words: Decision support systems; Magnetic resonance imaging; Magnetic resonance spectroscopy; Diffusion weighted imaging; Diffusion tensor imaging; Perfusion weighted imaging; Pattern recognition

Core tip: The quantification of the imaging profile of brain neoplasms by combining conventional magnetic resonance imaging and advanced imaging techniques introduces critical underlying pathophysiological information which seems to be the key to success. Thus, it is evident that the pursuit of this goal should be oriented towards the development of decision support software that will utilize large amounts of clinical data with extremely significant diagnostic value which often remain unexploited, hence resulting in a more valid and precise method of differential diagnosis and the selection of the most successful treatment scheme.

Tsolaki E, Kousi E, Svolos P, Kapsalaki E, Theodorou K, Kappas C, Tsougos I. Clinical decision support systems for brain tumor characterization using advanced magnetic resonance imaging techniques. *World J Radiol* 2014; 6(4): 72-81 Available from:

URL: http://www.wjgnet.com/1949-8470/full/v6/i4/72.htm DOI: http://dx.doi.org/10.4329/wjr.v6.i4.72

INTRODUCTION

The introduction of magnetic resonance imaging (MRI) systems has induced revolutionary changes in the medical imaging field and has contributed much on a diagnostic and therapeutic level. In recent years, there has been a shift towards advanced MRI techniques, such as magnetic resonance spectroscopy (^{1}H-MRS), diffusion weighted imaging (DWI), diffusion tensor imaging (DTI) and perfusion weighted imaging (PWI), in order to resolve demanding diagnostic problems. These techniques offer a more detailed and non-invasive evaluation of brain tumors[1-3] and have added incremental diagnostic information regarding brain tumor characterization over conventional MRI alone[4,5].

^{1}H-MRS has been studied for more than a decade as a promising diagnostic tool for a variety of pathologies. If coupled with the morphological features provided by MRI techniques, it can provide accurate identification and quantification of biologically important chemical compounds in soft tissue, thus increasing the understanding of the underlying pathologies. There have been numerous studies that indicate the significant contribution of ^{1}H-MRS for the characterization of brain tumors[6-8], and fewer studies have concentrated on pediatric tumors[9,10]. Even if ^{1}H-MRS does not change the final diagnosis, it may significantly rule out a differential diagnosis and thereby reduce the need for biopsy. However, challenges still remain in brain lesion classification regarding the use of ^{1}H-MRS. The most important one is the limited number of available spectra per lesion type which may induce difficulties in reaching specific conclusions. Moreover, the simultaneous analysis and evaluation of multiple spectroscopic parameters is a time-consuming process, required specific expertise and may not be practical in a clinical environment.

In addition to ^{1}H-MRS, the other advanced MRI techniques, DWI[11], DTI[12] and PWI have already found increasing use in the evaluation of cerebral tumors and still remain a subject of intense research[1,13,14]. DWI probes local tissue microstructure reflected by the freedom of microscopic motion of water molecules and provides a sensitive means to detect alterations in the integrity of white matter structures, while PWI facilitates the prediction of brain lesion progression in conjunction with histopathology[15].

It is evident that the continuously developing magnetic resonance systems have transformed from pure imaging systems to extremely precise metric systems that produce a considerable amount of numerical data that originate from the application of the aforementioned advanced MRI techniques. Taking into account the complex structure of the clinical data and the difficulty of brain tumor discrimination due to their intrinsic heterogeneity, the research community has shifted towards the application of machine learning algorithms, in order to assign different tissue types to specific patterns. Several studies have previously investigated the differentiation of brain tumors in adults based on machine learning techniques[16-20], as well as the discrimination of pediatric brain tumors[21,22].

By importing and utilizing these intelligent techniques in a clinical decision support system (CDSS), several advanced MRI techniques may become a part of the clinical routine in order to resolve demanding diagnostic problems. CDSSs based on pattern recognition have been widely accepted in medical applications, due to their capability for optimization, flexibility, accuracy for predictive inference and interpretability[23].

A CDSS according to van Bemmel *et al*[24] is defined as any piece of software that takes, as input data, the information about a clinical situation and produces, as output, the inferences regarding the clinical situation that can assist practitioners with their decision-making, and that would be judged as "intelligent" by the program's users.

Regarding brain tumor diagnosis, great efforts have been made in the implementation of intelligent systems for brain tumor differentiation, automatic processing, classification, evaluation and representation of clinical data. This effort is facilitated further by the evolvement of computer power that is available for the processing needs of these systems.

The purpose of the present study is to provide a literature review that focuses in the development of the CDSS, based on advanced MRI techniques for brain tumor characterization: (1) the first part provides an overview and an extensive description of the already developed CDSSs; and (2) in the second part, the study concludes to future objectives concerning the development of CDSSs for brain lesion characterization.

LITERATURE REVIEW

A thorough literature review was executed during the period 2000-2013. Initially, the research was limited to CDSS for brain tumor discrimination and the inclusion criterion was the kind of biomedical data that was utilized for their development. Specifically, the literature review was focused on the use of ^{1}H-MRS, DWI, DTI and PWI data in CDSS development. To the best of our knowledge, up to this point none of the CDSS was developed using features extracted from DWI, DTI or PWI techniques. However, the interest of the scientific community focused on the use of spectroscopic data in order to develop these systems. Thus, the research identified articles that corresponded to clinical systems that were implemented using chemical shift imaging (CSI) or single voxel MRS[25,26]. Furthermore, a number of articles and congress proceedings regarding the usability and effectiveness of these CDSS were collected.

Table 1 Validation results of the clinical decision support systems based on chemical shift imaging data

Ref.	Voxel assignment	Accuracy
De Edelenyi *et al*[27]	Low-grade gliomas	92.9%
	High-grade gliomas	79.16%
	Metastasis	60%
	Meningiomas	100%
	Necrosis	100%
	Healthy tissue	100%
	Cerebrospinal fluid	100%
Simonetti *et al*[29]	Healthy tissue	100%
	Cerospinal fluid	97%
	Glioma grade Ⅱ	83%
	Glioma grade Ⅲ	88%
	Glioma grade Ⅳ	100%
Luts *et al*[32]	Glioma Ⅱ	66.6%
	Glioma Ⅱ / Ⅲ	100%
	Glioma Ⅳ	100%
	Meningioma	100%
McKnight *et al*[28]	Low grade gliomas *vs* grade Ⅲ	89%
Li *et al*[34]	Glioblastoma multiforme	100%
	Glioma Ⅱ	100%

BRAIN TUMOR CDSS

CSI MRS data

The research revealed eight studies focused on the development of DSS based on proton MRSI, in order to gain information about the size, shape and the heterogeneity of the tumor. All of these studies used statistical or classification techniques in order to assign each voxel of the spectra to a specific tumor type and grade.

De Edelenyi *et al*[27] presented the first CDSS for brain tumor diagnosis focusing on CSI data. The authors proposed a method to create a "nosologic image" in order to extract information about the brain tumor type and the grade based on long TE ^{1}H-MRSI data, since biopsy does not always reveal the real grade of the tumor, due to tumor heterogeneity. Regarding this heterogeneity, each voxel of the spectroscopic image was colored according to the assigned histopathologic class (low or high grade glioma, metastasis and meningioma). However, McKnight *et al*[28] followed a different approach to extract image maps of long TE MV spectral data. Regarding the N-acetylaspartate and Cho levels of the spectrum, they investigated a score that was used to differentiate areas that present normal metabolite levels from regions that correspond to gliomas. Then, they utilized this score as a degree of abnormality throughout the lesion area. Afterwards, Simonetti *et al*[29] extracted nosologic images based not only to metabolic information but also exploiting the image variables of each voxel. They investigated the overlap between different classes (healthy, cerebrospinal fluid, grade Ⅱ, grade Ⅲ, grade Ⅳ) in the featured space, and constructed a probability map that corresponded to the probabilities of classification based on MRI and MRS data. Similarly to De Edelenyi *et al*[27], Simonetti *et al*[29] focused only on the metabolite and image characteristics of each voxel, ignoring the spatial information of the area under study. De Vos *et al*[30] used Short TE spectra to create nosologic images. They applied canonical correlation analysis in order to investigate the tumor type and the heterogeneity of the region of interest. Similarly, Laudadio *et al*[31] applied canonical correlation analysis to 2-dimensional turbo MRSI data in order to combine spectra and spatial MRS information. The resulting correlation maps were used to construct nosologic images where all the detected tissue types were visualized. From the same research group, Luts *et al*[32] proposed a new method to generate nosologic images of the brain comparing to previous approaches. They used digital brain atlases presented by Prastawa *et al*[33] in order to investigate the incremental value of MRI over MRSI data. They added subject-specific abnormal tissue for image segmentation purposes, and the resulting framework was more flexible and able to exploit spatial information more efficiently, leading to improved nosologic images. Contrary to previous studies, Li *et al*[34] used unsupervised classification methods to construct nosologic images, in order to overcome the need of large datasets to train classifiers. Another difference was that they provided an error map along with the nosologic image in order to underline spectra variations due to tumor inhomogeneity.

The validation results of the majority of the clinical systems described previously are presented in Table 1.

Single voxel MRS data

Regarding the use of single voxel MRS data for CDSS development, during the last 10 years, four projects, the International Network for Pattern Recognition of Tumors Using Magnetic Resonance (INTERPRET) (2000-2002), eTUMOUR (2004-2009), HealthAgents (2005-2008) and CURIAM BT (2004-2010), were developed.

INTERPRET

INTERPRET was the outcome of a multicenter European collaboration[35,36] that was funded under the 5th EU Framework Programme IST-1999-10310. A computer-based CDSS was developed in order to enable clinicians who have minimum knowledge of the MR spectrum to evaluate MR spectra and to discriminate between different brain tumors. During the INTERPRET development, one significant achievement was the creation of an important repository of brain tumors that contained 304 histopathological validated Short TE cases low grade gliomas [astrocytomas, oligodendrogliomas, oligoastrocytomas World Health Organization (WHO) grade Ⅱ], meningiomas (WHO grade Ⅰ and Ⅱ) and high grade malignant tumors (glioblastomas, metastases). Another important achievement was the definition of a data acquisition protocol to ensure the compatibility between the MRS data coming from different clinical collaborative centers as well as the quality control protocol development, in order to define the quality requirements that MR spectra should fulfill.

Furthermore, a single voxel INTERPRET graphical user interface (GUI) was developed, providing easy access to the spectra database, to images and clinical informa-

Table 2 Validation results of the clinical decision support systems based on single voxel data

Ref.	CDSS	Differentiation problem	Accuracy				Supportive raw files
			Short TE		Long TE	Short + Long TE	
Pérez-Ruiz *et al*[38]	INTERRET	Low grade meningiomas *vs* low grade glial tumors	94[a]	89[b] 89[c]	83[b]	84[c] 89[c]	
		Pseudotumoural disease[d] *vs* tumors[e] *vs* normal brain		86[c]	81[c]	92[c]	
García-Gómez *et al*[41]	eTUMOUR	Low grade glioma *vs* high grade tumor		92	84	92	1.5 Tesla MRS data of Philips (sdat/spar) GE up to 9X (SAGE Pxxxx with an shf or sdf/shf) siemens scanners (numaris 4) jMRUI[58] text file
		Meningioma *vs* glioma/Met		92	78	94	
		Low men *vs* glioma/Met *vs* low grade glioma		87	75	90	
Sáez *et al*[44]	HealthAgents	Aggressive tumor *vs* meningioma *vs* low grade glial		94	-		
		Meningioma *vs* metastasis		91	-		
		High grade tumor *vs* low grade tumor		87	68 (ch)		
		Affected tissue *vs* non affected tissue		99	-		
		Tumor *vs* non tumor		97	-		
		Aggressive tumor *vs* non aggressive tumor		81	72 (ch)		
		Glioma *vs* embryonal tumor		-	72 (ch)		
		Glioblastoma *vs* low grade glioma		84	-		
		Glioblastoma *vs* meningioma		91	-		
		Meningioma *vs* low grade glioma		92	-		
		Metastasis *vs* low grade glioma		85	-		
Vicente *et al*[46]	CURIAM BT	Aggressive tumor *vs* non aggressive tumor		85	87 (ch)		1.5 or 3 Tesla MRS data of different manufactures (Siemens, GE, Philips) by means of jMRUI[58] and jDMS[36]
		Pilocytic astrocytoma/ependymoma grade Ⅱ *vs* medulloblastoma		88 (ch)	85 (ch)	89 (ch)	
		Pilocytic astrocytoma *vs* medulloblastoma		92 (ch)	94 (ch)	95 (ch)	
		Pilocytic astrocytoma *vs* ependymoma grade Ⅱ *vs* medulloblastoma		76 (ch)	69 (ch)	92 (ch)	

It is indicated where the classification accuracy corresponds to classifier trained on pediatric tumor data (ch). [a]International Network for Pattern Recognition of Tumors Using Magnetic Resonance (INTERPRET) version 1.1; [b]INTERPRET version 2.0; [c]INTERPRET version 3.0; [d]Pseudotumoural disease: Acute infarct, multiple sclerosis, acute disseminated encephalomyelitis, and no specific pseudotumoral disease; eTumors: Astrocytoma World Health Organization (WHO) grade Ⅱ, oligodendroglioma WHO grade Ⅱ, oligoastrocytoma WHO grade Ⅱ, astrocytoma WHO grade Ⅲ, oligoastrocytoma WHO grade Ⅲ. CDSS: Clinical decision support systems; MRS: Magnetic resonance spectroscopy; MRUI: Magnetic Resonance User Interface.

tion from all the validated cases of human brain tumors. It was designed to provide the display of classification plots, which is useful for the automatic classification of tumor spectra[37]. The differentiation between different tumor groups was achieved by plotting the boundaries that were defined by the bisectors between the centroids of each class[38]. The users could enter their own spectrum, position it automatically among the tumor groups of the system and compare it with other spectra.

Until 2010 many improvements have been gradually released in successive versions and can be categorized in three different aspects: GUI enhancements, increased analysis capabilities, and data quality and assessment checks[38]. Specifically in the last version, an embedded database was developed for the permanent storage of the data into the system, more MRS data were supported compared to the previous versions (Short TE, Long TE and concatenated Short TE and Long TE Spectra) and six more classifiers were embedded to the system. Hence, the final version of INTERPRET not only offers the ability to differentiate common tumor types as in its first release, but also to differentiate among tumoral and pseudotumoral diseases (acute infarct, multiple sclerosis, acute disseminated encephalomyelitis). To address the latter classification problem, the metabolite ratios of the spectra were also used. The evaluation results of the different versions of INTERPRET CDSS are shown to Table 2.

eTUMOUR

Another European project eTUMOUR took up the research on the development of CDSS[39]. A more complex CDSS was developed that combined single voxel and CSI MRS data. The eTUMOUR CDSS upgraded and facilitated the clinical application of MRS in adult and pediatric brain tumor diagnosis, prognosis and treatment selection by using a combination of histology results, high resolution metabolic profiles (HR-MAS) and transcriptomic (DNA micro-arrays) *ex vivo* data to define the classification outcome[40]. Regarding the acquisition and quality control procedure, the experience obtained from the INTERPRET project was used, whereas suitable protocols for the techniques of tissue analysis (HR-MAS, DNA microarrays and micro-RNA) were defined.

A web-based database (eTDB) was created, which was able to manage a wide range of data types such as clinical information, histological images, MRI, single voxel, MRSI, HR-MAS and DNA microarray data. This database comprised a complete and detailed GUI and also a structure for online uploading and downloading data *via* the web.

A user friendly computer aided decision system (CADS) DSS was developed and tested in eTUMOUR project.

The embedded classifiers were trained to solve three different discrimination problems (meningioma *vs* non-meningioma, aggressive tumor *vs* low grade glial and meningioma *vs* aggressive tumor *vs* low grade glial) using short time echo spectrum, long time echo spectrum and combination of both spectra (Table 2). Furthermore, the design of the DSS provided a comparative analysis with the average spectra of 12 standard brain tumor types of an unknown brain tumor. During the classification procedure the assigned class as well as the posterior probabilities of each class were displayed to the system[39,41].

HealthAgents

HealthAgents[42] was a distributed DSS (d-DSS) built upon INTERPRET and eTUMOUR projects. The great difference of this project was its architectural structure since it was based on agent-based architecture in order to decentralize the process of brain tumor differentiation in a distributed decision support framework that supports data partitioning and sharing[43]. Since the accumulation of a sufficient number of cases for each tumor type or less common adult or childhood tumors was a very difficult and time consuming procedure, a collaborative network of different medical centers was constructed that contributed to the development of a repository of brain tumors, used for the training of robust classifiers for brain tumor differentiation.

The user, utilizes a local web-based GUI to enter the clinical data of a patient into the system and to request the appropriate classifiers from the network. These classifiers could be located anywhere on the collaborative HealthAgents network that consisted of different medical centers with their local existing databases of cases and their classifiers. Finally, the system would suggest the appropriate classifiers and indicate their specific location. Furthermore, a ranking tool was provided to the user, since many different classifiers coexisted in the system, in order to identify the classifiers that are more suitable for the diagnosis of particular case, to rank the obtained results from a set of classifiers and to solve possible conflicts between classifiers, by giving contradictory answers, which could occur when a test case was close to a decision boundary in one or more classifiers[44].

Regarding the classification framework of the HealthAgents DSS its primary functionality was based on the INTERPRET DSS system. Until 2011, 25 classifiers were embedded and shared the system for the differentiation of aggressive tumors, like glioblastomas and metastases, benign meningiomas and low-glial mixture, such as astrocytomas grade Ⅱ, oligodendrogliomas and oligoastrocytomas. The classification procedure was based on short time echo MRS data, long time echo MRS data and on the combination of them. The optimum classification results are presented to Table 2.

Curiam BT

Curiam BT[45,46] was developed in parallel to eTUMOUR and HealthAgents projects. CURIAM BT supported any kind of metabolic data either on short or long TE or both of different manufactures. Regarding the classification framework of this clinical system, it was able to determine the aggressiveness of a brain tumor in adults (non aggressive: grades Ⅰ and Ⅱ *vs* aggressive: grade Ⅲ and Ⅳ) and to discriminate among the three most common pediatric brain tumors such as ependymoma grade Ⅱ, pilocytic astrocytoma and medulloblastoma. Furthermore, compared with previous systems an additional opportunity was included, according to which the user could embed new classifiers to the system. Similar to the ranking tool in HealthAgents DSS, the audit and similarity methods were incorporated to the system to address the generalization ability of the coexisting classifiers. These methods proved to be significant as they provided the clinicians with the appropriate classifiers set regarding each differentiation problem and a specificity score of each classifier that determines its discrimination accuracy over time.

USABILITY AND EVALUATION OF CDSS

Regarding the evaluation of the single voxel CDSSs, there are several studies that reported their effectiveness and usability in the classification of different brain tumors during the clinical routine. These studies demonstrate the accuracy values that CDSSs present in various diagnostic problems, evaluate their contribution in combination with other diagnostic outcomes and survey CDSS usability regarding their user friendly module and acceptance by the clinical community. Considering the CDSSs that were based on CSI data, more research is needed since there is not a sufficient number of articles to demonstrate the overall contribution of these clinical systems to the clinical routine.

Fellows *et al*[47] investigated the discrimination ability of INTERPRET version 2.0 in order to differentiate high and low grade tumors. The classification outcome of the system was compared with the neuroradiological tissue diagnosis and the conclusion of the spectroscopists. The results did not reveal significant differentiations between the accuracy levels of each participating modality.

INTERPRET version 3.0 proved to be superior for the characterization of grade Ⅲ astrocytomas when compared to the spectroscopic and the radiologists' evaluation[48].

Regarding the clinical evaluation of eTUMOUR, an agreement of 79.1% was obtained between the DSS outcome and the radiologic diagnosis. This rate increased up to 88.4% when the averaged spectra from DSS were used for brain tumor classification. When the CDSS, averaged spectra and radiologic findings were compared with the histopathological diagnosis, agreement scores of 76.7%, 79.1% and 81.4% were respectively achieved[49].

When the CDSS results were compared with MRI, the overall percentage of correct predictions were 82.2% and 78.48%, respectively. Furthermore, the CDSS classification outcome was also compared with the corresponding outcome of MRI for the differentiation of

low grade gliomas, high grade gliomas and meningiomas. Specifically, the sensitivity and specificity values in low *vs* high grade gliomas classification problem, CDSS proved superior to the MRI corresponding values. Finally, the usefulness and applicability of the CADS was rated 86% and 71%, respectively[50].

Regarding the HealthAgents CDSS, an evaluation about its incremental diagnostic value was executed, and consequently 26 expert physicians were interviewed. As an overall response, they believed that the use of the CDSS would be beneficial for improving the quality of their brain tumor diagnoses. In addition, they considered the system easy to use, which is an important point in a DSS, especially in a clinical environment[44].

When the evaluation of CURIAM BT was carried out, it reached 71% and 85% regarding the user's perspective on its usefulness and convenience, respectively[51]. A comparing test was also executed in order to evaluate the contribution of CURIAM BT in the clinical routine. In that case, no significant differences were observed between the established diagnosis when conventional MRI, DWI and PWI were used, and the diagnosis derived from the above techniques combined with CDSS. Only in the case of high grade and low grade gliomas, did the observed differences reach 70%. Hence, a further evaluation should be implemented in order to investigate the CURIAM BT contribution in different diagnostic problems.

FUTURE PERSPECTIVES

One should consider CDSS as a supportive tool by providing additional information about the patient's state of health from which the clinician may establish a more educated and informed decision. As described in the "Usability and evaluation of CDSS" section, most of the studies proved the efficacy of the additional information that CDSS provide regarding improvements in clinical outcome. However, it is also evident that further evaluation should be implemented in order to investigate the CDSS contribution in different diagnostic problems. In addition, CDSS development involves much more than just the implementation of a software application. It requires adaptation by clinicians to use and engage in the refinement of CDSS both as a process and as a tool, as we move toward the goal of healthcare delivery that is consistent, effective, and of high quality[52]. In order to accomplish the above objectives and to reinforce the application of CDSS in clinical routine, there are a number of future perspectives that should be implemented.

Regarding the classification framework of the clinical systems, there are two significant issues which arise. First, the improvement of the classification performance and second, the inclusion of more difficult differential diagnostic problems such as glioblastomas *vs* solitary metastasis. Hence, the retraining of the existing classifiers and the development of new ones, are necessary in order to optimize the classification performance and to extend the discrimination ability of the CDSS.

Until now all the CDSSs developed for brain tumor differentiation are based on static classification methods. The use of static classifiers results in an implicit assumption that the learning procedure stops when the training set has been processed. The performance of a classifier strongly depends on the size of the training set for each class. Nevertheless, the accumulation of biomedical data is often a time-consuming and expensive procedure, and hence it may be not practical, especially in cases of uncommon cerebral pathologies like abscesses and lymphomas or pediatric brain tumors. In such cases, the implementation of incremental learning algorithms is a promising solution for clinical environments. Tortajada *et al*[53] evaluated the performance of an incremental classifier based on single voxel Short TE spectra in comparison to static classifiers. The results revealed that the classification performance was improved when the incremental classifiers were used comparing to performance of the static classifies.

Another future objective is to incorporate metabolic data from both ^{1}H-MRS techniques (single voxel-CSI) into the classification framework of a DSS. The two techniques can be utilized simultaneously in order to investigate tumor heterogeneity whereas; the advantages of each spectroscopic technique can be exploited. Therefore, the metabolic characteristics of different tumor regions could be summarized into one image and the corresponding biochemical compounds can be studied. Hence, the spatial and the quantitative data of the spectrum will be used for an overall evaluation of the tumor. The complementary use of the spectroscopic techniques may contribute to the optimization and the accuracy of the preoperative diagnosis, and it may increase the understanding of the underlying pathologies.

An important future aspect is to enrich the DSS datasets with metabolic data from the peritumoral and contralateral regions regarding the brain tumor under study. With this perspective, the pattern recognition methods will be extended towards a more accurate differentiation scheme of brain tumors.

Growing intracranial neoplasms exhibit various effects in their peritumoral area. According to Chernov *et al*[54] lactate-producing neoplasms are associated with more prominent reduction of the relative NAA content in the surrounding cerebral tissue, independently on the presence or absence of any other factor. According to Fan *et al*[55] both a high Cho peak and elevated Cho/Cr ratio were found in the peritumoral regions of high-grade gliomas, but not in metastases. This suggests that the infiltration of adjacent brain tissue by tumor is a unique feature of high-grade glioma.

Another plan is to incorporate quantitative data from other MR-based methodologies. Di-Costanzo *et al*[56] showed that in the case of brain tumor classification, when ^{1}H-MRS parameters were considered as features, 83.3% of brain tumors were correctly classified. Whereas, when ^{1}H-MRS variables were combined with relative cerebral blood volume (rCBV) values from perfusion MRI, a 100% classification accuracy between high- and low-grade gliomas was achieved. They also showed that in a

peri-enhancing tumor region 73.7% of the cases were correctly classified when considering only ^{1}H-MRSI variables, 84.2% when considering ^{1}H-MRSI variables and apparent diffusion coefficient (ADC), and 89.5% when considering ^{1}H-MRSI variables, ADC and rCBV. Zonari *et al*[57] achieved 80% sensitivity and 78.6% specificity when using rCBV parameter alone in grading cerebral neoplasms, and when combined with ^{1}H-MRS the sensitivity increased to 87.7% and specificity dropped to 76.2%.

Hence, it is evident that the continuous progress of imaging systems has induced revolutionary changes in the medical imaging field and has contributed utmost on a diagnostic and therapeutic level. The most important aspect however is that the continuous development of imaging techniques have transformed these modalities from conventional imaging to high-level metric systems, which may provide a quite large amount of quantitative information.

These large amounts of numeric data with an extremely significant diagnostic value may often remain unexploited during the clinical routine. The main reason for this is that the simultaneous analysis and evaluation of multiple parameters, is a time consuming process, requires specific expertise and may not be feasible during the clinical routine. It is prudent to mention that the available clinical time per patient may be estimated at about 30 min, while the process and evaluation of data from MRS and DTI usually takes more than 1 h. Especially when a specialized medical physicist for data manipulation is unavailable, these techniques are often handled by radiologists under a qualitative perspective rather than quantitative, which may lead to a biased differential diagnosis.

Therefore, an automatic evaluation of these data and a rapid display of the results are the minimum requirement during the clinical interpretation of an examination that will lead to a better clinical management of the patients, since the evaluation of the data will be done in an easier, and more effective way, which would ultimately lead to cost effectiveness by avoiding misdiagnosed cases. Towards this direction, the objective and future perspective would be to design and develop a CDSS, using incremental machine learning methods, based on all numeric data from the aforementioned advanced imaging techniques. The system should integrate and combine all the available metabolic, diffusion and perfusion data. The hypothesis is that the combination of multiple data from the aforementioned imaging modalities is expected to optimize the differential diagnosis of brain pathologies, which will be eventually beneficiary for tailored patient treatment.

Hence, these kind of systems should be specifically designed in such a way that the user (that is: radiologist, medical physicist and in general neuroscientists), with minimum knowledge of pattern recognition analysis, will be able to: (1) categorize and illustrate the clinical data on a single template in order to ensure that the data will not be dispersed; (2) perform a fully automated pattern recognition analysis towards the optimum differential diagnosis; (3) quantify the degree of uncertainty in the prediction of ambiguous diagnostic problems by offering a diagnostic orientation; and (4) use the system as a supportive tool for the selection of the most appropriate treatment strategy and the most successful treatment scheme.

From our personal experience, it should be stressed that a CDSS by no means substitutes for the expert's diagnostic decision, but rather supports the clinician by evaluating simultaneously a large amount of complicated MR data. Thorough analysis and evaluation of these data requires additional time, which exceeds by far the available clinical time per patient, hence this information may remain unexploited.

Furthermore, despite the good discrimination ability of the embedded classification schemes, it should be emphasized that the decision-making process with the use of a clinical decision system should be a procedure of two individual parts. The first part should include the classification result or a good orientation towards a clinical outcome, based on the evaluation of quantitative MRI data and the second part should involve the co-evaluation of the aforementioned result with all the available diagnostic and imaging information. Under these perspectives, a well designed CDSS may be used as an assistant diagnostic tool which can be implemented into the clinical routine and substantially aid the interpretation of an exam and optimize decision making.

CONCLUSION

Diagnosis and consequently treatment of brain neoplasms may greatly benefit from the introduction and utilization of intelligent systems in the form of CDSS for automatic processing, classification, evaluation and representation of the spectroscopic data as part of the clinical routine. Major progress has been made in the last few years towards this direction, as several systems exist and are continuously developing. Nevertheless, the quantification of the imaging profile of neoplasms by combining conventional MRI and advance imaging techniques (MRS, DWI, DTI and PWI) introduces critical underlying pathophysiological information which seems to be the key to success.

Thus, it is evident that the future directions should be oriented towards the development of software that will be implemented in the clinical routine, by utilizing large amounts of clinical data with extremely significant diagnostic value which often remain unexploited, resulting in a more valid and precise method for differential diagnosis of brain pathologies and the selection of the most successful treatment scheme.

REFERENCES

1 **Chiang IC**, Kuo YT, Lu CY, Yeung KW, Lin WC, Sheu FO,

Liu GC. Distinction between high-grade gliomas and solitary metastases using peritumoral 3-T magnetic resonance spectroscopy, diffusion, and perfusion imagings. *Neuroradiology* 2004; **46**: 619-627 [PMID: 15243726 DOI: 10.1007/s00234-004-1246-7]

2 **Liu X**, Tian W, Kolar B, Yeaney GA, Qiu X, Johnson MD, Ekholm S. MR diffusion tensor and perfusion-weighted imaging in preoperative grading of supratentorial nonenhancing gliomas. *Neuro Oncol* 2011; **13**: 447-455 [PMID: 21297125 DOI: 10.1093/neuonc/noq197]

3 **Tsougos I**, Svolos P, Kousi E, Fountas K, Theodorou K, Fezoulidis I, Kapsalaki E. Differentiation of glioblastoma multiforme from metastatic brain tumor using proton magnetic resonance spectroscopy, diffusion and perfusion metrics at 3 T. *Cancer Imaging* 2012; **12**: 423-436 [PMID: 23108208 DOI: 10.1102/1470-7330.2012.0038]

4 **Chang SC**, Lai PH, Chen WL, Weng HH, Ho JT, Wang JS, Chang CY, Pan HB, Yang CF. Diffusion-weighted MRI features of brain abscess and cystic or necrotic brain tumors: comparison with conventional MRI. *Clin Imaging* 2002; **26**: 227-236 [PMID: 12140151]

5 **Reiche W**, Schuchardt V, Hagen T, Il'yasov KA, Billmann P, Weber J. Differential diagnosis of intracranial ring enhancing cystic mass lesions--role of diffusion-weighted imaging (DWI) and diffusion-tensor imaging (DTI). *Clin Neurol Neurosurg* 2010; **112**: 218-225 [PMID: 20053496 DOI: 10.1016/j.clineuro.2009.11.016]

6 **Möller-Hartmann W**, Herminghaus S, Krings T, Marquardt G, Lanfermann H, Pilatus U, Zanella FE. Clinical application of proton magnetic resonance spectroscopy in the diagnosis of intracranial mass lesions. *Neuroradiology* 2002; **44**: 371-381 [PMID: 12012120 DOI: 10.1007/s00234-001-0760-0]

7 **Hollingworth W**, Medina LS, Lenkinski RE, Shibata DK, Bernal B, Zurakowski D, Comstock B, Jarvik JG. A systematic literature review of magnetic resonance spectroscopy for the characterization of brain tumors. *AJNR Am J Neuroradiol* 2006; **27**: 1404-1411 [PMID: 16908548]

8 **Kousi E**, Tsougos I, Tsolaki E, Fountas KN, Theodorou K, Fezoulidis I, Kapsalaki E, Kappas C. Spectroscopic evaluation of glioma grading at 3T: the combined role of short and long TE. *ScientificWorldJournal* 2012; **2012**: 546171 [PMID: 22919334 DOI: 10.1100/2012/546171]

9 **Astrakas LG**, Zurakowski D, Tzika AA, Zarifi MK, Anthony DC, De Girolami U, Tarbell NJ, Black PM. Noninvasive magnetic resonance spectroscopic imaging biomarkers to predict the clinical grade of pediatric brain tumors. *Clin Cancer Res* 2004; **10**: 8220-8228 [PMID: 15623597 DOI: 10.1158/1078-0432.CCR-04-0603]

10 **Panigrahy A**, Krieger MD, Gonzalez-Gomez I, Liu X, McComb JG, Finlay JL, Nelson MD, Gilles FH, Blüml S. Quantitative short echo time 1H-MR spectroscopy of untreated pediatric brain tumors: preoperative diagnosis and characterization. *AJNR Am J Neuroradiol* 2006; **27**: 560-572 [PMID: 16551993]

11 **Schaefer PW**, Grant PE, Gonzalez RG. Diffusion-weighted MR imaging of the brain. *Radiology* 2000; **217**: 331-345 [PMID: 11058626]

12 **Tang CY**, Friedman J, Shungu D, Chang L, Ernst T, Stewart D, Hajianpour A, Carpenter D, Ng J, Mao X, Hof PR, Buchsbaum MS, Davis K, Gorman JM. Correlations between Diffusion Tensor Imaging (DTI) and Magnetic Resonance Spectroscopy (1H MRS) in schizophrenic patients and normal controls. *BMC Psychiatry* 2007; **7**: 25 [PMID: 17578565 DOI: 10.1186/1471-244X-7-25]

13 **Zhang H**, Rödiger LA, Shen T, Miao J, Oudkerk M. Perfusion MR imaging for differentiation of benign and malignant meningiomas. *Neuroradiology* 2008; **50**: 525-530 [PMID: 18379768 DOI: 10.1007/s00234-008-0373-y]

14 **Sentürk S**, Oğuz KK, Cila A. Dynamic contrast-enhanced susceptibility-weighted perfusion imaging of intracranial tumors: a study using a 3T MR scanner. *Diagn Interv Radiol* 2009; **15**: 3-12 [PMID: 19263367]

15 **Järnum H**, Steffensen EG, Knutsson L, Fründ ET, Simonsen CW, Lundbye-Christensen S, Shankaranarayanan A, Alsop DC, Jensen FT, Larsson EM. Perfusion MRI of brain tumours: a comparative study of pseudo-continuous arterial spin labelling and dynamic susceptibility contrast imaging. *Neuroradiology* 2010; **52**: 307-317 [PMID: 19841916 DOI: 10.1007/s00234-009-0616-6]

16 **Lukas L**, Devos A, Suykens JA, Vanhamme L, Howe FA, Majós C, Moreno-Torres A, Van der Graaf M, Tate AR, Arús C, Van Huffel S. Brain tumor classification based on long echo proton MRS signals. *Artif Intell Med* 2004; **31**: 73-89 [PMID: 15182848 DOI: 10.1016/j.artmed.2004.01.001]

17 **Devos A**, Lukas L, Suykens JA, Vanhamme L, Tate AR, Howe FA, Majós C, Moreno-Torres A, van der Graaf M, Arús C, Van Huffel S. Classification of brain tumours using short echo time 1H MR spectra. *J Magn Reson* 2004; **170**: 164-175 [PMID: 15324770 DOI: 10.1016/j.jmr.2004.06.010]

18 **Dimou I**, Tsougos I, Tsolaki E, Kousi E, Kapsalaki E, Theodorou K, Kounelakis M, Zervakis M. Brain lesion classification using 3T MRS spectra and paired SVM kernels. *Biomed Signal Process Control* 2011; **6**: 314-320 [DOI: 10.1016/j.bspc.2011.01.001]

19 **Tsolaki E**, Svolos P, Kousi E, Kapsalaki E, Fountas K, Theodorou K, Tsougos I. Automated differentiation of glioblastomas from intracranial metastases using 3T MR spectroscopic and perfusion data. *Int J Comput Assist Radiol Surg* 2013; **8**: 751-761 [PMID: 23334798 DOI: 10.1007/s11548-012-0808-0]

20 **Svolos P**, Tsolaki E, Kapsalaki E, Theodorou K, Fountas K, Fezoulidis I, Tsougos I. Investigating brain tumor differentiation with diffusion and perfusion metrics at 3T MRI using pattern recognition techniques. *Magn Reson Imaging* 2013; **31**: 1567-1577 [PMID: 23906533 DOI: 10.1016/j.mri.2013.06.010]

21 **Davies NP**, Wilson M, Harris LM, Natarajan K, Lateef S, Macpherson L, Sgouros S, Grundy RG, Arvanitis TN, Peet AC. Identification and characterisation of childhood cerebellar tumours by in vivo proton MRS. *NMR Biomed* 2008; **21**: 908-918 [PMID: 18613254 DOI: 10.1002/nbm.1283]

22 **Raschke F**, Davies NP, Wilson M, Peet AC, Howe FA. Classification of single-voxel 1H spectra of childhood cerebellar tumors using LCModel and whole tissue representations. *Magn Reson Med* 2013; **70**: 1-6 [PMID: 22886824 DOI: 10.1002/mrm.24461]

23 **Lisboa PJ**, Wong H, Harris P, Swindell R. A Bayesian neural network approach for modelling censored data with an application to prognosis after surgery for breast cancer. *Artif Intell Med* 2003; **28**: 1-25 [PMID: 12850311 DOI: 10.1016/S0933-3657(03)00033-2)]

24 **van Bemmel JH**, Musen MA. Modeling for Decision Support. In: Handbook of Medical Informatics. Springer-Verlag, 1997

25 **Law M**, Cha S, Knopp EA, Johnson G, Arnett J, Litt AW. High-grade gliomas and solitary metastases: differentiation by using perfusion and proton spectroscopic MR imaging. *Radiology* 2002; **222**: 715-721 [PMID: 11867790 DOI: 10.1148/radiol.2223010558]

26 **Kousi E**, Tsougos I, Kapsalaki E. Proton Magnetic Resonance Spectroscopy of the Central Nervous System. In: Novel Frontiers of Advanced Neuroimaging. InTech, 2013: 19-50 [DOI: 10.5772/53892]

27 **De Edelenyi FS**, Rubin C, Estève F, Grand S, Décorps M, Lefournier V, Le Bas JF, Rémy C. A new approach for analyzing proton magnetic resonance spectroscopic images of brain tumors: nosologic images. *Nat Med* 2000; **6**: 1287-1289 [PMID: 11062544 DOI: 10.1038/81401]

28 **McKnight TR**, Noworolski SM, Vigneron DB, Nelson SJ. An automated technique for the quantitative assessment of 3D-MRSI data from patients with glioma. *J Magn Reson Imaging*

2001; **13**: 167-177 [PMID: 11169821 DOI: 10.1002/1522-2586(200102)13:2<167::AID-JMRI1026>3.0.CO;2-K]
29 **Simonetti AW**, Melssen WJ, van der Graaf M, Postma GJ, Heerschap A, Buydens LM. A chemometric approach for brain tumor classification using magnetic resonance imaging and spectroscopy. *Anal Chem* 2003; **75**: 5352-5361 [PMID: 14710812]
30 **De Vos M**, Laudadio T, Simonetti AW, Heerschap A, Van Huffel S. Fast nosologic imaging of the brain. *J Magn Reson* 2007; **184**: 292-301 [PMID: 17118683 DOI: 10.1016/j.jmr.2006.10.017]
31 **Laudadio T**, Martínez-Bisbal MC, Celda B, Van Huffel S. Fast nosological imaging using canonical correlation analysis of brain data obtained by two-dimensional turbo spectroscopic imaging. *NMR Biomed* 2008; **21**: 311-321 [PMID: 17907275 DOI: 10.1002/nbm.1190]
32 **Luts J**, Laudadio T, Idema AJ, Simonetti AW, Heerschap A, Vandermeulen D, Suykens JA, Van Huffel S. Nosologic imaging of the brain: segmentation and classification using MRI and MRSI. *NMR Biomed* 2009; **22**: 374-390 [PMID: 19105242 DOI: 10.1002/nbm.1347]
33 **Prastawa M**, Bullitt E, Ho S, Gerig G. A brain tumor segmentation framework based on outlier detection. *Med Image Anal* 2004; **8**: 275-283 [PMID: 15450222 DOI: 10.1016/j.media.2004.06.007]
34 **Li Y**, Sima DM, Van Cauter S, Himmelreich U, Croitor Sava AR, Pi Y, Liu Y, Van Huffel S. Unsupervised nosologic imaging for glioma diagnosis. *IEEE Trans Biomed Eng* 2013; **60**: 1760-1763 [PMID: 23192480 DOI: 10.1109/TBME.2012.2228651]
35 INTERPRET Consortium. Available from: URL: http: //azizu.uab.es/INTERPRET/
36 **Tate AR**, Underwood J, Acosta DM, Julià-Sapé M, Majós C, Moreno-Torres A, Howe FA, van der Graaf M, Lefournier V, Murphy MM, Loosemore A, Ladroue C, Wesseling P, Luc Bosson J, Cabañas ME, Simonetti AW, Gajewicz W, Calvar J, Capdevila A, Wilkins PR, Bell BA, Rémy C, Heerschap A, Watson D, Griffiths JR, Arús C. Development of a decision support system for diagnosis and grading of brain tumours using in vivo magnetic resonance single voxel spectra. *NMR Biomed* 2006; **19**: 411-434 [PMID: 16763971 DOI: 10.1002/nbm.1016]
37 Single voxel DSS tutorial. Available from: URL: http: //azizu.uab.es/INTERPRET/sv_tutorial/index.php#description
38 **Pérez-Ruiz A**, Julià-Sapé M, Mercadal G, Olier I, Majós C, Arús C. The INTERPRET Decision-Support System version 3.0 for evaluation of Magnetic Resonance Spectroscopy data from human brain tumours and other abnormal brain masses. *BMC Bioinformatics* 2010; **11**: 581 [PMID: 21114820 DOI: 10.1186/1471-2105-11-581]
39 Web accessible MR Decision Support System for Brain Tumour Diagnosis and Prognosis, Incorporating in vivo and ex vivo genomic and metabolic data. Available from: URL: http: //cordis.europa.eu/documents/documentlibrary/127824941EN19.doc
40 **Arus C**, Celda B, Dasmahaptra S, Dupplaw D, Gonzalez-Velez H, Van Huffel S, Lewis P, Lluch i Ariet M , Mier M, Peet A, Robles M. On the Design of a Web-Based Decision Support System for Brain Tumour Diagnosis Using Distributed Agents. Hong Kong, 2006: 208-211 [DOI: 10.1109/WI-IATW.2006.97]
41 **García-Gómez JM**. Pattern Recognition Approaches for Biomedical Data in Computer-Assisted Cancer Research, PhD thesis, Universidad Politécnica de Valencia, Departamento de Sistemas Informáticosy Computación Inteligencia Artificial, Reconocimiento de Formas e Imagen Digital. 2009
42 **Gonzalez-Velez H**, Mier M, Julià-Sapé M, Garcia-Gomez TN, Robles JM, Peet A, Arus C, Celda B, Van Huffel S, Lewis P, Dupplaw D, Dasmahapatra S. HealthAgents: Distributed Multi-Agent Brain Tumor Diagnosis and Prognosis. *J Appl Intel* 2009; **30**: 191-202 [DOI: 10.1007/s10489-007-0085-8]
43 **Hu B**, Croitoru M, Roset R, Dupplaw D, Lurgi M, Dasmahapatra S, Lewis P, Martínez-Miranda J, Sáez C. The HealthAgents ontology: how to represent the knowledge behind a brain tumour distributed decision system. *Knowl Eng Rev* 2011; **26**: 303-328
44 **Sáez C**, García-Gómez JM, Vicente J, Tortajada S, Luts J, Dupplaw D, Van Huffel S, Robles M. A generic and extensible automatic classification framework applied to brain tumour diagnosis in HealthAgents. *Knowl Eng Rev* 2011; **26**: 283-301 [DOI: 10.1017/S0269888911000129]
45 **Sáez C**, García-Gómez JM, Vicente J, Tortajada S, Fuster E, Esparza M, Navarro A, Robles M. Curiam BT 1.0, Decision Support System for Brain Tumour Diagnosis. In ESMRMB Congress. Antalya, Turkey: EPOS Posters/Paper Posters/Info-RESO, 2009: 538
46 **Vicente J**. Clinical Decision Support Systems for Brain Tumour Diagnosis: Classification and Evaluation Approaches. Departamento de Física Aplicada - Departament de Física Aplicada, 2012
47 **Fellows GA**, Wright AJ, Sibtain NA, Rich P, Opstad KS, McIntyre DJ, Bell BA, Griffiths JR, Howe FA. Combined use of neuroradiology and 1H-MR spectroscopy may provide an intervention limiting diagnosis of glioblastoma multiforme. *J Magn Reson Imaging* 2010; **32**: 1038-1044 [PMID: 21031506 DOI: 10.1002/jmri.22350]
48 **Julià-Sapé M**, Coronel I, Majós C, Candiota AP, Serrallonga M, Cos M, Aguilera C, Acebes JJ, Griffiths JR, Arús C. Prospective diagnostic performance evaluation of single-voxel 1H MRS for typing and grading of brain tumours. *NMR Biomed* 2012; **25**: 661-673 [PMID: 21954036 DOI: 10.1002/nbm.1782]
49 **Celda B**, Cano JG, Martinez-Bisbal MC, Martinez-Granados B. Clinical evaluation of a fully automated Computer Aid Decision System (CADS) for brain tumour supported diagnosis. eTUMOUR project FP6-2002-LSH-503094. In Joint Annual Meeting ISMRM-ESMRMB; May 1-7, Stockholm, Sweden, 2010
50 **Celda B**, Monleon D, Pla P, Gil-Cano J, Martinez-Granados B, Molla E, Revert A, Mart-Bonmati L, Leon J. Computer Aid Decision System (CADS) of eTUMOUR. Initial results of clinical evaluation for brain tumour classification In ESMRMB Congress, October 1-3, Antalya, Turkey, 2009
51 **Sáez C**, García-Gómez JM, Alberich-Bayarri Á, Edo MÁ., Vanyó M, Català-Gregori A, Barber C, Poyatos C, Mollà E, Martí-Bonmatí L, Robles M. Clinical Validation of the Added Value of a Clinical Decision Support System for Brain Tumour Diagnosis-Based on SV 1H MRS: Randomized Controlled Trial of Effectiveness and Qualitative Evaluation. Proceedings of 24th European Medical Informatics (MIE) Conference; 2012, August 26-29; Pisa-Italy: Quality of Life through Quality of Information
52 **Bryan C**, Boren SA. The use and effectiveness of electronic clinical decision support tools in the ambulatory/primary care setting: a systematic review of the literature. *Inform Prim Care* 2008; **16**: 79-91 [PMID: 18713524]
53 **Tortajada S**, Fuster-Garcia E, Vicente J, Wesseling P, Howe FA, Julià-Sapé M, Candiota AP, Monleón D, Moreno-Torres A, Pujol J, Griffiths JR, Wright A, Peet AC, Martínez-Bisbal MC, Celda B, Arús C, Robles M, García-Gómez JM. Incremental Gaussian Discriminant Analysis based on Graybill and Deal weighted combination of estimators for brain tumour diagnosis. *J Biomed Inform* 2011; **44**: 677-687 [PMID: 21377545 DOI: 10.1016/j.jbi.2011.02.009]
54 **Chernov MF**, Kubo O, Hayashi M, Izawa M, Maruyama T, Usukura M, Ono Y, Hori T, Takakura K. Proton MRS of the peritumoral brain. *J Neurol Sci* 2005; **228**: 137-142 [PMID: 15694194 DOI: 10.1016/j.jns.2004.11.039]
55 **Fan G**, Sun B, Wu Z, Guo Q, Guo Y. In vivo single-voxel proton MR spectroscopy in the differentiation of high-grade gliomas and solitary metastases. *Clin Radiol* 2004; **59**: 77-85

[PMID: 14697379 DOI: 10.1016/j.crad.2003.08.006]
56 **Di Costanzo A**, Scarabino T, Trojsi F, Popolizio T, Catapano D, Giannatempo GM, Bonavita S, Portaluri M, Tosetti M, d' Angelo VA, Salvolini U, Tedeschi G. Proton MR spectroscopy of cerebral gliomas at 3 T: spatial heterogeneity, and tumour grade and extent. *Eur Radiol* 2008; **18**: 1727-1735 [PMID: 18389246 DOI: 10.1007/s00330-008-0938-5]
57 **Zonari P**, Baraldi P, Crisi G. Multimodal MRI in the characterization of glial neoplasms: the combined role of single-voxel MR spectroscopy, diffusion imaging and echo-planar perfusion imaging. *Neuroradiology* 2007; **49**: 795-803 [PMID: 17619871 DOI: 10.1007/s00234-007-0253-x]
58 Magnetic Resonance User Interface (MRUI). Available from: URL: http: //sermn02.uab.es/mrui/

P- Reviewers: Lichtor T, Schoenhagen P, Triantopoulou C
S- Editor: Gou SX **L- Editor**: Cant MR **E- Editor**: Liu SQ

World Journal of Radiology

Online Submissions: http://www.wjgnet.com/esps/
bpgoffice@wjgnet.com
doi:10.4329/wjr.v6.i4.82

World J Radiol 2014 April 28; 6(4): 82-92
ISSN 1949-8470 (online)

REVIEW

Role of interventional radiology in the management of acute gastrointestinal bleeding

Raja S Ramaswamy, Hyung Won Choi, Hans C Mouser, Kazim H Narsinh, Kevin C McCammack, Tharintorn Treesit, Thomas B Kinney

Raja S Ramaswamy, Hyung Won Choi, Kazim H Narsinh, Kevin C McCammack, Tharintorn Treesit, Thomas B Kinney, Department of Vascular and Interventional Radiology, University of California San Diego Medical Center, San Diego, CA 92103, United States
Hans C Mouser, Department of Radiology, Indiana University Medical Center, Indianapolis, IN 46202, United States
Author contributions: All authors contributed equally to this paper.
Correspondence to: Raja S Ramaswamy, MD, Department of Vascular and Interventional Radiology, University of California San Diego Medical Center, 200 West Arbor Drive, #8756, San Diego, CA 92103, United States. rramaswamy@ucsd.edu
Telephone: +1-619-5436222 Fax: +1-619-5431234
Received: December 15, 2013 Revised: February 20, 2014
Accepted: March 11, 2014
Published online: April 28, 2014

Abstract

Acute gastrointestinal bleeding (GIB) can lead to significant morbidity and mortality without appropriate treatment. There are numerous causes of acute GIB including but not limited to infection, vascular anomalies, inflammatory diseases, trauma, and malignancy. The diagnostic and therapeutic approach of GIB depends on its location, severity, and etiology. The role of interventional radiology becomes vital in patients whose GIB remains resistant to medical and endoscopic treatment. Radiology offers diagnostic imaging studies and endovascular therapeutic interventions that can be performed promptly and effectively with successful outcomes. Computed tomography angiography and nuclear scintigraphy can localize the source of bleeding and provide essential information for the interventional radiologist to guide therapeutic management with endovascular angiography and transcatheter embolization. This review article provides insight into the essential role of Interventional Radiology in the management of acute GIB.

Key words: Interventional radiology; Angiography; Therapeutic management; Upper gastrointestinal bleeding; Lower gastrointestinal bleeding; Embolization

Core tip: Acute gastrointestinal bleeding can lead to significant morbidity and mortality without appropriate treatment. The role of interventional radiology is crucial in patients that have persistent bleeding despite medical and endoscopic treatment. Computed tomography angiography and nuclear scintigraphy can localize lesions and provide information helpful for the Interventional Radiologist. The source of bleeding can be then be stabilized with endovascular angiography/transcatheter arterial embolization which is safe and effective with minimal complications due to the advances in catheter technology.

Ramaswamy RS, Choi HW, Mouser HC, Narsinh KH, McCammack KC, Treesit T, Kinney TB. Role of interventional radiology in the management of acute gastrointestinal bleeding. *World J Radiol* 2014; 6(4): 82-92 Available from: URL: http://www.wjgnet.com/1949-8470/full/v6/i4/82.htm DOI: http://dx.doi.org/10.4329/wjr.v6.i4.82

INTRODUCTION

Acute gastrointestinal bleeding (GIB) is a common clinical presentation that can lead to significant morbidity and mortality without appropriate treatment. The estimated annual incidence is approximately 40-150 cases per 10000 persons for upper GIB and 20-27 cases per 100000 persons for lower GIB[1,2]. Mortality rate for both upper and lower GIB is estimated to be around 4%-10%[1,2]. GIB can be a sequelae of many different etiologies, such as infec-

tion, vascular anomaly, inflammatory diseases, trauma, and malignancy[2-9]. GIB is conventionally categorized by the anatomical location of the bleeding source. A GIB source proximal to the ligament of Treitz, which occurs more frequently, is classified as part of upper gastrointestinal (GI), and a source distal to the ligament of Treitz is considered to be part of lower GI. Diagnostic and treatment approach of GIB depends on its location, severity, and etiology. The role of radiology becomes especially important in patients whose GIB remains resistant to medical and endoscopic treatment. Radiology offers diagnostic imaging studies and endovascular therapeutic interventions that can be performed promptly and effectively.

CLINICAL EVALUATION AND MANAGEMENT OF THE PATIENT

Initial evaluation of patients with GIB begins with a history and physical examination[10,11]. GIB can manifest with various signs, such as tachycardia, orthostatic hypotension, and chronic anemia[11,12]. In patients who are hemodynamically unstable, resuscitation with fluid replacement and blood product administration should occur promptly to maintain intravascular volume and stabilize vital signs[10]. Correction of coagulopathy may also be needed in certain cases[10]. Diagnostic workup should immediately follow assessment and resuscitation, if not occurring simultaneously, to minimize adverse patient outcomes[10,13,14].

Patient history and physical examination can help to determine whether GIB is of upper or lower GI source and guide subsequent workup[11,15]. GIB that manifests as hematemesis or melena are commonly due to an upper GI source[11,13]. Patients with active brisk upper GIB can also present with hematochezia and without any associated hematemesis or melena[11,13,15]. Nasogastric tube lavage is sometimes performed to confirm an upper GI source of bleeding, but a negative result does not necessarily rule it out[11,13,15]. Because of the intermittent nature of GIB and the possibility of a bleeding source distal to the pylorus, gastric lavage test is expected to yield negative results in certain cases. Approximately one quarter of upper GI hemorrhage is due to peptic ulcer disease and often associated with non-steroidal anti-inflammatory drug use and *Helicobacter pylori* infection[15,16]. Other causes of acute upper GIB include varices, vascular abnormalities, angiodysplasia, gastritis, esophagitis, post Endoscopic Retrograde Cholangiopancreatography-papillotomy, and neoplasms[2,4,10].

Patients with lower GIB commonly presents with hematochezia as most lower GIB sources are located in the colon. Less commonly, patients may present with melena if the source of bleeding is located in the small bowel or right colon. Of note, 10% to 15% of patients with hematochezia are reported to have an upper GI bleeding site[17]. Diverticulosis is the most common cause of hematochezia, with the incidence increasing with ages older than 65. Other causes include inflammatory bowel disease, ischemic colitis, neoplasia, polyps, vascular malformations, post-polypectomy, and angiodysplasia[12,18]. Although most lower GIB resolves spontaneously with conservative management, 10%-15% of cases eventually require endovascular intervention[19].

Endoscopy is the first diagnostic and therapeutic intervention of choice for both upper and lower GIB and thus a consultation with a gastroenterologist should not be delayed when a patient presents with GIB. For patients suspected of having an upper GI source of bleeding, esophagoduodenoscopy (EGD) is performed. Factors that may predict endoscopic treatment failure include patients that present with shock, hemoglobin less than 10, greater than six units of blood transfused, and significant comorbidities.

With regards to upper GI bleeding, larger ulcer size and location of an ulcer on the posterior wall of the duodenal bulb are also associated with increased rates of technical failure[20,21].

Patients that present with hematochezia and suspected of having a lower GI source, colonoscopy is the initial diagnostic test of choice. For active lower GIB that is rapid and heavy, endoscopic view may be limited and yield inconclusive results. If a colonoscopy fails to identify the source of bleeding, then EGD may be performed in addition. Some studies have shown that endoscopy has a 92% sensitivity and near 100% specificity of identifying upper GI lesions and sensitivity of 90% and positive predictive value of 87% for identifying lower GI lesions[22,23]. An unprepared colon limits the colonoscopy study and while blood may be seen within the colon lumen the exact site of bleeding is difficult to identify[23].

If a lesion is identified endoscopically, therapeutic intervention can be done to effectively stabilize bleeding. Endoscopic therapies include epinephrine injection, sclerotherapy, and metal clip placement. Metal clips are especially useful in patients who require transcatheter or surgical intervention later on as clips can be visualized by imaging studies and facilitate lesion localization during angiography or surgery[9,17].

INDICATIONS FOR ANGIOGRAPHY

When a patient has non-diagnostic endoscopic results or remains refractory to medical and endoscopic treatment, radiologic imaging and endovascular intervention are the next intervention of choice. Non-invasive radiologic imaging options include computed tomography angiography (CTA) and nuclear scintigraphy. However, these imaging modalities are only diagnostic and require subsequent endovascular or surgical intervention to stabilize bleeding[24,25].

COMPUTED TOMOGRAPHY

CTA can detect flow rates as low as 0.3 mL/min and has a sensitivity of 50%-86% and specificity of 92%-95% for identifying lesions responsible for GIB[24,26,27]. In addition to identifying the site of bleeding; CTA can often identify the etiology of GIB which may be useful for further

management.

At our institution, we use the following protocol for CTA: noncontrast (unenhanced), arterial phase, and portal venous phase with intravenous contrast at 4-5 mL/s. We also recommend the following acquisition parameters: section thickness of 1 mm with reconstruction interval of 0.8 mm, pitch of 0.900, rotation time of 0.5 s, tube voltage of 120 kV, and automatic tube current modulation in the x/y/z axis directions. We do not administer oral contrast as this may mask the bleeding source.

On nonenhanced CT, focal hyperattenuation within the bowel is indicative of recent hemorrhage and may represent a "sentinel clot". Extravasation of contrast is the hallmark finding used to determine the source of bleeding. Further, a changing appearance of the focus of extravasated contrast with time between phases confirms the presence of active bleeding[25]. Although CTA can only serve as a diagnostic tool; it provides important information about vascular anatomy variance that becomes useful for endovascular intervention or surgical planning.

NUCLEAR SCINTIGRAPHY

The role of nuclear medicine for the detection of acute GI bleeding varies on an institutional basis. Nuclear scintigraphy plays a very important role in the detection of lower GI bleeding and when positive, has the ability to stratify patients that would benefit from intervention versus medical management. Although there is significant variability in reported detection of bleeding site by scintigraphy, the Society of Nuclear Medicine procedure guidelines states that bleeding rates as low as 0.1-0.35 mL/min can be detected[28]. Tc-99m labeled red blood cell studies have an overall sensitivity of 95% and specificity of 93%[29]. Patients with immediate blush on red blood cell scintigraphy are more likely to require urgent angiography and those with delayed blush have low angiographic yield[30]. GI bleeding often is intermittent and nuclear scintigraphy has the advantage of continuous monitoring to localize sites of intermittent bleeding for potential angiography and intervention[31].

ANGIOGRAPHIC EVALUATION OF ACUTE GI HEMORRHAGE

In emergent cases or in hospitals where CTA or nuclear scintigraphy is not available, patients with active GIB who fail medical and endoscopic intervention should undergo endovascular angiographic evaluation. Angiography is able to identify an active bleeding rate of at least 0.5 to 1 mL/min[32,33]. For lower GIB, angiography performed with digital subtraction has a sensitivity of 60%, specificity of 100%, positive and negative predictive values of 100% and 24%, respectively[34].

Access for endovascular angiography is gained *via* the common femoral artery[35,36]. The aim of endovascular angiography is to identify bleeding vessel(s) and use selective catheterization to prepare for embolization[36,37]. At our institution, based on clinical scenario (patient history, CTA, endoscopic findings) the most suspected bleeding vessel is first studied. For suspected upper GIB, the celiac artery is commonly interrogated first as a majority of upper GIB is caused by gastroduodenal ulcers which are supplied by branches of the celiac artery[35-38] (Figure 1). If angiographically negative, selective left gastric and the gastroduodenal artery evaluation is done. If the source of bleeding is thought to be in the small bowel or if no evidence of bleeding is seen upon interrogation of the celiac artery or its branches, the superior mesenteric artery (SMA) is evaluated next[36,37]. If these angiographic studies are all negative, then evaluation of the inferior mesenteric artery (IMA) is considered. Selective injections are used to confirm any findings that are suspicious on nonselective angiograms[36,37].

For suspected lower GIB, the SMA and IMA are examined[36]. If bleeding appears to originate the proximal colon, the SMA is initially evaluated. If bleeding appears to originate in the distal colon, the IMA is selected[36,39]. The two most common causes of lower GIB are colonic diverticular disease and angiodysplasia[2,32] (Figures 2 and 3). However, when congenital variant vascular anatomy is suspected, such as in cases where a lower GI bleed simulates an upper GI bleed, all three major arterial supplies should be evaluated[36]. If negative, the internal iliac arteries should be evaluated as the middle and inferior rectal arteries can be a source of hemorrhage[36,39].

At our institution, under fluoroscopy we use nonionic contrast is injected at a flow rate of 5-7 mL/s for celiac and super mesenteric arteriography, and 2-3 mL/s for inferior mesenteric arteriography. Digital subtraction angiogram is used to better visualize the vasculature by subtracting pre-contrast image from later images and effectively removing soft tissue and bones from the images. This is limited by peristalsis (consider giving glucagon) or patient breathing (which can be dealt with by studying unsubtracted images). Extravasation of contrast agent is indicative of active bleeding[36]. Positive findings include mucosal blushes with abnormal vessels suggestive of tumor, prolonged contrast spots suggestive of inflammation, and visualization of arteries and veins on the same phase of the study suggestive of an arteriovenous malformation. Other lesions to consider include pseudoaneurysms and arteriovenous fistulas[36,39].

There are several artifacts that mimic extravasation including bowel subtraction artifact, hypervascular mucosa, parts of the renal collecting system, and adrenal gland opacification[39]. With respect to angiography, contrast extravasation may not been seen; however, a pathologic finding may indicate the source of bleeding. For example, visualization of varices at unsuspected sites may indicate the site of pathology. Further, angiodysplasia is often diagnosed by early and persistent filling of a draining vein and by abnormal clusters of vessels within the bowel wall. Possible pitfalls for failing to identify the bleeding focus include bleeding from a venous origin and technically related issues such as failure to inject the correct

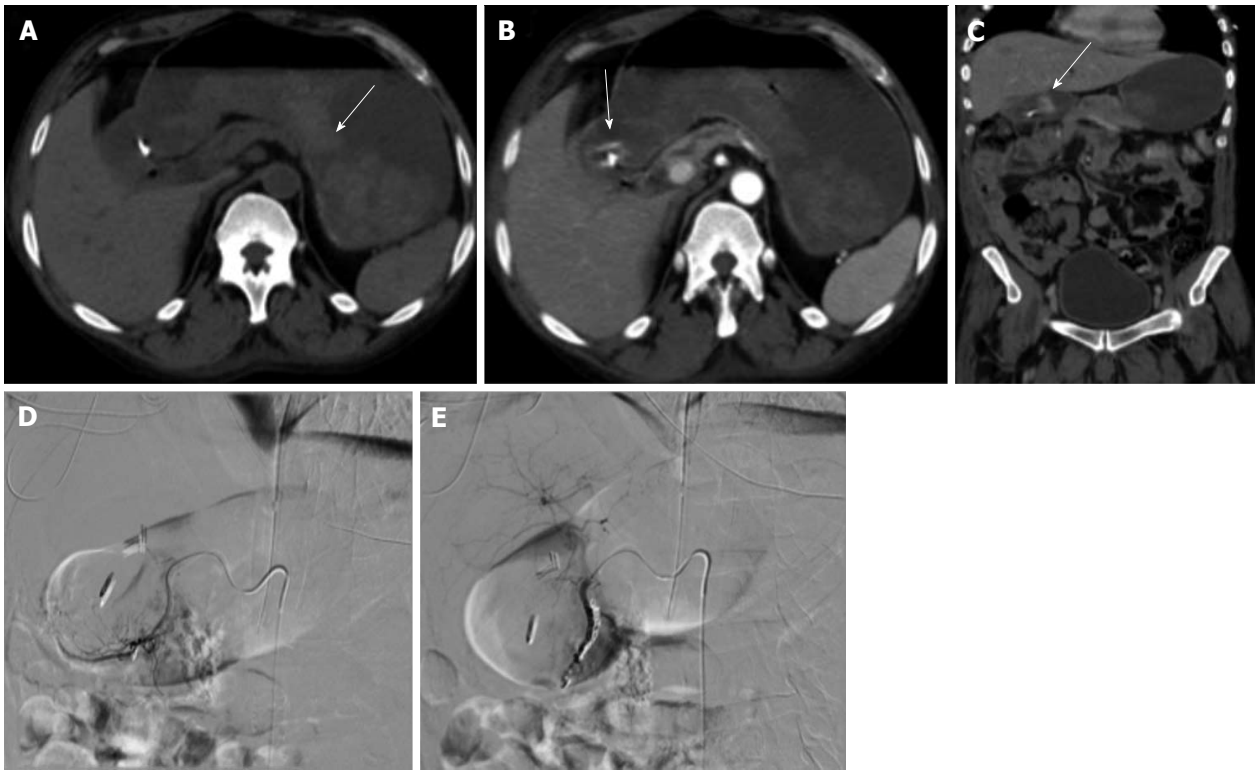

Figure 1 Upper gastrointestinal bleed secondary to gastric/duodenal ulcers. Fifty-four-year-old male with history of gastric ulcers which were treated by clipping through endoscopy. Despite endoscopic intervention, the patient presented with dropping hematocrit requiring transfusion. A: Noncontrast; B and C: contrast enhanced computed tomography imaging demonstrates active extravasation at the level of the gastric antrum with blood product filling the stomach; D and E: Active extravasation was found at the gastroduodenal artery (not shown) which was embolized with coils and gelfoam.

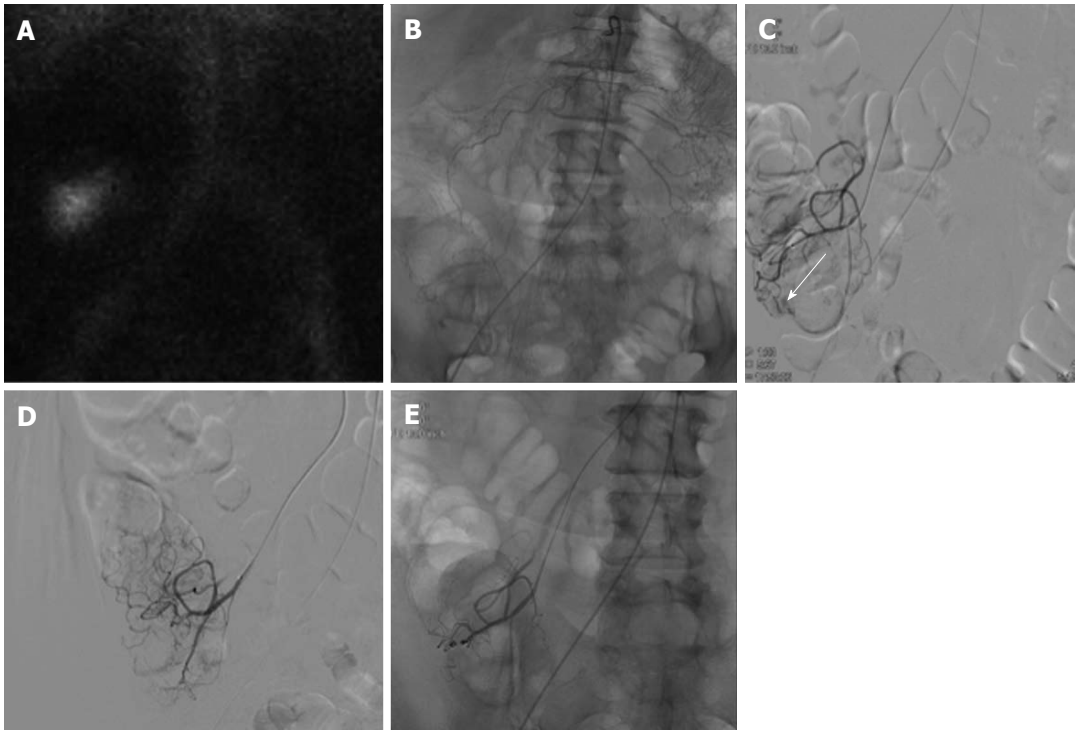

Figure 2 Lower gastrointestinal bleeding secondary to angiodysplasia. Sixty-one-year-old female with multiple bloody stools prior to admission and negative colonoscopy. A: Tc-99m red blood cell study demonstrates active bleeding in the region of the cecum; B and C: Selective catheterization of the distal ileocolic artery demonstrates a small focus of hemorrhage consistent with an area of angiodysplasia; D and E: Coil embolization was performed with two 3 mm coils. Post embolization images demonstrates resolved bleeding.

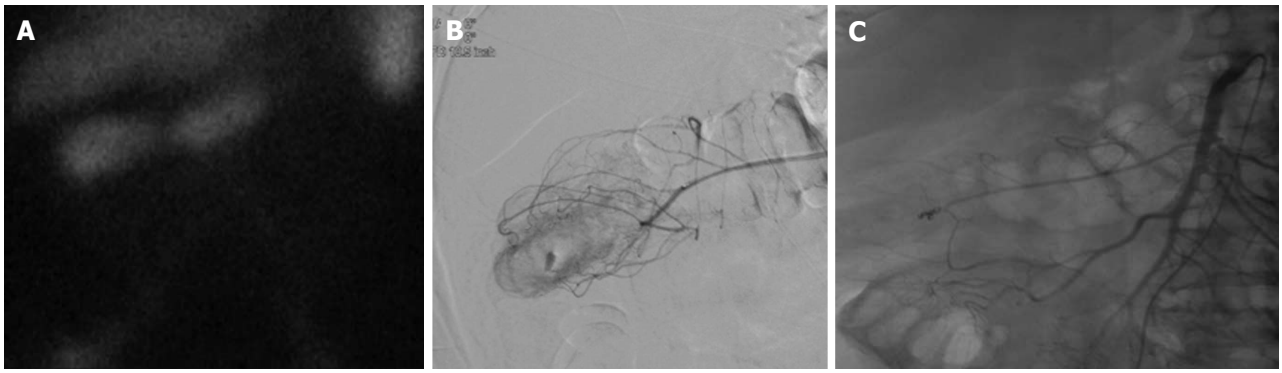

Figure 3 Lower gastrointestinal bleed secondary to diverticulitis. Sixty-eight-year-old male with history of esophageal carcinoma with acute diverticulitis with drifting hematocrit. A: Tc-99m labeled red blood cell study demonstrates bleeding at the hepatic flexure of the colon; B: Selective catheter angiography at the middle colic artery demonstrates active extravasation into a diverticulum present at the hepatic flexure the colon; C: Coil embolization of the right lateral aspect of the middle colic artery, across a small perforating vessel associated with a diverticular hemorrhage.

artery and bleeding outside the field of imaging[39,40].

If patient is not actively bleeding or contrast extravasation is not visualized under fluoroscopy, the interventional radiologist may choose to restudy the same vessels or sub-selectively catheterize vessels likely supplying the suspected site of bleeding identified by prior endoscopic clipping or imaging studies to help increase the diagnostic yield and reduce false negative studies[39,40].

ANGIOGRAPHIC MANAGEMENT OF ACUTE GI HEMORRHAGE

One of the advantages of endovascular angiography is that it can be both a diagnostic and therapeutic tool. Also, endovascular angiography can be performed emergently without any bowel preparation. However, if the patient had prior oral contrast this may limit the diagnostic ability of a mesenteric angiogram thus oral contrast should be avoided in patients who undergo CT imaging prior to angiographic intervention[40-42].

Endovascular angiography serves as an effective and safe alternative to surgical intervention for patients whose GIB is refractory to medical and endoscopic treatment. Hemostasis is achieved by reducing blood flow to the bleeding vessel and thus decreasing perfusion pressure and facilitating clot formation at the site of bleeding[40-43].

TRANSCATHETER ARTERIAL EMBOLIZATION

Transcatheter arterial embolization (TAE) is effective for controlling acute GIB[41]. Some studies have shown that TAE is safer than surgical intervention in the high risk patient population and has a lower 30-d mortality rate[38,44]. TAE is a viable option and temporizing measure in circumstances where endoscopic and/or surgical approach is not ideal.

The goal of TAE is super-selective embolization of bleeding vessels to reduce arterial perfusion pressure while maintaining adequate collateral blood flow to minimize the risk of bowel infarction[43]. A 5 French angiographic catheter is used to access the celiac, superior mesenteric, or inferior mesenteric arteries depending on the suspected location of bleeding and its supplying vasculature. In some cases this catheter can be guided to the site of bleeding; however, if it does not reach the bleeding site, then a smaller coaxial 3 French microcatheter can be advanced through the 4 or 5 Fr catheter.

Smaller guidewires, such as 0.018 in or smaller are used to guide the microcatheters as close as possible to the bleeding site. Caution must be taken to move the guide wire and microcatheter as carefully and steadily as possible to avoid vessel perforation, dissection, and vasospasm while reaching as close as possible to the site of bleeding. When no contrast extravasation is visualized under fluoroscopy, blind embolization of suspected bleeding vessel may be done at the discretion of the interventional radiologist[38,45].

For upper GI bleeding, bleeding visualized in the stomach fundus is treated by left gastric artery embolization and bleeding in the gastric antrum/proximal duodenum by gastroduodenal embolization. When embolizing the gastroduodenal artery, if only the proximal portion is occluded, then bleeding may by the pancreaticoduodenal arcade, also known as bleeding *via* the "back door". mpiric embolization has also shown to be effective[40,42] (Figures 4 and 5).

For lower GI bleeding the catheter should be positioned as close to the bleeding site as possible. If the source is in the SMA, the catheter advanced to the vasa rectum and if in the IMA the catheter should be placed in the marginal or terminal artery if possible. Embolization should only be performed when the catheter has been advanced to the mesenteric border of the colon. The bowel distal to the ligament of Treitz does not have a dual supply; therefore, the risk of bowel infarction is higher[39,40,42] (Figures 6 and 7).

The type of embolic agent used is conventionally dependent on the interventional radiologist's experience and preference, etiology of bleeding, and availability of the agent. Embolic agents include coils, glue, onyx, Gelfoam,

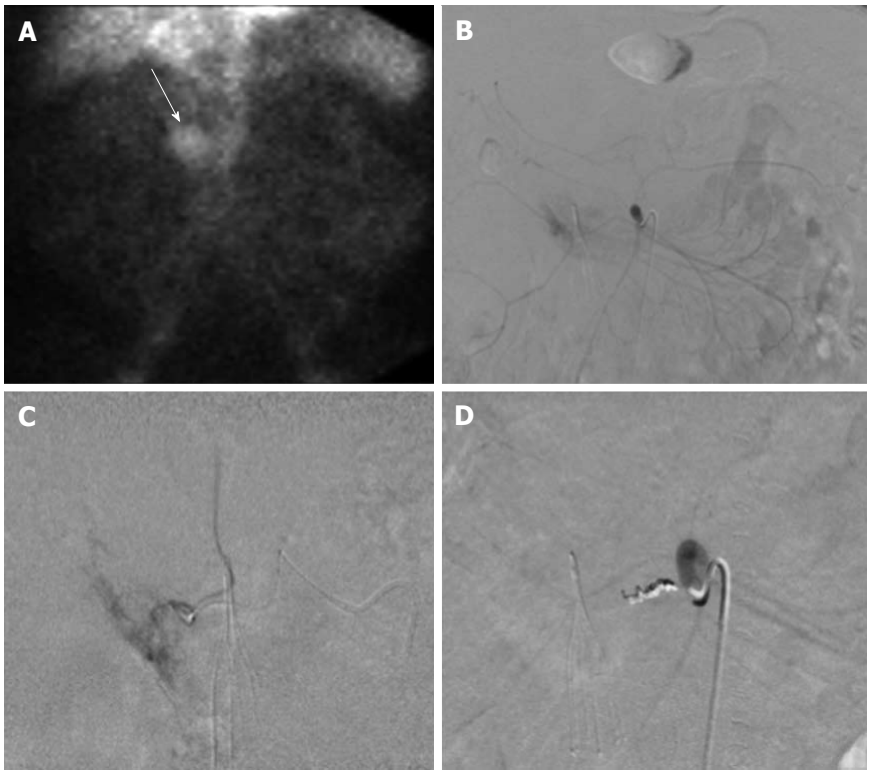

Figure 4 Sixty-six-year-old male with ongoing gastrointestinal hemorrhage requiring multiple transfusions over the last 72 h. EGD performed revealed ulcers in the first and second portion of the duodenum. A: Technetium-99m tagged RBC scan demonstrates brisk hemorrhage arising from the proximal small bowel/duodenum; B and C: Digitally subtracted images reveal active extravasation in the second portion of the duodenum from the inferior pancreaticoduodenal artery corresponding to area of hemorrhage on tagged RBC scan; D: Successful and uncomplicated coil embolization of the inferior pancreaticoduodenal artery with cessation of active hemorrhage. EGD: Esophagoduodenoscopy; RBC: Red blood cell.

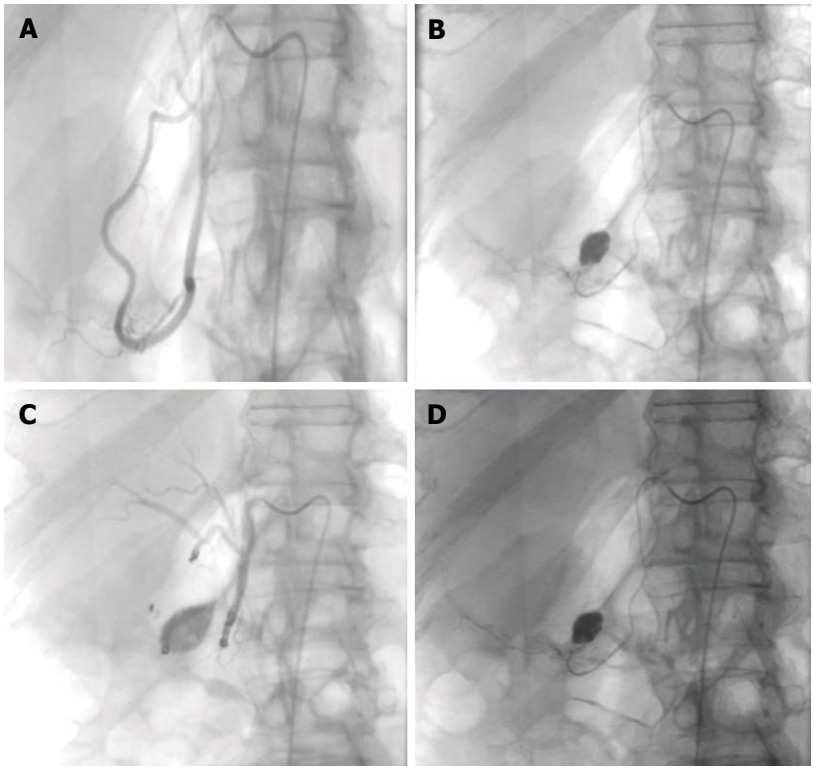

Figure 5 Seventy-two-year-old female with worsening abdominal pain and acute gastrointestinal hemorrhage. Upper gastrointestinal endoscopy reveals multiple large bleeding ulcers in the duodenum. A and B: Selective catheter angiography of the gastroduodenal and pancreaticoduodenal arteries demonstrates active extravasation; C: A combination of gelfoam slurry and coils were used to embolize branches of the pancreaticoduodenal and gastroduodenal artery; D: Representative post embolization image demonstrates no further evidence of active extravasation or bleeding.

polyvinyl alcohol particles (PVA), and Amplatzer vascular plugs. The most commonly used embolic agents are coils and PVA[46-49].

Coils come in a variety of sizes and shapes, ranging from sub-millimeter to centimeters. Coils are composed of a metal component that acts as a physical occlusion and a fiber component that stimulates the thrombogenic process. Coils can be visualized under fluoroscopy after placement which is an important advantage when compared to Gelfoam or PVA. Newer types of embolization coils have the ability to be removed after deployment if the initial placement is felt to be unsatisfactory[46,50].

Gelfoam (absorbable compressed sponge) is a temporary agent made of subcutaneous porcine adipose tissue that remains effective for weeks to months before recanalization occurs. For this reason, Gelfoam is not rec-

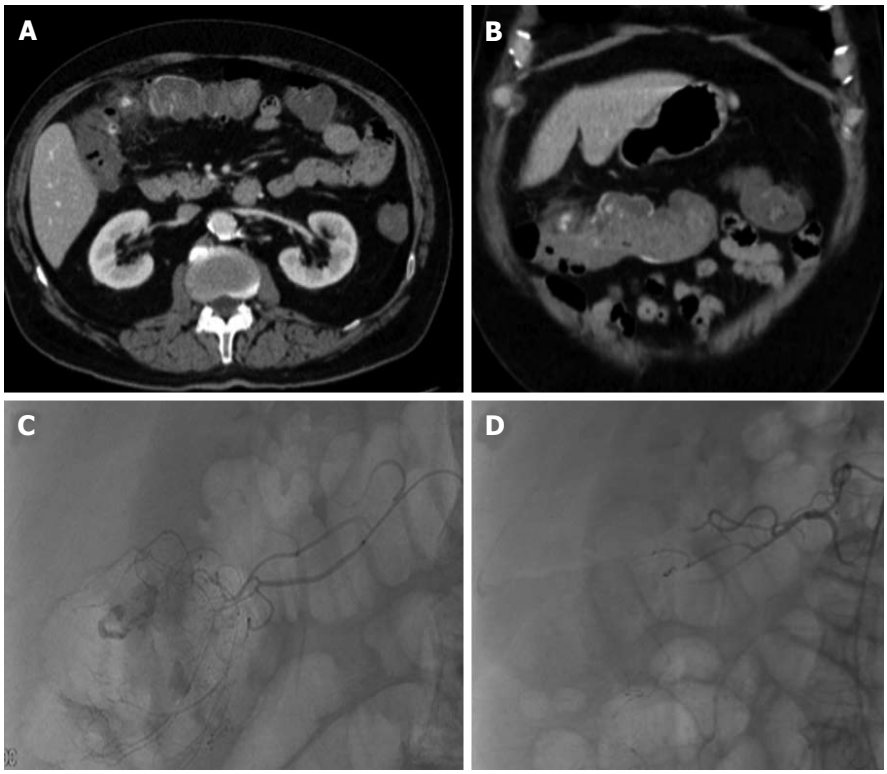

Figure 6 Lower gastrointestinal bleed from acute diverticulitis. Seventy-three-year-old male patient with bloody diarrhea, severely hypotensive (blood pressure 70/40) requiring 10 units of packed red blood cells. A and B: Contrast enhanced computed tomography abdomen demonstrates acute diverticulitis at the hepatic flexure, with active hemorrhage; C: Visceral angiography demonstrates the region of active bleeding in the ascending colon at the hepatic flexure; D: Successful distal Gelfoam and coil embolization of the supplying right colic artery branches.

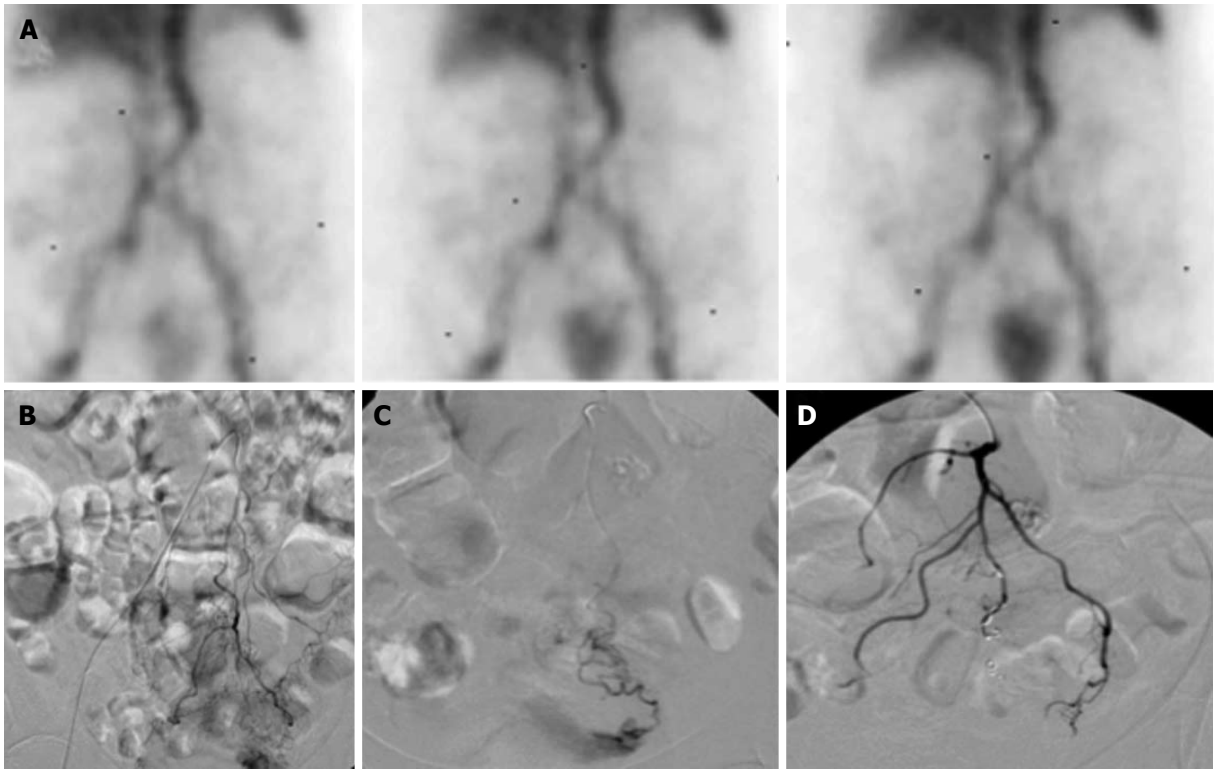

Figure 7 Lower gastrointestinal bleed secondary to supratherapeutic international normalized ratio. Seventy-six-year-old female with supratherapeutic INR (3.5) with painless hematochezia. A: Tc-99m labeled RBC study demonstrates brisk gastrointestinal bleeding localized to the sigmoid colon; B and C: Catheter angiography demonstrates active extravasation from a tertiary branch of the inferior mesenteric artery supplying the distal sigmoid colon which was subsequently embolized; D: With coils and no evidence of continued bleeding. RBC: Red blood cell.

ommended as a single agent. Gelfoam can also be mixed with saline to form a slurry, which helps with delivery. Advantages of gelfoam include: widespread availability, cost-effectiveness, and allows future access to embolized vessels after resorption. Disadvantages include that the preparation of particles can be time consuming and recanalization of vessels is unpredictable[51]. In addition, because Gelfoam is made of small particulates, it is dif-

ficult to control its placement and can be deployed more distally than intended, which can result in higher risk of bowel ischemia from embolization of nearby collateral vessels[36,50,51].

Several studies have shown that recurrent bleeding is more likely to occur when PVA particles, Gelfoam, or coils are used alone[46,48,52]. Using coils with Gelfoam or PVA particles on both sides of the bleeding vessel is recommended to avoid "backdoor" bleeding and decrease the risk of recurrent bleeding[48,53]. Some studies have shown that for upper GIB, which is commonly due to gastroduodenal ulcers, successful hemostasis can be achieved by embolizing the gastroduodenal artery or pancreaticoduodenal artery using coils alone[54-56], or using coils and Gelfoam together to embolize distally and proximally in the gastroduodenal arterial trunk[46,48,52]. Clinical success rate of embolization for upper GIB have been cited to be around 44%-100%[41,44,46,57].

For lower GIB, some studies recommend against using Gelfoam, and instead advocate using coils and larger PVA particles[43,58,59]. Small PVA particles, less than 250 μm, and Gelfoam particles may travel distally and occlude vessels at the arteriolar level. This results in occlusion of intramural circulation or submucosal plexus beyond the level of collateralization and increases the risk of bowel infarction[59,60]. More peripheral embolization just proximal to the vasa recta is recommended to minimize the length of bowel at risk for ischemia. In most of the reported series in the literature, the target artery of embolization was the vasa recta and in technically difficult cases the marginal artery or more proximally[57,61,62].

Anecdotally, coil embolization at the marginal artery may result in a higher rebleeding rate. Further, if a secondary intervention is required, this may close the door for future access to the bleeding vessel. Advantages to using microcoils include the ability to visualize under direct fluoroscopy and permitting decreasing perfusion pressure while collateral flow prevents infarction. Early rebleeding (less than 30 d) is reported to range from 10%-30%. Rebleeding may be secondary to a new site of bleed or recanalization of the previously embolized artery. Success rate for embolization of lower GIB has ranged from 88%-93%[43,57,60].

N-butyl 2-cyanoacrylate (NBCA) glue or ethylene-vinyl alcohol copolymer (Onyx®, Micro Therapeutics, Inc., Irvine, CA, United States of America) is a promising newer embolic agent to control GI bleeding. There is a growing body of evidence that supports the use of cyanoacrylates in embolization for lower GI hemorrhage. Advantages of using NBCA include the ability to occlude vessel beyond the most distal site of microcatheter advancement, permanent vessel closure, the option for using ultra-microcatheters not suitable for microcoil delivery, and more efficient obliteration of bleeding pseudoaneurysms with complex anatomy. Further, the rebleeding rate after use of cyanoacrylate is 4%-15%, which appears lower than the rate reported from employing coils or particles 0%-26%[39,63-66].

However, NBCA is considerably more expensive and requires a steeper learning curve. It has been reported in the literature that the time for TAE using NBCA was significantly lower than when using other liquid agents[49,55]. There is a significant risk of glue reflux, bowel infarction, and future bowel stenosis[67]. Also, the glue may polymerize with the catheter tip, which may subsequently get stripped off as the catheter is retracted. This poses the risk of non-target embolization or the catheter becoming adherent to the artery. Prompt catheter removal and aspiration of the guide catheter after microcatheter removal can significantly reduce this risk[52,68].

Another potential agent, Onyx, is a liquid embolic agent composed of ethylene-vinyl alcohol copolymer dissolved in dimethyl sulphoxide (DMSO). In 2010, Lenhart *et al*[69] reported their experience with the use of Onyx in the setting of acute upper GIB, becoming the first study published on arterial embolotherapy with Onyx as an embolic agent in the gastrointestinal tract. Their reported success rate was 81% and the complication rate minimal. The main advantages of Onyx® are its nonadhesive properties, high radiopacity and long solidification periods which make the embolization procedure more predictable. The DMSO solvent has disadvantages including severe vasospasm, excretion *via* respiration/perspiration which can cause an odor for days. The most prohibitive and restrictive factor however is its high cost and requirement for DMSO compatible catheters[52,69].

VASOPRESSIN INFUSION

Vasopressin infusion is a less frequently used treatment for acute GIB[58]. It was more commonly used before the advancement and improvement of transcatheter technique. Vasopressin acts by constricting arteries and reducing blood flow to the target site, but can also cause systemic side effects such as cardiac arrhythmia and bowel ischemia. In addition, vasopressin infusion has a high rebleeding rate after infusion is stopped. It requires much longer procedure time including catheter placement for 24-48 h and intensive monitoring during vasopressin infusion. However, when GIB is caused by diffuse lesions or super-selective catheterization is not possible, vasopressin infusion may be the remaining therapeutic option before surgical intervention. Vasopressin infusion is used more often for lower GIB than upper GIB as vessels responsible for lower GIB tend to be smaller in diameter and thus more responsive to the constricting effect of vasopressin[58,70]. Some studies have shown that the cardiac side effects of vasopressin can be alleviated by using intravenous nitroglycerin infusion to increase coronary blood flow and cardiac output[70]. Vasopressin infusion has a success rate of 59%-90% and a high rate of rebleeding rate of up to 36%-43%[70].

COMPLICATIONS

Endovascular embolization and vasopressin infusion can increase the risk of bowel ischemia by reducing blood flow to the segment of bowel supplied by the target ves-

sel[71,72]. Non-target embolization can occur as well[41]. However, the advancement of super-selective catheterization technique has helped to reduce such risk in recent years[42,73]. Other complications with transcatheter intervention include arterial injury such as dissection, perforation, pseudoaneurysm, and vasospasm. For vasopressin infusion, there is a higher risk of catheter associated infection or thrombus formation because of the need for much longer duration of catheter placement[74,75]. Contrast use during fluoroscopy can induce nephropathy, but with adequate hydration and vigilance of contrast use, the risk can be decreased[76,77]. Hematoma is a common minor complication associated with puncture site. Patients may complain of temporary minor abdominal pain after the procedure but this most often resolves spontaneously.

CONCLUSION

Although many cases of acute GIB resolve spontaneously or respond to medical and endoscopic treatment, patients with GIB refractory to such treatment are at higher risk for adverse outcome. Various subspecialties contribute to the care of bleeding patients. Patients with acute GIB should be considered for prompt radiologic imaging studies and endovascular intervention to prevent morbidity and mortality. CTA can localize lesions and provide information helpful for endovascular intervention and surgery. Rapid GIB stabilization can be achieved with endovascular angiography and transcatheter embolization. It is a safe and effective alternative to surgery.

REFERENCES

1 **Manning-Dimmitt LL**, Dimmitt SG, Wilson GR. Diagnosis of gastrointestinal bleeding in adults. *Am Fam Physician* 2005; **71**: 1339-1346 [PMID: 15832537]

2 **Longstreth GF**. Epidemiology and outcome of patients hospitalized with acute lower gastrointestinal hemorrhage: a population-based study. *Am J Gastroenterol* 1997; **92**: 419-424 [PMID: 9068461]

3 **Boonpongmanee S**, Fleischer DE, Pezzullo JC, Collier K, Mayoral W, Al-Kawas F, Chutkan R, Lewis JH, Tio TL, Benjamin SB. The frequency of peptic ulcer as a cause of upper-GI bleeding is exaggerated. *Gastrointest Endosc* 2004; **59**: 788-794 [PMID: 15173790]

4 **Cook DJ**, Fuller HD, Guyatt GH, Marshall JC, Leasa D, Hall R, Winton TL, Rutledge F, Todd TJ, Roy P. Risk factors for gastrointestinal bleeding in critically ill patients. Canadian Critical Care Trials Group. *N Engl J Med* 1994; **330**: 377-381 [PMID: 8284001 DOI: 10.1056/NEJM199402103300601]

5 **Enestvedt BK**, Gralnek IM, Mattek N, Lieberman DA, Eisen G. An evaluation of endoscopic indications and findings related to nonvariceal upper-GI hemorrhage in a large multicenter consortium. *Gastrointest Endosc* 2008; **67**: 422-429 [PMID: 18206878 DOI: 10.1016/j.gie.2007.09.024]

6 **Hreinsson JP**, Kalaitzakis E, Gudmundsson S, Björnsson ES. Upper gastrointestinal bleeding: incidence, etiology and outcomes in a population-based setting. *Scand J Gastroenterol* 2013; **48**: 439-447 [PMID: 23356751 DOI: 10.3109/00365521.2012.763174]

7 **Longstreth GF**. Epidemiology of hospitalization for acute upper gastrointestinal hemorrhage: a population-based study. *Am J Gastroenterol* 1995; **90**: 206-210 [PMID: 7847286]

8 **van Leerdam ME**. Epidemiology of acute upper gastrointestinal bleeding. *Best Pract Res Clin Gastroenterol* 2008; **22**: 209-224 [PMID: 18346679 DOI: 10.1016/j.bpg.2007.10.011]

9 **Zuccaro G**. Epidemiology of lower gastrointestinal bleeding. *Best Pract Res Clin Gastroenterol* 2008; **22**: 225-232 [PMID: 18346680 DOI: 10.1016/j.bpg.2007.10.009]

10 **Ahmed A**, Stanley AJ. Acute upper gastrointestinal bleeding in the elderly: aetiology, diagnosis and treatment. *Drugs Aging* 2012; **29**: 933-940 [PMID: 23192436 DOI: 10.1007/s40266-012-0020-5]

11 **Srygley FD**, Gerardo CJ, Tran T, Fisher DA. Does this patient have a severe upper gastrointestinal bleed? *JAMA* 2012; **307**: 1072-1079 [PMID: 22416103 DOI: 10.1001/jama.2012.253]

12 **Strate LL**, Orav EJ, Syngal S. Early predictors of severity in acute lower intestinal tract bleeding. *Arch Intern Med* 2003; **163**: 838-843 [PMID: 12695275 DOI: 10.1001/archinte.163.7.838]

13 **Barkun A**, Bardou M, Marshall JK, Nonvariceal Upper GI Bleeding Consensus Conference Group. Consensus recommendations for managing patients with nonvariceal upper gastrointestinal bleeding. *Ann Intern Med* 2003; **139**: 843-857 [PMID: 14623622]

14 **Barnert J**, Messmann H. Diagnosis and management of lower gastrointestinal bleeding. *Nat Rev Gastroenterol Hepatol* 2009; **6**: 637-646 [PMID: 19881516 DOI: 10.1038/nrgastro.2009.167]

15 **Wilkins T**, Khan N, Nabh A, Schade RR. Diagnosis and management of upper gastrointestinal bleeding. *Am Fam Physician* 2012; **85**: 469-476 [PMID: 22534226]

16 **Prasad Kerlin M**, Tokar JL. Acute gastrointestinal bleeding. *Ann Intern Med* 2013; **159**: ITC2-IT1, ITC2-IT1, ITC2-IT1, ITC2-IT1, ITC2-IT1, ITC2-IT1, ITC2-IT1, ITC2-IT1, ITC2-IT1, ITC2-IT1, ITC2-IT1, ITC2-IT1, ITC2-IT1, ITC2-IT1, ITC2-IT1, quiz ITC2-IT1 [PMID: 23922080 DOI: 10.7326/0003-4819-159-3-201308060-01002]

17 **Zuccaro G**. Management of the adult patient with acute lower gastrointestinal bleeding. American College of Gastroenterology. Practice Parameters Committee. *Am J Gastroenterol* 1998; **93**: 1202-1208 [PMID: 9707037 DOI: 10.1111/j.1572-0241.1998.00395.x]

18 **Strate LL**. Lower GI bleeding: epidemiology and diagnosis. *Gastroenterol Clin North Am* 2005; **34**: 643-664 [PMID: 16303575 DOI: 10.1016/j.gtc.2005.08.007]

19 **Billingham RP**. The conundrum of lower gastrointestinal bleeding. *Surg Clin North Am* 1997; **77**: 241-252 [PMID: 9092113]

20 **Brullet E**, Calvet X, Campo R, Rue M, Catot L, Donoso L. Factors predicting failure of endoscopic injection therapy in bleeding duodenal ulcer. *Gastrointest Endosc* 1996; **43**: 111-116 [PMID: 8635702]

21 **Siva R**, Al Zubaidi G, Masoud AK, Nihar M. Predictive factors for failure of endoscopic management therapy in peptic ulcer bleeding. *Saudi J Gastroenterol* 2002; **8**: 17-21 [PMID: 19861786]

22 **Smith GA**, O'Dwyer PJ. Sensitivity of double contrast barium enema and colonoscopy for the detection of colorectal neoplasms. *Surg Endosc* 2001; **15**: 649-652 [PMID: 11591961 DOI: 10.1007/s004640000372]

23 **Zuckerman GR**, Prakash C, Askin MP, Lewis BS. AGA technical review on the evaluation and management of occult and obscure gastrointestinal bleeding. *Gastroenterology* 2000; **118**: 201-221 [PMID: 10611170]

24 **Chua AE**, Ridley LJ. Diagnostic accuracy of CT angiography in acute gastrointestinal bleeding. *J Med Imaging Radiat Oncol* 2008; **52**: 333-338 [PMID: 18811756 DOI: 10.1111/j.1440-1673.2008.01964.x]

25 **Artigas JM**, Martí M, Soto JA, Esteban H, Pinilla I, Guillén E. Multidetector CT angiography for acute gastrointestinal bleeding: technique and findings. *Radiographics* 2013; **33**: 1453-1470 [PMID: 24025935 DOI: 10.1148/rg.335125072]

26 **García-Blázquez V**, Vicente-Bártulos A, Olavarria-Delgado A, Plana MN, van der Winden D, Zamora J, EBM-Connect Collaboration. Accuracy of CT angiography in the diagnosis of acute gastrointestinal bleeding: systematic review and meta-analysis. *Eur Radiol* 2013; **23**: 1181-1190 [PMID: 23192375 DOI: 10.1007/s00330-012-2721-x]

27 **Rondonotti E**, Marmo R, Petracchini M, de Franchis R, Pennazio M. The American Society for Gastrointestinal Endoscopy (ASGE) diagnostic algorithm for obscure gastrointestinal bleeding: eight burning questions from everyday clinical practice. *Dig Liver Dis* 2013; **45**: 179-185 [PMID: 22921043 DOI: 10.1016/j.dld.2012.07.012]

28 **Ford PV**, Bartold SP, Fink-Bennett DM, Jolles PR, Lull RJ, Maurer AH, Seabold JE. Procedure guideline for gastrointestinal bleeding and Meckel's diverticulum scintigraphy. Society of Nuclear Medicine. *J Nucl Med* 1999; **40**: 1226-1232 [PMID: 10405149]

29 **Bunker SR**, Lull RJ, Tanasescu DE, Redwine MD, Rigby J, Brown JM, Brachman MB, McAuley RJ, Ramanna L, Landry A. Scintigraphy of gastrointestinal hemorrhage: superiority of 99mTc red blood cells over 99mTc sulfur colloid. *AJR Am J Roentgenol* 1984; **143**: 543-548 [PMID: 6331732 DOI: 10.2214/ajr.143.3.543]

30 **Ng DA**, Opelka FG, Beck DE, Milburn JM, Witherspoon LR, Hicks TC, Timmcke AE, Gathright JB. Predictive value of technetium Tc 99m-labeled red blood cell scintigraphy for positive angiogram in massive lower gastrointestinal hemorrhage. *Dis Colon Rectum* 1997; **40**: 471-477 [PMID: 9106699]

31 **Allen TW**, Tulchinsky M. Nuclear medicine tests for acute gastrointestinal conditions. *Semin Nucl Med* 2013; **43**: 88-101 [PMID: 23414825 DOI: 10.1053/j.semnuclmed.2012.11.001]

32 **Zuckerman GR**, Prakash C. Acute lower intestinal bleeding. Part II: etiology, therapy, and outcomes. *Gastrointest Endosc* 1999; **49**: 228-238 [PMID: 9925703]

33 **Winzelberg GG**, Froelich JW, McKusick KA, Waltman AC, Greenfield AJ, Athanasoulis CA, Strauss HW. Radionuclide localization of lower gastrointestinal hemorrhage. *Radiology* 1981; **139**: 465-469 [PMID: 6971455 DOI: 10.1148/radiology.139.2.6971455]

34 **Defreyne L**, Uder M, Vanlangenhove P, Van Maele G, Kunnen M, Kramann B. Angiography for acute lower gastrointestinal hemorrhage: efficacy of cut film compared with digital subtraction techniques. *J Vasc Interv Radiol* 2003; **14**: 313-322 [PMID: 12631635]

35 **Navuluri R**, Patel J, Kang L. Role of interventional radiology in the emergent management of acute upper gastrointestinal bleeding. *Semin Intervent Radiol* 2012; **29**: 169-177 [PMID: 23997408 DOI: 10.1055/s-0032-1326925]

36 **Walker TG**, Salazar GM, Waltman AC. Angiographic evaluation and management of acute gastrointestinal hemorrhage. *World J Gastroenterol* 2012; **18**: 1191-1201 [PMID: 22468082 DOI: 10.3748/wjg.v18.i11.1191]

37 **Walker TG**. Acute gastrointestinal hemorrhage. *Tech Vasc Interv Radiol* 2009; **12**: 80-91 [PMID: 19853226 DOI: 10.1053/j.tvir.2009.08.002]

38 **Eriksson LG**, Ljungdahl M, Sundbom M, Nyman R. Transcatheter arterial embolization versus surgery in the treatment of upper gastrointestinal bleeding after therapeutic endoscopy failure. *J Vasc Interv Radiol* 2008; **19**: 1413-1418 [PMID: 18755604 DOI: 10.1016/j.jvir.2008.06.019]

39 **Valji K**. The practice of interventional radiology with online cases and videos. Philadelphia, PA: Elsevier/Saunders, 2012

40 **Funaki B**. On-call treatment of acute gastrointestinal hemorrhage. *Semin Intervent Radiol* 2006; **23**: 215-222 [PMID: 21326767 DOI: 10.1055/s-2006-948758]

41 **Yap FY**, Omene BO, Patel MN, Yohannan T, Minocha J, Knuttinen MG, Owens CA, Bui JT, Gaba RC. Transcatheter embolotherapy for gastrointestinal bleeding: a single center review of safety, efficacy, and clinical outcomes. *Dig Dis Sci* 2013; **58**: 1976-1984 [PMID: 23361570 DOI: 10.1007/s10620-012-2547-z]

42 **Funaki B**, Kostelic JK, Lorenz J, Ha TV, Yip DL, Rosenblum JD, Leef JA, Straus C, Zaleski GX. Superselective microcoil embolization of colonic hemorrhage. *AJR Am J Roentgenol* 2001; **177**: 829-836 [PMID: 11566683 DOI: 10.2214/ajr.177.4.1770829]

43 **Evangelista PT**, Hallisey MJ. Transcatheter embolization for acute lower gastrointestinal hemorrhage. *J Vasc Interv Radiol* 2000; **11**: 601-606 [PMID: 10834491]

44 **Mirsadraee S**, Tirukonda P, Nicholson A, Everett SM, McPherson SJ. Embolization for non-variceal upper gastrointestinal tract haemorrhage: a systematic review. *Clin Radiol* 2011; **66**: 500-509 [PMID: 21371695 DOI: 10.1016/j.crad.2010.11.016]

45 **Eriksson LG**, Sundbom M, Gustavsson S, Nyman R. Endoscopic marking with a metallic clip facilitates transcatheter arterial embolization in upper peptic ulcer bleeding. *J Vasc Interv Radiol* 2006; **17**: 959-964 [PMID: 16778228 DOI: 10.1097/01.RVI.0000223719.79371.46]

46 **Aina R**, Oliva VL, Therasse E, Perreault P, Bui BT, Dufresne MP, Soulez G. Arterial embolotherapy for upper gastrointestinal hemorrhage: outcome assessment. *J Vasc Interv Radiol* 2001; **12**: 195-200 [PMID: 11265883]

47 **Loffroy R**, Guiu B, D'Athis P, Mezzetta L, Gagnaire A, Jouve JL, Ortega-Deballon P, Cheynel N, Cercueil JP, Krausé D. Arterial embolotherapy for endoscopically unmanageable acute gastroduodenal hemorrhage: predictors of early rebleeding. *Clin Gastroenterol Hepatol* 2009; **7**: 515-523 [PMID: 19418601 DOI: 10.1016/j.cgh.2009.02.003]

48 **Loffroy R**, Guiu B, Mezzetta L, Minello A, Michiels C, Jouve JL, Cheynel N, Rat P, Cercueil JP, Krausé D. Short- and long-term results of transcatheter embolization for massive arterial hemorrhage from gastroduodenal ulcers not controlled by endoscopic hemostasis. *Can J Gastroenterol* 2009; **23**: 115-120 [PMID: 19214287]

49 **Toyoda H**, Nakano S, Kumada T, Takeda I, Sugiyama K, Osada T, Kiriyama S. Estimation of usefulness of N-butyl-2-cyanoacrylate-lipiodol mixture in transcatheter arterial embolization for urgent control of life-threatening massive bleeding from gastric or duodenal ulcer. *J Gastroenterol Hepatol* 1996; **11**: 252-258 [PMID: 8742922]

50 **Frisoli JK**, Sze DY, Kee S. Transcatheter embolization for the treatment of upper gastrointestinal bleeding. *Tech Vasc Interv Radiol* 2004; **7**: 136-142 [PMID: 16015558]

51 **Abdel-Aal AK**, Bag AK, Saddekni S, Hamed MF, Ahmed FY. Endovascular management of nonvariceal upper gastrointestinal hemorrhage. *Eur J Gastroenterol Hepatol* 2013; **25**: 755-763 [PMID: 23492985 DOI: 10.1097/MEG.0b013e32835fb9a9]

52 **Loffroy RF**, Abualsaud BA, Lin MD, Rao PP. Recent advances in endovascular techniques for management of acute nonvariceal upper gastrointestinal bleeding. *World J Gastrointest Surg* 2011; **3**: 89-100 [PMID: 21860697 DOI: 10.4240/wjgs.v3.i7.89]

53 **Lubarsky M**, Ray CE, Funaki B. Embolization agents-which one should be used when? Part 1: large-vessel embolization. *Semin Intervent Radiol* 2009; **26**: 352-357 [PMID: 21326545 DOI: 10.1055/s-0029-1242206]

54 **Ledermann HP**, Schoch E, Jost R, Decurtins M, Zollikofer CL. Superselective coil embolization in acute gastrointestinal hemorrhage: personal experience in 10 patients and review of the literature. *J Vasc Interv Radiol* 1998; **9**: 753-760 [PMID: 9756062]

55 **Toyoda H**, Nakano S, Takeda I, Kumada T, Sugiyama K, Osada T, Kiriyama S, Suga T. Transcatheter arterial embolization for massive bleeding from duodenal ulcers not controlled by endoscopic hemostasis. *Endoscopy* 1995; **27**: 304-307 [PMID: 7555935 DOI: 10.1055/s-2007-1005697]

56 **van Vugt R**, Bosscha K, van Munster IP, de Jager CP, Rutten MJ. Embolization as treatment of choice for bleeding peptic ulcers in high-risk patients. *Dig Surg* 2009; **26**: 37-42 [PMID: 19155626 DOI: 10.1159/000193476]

57 **Defreyne L**, Vanlangenhove P, De Vos M, Pattyn P, Van Maele G, Decruyenaere J, Troisi R, Kunnen M. Embolization as a first approach with endoscopically unmanageable acute nonvariceal gastrointestinal hemorrhage. *Radiology* 2001; **218**: 739-748 [PMID: 11230648 DOI: 10.1148/radiology.218.3.r01mr05739]

58 **Darcy M**. Treatment of lower gastrointestinal bleeding: vasopressin infusion versus embolization. *J Vasc Interv Radiol* 2003; **14**: 535-543 [PMID: 12761306]

59 **Kusano S**, Murata K, Ohuchi H, Motohashi O, Atari H. Low-dose particulate polyvinylalcohol embolization in massive small artery intestinal hemorrhage. Experimental and clinical results. *Invest Radiol* 1987; **22**: 388-392 [PMID: 3496319]

60 **Gordon RL**, Ahl KL, Kerlan RK, Wilson MW, LaBerge JM, Sandhu JS, Ring EJ, Welton ML. Selective arterial embolization for the control of lower gastrointestinal bleeding. *Am J Surg* 1997; **174**: 24-28 [PMID: 9240947 DOI: 10.1016/S0002-9610(97)00044-5]

61 **Nicholson AA**, Ettles DF, Hartley JE, Curzon I, Lee PW, Duthie GS, Monson JR. Transcatheter coil embolotherapy: a safe and effective option for major colonic haemorrhage. *Gut* 1998; **43**: 79-84 [PMID: 9771409]

62 **Peck DJ**, McLoughlin RF, Hughson MN, Rankin RN. Percutaneous embolotherapy of lower gastrointestinal hemorrhage. *J Vasc Interv Radiol* 1998; **9**: 747-751 [PMID: 9756061]

63 **Hur S**, Jae HJ, Lee M, Kim HC, Chung JW. Safety and efficacy of transcatheter arterial embolization for lower gastrointestinal bleeding: a single-center experience with 112 patients. *J Vasc Interv Radiol* 2014; **25**: 10-19 [PMID: 24286939 DOI: 10.1016/j.jvir.2013.09.012]

64 **Yata S**, Ihaya T, Kaminou T, Hashimoto M, Ohuchi Y, Umekita Y, Ogawa T. Transcatheter arterial embolization of acute arterial bleeding in the upper and lower gastrointestinal tract with N-butyl-2-cyanoacrylate. *J Vasc Interv Radiol* 2013; **24**: 422-431 [PMID: 23380738 DOI: 10.1016/j.jvir.2012.11.024]

65 **Huang CC**, Lee CW, Hsiao JK, Leung PC, Liu KL, Tsang YM, Liu HM. N-butyl cyanoacrylate embolization as the primary treatment of acute hemodynamically unstable lower gastrointestinal hemorrhage. *J Vasc Interv Radiol* 2011; **22**: 1594-1599 [PMID: 21875815 DOI: 10.1016/j.jvir.2011.07.018]

66 **Frodsham A**, Berkmen T, Ananian C, Fung A. Initial experience using N-butyl cyanoacrylate for embolization of lower gastrointestinal hemorrhage. *J Vasc Interv Radiol* 2009; **20**: 1312-1319 [PMID: 19800541 DOI: 10.1016/j.jvir.2009.06.031]

67 **Lang EK**. Transcatheter embolization in management of hemorrhage from duodenal ulcer: long-term results and complications. *Radiology* 1992; **182**: 703-707 [PMID: 1535883 DOI: 10.1148/radiology.182.3.1535883]

68 **Lee CW**, Liu KL, Wang HP, Chen SJ, Tsang YM, Liu HM. Transcatheter arterial embolization of acute upper gastrointestinal tract bleeding with N-butyl-2-cyanoacrylate. *J Vasc Interv Radiol* 2007; **18:** 209-216 [PMID: 17327553 DOI: 10.1016/j.jvir.2006.12.003]

69 **Lenhart M**, Paetzel C, Sackmann M, Schneider H, Jung EM, Schreyer AG, Feuerbach S, Zorger N. Superselective arterial embolisation with a liquid polyvinyl alcohol copolymer in patients with acute gastrointestinal haemorrhage. *Eur Radiol* 2010; **20**: 1994-1999 [PMID: 20379821 DOI: 10.1007/s00330-010-1762-2]

70 **Bush HL**, Nabseth DC. Intravenous nitroglycerin to improve coronary blood flow and left ventricular performance during vasopressin therapy. *Surg Forum* 1979; **30**: 226-228 [PMID: 120016]

71 **Gomes AS**, Lois JF, McCoy RD. Angiographic treatment of gastrointestinal hemorrhage: comparison of vasopressin infusion and embolization. *AJR Am J Roentgenol* 1986; **146**: 1031-1037 [PMID: 3485897 DOI: 10.2214/ajr.146.5.1031]

72 **Leitman IM**, Paull DE, Shires GT. Evaluation and management of massive lower gastrointestinal hemorrhage. *Ann Surg* 1989; **209**: 175-180 [PMID: 2783842]

73 **Bandi R**, Shetty PC, Sharma RP, Burke TH, Burke MW, Kastan D. Superselective arterial embolization for the treatment of lower gastrointestinal hemorrhage. *J Vasc Interv Radiol* 2001; **12**: 1399-1405 [PMID: 11742013]

74 **Mallory A**, Schaefer JW, Cohen JR, Holt SA, Norton LW. Selective intra-arterial vasopression in fusion for upper gastrointestinal tract hemorrhage: a controlled trial. *Arch Surg* 1980; **115**: 30-32 [PMID: 6985789]

75 **Formanek G**, Frech RS, Amplatz K. Arterial thrombus formation during clinical percutaneous catheterization. *Circulation* 1970; **41**: 833-839 [PMID: 5444526]

76 **Barrett BJ**, Parfrey PS. Clinical practice. Preventing nephropathy induced by contrast medium. *N Engl J Med* 2006; **354**: 379-386 [PMID: 16436769 DOI: 10.1056/NEJMcp050801]

77 **Murphy SW**, Barrett BJ, Parfrey PS. Contrast nephropathy. *J Am Soc Nephrol* 2000; **11**: 177-182 [PMID: 10616853]

P- Reviewers: Chan WP, Murata S, Metwalli ZA
S- Editor: Song XX **L- Editor**: A **E- Editor**: Liu SQ

World Journal of Radiology

Online Submissions: http://www.wjgnet.com/esps/
bpgoffice@wjgnet.com
doi:10.4329/wjr.v6.i4.93

World J Radiol 2014 April 28; 6(4): 93-105
ISSN 1949-8470 (online)

REVIEW

FMRI contributions to addressing autobiographical memory impairment in temporal lobe pathology

Ekaterina J Denkova, Liliann Manning

Ekaterina J Denkova, Liliann Manning, Department of Psychology, University of Strasbourg, 67000 Strasbourg, France
Liliann Manning, Cognitive Neuropsychology and Physiopathology of Schizophrenia, INSERM U1114, 67000 Strasbourg, France
Author contributions: Denkova EJ and Manning L contributed to this review equally.
Correspondence to: Dr. Ekaterina J Denkova, Department of Psychology, University of Strasbourg, 12 rue Goethe, 67000 Strasbourg, France. ekaterina.denkova@yahoo.ca
Telephone: +33-3-68851927 Fax: +33-3-68851947
Received: December 17, 2013 Revised: February 20, 2014
Accepted: March 13, 2014
Published online: April 28, 2014

Abstract

Episodic autobiographical memory (AM) allows one, through the recollection of sensory-perceptual details, thoughts and feelings, to become aware of an event as belonging to one's own past as well as being able to project into one's future. Because AM provides a sense of self-continuity, contributes to the integrity of the self, and helps predicting future experiences, any deficit of AM may have debilitating consequences for everyday life functioning. Understanding AM failure and the underlying neural mechanisms has the potential to shed light on brain reorganization mechanisms and engagement of compensatory processes. Functional magnetic resonance imaging (fMRI) provides the most promising imaging method to tackle these issues. We reviewed evidence from the few studies that used fMRI to investigate the functionality of the residual tissue, the neural reorganization and compensatory mechanisms in patients with neurological conditions due to impaired medial temporal lobe. Overall, these studies highlight the importance of the left hippocampus, which when atrophied and not functional leads to AM deficits but its residual functionality may support relatively normal AM recollection. When damaged hippocampal tissue is not functional, other brain regions (*e.g.*, the medial prefrontal cortex) may be involved to compensate impairment, but they appear generally ineffective to support detailed episodic recollection.

Key words: Functional magnetic resonance imaging; Autobiographical memory; Amnesia; Medial temporal lobe; Memory deficit; Reorganization

Core tip: Functional magnetic resonance imaging investigations of patients with impaired autobiographical memory (AM) can greatly contribute to further our understanding of brain reorganization mechanisms and engagement of compensatory processes after damage to the medial temporal lobe. These investigations are reviewed here. Overall, they highlight the importance of the left hippocampus, which when atrophied and not functional leads to deficits in AM but its residual functionality may support relatively normal AM recollection. When damaged hippocampal tissue is not functional, other brain regions (*e.g.*, the medial prefrontal cortex) may be involved to compensate impairment, but they appear generally ineffective to support detailed recollection.

Denkova EJ, Manning L. FMRI contributions to addressing autobiographical memory impairment in temporal lobe pathology. *World J Radiol* 2014; 6(4): 93-105 Available from: URL: http://www.wjgnet.com/1949-8470/full/v6/i4/93.htm DOI: http://dx.doi.org/10.4329/wjr.v6.i4.93

INTRODUCTION

Remembering autobiographical memories (AM) involves recollection of contextual information (time and place)

and sensory-perceptual and affective details of personal experiences with a sense of self-awareness[1-3]. AM, not surprisingly, contributes to both one's sense of personal identity (who we are) and sense of self-continuity. Over the last two decades, there has been a growing interest in understanding the neural correlates of normal AM and, more recently, impaired AM. The reasons of the remarkable increase in the number of studies in this topic is, very likely, the mentioned AM contribution to the construction of the sense of self across time, but also the important social role AM plays in the development of new relationships and the nurturing of existing ones, and most particularly, its role as a directive function, where the past serves as a basis for guiding present and future behaviors[4,5]. In the context of the broader issue under consideration in this special topic [with focus on functional magnetic resonance imaging (fMRI)], the present review aims to discuss emerging research that highlights the usefulness of fMRI in the examination of AM in patients with damage to the core memory structures in the medial temporal lobe (MTL). The emphasis of this review is, therefore, on fMRI investigations of AM impairment due to neurological conditions affecting the MTL. The decision to focus on the MTL is driven by evidence that MTL plays a pivotal role in normal AM functioning and its damage typically leads to amnesia for past events[6-9] (but see also[10]) and that fMRI examinations of AM in neurological patients, which to date are limited in number, have been more often reported in the case of patients with damage to the MTL. The underlying question we would like to tackle is to what extent these investigations shed light on the functionality of the residual tissue, the neural reorganization and compensatory mechanisms (either efficient or not) in the case of damage to the MTL. Before discussing the fMRI studies of AM in patients with MTL damage, we introduce AM and summarize the highlights of neuroimaging evidence in healthy participants to provide the context to discuss functional neuroimaging findings in pathology.

THEORETICAL CONSIDERATIONS OF AM

Episodic AM allows one to become aware of an event as belonging to one's own past as well as being able to project into one's future. This sense of self-continuity across time[2,3,11] is grounded in the recollection of sensory-perceptual details, thoughts and feelings. Typically, episodic memory has been distinguished from semantic memory, which refers to general knowledge, knowledge about public facts and people, as well as personal knowledge (*e.g.*, date of birth, the name of our parents and friends). However, these systems are highly interdependent[12] in relation to the self. Turning back to episodic AM, some authors consider that it is a uniquely human system[13] (but see[14] for a different standpoint). Moreover, Tulving's Serial Parallel Independent model places this memory system at the apex of a pyramid, which implies the highest memory achievement in evolution[15]. Tulving *et al*[2] defined AM as consisting of three major constructs: sense of self, autonoetic consciousness and subjectively sensed time. But even more closely related to the self, is Conway's Self Memory System[1,12]. Very briefly, Conway views episodic memories and conceptual autobiographical knowledge as discrete systems that both operate with the "working self" in a bidirectional manner. The working self is conceived as a mechanism that controls access to memories according to the individual's present goals. Importantly, the working self is constrained by the memories and knowledge within the autobiographical knowledge base.

Recently, some studies show that the contribution of AM to the sense of self is not crucial. Klein[16,17] and Klein *et al*[18] presented a series of patients both studied by him and reported in the literature, who have lost the entire fund of episodic memory and who are unable to simulate future personal events, but retain the sense of self. However, a distinction is made between the sense of self, which is preserved in amnesic patients[19] and the sense of self-continuity across time, which depends on AM (Klein SB, personal communication to LM, December, 2013).

Importantly, recollection of past personal experience is considered to be a reconstructive process with memories recreated from their constituent elements. Particularly, autobiographical memories are not static records of the past; rather they are considered as mental reconstructions, which are constrained by two simultaneous, even contradictory, demands: correspondence with the real event and coherence, as time goes by, with the individual's self-image. More precisely, memory reconstruction must reflect reality by providing sensory-perceptive and eventually affective details that represent, as closely as possible, the experience and also be in accordance with the rememberer's current self-image and goals[12]. By making available memories that match current self-beliefs and goals, the main function of AM would be to maintain the integrity of the self[12].

Bearing in mind that AM provides a sense of self-continuity, contributes to the integrity of the self, and helps predicting future experiences, it is not surprising that AM impairment may have debilitating consequences for everyday life functioning. Consequently, understanding AM failure and the underlying neural mechanisms has the potential not only to strengthen the progress of memory research, but importantly, to shed light on brain reorganization mechanisms and eventually to help in planning treatment and in monitoring the effects of therapeutical interventions with the final aim to achieve better management of patients with AM deficits.

FMRI EXAMINATION OF NORMAL AM FUNCTIONING

The advent of fMRI made the examination *in vivo* of different human abilities, in general, possible. More particularly, fMRI (in contrast to earlier neuroimaging techniques, such as positron emission tomography) provides

the most promising new imaging method and offers a number of important advantages in the study of neural correlates of human memory. Among the main fMRI strengths are the improved spatial resolution, the fast speed of data acquisition which allows more flexible experimental designs and the unrestricted number of observations due to the absence of radiation exposure. Moreover, in the last decade, fMRI has undergone a rapid development and provided new ways to design experiments (*e.g.*, event-related, self-paced designs) and to analyze data (*e.g.*, independent component analysis, spatiotemporal partial least squares analysis, psychophysiological interactions analysis, dynamic causal modelling, multi-voxel pattern analysis) allowing segregation of the time-course of memory retrieval processes, examination of the connectivity among brain regions and investigation of memory representation in specific brain regions. This continuous progress has led to improved and refined testing of hypotheses about the neural correlates of both normal and impaired AM.

Evidence from fMRI studies in healthy participants allowed the establishing of a brain network of AM retrieval comprising the MTL, prefrontal cortex (PFC) and posterior cortices[20-22]. Despite the proliferation of functional neuroimaging studies of AM over the last 10-15 years, many of the critical issues (*e.g.*, MTL involvement according to the remoteness of memories, lateralization of the AM networks) continue to be debated, leading nevertheless to greater refinement of the theories derived from the lesion research. For instance, there is a debate regarding the involvement of MTL, especially the hippocampus, in retrieval of personal events according to the age of memories. This debate originated from the lesion studies and is reflected in fMRI studies in healthy subjects. On the one hand, the Standard Consolidation Theory states that memories (without making a distinction between episodic and semantic memories) are initially dependant on the MTL but over time, they undergo consolidation in the neocortical structures and eventually become independent of the MTL[23]. On the other hand, the Multiple Trace Theory postulates a lifelong involvement of the MTL for retrieval of episodic and context-specific memories[6,24]. Recently, the latter has been updated to explicitly include a transformation account of memory, which considers the dynamic nature of memories and suggests that episodic memories may transform to semantic or gist-like versions represented in neocortical areas outside of the hippocampus, but those that continue to contain rich episodic/contextual details remain dependant on the hippocampus[25,26].

MTL

Neuroimaging evidence suggests that the MTL is a crucial node in the AM retrieval network[21,27] involved in binding together the multimodal representations of an episode. Specifically, studies directly comparing autobiographical to semantic memory retrieval revealed greater engagement of the MTL, particularly on the left side[28-30]. Of note, MTL activation observed by some semantic memory studies involving famous people recognition[31,32] could be explained by the association of this semantic information with autobiographical memories[33], as suggested by lesion research[34,35]. As for the MTL's involvement according to age of memories, an increasing number of fMRI studies provided evidence that, when phenomenological qualities and especially vividness are considered, MTL activations are observed for retrieval of rich and vivid and both recent and remote autobiographical memories[36-41], which resonates with the Multiple Trace Theory positing long-life involvement of MTL for vivid context-specific recollections.

Prefrontal cortex

Available evidence also highlights the role of different PFC sub-regions in AM retrieval[22,27]. Specifically, among the PFC sub-regions, the ventrolateral PFC and the medial PFC appear to be systematically linked to retrieval of personal events[27,38].

Lateral PFC: Systematic activation of the ventrolateral PFC during recollection of autobiographical memories is associated with successful memory retrieval, involving initial strategic search and selection of appropriate information[27,42,43]. Specifically, activity in the lateral PFC has been observed early during retrieval[28,29,44], supporting therefore its role in strategic search operations and initial recovery processes consistent with current models of AM[1] that emphasize the reconstructive retrieval of memories. Additionally, the more ventral (orbital) portion of the lateral PFC, part of the frontotemporal junction interconnected through the ventral branch of the uncinate fascicle, has been attributed a crucial role in ecphory (triggering) of memory retrieval[45,46] and synchronisation of emotional and factual components of the personal memories during conscious self re-experiencing[47-49]. The latter is also supported by recent evidence suggesting the involvement of parts of the ventrolateral PFC in enhanced re-experiencing of emotional autobiographical memories[50].

Medial PFC: Activation of the medial PFC is also systematically reported during recollection of autobiographical memories[27] and linked to the role of medial PFC in self-referential processes[51], of which AM is an essential part. Indeed, there is evidence that increased activity in medial PFC distinguished real life AM from laboratory-based episodic memory imaging studies[38,52,53] and its more ventral portions are associated with real self-relevant events[54] and self-perspective[55]. Recently, ventromedial PFC has been found to contain more information about remote memories (although both recent and remote memories are represented there[37]). It should be noted that overall in the neuroimaging research, the medial PFC is linked to a variety of functions[56], such as self-referential[51] and emotional[57] processing, mentalizing[58,59], intuitive assessment of "felt rightness"[60] as well as in some regulatory

mechanisms[61]. Therefore, it can be suggested that medial PFC might in general be supporting processes related to self-awareness and self-regulation.

Posterior cortices

Retrieval of autobiographical memories in healthy participants also leads to activations in the posterior cortices (*e.g.*, precuneus, visual cortices), which are considered to support the multimodal and visual representations associated with the event and visual imagery (and visualized re-experiencing)[20,62]. Specifically, fMRI studies provided evidence that posterior cortices are later involved during (re)construction of autobiographical memories[28,29] to support the retrieval of specific details. For instance, precuneus because of its role in egocentric (view-dependant, relative to the observer) representation of a place, has been thought critical for autonoetic awareness in remembering events from a first person perspective[63]. This is by comparison to MTL, which is involved in allocentric (view-independent) representations[64], but only those that are rich instead of schematic[7].

In summary, fMRI investigations of AM in normal conditions have been very informative in establishing what is called the typical AM brain network, which can be used as a framework for investigation and better understanding of neural correlates of AM impairment.

FMRI INVESTIGATION OF AM IMPAIRMENT IN PATHOLOGIES AFFECTING MTL

Over the past decade, the rapid development of functional neuroimaging techniques and experimental designs (more flexible event-related, self-paced designs, shortened repetition times, new analyzing tools) has made the use of functional neuroimaging protocols in patients possible, which, besides clinical issues, advances our understanding of the neural networks of memory[65,66] and its reorganization in case of damage. The use of functional neuroimaging techniques in brain damaged patients can help to better understand not only how damage alters the neural network supporting AM retrieval, but also potential reorganization of this network through compensatory mechanisms (efficient or not) solicited to cope with memory impairment. It is important to note, however, that the combined use of neuropsychological and neuroimaging methods has advantages over the use of either approach alone[65,66]. The purpose of the review is not to provide an exhaustive literature review of memory impairment due to brain damage and its assessment with neuroimaging in general (for more general reviews on human memory disorders and the application of neuroimaging, we refer the readers to[65,67,68]). Rather the aim is to present and discuss examples of studies that have used fMRI in particular (as the most advanced neuroimaging method and targeted by the scope of the present special topic) to investigate AM impairment in patients with damage to the MTL regions, because of their critical importance for retrieval of specific autobiographical events as highlighted by functional neuroimaging research in normal subjects and lesion research (although the latter still continues to debate the long-life involvement of the hippocampus). Therefore, we will discuss studies that use fMRI protocols to investigate AM in patients with different neurological conditions affecting the MTL and hence, shed light on the functionality of damaged MTL and the potential reorganization of the AM network. We selected the studies based on that they examine AM through fMRI in pathologies with overt damage to the MTL (Table 1). The neurological conditions presented below differ in terms of the age at which they occur, their focal or diffuse nature, and progression.

Developmental amnesia

Developmental amnesia is a memory disorder associated with selective hippocampal damage resulting from hypoxic/ischemic episodes that occur perinatally or early in childhood[69]. Typically, developmental amnesia is characterized by severely impaired episodic AM and relatively preserved semantic memory[70,71], which makes it possible to investigate developmental deficits selectively and to shed light on the neural reorganisation of the AM network due to early life damage. In fact, among the first neuroimaging studies of AM in amnesic patients is the study carried out by Maguire *et al*[72], who used fMRI in the case of a developmental amnesic patient, Jon (initially reported by Vargha-Khadem *et al*[71]). Jon presented with impaired AM (but he was able to recall some personal memories) and had a relatively preserved semantic memory[72]. Jon showed a similar pattern of brain activations to control subjects during memory retrieval but the activations and the interactions among them were different from those observed in controls. Of particular interest, Jon's retrieval of autobiographical events was associated with increased bilateral activity of the hippocampus, in spite of the 50% volume loss bilaterally. Moreover, hippocampus and medial PFC were significantly more activated during retrieval of events for which Jon had clear and conscious recollection (autonoetic consciousness) compared to those he knew but could not remember experiencing. Overall, the findings suggest that the residual hippocampal tissue was functional and contributed to retrieval of the few preserved autobiographical "islands". Moreover, they point out the crucial role of autonoetic awareness during AM retrieval mediated, very likely, by the medial PFC. Therefore, these findings provide insights to mechanisms of brain plasticity[73].

Hypoxia (in adulthood)

Deprivation of oxygen supply (hypoxia) in adulthood also leads to damage to the MTL, specifically the hippocampus, and severe deficit in memory of past events[74-76]. By comparison to patients with developmental amnesia, patients with hypoxic MTL damage in adulthood showed a much more severe pattern of memory impairment. In

Table 1 Summaries of functional magnetic resonance imaging studies investigating autobiographical memory in patients with medial temporal lobe damage

Ref.	Pathology	Patients	Lesion side	Remote memory profile	Compensatory Activations
Addis *et al*[97]	Temporal lobe epilepsy	11 patients	Left	Mild impairment episodic AM	mPFC, posterior medial structures
				Relative preservation semantic AM	mPFC-PHG connectivity
Berry *et al*[124]	Limbic encephalitis	Single-case, Mrs B	Bilateral	Impaired AM (recent events)	Left vlPFC, posterior cortices
Maguire *et al*[72]	Developmental amnesia	Single-case, patient Jon	Bilateral	Impaired AM (few preserved events) relatively normal semantic memory	Functional residual hippocampi mPFC
Maguire *et al*[77]	Hypoxia in late age	Single-case, patient VC	Bilateral	Severe impairment AM	Lateral temporal areas (for personal facts)
Maguire *et al*[110]	Semantic dementia	Single-case, patient AM	Initially left later bilateral	Initially relatively intact AM followed by gradual deterioration	Year 1: Initially functional right and residual left hippocampi, Year2: mPFC, vlPFC, precuneus, Year 3: few occipito-temporal areas
Manning *et al*[98]	Temporal lobe epilepsy	Single-case, patient JR	Left	Preserved AM, impaired public memory	Contro-lesional right MTL, mPFC, posterior cortices
Meulenbroek *et al*[113]	Alzheimer's disease	21 patients	Bilateral	Episodic-to-semantic shift	mPFC, left vlPFC, posterior cortices
Viard *et al*[111]	Semantic dementia	Patients JPL and EP	JPL: bilateral	JPL: impaired AM	JPL: right hippocampus, vlPFC, occipital areas
			EP: bilateral but sparing hippocampi	EP: initially relatively preserved AM	EP: both hippocampi

AM: Autobiographical memory; mPFC: Medial prefrontal cortex; vlPFC: Ventro-lateral prefrontal cortex; MTL: Medial temporal lobe; PHG: Parahippocampal gyrus.

an fMRI examination, Maguire *et al*[77] investigated memory in a patient, VC (initially reported by Cipolotti *et al*[75]), who had MTL damage due to hypoxia in late adulthood. Given that VC did not have reliable memory of personal past events to be investigated in a functional neuroimaging procedure[78,79], only his memory for personal facts and general knowledge were examined. In the context of broadly comparable to control subjects' memory network, VC exhibited increased activity in lateral temporal regions compared to controls and did not show any activity in the residual hippocampi, while hippocampal activations were revealed in controls as well as in developmental amnesic patient Jon for personal facts. These findings suggest that in the case of hypoxic MTL damage in adulthood, deficits of AM are much more severe and could be due to the absence of residual functionality in lesioned hippocampi. Overall, combined together findings from developmental and adult-acquired amnesia due to hypoxia point to the importance of age at which damage occurs, which is of great importance for reorganization and compensatory brain mechanisms. This issue clearly needs further investigation by systematic fMRI examination of patients with damage occurring at different periods of life.

Temporal lobe epilepsy

Temporal lobe epilepsy (TLE) is a chronic neurological condition characterized by partial epileptic seizures originating in the temporal lobe, accompanied usually by hippocampus sclerosis[80] and associated with memory deficit[81]. Overall, memory for the past has been much less investigated than anterograde memory (*i.e.*, acquisition of new information) in patients with TLE. However, in the last decade an increasing number of studies also explored remote memory in TLE patients[82-88]. They revealed that TLE affects remote memory, particularly AM, with left TLE leading to severe AM deficit. Similarly to clinical neuropsychological studies, the majority of the functional neuroimaging studies focused on testing anterograde memory[89,90] and on pre-surgical evaluation to predict post-surgical memory changes[91-96], while only a handful of functional neuroimaging studies examined the neural correlates of AM in patients with TLE[97,98] (see also[99] for patients with transient epileptic amnesia). The studies by Manning *et al*[98] and Addis *et al*[97] presented left TLE patients with different AM profiles, which illustrates the fact that the same disease can lead to different patterns of memory performance and brain reorganization.

In a single-case report, Manning *et al*[98] investigated the interaction between AM and semantic memory in a patient, JR (initially reported by Manning *et al*[100]), who underwent surgical resection of the left MTL for treatment of long-standing TLE with teenage onset of seizures. JR presented a very rare pattern of remote memory dissociation, such as preserved AM and selectively impaired semantic memory for public events and famous people. During retrieval of autobiographical episodes associated with famous people, JR showed increased activations in the intact right MTL (parahippocampal gyrus), several posterior cortices (posterior cingulate cortex, precuneus, temporo-occipital junction) and medial PFC. These findings suggest that contralesional right MTL may be sufficient to adaptively take charge of AM in case of left MTL damage according to the age at which epilepsy

occurred and the developmental course of AM ability, which typically emerges gradually across the preschool years.

Addis *et al*[97] investigated the AM cerebral network in a group of patients with left TLE with significant left hippocampal atrophy and mild AM impairment (reflected in reduction of the episodic details of memories). The authors found that in the absence of significant activation and connections of the residual left hippocampal tissue, retrieval of personal memories in left TLE patients was associated with increased activations in the posterior cortices, including posterior cingulate/retrosplenial and precuneus, right hippocampus (albeit sub-threshold) as well as strong direct connections between the left medial posterior cortices (posterior cingulate/retrosplenial) and left medial PFC, and between left parahippocampal gyrus and left medial PFC. These findings suggest that the AM impairment in left TLE could be due to reduced engagement and connections of the lesioned left hippocampus, compensated to some degree by pathways involving medial PFC and medial posterior cortices, which were insufficient to support detailed episodic-specific recollections.

Overall, the above-mentioned studies provided complementary evidence that depending on the onset of the epilepsy, damage to the left hippocampus can differently affect AM and a different pattern of reorganization of the AM network can be observed, despite several apparent differences between the two studies (single case *vs* group study, after *vs* before surgical treatment). Specifically, in a case of late childhood/teenage occurring epilepsy, right MTL could be sufficient to successfully mediate AM. Otherwise, regions outside MTL could be solicited to compensate left MTL damage, such as medial PFC and medial posterior cortices, which support residual AM (less detailed memories) but appear inefficient to maintain an overall normal level of detailed, episodic-specific AM recollections.

Neurodegenerative diseases

Neurodegenerative diseases are neurological conditions characterized by progressive degeneration and/or death of neuronal cells. Of particular interest in the study of memory are semantic dementia, a form of frontotemporal dementia, and Alzheimer's disease since both involve neurodegenerative processes in the temporal lobes[101,102]. Usually in the memory literature, semantic dementia and Alzheimer's disease present a dissociable neuropsychological memory profile at an initial stage of the disease[103,104]. While semantic dementia is characterized by a profound and amodal loss of semantic memory in the context of relatively preserved episodic AM[105-107], Alzheimer's disease is typically characterized by severe impairment of episodic AM in the context of relative sparing of semantic memory[108,109]. Despite the interesting dissociation within remote memory observed in these two neurodegenerative diseases, there are only a handful of fMRI studies examining AM in patients with semantic dementia and Alzheimer's disease.

Semantic dementia: Only two studies, to our knowledge to date, have investigated the neural correlates of AM in semantic dementia using fMRI[110,111], one of them presenting a longitudinal fMRI follow-up of a semantic dementia patient[110]. The fMRI studies provided evidence of efficient and inefficient compensatory mechanisms, which led to relative initial maintenance of normal level of AM performance and to impaired, namely lacking episodic-specificity AM, performance, respectively.

In a single-case report, Maguire *et al*[110] used fMRI to investigate neural correlates of AM in a semantic dementia patient, AM, as a function of the progression of the dementia at three separate occasions (years 1, 2 and 3). Initially, the patient showed relatively normal AM scores, but with the progression of the disease his AM gradually deteriorated. To begin with, the patient had volume loss in the left hippocampus and left anterior lateral temporal cortex. However, at year 3, the atrophy encompassed the temporal lobes bilaterally, including both hippocampi. As for changes through time of the AM retrieval network, initially at year 1, the patient exhibited increased activations in regions of the consensual AM network, including the intact right hippocampus, and importantly increased activation of the remnant left hippocampus, which was not further observed during the following fMRI examinations (years 2 and 3). Moreover, at year 2, the patient showed increased activations of ventromedial PFC and precuneus, among other brain regions, to finally end up at year 3 with disengagement of the AM network, except for the occipitotemporal cortices. These findings reveal how the progression of dementia and MTL atrophy could affect AM retrieval and the associated neural correlates. Initially, despite the volume loss in the left hippocampus, the residual hippocampal tissue was still functional and therefore could support relatively preserved recollection of personal events. Over the course of the dementia process, the hippocampus became inactive and it seemed to be compensated by increased activity in the medial PFC and precuneus, which, with the progression of the dementia, appeared in turn to become non-operational.

Viard *et al*[111] used fMRI to investigate AM according to the remoteness of memories in two semantic dementia patients, JPL and EP, with different patterns of hippocampal atrophy and AM profiles. While JPL presented with impaired AM recollections (reflected in reduction of specific episodic details) and severe atrophy of both hippocampi, EP presented with initially preserved AM recollections with greater reliance on visual imagery than healthy controls and relative preservation of both hippocampi, despite atrophy in adjacent temporal cortices. In terms of brain activations and interactions, while JPL exhibited less activity in the left anterior hippocampus (remote memories) and increased activity in the right posterior hippocampus, functionally connected with the posterior occipital cortices, EP exhibited increased activity in both left and right anterior hippocampi (for both recent and remote memories), which were functionally connected to each other. These findings suggest that

atrophy together with absence of functionality in the residual hippocampal tissue might explain impaired AM, suggesting that activation in right posterior hippocampus and interactions with occipital cortices may have been recruited to compensate left hippocampal deficit, but that this compensatory mechanism was insufficient to support a normal level of rich episodic-specific recollections.

Overall, evidence from fMRI studies of AM in semantic dementia patients highlights the importance of the left hippocampus in retrieval of vivid and specific autobiographical memories, which when atrophied and not functional leads to impaired AM. In the case of late age and progressive damage of MTL, initial functionality of the remnant left hippocampus, rather than the right hippocampus, could support a relatively normal level of AM performance at an early stage of the disease. Subsequent increased engagement of medial PFC and precuneus could be seen as a compensatory mechanism reflecting attempts to maintain AM, although it had gradually declined. It could be also speculated that precuneus involvement could reflect retrieval processes that are based on a more egocentric representation and greater reliance on a self-referential perspective during recollection.

Alzheimer's disease: Episodic to semantic shift is usually reported in patients with Alzheimer's disease and deficit in episodic AM recollection is the hallmark of the disease, even being detected at the very preliminary stage of the disease, known as amnesic mild cognitive impairment[112]. The pattern of "semantization" of episodic AM has been observed in a group of 21 patients diagnosed with early stage, probable Alzheimer's disease who were examined using fMRI[113]. Specifically, these patients presented with a decline in episodic recollection of personal experiences, which contained more semantic and repetitive information and also atrophy in both hippocampi. At the level of brain activations, patients with Alzheimer's disease showed increased activity in ventromedial PFC, left ventrolateral PFC and posterior cortices (lingual gyrus and precuneus). Moreover, increased activity in ventromedial and ventrolateral PFC was linked to decreased volume in the hippocampus. These findings suggest that increased engagement of ventromedial and ventrolateral PFC could reflect a compensatory mechanism supporting retrieval of less detailed and more "semantized" autobiographical memories (*i.e.*, episodic-to-semantic shift in the quality of recollection), very likely relying on some kind of self-involvement.

Encephalitis

Encephalitis is a neurological condition characterized by an acute inflammation of the brain, generally caused by a virus or autoimmunity (*e.g.*, herpes encephalitis, limbic encephalitis). There is usually extensive damage to the temporal lobes, including the medial temporal regions[114-116] and extending to the PFC[117,118], although not necessarily[119], and a severe memory impairment[114]. More specifically, neuropsychological research provides evidence of retrograde amnesia, particularly for autobiographical events[116,120-123]. Despite evidence that encephalitis severely affects retrograde memory, especially AM, and may lead to interesting dissociations in relation to the side of damage[120], fMRI investigations of AM in encephalitic patients are very rare[124]. In a single-case fMRI study, Berry *et al*[124] examined the neural correlates underlying "rehearsed" (reviewed) personal episodes in a woman, Mrs B, diagnosed with limbic encephalitis five years before the neuroimaging investigation and presenting with impaired memory for autobiographical events. The patient used a wearable camera, SenseCam (Microsoft Research, Cambridge) to recode images during personal events, and then reviewed the images approximately every two days during three weeks. During scanning, Mrs B viewed rehearsed SenseCam images, together with never reviewed and new images as well as events recorded in a written diary and also rehearsed every two days during three weeks. At the behavioral level, the patient showed better performance for "rehearsed" SenseCam images, which at the neural level was associated with increased activity in the left ventrolateral PFC, lateral temporal, parietal and occipital regions in the absence of MTL activations. This study suggests a potentially effective way of alleviating AM deficit with a rehearsal-based training using visual material and supported by frontal and posterior activations, which very likely reflects a more general recognition of the event rather than detailed specific recollection, especially given that during scanning, events were not remembered in detail but just recognized (as known or familiar). Further investigation involving detailed recollection of personal events would help better understand the effects of training procedures on AM brain network.

Summary

Altogether, the above-presented fMRI studies in patients with MTL damage highlight the importance of the left hippocampus, which when atrophied and not functional leads to deficits in AM. Available fMRI evidence suggests that atrophy in the left hippocampus does not necessary lead to alteration in its activation pattern and to severe AM impairment; namely, residual functionality in the damaged hippocampus may underpin relatively normal AM recollection. When residual hippocampal tissue is not functional, other brain mechanisms come into play to compensate its silence. In some cases, engagement of contralesional MTL structures could be sufficient to support AM, but very likely only in some circumstances, dependent on the age at which damage occurred. In other cases, PFC, more often medial PFC, and posterior cortices could support compensatory processes engaged to deal with the AM deficit, but not necessarily always efficient to support rich and detailed recollections (Table 1). Given the evidence that medial PFC has been associated with processes related to the self[51] and contains more information for remote memories[37] in healthy subjects, it could be speculated that involvement of medial PFC in case of damage could reflect retrieval of more stable

gist-like aspects containing less episodic details of the memories (rather than true detailed episodic-specific recollection supported by hippocampus) accompanied by the overall sense of self-involvement.

CONCLUSION

Overall, the present review of fMRI studies in patients with AM impairment due to damage in MTL core memory structures summarizes the importance of fMRI data in providing insights on how brain damage affects the neural network supporting retrieval of autobiographical memories and how the brain appears to cope with damage by engaging compensatory mechanisms, which can either be efficient or not, so to mediate AM recollection. FMRI may supply additional information over that provided by neuropsychological assessment and structural MRI and combining them together during examination of brain damaged patients would lead to a better and more reliable understanding of memory disorders and the underlying brain activations pattern and, ultimately, better management of the patients. The studies discussed in the present review, presenting different pathological entities affecting MTL and associated with different patterns of AM loss, provide relevant theoretical and clinical information that can guide future functional neuroimaging research of memory impairment. Although the present review focused on the use of fMRI in patients with MTL damage, for completeness, it should be noted that fMRI has started to be used in other pathologies characterized by AM impairment, some of which we briefly enumerate below.

Traumatic brain injury

Traumatic brain injury (TBI) has usually been associated with impaired AM[125-127] together with diffuse axonal injury mainly affecting the connection between frontal and temporal regions[126,128]. Given the diffuse nature of damage, TBI presents a challenge in understanding impairment of AM, which might be linked to a more general deficit in executive functions and alteration of the sense of self. A recent single-case fMRI investigation[129] of a TBI patient, ML (initially reported by Levine *et al*[125]), revealed decreased involvement of the medial prefrontal and posterior cortices for recently encoded personal events, of which retrieval is lacking specificity and autonoetic awareness[125]. This finding underscores the link between autonoetic awareness and medial PFC, which could be involved as a compensatory mechanism only when autonoetic awareness is relatively preserved.

Psychogenic amnesia

While all the above-presented findings underscore the importance of considering fMRI examination in patients with AM impairment due to overt brain damage, it should be also mentioned that fMRI can be used in patients without overt brain damage but who present with a specific deficit in AM, such as psychogenic amnesia (known also as dissociative amnesia)[130,131], which affects the ventrolateral PFC[132] associated with retrieval of emotional memories (see above) and is linked to reduced MTL engagement[133].

Affective disorders

Dysfunctions of AM are also widely reported in affective disorders, such as depression and post-traumatic stress disorder (PTSD)[134-137], which are characterized by intrusions of memory of the traumatic event, bias toward negative memories and an overgeneralization (lacking specificity) of retrieval[138,139]. Recently, there are some studies examining the neural correlates of AM in depression[140,141] and PTSD[142,143], which highlight the abnormal involvement of the PFC and/or emotion-related MTL region, *i.e.*, amygdala. Overall, the fMRI investigations in psychogenic amnesia and affective disorders could also be very informative regarding the interplay between memory and emotion, which has long been neglected, while there is no doubt of emotional and motivational influences on AM.

Psychiatric disorders: The case of schizophrenia

Schizophrenia has been also associated with impaired AM[144-146] in the context of deficits in several cognitive operations (perception, memory) and emotional processing, caused very likely by a more general cognition – emotion disintegration[147]. FMRI examination of AM in schizophrenia revealed an abnormal pattern of activation and correlations with memory performance in the PFC and striatum, respectively[148]. Further fMRI investigations are needed to clearly understand AM deficits in schizophrenia and its link to a more general disturbance at the level of emotion-cognition interaction.

Finally, we would like to mention that it would also be of great use for investigating the effects of cognitive based training programs. Specifically, fMRI can be used before and after training programs to establish beneficial changes in neural activations leading to improved AM[149]. Investigations of this sort are remarkably scarce in the AM research, but hopefully they will emerge in the near future and provide new opportunities to understand reorganization of brain network activation and brain plasticity.

REFERENCES

1 **Conway MA**, Pleydell-Pearce CW. The construction of autobiographical memories in the self-memory system. *Psychol Rev* 2000; **107**: 261-288 [PMID: 10789197 DOI: 10.1037/0033-295X.107.2.261]

2 **Tulving E**. Episodic memory and common sense: how far apart? *Philos Trans R Soc Lond B Biol Sci* 2001; **356**: 1505-1515 [PMID: 11571040 DOI: 10.1098/rstb.2001.0937]

3 **Tulving E**. Episodic memory: from mind to brain. *Annu Rev Psychol* 2002; **53**: 1-25 [PMID: 11752477 DOI: 10.1146/annurev.psych.53.100901.135114]

4 **Bluck S**. Autobiographical memory: exploring its functions in everyday life. *Memory* 2003; **11**: 113-123 [PMID: 12820825 DOI: 10.1080/741938206]

5 **Rasmussen AS**, Habermas T. Factor structure of overall autobiographical memory usage: the directive, self and social functions revisited. *Memory* 2011; **19**: 597-605 [PMID:

21919587 DOI: 10.1080/09658211.2011.592499]
6 **Moscovitch M**, Nadel L, Winocur G, Gilboa A, Rosenbaum RS. The cognitive neuroscience of remote episodic, semantic and spatial memory. *Curr Opin Neurobiol* 2006; **16**: 179-190 [PMID: 16564688 DOI: 10.1016/j.conb.2006.03.013]
7 **Moscovitch M**, Rosenbaum RS, Gilboa A, Addis DR, Westmacott R, Grady C, McAndrews MP, Levine B, Black S, Winocur G, Nadel L. Functional neuroanatomy of remote episodic, semantic and spatial memory: a unified account based on multiple trace theory. *J Anat* 2005; **207**: 35-66 [PMID: 16011544 DOI: 10.1111/j.1469-7580.2005.00421.x]
8 **Preston AR**, Wagner AD. The medial temporal lobe and memory. In: Kesner RP, Martinez JL. Neurobiology of Learning and Memory. Amsterdam: Elsevier, 2007: 305-337
9 **Spiers HJ**, Maguire EA, Burgess N. Hippocampal amnesia. *Neurocase* 2001; **7**: 357-382 [PMID: 11744778 DOI: 10.1076/neur.7.5.357.16245]
10 **Bright P**, Buckman J, Fradera A, Yoshimasu H, Colchester AC, Kopelman MD. Retrograde amnesia in patients with hippocampal, medial temporal, temporal lobe, or frontal pathology. *Learn Mem* 2006; **13**: 545-557 [PMID: 17015852 DOI: 10.1101/lm.265906]
11 **Tulving E**. Episodic memory and autonoesis: Uniquely human? In: Terrace HS, Metcalfe J. The Missing Link in Cognition: Origins of Self-Reflective Consciousness. Oxford University Press, 2005: 3-56
12 **Conway MA**. Memory and the self. *J Mem Lang* 2005; **53**: 594-628 [DOI: 10.1016/j.jml.2005.08.005]
13 **Suddendorf T**, Addis DR, Corballis MC. Mental time travel and the shaping of the human mind. *Philos Trans R Soc Lond B Biol Sci* 2009; **364**: 1317-1324 [PMID: 19528013 DOI: 10.1098/rstb.2008.0301]
14 **Suddendorf T**, Corballis MC. Behavioural evidence for mental time travel in nonhuman animals. *Behav Brain Res* 2010; **215**: 292-298 [PMID: 19962409 DOI: 10.1016/j.bbr.2009.11.044]
15 **Tulving E**. Are there 256 kinds of memory? In: Nairne JS. The Foundations of Remembering: Essays in Honor of Henry L. Roediger: Psychology Press, 2007: 39-52
16 **Klein SB**. The Two Selves: Their Metaphysical Commitments and Functional Independence. New York: Oxford University Press, 2014
17 **Klein SB**. Self, memory, and the self-reference effect: an examination of conceptual and methodological issues. *Pers Soc Psychol Rev* 2012; **16**: 283-300 [PMID: 22291045 DOI: 10.1177/1088868311434214]
18 **Klein SB**, Nichols S. Memory and the Sense of Personal Identity. *Mind* 2012; **121**: 677-702 [DOI: 10.1093/mind/fzs080]
19 **Tulving E**. Elements of episodic memory. New York: Oxford Univiversity Press, 1983
20 **Cabeza R**, St Jacques P. Functional neuroimaging of autobiographical memory. *Trends Cogn Sci* 2007; **11**: 219-227 [PMID: 17382578 DOI: 10.1016/j.tics.2007.02.005]
21 **Maguire EA**. Neuroimaging studies of autobiographical event memory. *Philos Trans R Soc Lond B Biol Sci* 2001; **356**: 1441-1451 [PMID: 11571035 DOI: 10.1098/rstb.2001.0944]
22 **St Jacques PL**, Cabeza R. Neural correlates of autobiographical memory. In: Ghetti S, Bauer PJ. Origins and development of recollection. New York: Oxford University Press, 2012: 188-218
23 **Squire LR**, Alvarez P. Retrograde amnesia and memory consolidation: a neurobiological perspective. *Curr Opin Neurobiol* 1995; **5**: 169-177 [PMID: 7620304 DOI: 10.1016/0959-4388(95)80023-9]
24 **Nadel L**, Moscovitch M. Memory consolidation, retrograde amnesia and the hippocampal complex. *Curr Opin Neurobiol* 1997; **7**: 217-227 [PMID: 9142752 DOI: 10.1016/S0959-4388(97)80010-4]
25 **Winocur G**, Moscovitch M. Memory transformation and systems consolidation. *J Int Neuropsychol Soc* 2011; **17**: 766-780 [PMID: 21729403 DOI: 10.1017/S1355617711000683]
26 **Winocur G**, Moscovitch M, Bontempi B. Memory formation and long-term retention in humans and animals: convergence towards a transformation account of hippocampal-neocortical interactions. *Neuropsychologia* 2010; **48**: 2339-2356 [PMID: 20430044 DOI: 10.1016/j.neuropsychologia.2010.04.016]
27 **Svoboda E**, McKinnon MC, Levine B. The functional neuroanatomy of autobiographical memory: a meta-analysis. *Neuropsychologia* 2006; **44**: 2189-2208 [PMID: 16806314 DOI: 10.1016/j.neuropsychologia.2006.05.023]
28 **Botzung A**, Denkova E, Ciuciu P, Scheiber C, Manning L. The neural bases of the constructive nature of autobiographical memories studied with a self-paced fMRI design. *Memory* 2008; **16**: 351-363 [PMID: 18432480 DOI: 10.1080/09658210801931222]
29 **Daselaar SM**, Rice HJ, Greenberg DL, Cabeza R, LaBar KS, Rubin DC. The spatiotemporal dynamics of autobiographical memory: neural correlates of recall, emotional intensity, and reliving. *Cereb Cortex* 2008; **18**: 217-229 [PMID: 17548799 DOI: 10.1093/cercor/bhm048]
30 **Greenberg DL**, Rice HJ, Cooper JJ, Cabeza R, Rubin DC, Labar KS. Co-activation of the amygdala, hippocampus and inferior frontal gyrus during autobiographical memory retrieval. *Neuropsychologia* 2005; **43**: 659-674 [PMID: 15721179 DOI: 10.1016/j.neuropsychologia.2004.09.002]
31 **Douville K**, Woodard JL, Seidenberg M, Miller SK, Leveroni CL, Nielson KA, Franczak M, Antuono P, Rao SM. Medial temporal lobe activity for recognition of recent and remote famous names: an event-related fMRI study. *Neuropsychologia* 2005; **43**: 693-703 [PMID: 15721182 DOI: 10.1016/j.neuropsychologia.2004.09.005]
32 **Leveroni CL**, Seidenberg M, Mayer AR, Mead LA, Binder JR, Rao SM. Neural systems underlying the recognition of familiar and newly learned faces. *J Neurosci* 2000; **20**: 878-886 [PMID: 10632617]
33 **Denkova E**, Botzung A, Manning L. Neural correlates of remembering/knowing famous people: an event-related fMRI study. *Neuropsychologia* 2006; **44**: 2783-2791 [PMID: 16879842 DOI: 10.1016/j.neuropsychologia.2006.05.029]
34 **Snowden JS**, Griffiths HL, Neary D. Autobiographical experience and word meaning. *Memory* 1995; **3**: 225-246 [PMID: 8574865 DOI: 10.1080/09658219508253152]
35 **Westmacott R**, Black SE, Freedman M, Moscovitch M. The contribution of autobiographical significance to semantic memory: evidence from Alzheimer's disease, semantic dementia, and amnesia. *Neuropsychologia* 2004; **42**: 25-48 [PMID: 14615074 DOI: 10.1016/S0028-3932(03)00147-7]
36 **Addis DR**, Moscovitch M, Crawley AP, McAndrews MP. Recollective qualities modulate hippocampal activation during autobiographical memory retrieval. *Hippocampus* 2004; **14**: 752-762 [PMID: 15318333 DOI: 10.1002/hipo.10215]
37 **Bonnici HM**, Chadwick MJ, Lutti A, Hassabis D, Weiskopf N, Maguire EA. Detecting representations of recent and remote autobiographical memories in vmPFC and hippocampus. *J Neurosci* 2012; **32**: 16982-16991 [PMID: 23175849 DOI: 10.1523/JNEUROSCI.2475-12.2012]
38 **Gilboa A**. Autobiographical and episodic memory--one and the same? Evidence from prefrontal activation in neuroimaging studies. *Neuropsychologia* 2004; **42**: 1336-1349 [PMID: 15193941 DOI: 10.1016/j.neuropsychologia.2004.02.014]
39 **Sheldon S**, Levine B. Same as it ever was: vividness modulates the similarities and differences between the neural networks that support retrieving remote and recent autobiographical memories. *Neuroimage* 2013; **83**: 880-891 [PMID: 23845428 DOI: 10.1016/j.neuroimage.2013.06.082]
40 **Söderlund H**, Moscovitch M, Kumar N, Mandic M, Levine B. As time goes by: hippocampal connectivity changes with remoteness of autobiographical memory retrieval. *Hippocampus* 2012; **22**: 670-679 [PMID: 21404363 DOI: 10.1002/hipo.20927]

41 **Gilboa A**, Winocur G, Grady CL, Hevenor SJ, Moscovitch M. Remembering our past: functional neuroanatomy of recollection of recent and very remote personal events. *Cereb Cortex* 2004; **14**: 1214-1225 [PMID: 15166099 DOI: 10.1093/cercor/bhh082]

42 **Badre D**. Cognitive control, hierarchy, and the rostro-caudal organization of the frontal lobes. *Trends Cogn Sci* 2008; **12**: 193-200 [PMID: 18403252 DOI: 10.1016/j.tics.2008.02.004]

43 **Moscovitch M**, Winocur G. The frontal cortex and working with memory. In Stuss DT, Knight R. Principles of frontal lobe function. New York: Oxfor Univesrity Press, 2002: 188-209.

44 **Addis DR**, Knapp K, Roberts RP, Schacter DL. Routes to the past: neural substrates of direct and generative autobiographical memory retrieval. *Neuroimage* 2012; **59**: 2908-2922 [PMID: 22001264 DOI: 10.1016/j.neuroimage.2011.09.066]

45 **Markowitsch HJ**. Which brain regions are critically involved in the retrieval of old episodic memory? *Brain Res Brain Res Rev* 1995; **21**: 117-127 [PMID: 8866670 DOI: 10.1016/0165-0173(95)00007-0]

46 **Markowitsch HJ**. The functional neuroanatomy of episodic memory retrieval. *Trends Neurosci* 1997; **20**: 557-558 [PMID: 9416665]

47 **Brand M**, Markowitsch HJ. Memory processes and the orbitofrontal cortex. In: Zald DH, Rauch SL. The orbitofrontal cortex. Oxford: Oxford University Press, 2006: 285-230 [DOI: 10.1093/acprof:oso/9780198565741.003.0011]

48 **Brand M**, Markowitsch HJ. The role of the prefrontal cortex in episodic memory. In: Dere E, Huston JP, Easton A. Handbook of episodic memory. Amsterdam: Elsevier, 2008: 317-341

49 **Markowitsch HJ**, Thiel A, Reinkemeier M, Kessler J, Koyuncu A, Heiss WD. Right amygdalar and temporofrontal activation during autobiographic, but not during fictitious memory retrieval. *Behav Neurol* 2000; **12**: 181-190 [PMID: 11568430 DOI: 10.1155/2000/303651]

50 **Denkova E**, Dolcos S, Dolcos F. The Effect of Retrieval Focus and Emotional Valence on the Inferior Frontal Cortex Activity during Autobiographical Recollection. *Front Behav Neurosci* 2013; **7**: 192 [PMID: 24379766 DOI: 10.3389/fnbeh.2013.00192]

51 **Northoff G**, Heinzel A, de Greck M, Bermpohl F, Dobrowolny H, Panksepp J. Self-referential processing in our brain--a meta-analysis of imaging studies on the self. *Neuroimage* 2006; **31**: 440-457 [PMID: 16466680 DOI: 10.1016/j.neuroimage.2005.12.002]

52 **Cabeza R**, Prince SE, Daselaar SM, Greenberg DL, Budde M, Dolcos F, LaBar KS, Rubin DC. Brain activity during episodic retrieval of autobiographical and laboratory events: an fMRI study using a novel photo paradigm. *J Cogn Neurosci* 2004; **16**: 1583-1594 [PMID: 15622612 DOI: 10.1162/0898929042568578]

53 **McDermott KB**, Szpunar KK, Christ SE. Laboratory-based and autobiographical retrieval tasks differ substantially in their neural substrates. *Neuropsychologia* 2009; **47**: 2290-2298 [PMID: 19159634 DOI: 10.1016/j.neuropsychologia.2008.12.025]

54 **Summerfield JJ**, Hassabis D, Maguire EA. Cortical midline involvement in autobiographical memory. *Neuroimage* 2009; **44**: 1188-1200 [PMID: 18973817 DOI: 10.1016/j.neuroimage.2008.09.033]

55 **St Jacques PL**, Conway MA, Lowder MW, Cabeza R. Watching my mind unfold versus yours: an fMRI study using a novel camera technology to examine neural differences in self-projection of self versus other perspectives. *J Cogn Neurosci* 2011; **23**: 1275-1284 [PMID: 20521858 DOI: 10.1162/jocn.2010.21518]

56 **Amodio DM**, Frith CD. Meeting of minds: the medial frontal cortex and social cognition. *Nat Rev Neurosci* 2006; **7**: 268-277 [PMID: 16552413 DOI: 10.1038/nrn1884]

57 **Kober H**, Barrett LF, Joseph J, Bliss-Moreau E, Lindquist K, Wager TD. Functional grouping and cortical-subcortical interactions in emotion: a meta-analysis of neuroimaging studies. *Neuroimage* 2008; **42**: 998-1031 [PMID: 18579414 DOI: 10.1016/j.neuroimage.2008.03.059]

58 **Denny BT**, Kober H, Wager TD, Ochsner KN. A meta-analysis of functional neuroimaging studies of self- and other judgments reveals a spatial gradient for mentalizing in medial prefrontal cortex. *J Cogn Neurosci* 2012; **24**: 1742-1752 [PMID: 22452556 DOI: 10.1162/jocn_a_00233]

59 **Frith U**, Frith CD. Development and neurophysiology of mentalizing. *Philos Trans R Soc Lond B Biol Sci* 2003; **358**: 459-473 [PMID: 12689373 DOI: 10.1098/rstb.2002.1218]

60 **Moscovitch M**, Winocur G. The frontal cortex and working with memory. In: Stuss DT, Knight R. The Frontal Lobes. Oxford: Oxford University Press, 2002: 188-209

61 **Ochsner KN**, Silvers JA, Buhle JT. Functional imaging studies of emotion regulation: a synthetic review and evolving model of the cognitive control of emotion. *Ann N Y Acad Sci* 2012; **1251**: E1-E24 [PMID: 23025352 DOI: 10.1111/j.1749-6632.2012.06751.x]

62 **Hassabis D**, Maguire EA. Deconstructing episodic memory with construction. *Trends Cogn Sci* 2007; **11**: 299-306 [PMID: 17548229 DOI: 10.1016/j.tics.2007.05.001]

63 **Freton M**, Lemogne C, Bergouignan L, Delaveau P, Lehéricy S, Fossati P. The eye of the self: precuneus volume and visual perspective during autobiographical memory retrieval. *Brain Struct Funct* 2013; Epub ahead of print [PMID: 23553546]

64 **Burgess N**, Becker S, King JA, O'Keefe J. Memory for events and their spatial context: models and experiments. *Philos Trans R Soc Lond B Biol Sci* 2001; **356**: 1493-1503 [PMID: 11571039 DOI: 10.1098/rstb.2001.0948]

65 **Kapur N**, Kopelman MD. Advanced brain imaging procedures and human memory disorder. *Br Med Bull* 2003; **65**: 61-81 [PMID: 12697617 DOI: 10.1093/bmb/65.1.61]

66 **Mayes AR**, Montaldi D. Exploring the neural bases of episodic and semantic memory: the role of structural and functional neuroimaging. *Neurosci Biobehav Rev* 2001; **25**: 555-573 [PMID: 11595275 DOI: 10.1016/S0149-7634(01)00034-3]

67 **Kopelman MD**. Disorders of memory. *Brain* 2002; **125**: 2152-2190 [PMID: 12244076 DOI: 10.1093/brain/awf229]

68 **Kopelman MD**, Kapur N. The loss of episodic memories in retrograde amnesia: single-case and group studies. *Philos Trans R Soc Lond B Biol Sci* 2001; **356**: 1409-1421 [PMID: 11571032 DOI: 10.1098/rstb.2001.0942]

69 **Gadian DG**, Aicardi J, Watkins KE, Porter DA, Mishkin M, Vargha-Khadem F. Developmental amnesia associated with early hypoxic-ischaemic injury. *Brain* 2000; **123** Pt 3: 499-507 [PMID: 10686173 DOI: 10.1093/brain/123.3.499]

70 **Vargha-Khadem F**, Gadian DG, Mishkin M. Dissociations in cognitive memory: the syndrome of developmental amnesia. *Philos Trans R Soc Lond B Biol Sci* 2001; **356**: 1435-1440 [PMID: 11571034 DOI: 10.1098/rstb.2001.0951]

71 **Vargha-Khadem F**, Gadian DG, Watkins KE, Connelly A, Van Paesschen W, Mishkin M. Differential effects of early hippocampal pathology on episodic and semantic memory. *Science* 1997; **277**: 376-380 [PMID: 9219696 DOI: 10.1126/science.277.5324.376]

72 **Maguire EA**, Vargha-Khadem F, Mishkin M. The effects of bilateral hippocampal damage on fMRI regional activations and interactions during memory retrieval. *Brain* 2001; **124**: 1156-1170 [PMID: 11353732 DOI: 10.1093/brain/124.6.1156]

73 **Manning L**. Do some neurological conditions induce brain plasticity processes? *Behav Brain Res* 2008; **192**: 143-148 [PMID: 18479763 DOI: 10.1016/j.bbr.2008.04.001]

74 **Andelman F**, Hoofien D, Goldberg I, Aizenstein O, Neufeld MY. Bilateral hippocampal lesion and a selective impairment of the ability for mental time travel. *Neurocase* 2010; **16**: 426-435 [PMID: 20401802 DOI: 10.1080/13554791003623318]

75 **Cipolotti L**, Shallice T, Chan D, Fox N, Scahill R, Harrison G,

Stevens J, Rudge P. Long-term retrograde amnesia...the crucial role of the hippocampus. *Neuropsychologia* 2001; **39**: 151-172 [PMID: 11163373 DOI: 10.1016/S0028-3932(00)00103-2]
76 **Klein SB**, Loftus J, Kihlstrom JF. Memory and temporal experience: The effects of episodic memory loss on an amnesic patient's ability to remember the past and imagine the future. *Social Cognition* 2002; **20**: 353-379 [DOI: 10.1521/soco.20.5.353.21125]
77 **Maguire EA**, Frith CD, Rudge P, Cipolotti L. The effect of adult-acquired hippocampal damage on memory retrieval: an fMRI study. *Neuroimage* 2005; **27**: 146-152 [PMID: 15886022 DOI: 10.1016/j.neuroimage.2005.04.006]
78 **Price CJ**, Friston KJ. Scanning patients with tasks they can perform. *Hum Brain Mapp* 1999; **8**: 102-108 [PMID: 10524600]
79 **Price CJ**, Crinion J, Friston KJ. Design and analysis of fMRI studies with neurologically impaired patients. *J Magn Reson Imaging* 2006; **23**: 816-826 [PMID: 16649208 DOI: 10.1002/jmri.20580]
80 **Engel J Jr**. Introduction to temporal lobe epilepsy. *Epilepsy Res* 1996; **26**: 141-150 [PMID: 8985696 DOI: 10.1016/S0920-1211(96)00043-5]
81 **Snyder PJ**. Epilepsy as a "natural laboratory" for the study of human memory. *Brain Cogn* 1997; **35**: 1-4 [PMID: 9339298 DOI: 10.1006/brcg.1997.0924]
82 **Després O**, Voltzenlogel V, Hirsch E, Vignal JP, Manning L. [Memory improvement in patients with temporal lobe epilepsy at one-year postoperative]. *Rev Neurol* (Paris) 2011; **167**: 231-244 [PMID: 21159357 DOI: 10.1016/j.neurol.2010.08.008]
83 **Herfurth K**, Kasper B, Schwarz M, Stefan H, Pauli E. Autobiographical memory in temporal lobe epilepsy: role of hippocampal and temporal lateral structures. *Epilepsy Behav* 2010; **19**: 365-371 [PMID: 20875774 DOI: 10.1016/j.yebeh.2010.07.012]
84 **St-Laurent M**, Moscovitch M, Levine B, McAndrews MP. Determinants of autobiographical memory in patients with unilateral temporal lobe epilepsy or excisions. *Neuropsychologia* 2009; **47**: 2211-2221 [PMID: 19524089 DOI: 10.1016/j.neuropsychologia.2009.01.032]
85 **Viskontas IV**, McAndrews MP, Moscovitch M. Remote episodic memory deficits in patients with unilateral temporal lobe epilepsy and excisions. *J Neurosci* 2000; **20**: 5853-5857 [PMID: 10908628]
86 **Voltzenlogel V**, Despres O, Vignal JP, Kehrli P, Manning L. One-year postoperative autobiographical memory following unilateral temporal lobectomy for control of intractable epilepsy. *Epilepsia* 2007; **48**: 605-608 [PMID: 17326789 DOI: 10.1111/j.1528-1167.2006.00970.x]
87 **Voltzenlogel V**, Després O, Vignal JP, Steinhoff BJ, Kehrli P, Manning L. Remote memory in temporal lobe epilepsy. *Epilepsia* 2006; **47**: 1329-1336 [PMID: 16922877 DOI: 10.1111/j.1528-1167.2006.00555.x]
88 **St-Laurent M**, Moscovitch M, Tau M, McAndrews MP. The temporal unraveling of autobiographical memory narratives in patients with temporal lobe epilepsy or excisions. *Hippocampus* 2011; **21**: 409-421 [PMID: 20082294 DOI: 10.1002/hipo.20757]
89 **Dupont S**, Van de Moortele PF, Samson S, Hasboun D, Poline JB, Adam C, Lehéricy S, Le Bihan D, Samson Y, Baulac M. Episodic memory in left temporal lobe epilepsy: a functional MRI study. *Brain* 2000; **123** (Pt 8): 1722-1732 [PMID: 10908201 DOI: 10.1093/brain/123.8.1722]
90 **Sidhu MK**, Stretton J, Winston GP, Bonelli S, Centeno M, Vollmar C, Symms M, Thompson PJ, Koepp MJ, Duncan JS. A functional magnetic resonance imaging study mapping the episodic memory encoding network in temporal lobe epilepsy. *Brain* 2013; **136**: 1868-1888 [PMID: 23674488 DOI: 10.1093/brain/awt099]
91 **Bonelli SB**, Powell RH, Yogarajah M, Samson RS, Symms MR, Thompson PJ, Koepp MJ, Duncan JS. Imaging memory in temporal lobe epilepsy: predicting the effects of temporal lobe resection. *Brain* 2010; **133**: 1186-1199 [PMID: 20157009 DOI: 10.1093/brain/awq006]
92 **Bonelli SB**, Thompson PJ, Yogarajah M, Powell RH, Samson RS, McEvoy AW, Symms MR, Koepp MJ, Duncan JS. Memory reorganization following anterior temporal lobe resection: a longitudinal functional MRI study. *Brain* 2013; **136**: 1889-1900 [PMID: 23715092 DOI: 10.1093/brain/awt105]
93 **Cheung MC**, Chan AS, Lam JM, Chan YL. Pre- and postoperative fMRI and clinical memory performance in temporal lobe epilepsy. *J Neurol Neurosurg Psychiatry* 2009; **80**: 1099-1106 [PMID: 19389718 DOI: 10.1136/jnnp.2009.173161]
94 **Powell HW**, Koepp MJ, Richardson MP, Symms MR, Thompson PJ, Duncan JS. The application of functional MRI of memory in temporal lobe epilepsy: a clinical review. *Epilepsia* 2004; **45**: 855-863 [PMID: 15230713 DOI: 10.1111/j.0013-9580.2004.41603.x]
95 **Powell HW**, Richardson MP, Symms MR, Boulby PA, Thompson PJ, Duncan JS, Koepp MJ. Preoperative fMRI predicts memory decline following anterior temporal lobe resection. *J Neurol Neurosurg Psychiatry* 2008; **79**: 686-693 [PMID: 17898035 DOI: 10.1136/jnnp.2007.115139]
96 **Richardson MP**, Strange BA, Thompson PJ, Baxendale SA, Duncan JS, Dolan RJ. Pre-operative verbal memory fMRI predicts post-operative memory decline after left temporal lobe resection. *Brain* 2004; **127**: 2419-2426 [PMID: 15459025 DOI: 10.1093/brain/awh293]
97 **Addis DR**, Moscovitch M, McAndrews MP. Consequences of hippocampal damage across the autobiographical memory network in left temporal lobe epilepsy. *Brain* 2007; **130**: 2327-2342 [PMID: 17681983 DOI: 10.1093/brain/awm166]
98 **Manning L**, Denkova E, Unterberger L. Autobiographical significance in past and future public semantic memory: a case-study. *Cortex* 2013; **49**: 2007-2020 [PMID: 23266012 DOI: 10.1016/j.cortex.2012.11.007]
99 **Milton F**, Butler CR, Benattayallah A, Zeman AZ. The neural basis of autobiographical memory deficits in transient epileptic amnesia. *Neuropsychologia* 2012; **50**: 3528-3541 [PMID: 23036282 DOI: 10.1016/j.neuropsychologia.2012.09.027]
100 **Manning L**, Chassagnon S, Hirsch E, Kehrli P, Maitrot D. Selective memory impairment for public events in a patient with left temporal lobe epilepsy. *Epilepsy Res* 2005; **64**: 45-47 [PMID: 15820669 DOI: 10.1016/j.eplepsyres.2005.02.003]
101 **Chan D**, Fox NC, Scahill RI, Crum WR, Whitwell JL, Leschziner G, Rossor AM, Stevens JM, Cipolotti L, Rossor MN. Patterns of temporal lobe atrophy in semantic dementia and Alzheimer's disease. *Ann Neurol* 2001; **49**: 433-442 [PMID: 11310620 DOI: 10.1002/ana.92]
102 **Galton CJ**, Gomez-Anson B, Antoun N, Scheltens P, Patterson K, Graves M, Sahakian BJ, Hodges JR. Temporal lobe rating scale: application to Alzheimer's disease and frontotemporal dementia. *J Neurol Neurosurg Psychiatry* 2001; **70**: 165-173 [PMID: 11160463 DOI: 10.1136/jnnp.70.2.165]
103 **Hodges JR**. Alzheimer's disease and the frontotemporal dementias: contributions to clinico-pathological studies, diagnosis, and cognitive neuroscience. *J Alzheimers Dis* 2013; **33** Suppl 1: S211-S217 [PMID: 22766737]
104 **Irish M**, Piguet O, Hodges JR, Hornberger M. Common and unique gray matter correlates of episodic memory dysfunction in frontotemporal dementia and alzheimer's disease. *Hum Brain Mapp* 2014; **35**: 1422-1435 [PMID: 23670951 DOI: 10.1002/hbm.22263]
105 **Graham KS**, Hodges JR. Differentiating the roles of the hippocampal complex and the neocortex in long-term memory storage: evidence from the study of semantic dementia and Alzheimer's disease. *Neuropsychology* 1997; **11**: 77-89 [PMID: 9055272 DOI: 10.1037/0894-4105.11.1.77]
106 **Moss HE**, Kopelman MD, Cappelletti M, Davies Pde M, Jaldow E. Lost for words or loss of memories? Autobiographical memory in semantic dementia. *Cogn Neuropsychol* 2003; **20**: 703-732 [PMID: 20957590 DOI: 10.1080/026432902420009

16]
107 **Piolino P**, Desgranges B, Belliard S, Matuszewski V, Lalevée C, De la Sayette V, Eustache F. Autobiographical memory and autonoetic consciousness: triple dissociation in neurodegenerative diseases. *Brain* 2003; **126**: 2203-2219 [PMID: 12821510 DOI: 10.1093/brain/awg222]
108 **Addis DR**, Tippett LJ. Memory of myself: autobiographical memory and identity in Alzheimer's disease. *Memory* 2004; **12**: 56-74 [PMID: 15098621 DOI: 10.1080/09658210244000423]
109 **Greene JD**, Hodges JR, Baddeley AD. Autobiographical memory and executive function in early dementia of Alzheimer type. *Neuropsychologia* 1995; **33**: 1647-1670 [PMID: 8745122 DOI: 10.1016/0028-3932(95)00046-1]
110 **Maguire EA**, Kumaran D, Hassabis D, Kopelman MD. Autobiographical memory in semantic dementia: a longitudinal fMRI study. *Neuropsychologia* 2010; **48**: 123-136 [PMID: 19720072 DOI: 10.1016/j.neuropsychologia.2009.08.020]
111 **Viard A**, Desgranges B, Matuszewski V, Lebreton K, Belliard S, de La Sayette V, Eustache F, Piolino P. Autobiographical memory in semantic dementia: new insights from two patients using fMRI. *Neuropsychologia* 2013; **51**: 2620-2632 [PMID: 23954715 DOI: 10.1016/j.neuropsychologia.2013.08.007]
112 **Irish M**, Lawlor BA, O'Mara SM, Coen RF. Exploring the recollective experience during autobiographical memory retrieval in amnestic mild cognitive impairment. *J Int Neuropsychol Soc* 2010; **16**: 546-555 [PMID: 20298640 DOI: 10.1017/S1355617710000172]
113 **Meulenbroek O**, Rijpkema M, Kessels RP, Rikkert MG, Fernández G. Autobiographical memory retrieval in patients with Alzheimer's disease. *Neuroimage* 2010; **53**: 331-340 [PMID: 20570740 DOI: 10.1016/j.neuroimage.2010.05.082]
114 **Kapur N**, Barker S, Burrows EH, Ellison D, Brice J, Illis LS, Scholey K, Colbourn C, Wilson B, Loates M. Herpes simplex encephalitis: long term magnetic resonance imaging and neuropsychological profile. *J Neurol Neurosurg Psychiatry* 1994; **57**: 1334-1342 [PMID: 7964808 DOI: 10.1136/jnnp.57.11.1334]
115 **Kopelman MD**, Stanhope N, Kingsley D. Retrograde amnesia in patients with diencephalic, temporal lobe or frontal lesions. *Neuropsychologia* 1999; **37**: 939-958 [PMID: 10426519 DOI: 10.1016/S0028-3932(98)00143-2]
116 **Rosenbaum RS**, Moscovitch M, Foster JK, Schnyer DM, Gao F, Kovacevic N, Verfaellie M, Black SE, Levine B. Patterns of autobiographical memory loss in medial-temporal lobe amnesic patients. *J Cogn Neurosci* 2008; **20**: 1490-1506 [PMID: 18303977 DOI: 10.1162/jocn.2008.20105]
117 **Calabrese P**, Markowitsch HJ, Durwen HF, Widlitzek H, Haupts M, Holinka B, Gehlen W. Right temporofrontal cortex as critical locus for the ecphory of old episodic memories. *J Neurol Neurosurg Psychiatry* 1996; **61**: 304-310 [PMID: 8795604 DOI: 10.1136/jnnp.61.3.304]
118 **Kataoka H**, Furiya Y, Ueno S. Limbic encephalitis with involvement of prefrontal cortices and persistent amnesia. *Neurologist* 2008; **14**: 255-257 [PMID: 18617853 DOI: 10.1097/NRL.0b013e31816b73fe]
119 **Tanaka Y**, Miyazawa Y, Hashimoto R, Nakano I, Obayashi T. Postencephalitic focal retrograde amnesia after bilateral anterior temporal lobe damage. *Neurology* 1999; **53**: 344-350 [PMID: 10430424 DOI: 10.1212/WNL.53.2.344]
120 **Buccione I**, Fadda L, Serra L, Caltagirone C, Carlesimo GA. Retrograde episodic and semantic memory impairment correlates with side of temporal lobe damage. *J Int Neuropsychol Soc* 2008; **14**: 1083-1094 [PMID: 18954490 DOI: 10.1017/S1355617708080922]
121 **Cermak LS**, O'Connor M. The anterograde and retrograde retrieval ability of a patient with amnesia due to encephalitis. *Neuropsychologia* 1983; **21**: 213-234 [PMID: 6877576 DOI: 10.1016/0028-3932(83)90039-8]
122 **O'Connor M**, Butters N, Miliotis P, Eslinger P, Cermak LS. The dissociation of anterograde and retrograde amnesia in a patient with herpes encephalitis. *J Clin Exp Neuropsychol* 1992; **14**: 159-178 [PMID: 1572943 DOI: 10.1080/01688639208402821]
123 **Tsukiura T**, Ohtake H, Fujii T, Miura R, Ogawa T, Yamadori A. Preserved ability to recognize keywords related to remote events in the absence of retrieval of relevant knowledge: a case of postencephalitic amnesia. *Brain Cogn* 2003; **51**: 1-11 [PMID: 12633586 DOI: 10.1016/S0278-2626(02)00529-8]
124 **Berry E**, Hampshire A, Rowe J, Hodges S, Kapur N, Watson P, Browne G, Smyth G, Wood K, Owen AM. The neural basis of effective memory therapy in a patient with limbic encephalitis. *J Neurol Neurosurg Psychiatry* 2009; **80**: 1202-1205 [PMID: 19286742 DOI: 10.1136/jnnp.2008.164251]
125 **Levine B**, Black SE, Cabeza R, Sinden M, Mcintosh AR, Toth JP, Tulving E, Stuss DT. Episodic memory and the self in a case of isolated retrograde amnesia. *Brain* 1998; **121** (Pt 10): 1951-1973 [PMID: 9798749]
126 **Markowitsch HJ**, Calabrese P, Liess J, Haupts M, Durwen HF, Gehlen W. Retrograde amnesia after traumatic injury of the fronto-temporal cortex. *J Neurol Neurosurg Psychiatry* 1993; **56**: 988-992 [PMID: 8410040 DOI: 10.1136/jnnp.56.9.988]
127 **Piolino P**, Desgranges B, Manning L, North P, Jokic C, Eustache F. Autobiographical memory, the sense of recollection and executive functions after severe traumatic brain injury. *Cortex* 2007; **43**: 176-195 [PMID: 17405665 DOI: 10.1016/S0010-9452(08)70474-X]
128 **Kroll NE**, Markowitsch HJ, Knight RT, von Cramon DY. Retrieval of old memories: the temporofrontal hypothesis. *Brain* 1997; **120** (Pt 8): 1377-1399 [PMID: 9278629]
129 **Levine B**, Svoboda E, Turner GR, Mandic M, Mackey A. Behavioral and functional neuroanatomical correlates of anterograde autobiographical memory in isolated retrograde amnesic patient M.L. *Neuropsychologia* 2009; **47**: 2188-2196 [PMID: 19154750 DOI: 10.1016/j.neuropsychologia.2008.12.026]
130 **Kopelman MD**. Focal retrograde amnesia and the attribution of causality: An exceptionally critical view. *Cogn Neuropsychol* 2000; **17**: 585-621 [PMID: 20945196 DOI: 10.1080/02643290750002172]
131 **Markowitsch HJ**. Psychogenic amnesia. *Neuroimage* 2003; **20** Suppl 1: S132-S138 [PMID: 14597306 DOI: 10.1016/j.neuroimage.2003.09.010]
132 **Brand M**, Eggers C, Reinhold N, Fujiwara E, Kessler J, Heiss WD, Markowitsch HJ. Functional brain imaging in 14 patients with dissociative amnesia reveals right inferolateral prefrontal hypometabolism. *Psychiatry Res* 2009; **174**: 32-39 [PMID: 19783409 DOI: 10.1016/j.pscychresns.2009.03.008]
133 **Botzung A**, Denkova E, Manning L. Psychogenic memory deficits associated with functional cerebral changes: an FMRI study. *Neurocase* 2007; **13**: 378-384 [PMID: 18781436 DOI: 10.1080/13554790701851528]
134 **Brewin CR**, Hunter E, Carroll F, Tata P. Intrusive memories in depression: an index of schema activation? *Psychol Med* 1996; **26**: 1271-1276 [PMID: 8931173 DOI: 10.1017/S0033291700035996]
135 **Brewin CR**, Reynolds M, Tata P. Autobiographical memory processes and the course of depression. *J Abnorm Psychol* 1999; **108**: 511-517 [PMID: 10466275 DOI: 10.1037/0021-843X.108.3.511]
136 **Rubin DC**, Berntsen D, Bohni MK. A memory-based model of posttraumatic stress disorder: evaluating basic assumptions underlying the PTSD diagnosis. *Psychol Rev* 2008; **115**: 985-1011 [PMID: 18954211 DOI: 10.1037/a0013397]
137 **Rubin DC**, Dennis MF, Beckham JC. Autobiographical memory for stressful events: the role of autobiographical memory in posttraumatic stress disorder. *Conscious Cogn* 2011; **20**: 840-856 [PMID: 21489820 DOI: 10.1016/j.concog.2011.03.015]
138 **Watson LA**, Berntsen D, Kuyken W, Watkins ER. The characteristics of involuntary and voluntary autobiographical

memories in depressed and never depressed individuals. *Conscious Cogn* 2012; **21**: 1382-1392 [PMID: 22850328 DOI: 10.1016/j.concog.2012.06.016]

139 **Brown AD**, Root JC, Romano TA, Chang LJ, Bryant RA, Hirst W. Overgeneralized autobiographical memory and future thinking in combat veterans with posttraumatic stress disorder. *J Behav Ther Exp Psychiatry* 2013; **44**: 129-134 [PMID: 22200095 DOI: 10.1016/j.jbtep.2011.11.004]

140 **Whalley MG**, Rugg MD, Brewin CR. Autobiographical memory in depression: an fMRI study. *Psychiatry Res* 2012; **201**: 98-106 [PMID: 22386970 DOI: 10.1016/j.pscychresns.2011.08.008]

141 **Young KD**, Bellgowan PS, Bodurka J, Drevets WC. Behavioral and neurophysiological correlates of autobiographical memory deficits in patients with depression and individuals at high risk for depression. *JAMA Psychiatry* 2013; **70**: 698-708 [PMID: 23677007 DOI: 10.1001/jamapsychiatry.2013.1189]

142 **St Jacques PL**, Botzung A, Miles A, Rubin DC. Functional neuroimaging of emotionally intense autobiographical memories in post-traumatic stress disorder. *J Psychiatr Res* 2011; **45**: 630-637 [PMID: 21109253 DOI: 10.1016/j.jpsychires.2010.10.011]

143 **St Jacques PL**, Kragel PA, Rubin DC. Neural networks supporting autobiographical memory retrieval in posttraumatic stress disorder. *Cogn Affect Behav Neurosci* 2013; **13**: 554-566 [PMID: 23483523 DOI: 10.3758/s13415-013-0157-7]

144 **Danion JM**, Cuervo C, Piolino P, Huron C, Riutort M, Peretti CS, Eustache F. Conscious recollection in autobiographical memory: an investigation in schizophrenia. *Conscious Cogn* 2005; **14**: 535-547 [PMID: 16091269 DOI: 10.1016/j.concog.2005.01.005]

145 **D'Argembeau A**, Raffard S, Van der Linden M. Remembering the past and imagining the future in schizophrenia. *J Abnorm Psychol* 2008; **117**: 247-251 [PMID: 18266503 DOI: 10.1037/0021-843X.117.1.247]

146 **Riutort M**, Cuervo C, Danion JM, Peretti CS, Salamé P. Reduced levels of specific autobiographical memories in schizophrenia. *Psychiatry Res* 2003; **117**: 35-45 [PMID: 12581819 DOI: 10.1016/S0165-1781(02)00317-7]

147 **Anticevic A**, Corlett PR. Cognition-emotion dysinteraction in schizophrenia. *Front Psychol* 2012; **3**: 392 [PMID: 23091464 DOI: 10.3389/fpsyg.2012.00392]

148 **Cuervo-Lombard C**, Lemogne C, Gierski F, Béra-Potelle C, Tran E, Portefaix C, Kaladjian A, Pierot L, Limosin F. Neural basis of autobiographical memory retrieval in schizophrenia. *Br J Psychiatry* 2012; **201**: 473-480 [PMID: 22539776 DOI: 10.1192/bjp.bp.111.099820]

149 **Ernst A**, Botzung A, Gounot D, Sellal F, Blanc F, de Seze J, Manning L. Induced brain plasticity after a facilitation programme for autobiographical memory in multiple sclerosis: a preliminary study. *Mult Scler Int* 2012; **2012**: 820240 [PMID: 23125932 DOI: 10.1155/2012/820240]

P- Reviewers: Kawabori M, Quattrocchi CC **S- Editor**: Zhai HH
L- Editor: Roemmele A **E- Editor**: Liu SQ

World Journal of Radiology

Online Submissions: http://www.wjgnet.com/esps/
bpgoffice@wjgnet.com
doi:10.4329/wjr.v6.i4.106

World J Radiol 2014 April 28; 6(4): 106-115
ISSN 1949-8470 (online)

MINIREVIEWS

Orbital inflammatory disease: Pictorial review and differential diagnosis

Michael N Pakdaman, Ali R Sepahdari, Sahar M Elkhamary

Michael N Pakdaman, Ali R Sepahdari, Department of Radiological Sciences, David Geffen School of Medicine, University of California Los Angeles, Los Angeles, CA 90095, United States
Sahar M Elkhamary, Radiology Department, King Khaled Eye Specialist Hospital, Saudi Arabia and Diagnostic Radiology Department, Mansoura Faculty of Medicine, Riyadh 12329, Egypt
Author contributions: Pakdaman MN, Sepahdari AR and Elkhamary SM contributed equally to this work; Sepahdari AR designed the review article structure; Pakdaman MN and Sepahdari AR performed literature review and write-up of this review manuscript; Elkhamary SM analyzed the clinical relevance and relevance of supporting articles, and contributed to drafting and revision of the manuscript; Sepahdari AR provided final approval of the version to be published.
Correspondence to: Ali R Sepahdari, MD, Assistant Professor, Department of Radiological Sciences, David Geffen School of Medicine, University of California Los Angeles, 757 Westwood Plaza, Suite 1621D, Los Angeles, CA 90095, United States. asepahdari@mednet.ucla.edu
Telephone: +1-310-2676708 Fax: +1-310-2673635
Received: December 16, 2013 Revised: January 21, 2014
Accepted: April 11, 2014
Published online: April 28, 2014

Abstract

Orbital inflammatory disease (OID) represents a collection of inflammatory conditions affecting the orbit. OID is a diagnosis of exclusion, with the differential diagnosis including infection, systemic inflammatory conditions, and neoplasms, among other conditions. Inflammatory conditions in OID include dacryoadenitis, myositis, cellulitis, optic perineuritis, periscleritis, orbital apicitis, and a focal mass. Sclerosing orbital inflammation is a rare condition with a chronic, indolent course involving dense fibrosis and lymphocytic infiltrate. Previously thought to be along the spectrum of OID, it is now considered a distinct pathologic entity. Imaging plays an important role in elucidating any underlying etiology behind orbital inflammation and is critical for ruling out other conditions prior to a definitive diagnosis of OID. In this review, we will explore the common sites of involvement by OID and discuss differential diagnosis by site and key imaging findings for each condition.

Key words: Orbit; Inflammation; Pseudotumor; Orbital inflammatory disease; Nonspecific orbital inflammation; Dacryoadenitis; Myositis; Orbital cellulitis; Optic perineuritis; Orbital apicitis

Core tip: This review provides a pictorial summary of orbital inflammatory disease (OID). It outlines many key aspects of OID on imaging that can be used to distinguish from other pathologic conditions. The review also provides an up-to-date overview of the best approaches to imaging workup when suspecting OID.

Pakdaman MN, Sepahdari AR, Elkhamary SM. Orbital inflammatory disease: Pictorial review and differential diagnosis. *World J Radiol* 2014; 6(4): 106-115 Available from: URL: http://www.wjgnet.com/1949-8470/full/v6/i4/106.htm DOI: http://dx.doi.org/10.4329/wjr.v6.i4.106

INTRODUCTION

Orbital inflammatory disease (OID, aka orbital inflammatory pseudotumor, idiopathic orbital inflammatory syndrome, nonspecific orbital inflammation)[1-3] was first described by Gleason in 1903[4] and accounts for 6% of diseases involving the orbit. It is the third most common orbital disease after Grave's orbitopathy and lymphoproliferative diseases[5]. OID is most commonly unilateral with symptoms and clinical findings depending on the site involved as well as the degree of inflammation, fibrosis, and any mass effect. Generally, acute OID presents with proptosis, extraocular motility disturbance, pain, erythema, and chemosis[2]. As OID is a diagnosis

Table 1 Differential diagnosis of orbital inflammatory disease by site

Structure involved	Clinical condition	Common imaging findings	Differential diagnosis
Lacrimal gland	Dacryoadenitis	Diffuse lacrimal gland enlargement	Epithelial neoplasm, lymphoma
Extraocular muscles	Myositis	Unilateral EOM inflammation, usually involving surrounding fat and myotendinous junction	Dysthyroid orbitopathy
Optic nerve sheath	Perineuritis	Peripheral enhancement about the optic nerve, with varying infiltration of surrounding fat. Variable enhancement of the nerve substance	Optic nerve sheath meningioma, demyelinating optic neuritis
Orbital/periorbital fat	Cellulitis	Enhancing periorbital soft tissue with possible intraconal extension	Infectious orbital cellulitis, carotid cavernous fistula, cavernous sinus thrombosis
Orbital apex	Orbital apicitis, Tolosa-Hunt syndrome	Ill-defined, T2 hypointense enhancing tissue at orbital apex, variably involving middle cranial fossa and cavernous sinus	Meningioma, other dural infiltrative process
Periscleral	Periscleritis	Scleral thickening with periscleral edema and fluid in Tenon's capsule	Endophthalmitis

EOM: Extraocular muscles.

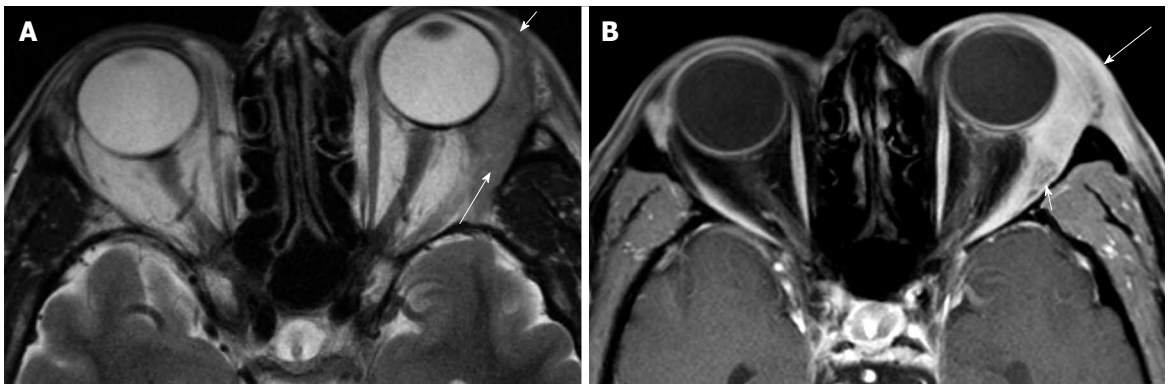

Figure 1 Dacryoadenitis. A: Axial T2 shows diffuse enlargement of the left lacrimal gland. Note the tapered posterior margin (long arrow), as well as the involvement of the orbital lobe (short arrow). These findings suggest a lymphoid or inflammatory process rather than an epithelial neoplasm; B: Axial fat-suppressed contrast-enhanced T1 shows infiltration of the preseptal (long arrow) and post septal (short arrow) fat. These features suggest orbital inflammatory disease rather than orbital lymphoma.

of exclusion, patients must be evaluated to rule out any malignancy, infection, systemic inflammatory process, or other concomitant medical conditions[6]. The differential diagnosis includes local and systemic inflammatory conditions caused by neoplasm, infection, vascular malformation, and trauma[5].

Inflammation occurs as a non-specific response to potentially harmful stimuli and is marked by increased blood flow and vascular permeability, vasodilatation, release of soluble mediators, extravasation of fluids, and cellular influx[7]. Imaging findings in inflammatory disease are most often related to increased blood-tissue permeability resulting in contrast enhancement, which is often best seen with the use of fat suppression. Other common imaging findings in inflammation include fibrosis and edema[8].

The site of involvement by OID dictates the radiological differential diagnosis, which can be especially important given that the symptoms may be nonspecific. We will review the common sites of involvement by OID and discuss differential diagnosis by site, as outlined in Table 1. However, it is important to note that OID commonly involves multiple sites, and that this feature is often important in suggesting OID ahead of other lesions.

Dacryoadenitis

Inflammation of the lacrimal gland, termed "dacryoadenitis", is commonly seen in OID. Clinically, dacryoadenitis presents as a painful, firm, erythematous mass with edema in the lateral upper lid, and possible ptosis[9,10]. Because the abnormality diffusely involves the lymphoid structures of the lacrimal gland, the classic appearance is of diffuse enlargement of the gland, including the orbital and palpebral lobes (Figure 1)[10,11]. This is an important feature in distinguishing inflammatory disease from an epithelial neoplasm, which will typically only involve a portion of the lacrimal gland, usually the orbital lobe (Figure 2). Additional features that suggest an inflammatory process are a compressed, "almond-shaped" appearance of the gland as well as a tapered posterior margin of the gland. In contrast, an epithelial neoplasm will typically be seen as well-circumscribed and round to oval in shape[10,12]. The axial T2 magnetic resonance imaging (MRI) in Figure 1A shows diffuse enlargement of the left lacrimal gland. Note the tapered posterior margin, as well as the involvement of the orbital lobe. These findings suggest a lymphoid or inflammatory process rather than an epithelial neoplasm.

Although it is usually relatively straightforward to dis-

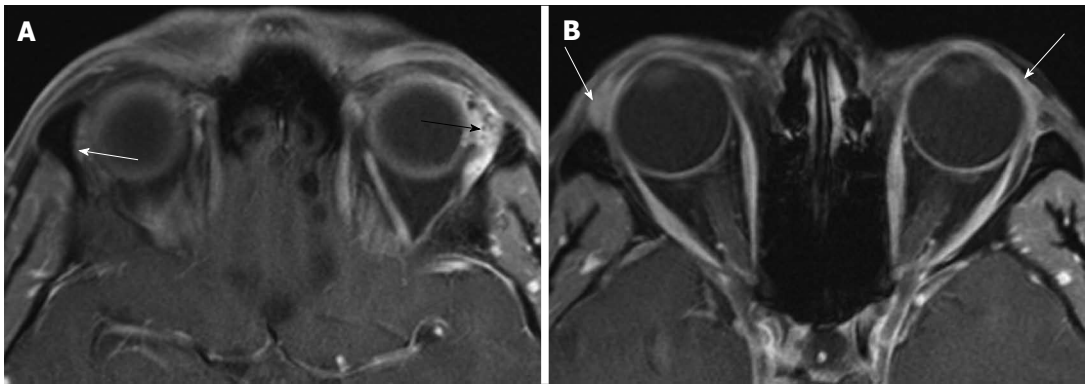

Figure 2 Adenoid cystic carcinoma of the lacrimal gland. A: Axial T1 non-enhanced MRI showing an enlarged, heterogeneous left lacrimal gland (black arrow). Compare this to the contralateral normal gland (white arrow); B: Axial T1 non-enhanced MRI showing sparing of the palpebral lobe (arrows). MRI: Magnetic resonance imaging.

tinguish an epithelial lacrimal gland neoplasm from a process involving the glandular lymphoid tissue, it is not always easy to distinguish lymphoma of the lacrimal gland from inflammatory disease. There are a few features that can aid in this distinction. First, inflammatory disease is more commonly bilateral (30% of chronic and 20% of acute inflammatory disease *vs* 12%-18% of lymphoma cases)[13-15]. Second, inflammatory disease is more commonly associated with inflammation of the surrounding soft tissues. Figure 1B is an axial fat-suppressed contrast-enhanced T1 that shows infiltration of the preseptal and post septal fat. These features suggest OID rather than orbital lymphoma. There are exceptions to these rules, however. Sarcoid commonly produces diffuse lacrimal gland enlargement without infiltration of surrounding fat, a pattern that is more suggestive of lymphoma. Lymphoma may also have a surrounding inflammatory component in some cases[12].

Diffusion-weighted imaging (DWI) is perhaps the most reliable technique to distinguish lymphoma from inflammatory disease. The densely packed cells in lymphoma inhibit the non-random motion of water, causing lymphoma to appear bright on DWI, with associated reduction in apparent diffusion coefficient (ADC) (Figure 3). An ADC of less than 0.92×10^{-3} mm^2/s was shown to be 100% sensitive and specific in distinguishing lymphoma from inflammatory disease[3], though we have seen a handful of exceptions to this rule. Politi *et al*[13] found an ADC threshold of 0.775×10^{-3} mm^2/s was 96% sensitive and 93% specific for diagnosing ocular adnexal lymphoma.

Myositis

Orbital myositis is a non-infectious inflammatory condition primarily affecting the extraocular muscles (EOM)[16]. Clinically, it presents with unilateral orbital or periorbital pain (17%-69%), painful and restricted eye movement (46%-54%), proptosis (32%-82%), periorbital edema (42%-75%), and hyperemia of the conjunctiva (33%-48%)[17]. The classic appearance of EOM myositis includes a unilateral thickening of one or two EOMs, often also involving the surrounding fat, tendon, and myotendinous junction (Figure 4). These are important features in distinguishing myositis from thyroid orbitopathy, which typically produces bilateral inflammation of EOM and spares the myotendinous junction. Of note, sparing of the myotendinous junction alone does not exclude OID. The lateral rectus and superior oblique muscles are also relatively spared early in the disease course in thyroid orbitopathy, and the condition often presents clinically with proptosis, chemosis, and diplopia. These findings may also suggest IgG4-related disease (IgG4-RD), which may present with similar clinical symptoms. The lymphocytic infiltration characteristic of IgG4-RD is often seen as inflammation of bilateral lacrimal glands and EOM's[18]. The most frequently affected muscle is the inferior rectus. In patients with normal thyroid stimulating hormone and thyroid, these findings may suggest IgG4-RD and a serum IgG4 level may be considered.

The differential diagnosis for myositis also includes orbital cellulitis, which is commonly accompanied by fever, leukocytosis, and a clinical history of head and neck infection. Contrast-enhanced computed tomography (CT) imaging may identify the source of spread to the orbit and may also help identify any abscess that requires surgical intervention[17]. Figure 5 demonstrates a case of infectious orbital cellulitis where corresponding sinus disease can be appreciated. Metastases and lymphoma may also mimic myositis and are often seen as a focal mass with increased signal intensity in the EOM's[17]. Patients with low-flow carotid cavernous fistula (CCF) may also share features with myositis, as the venous congestion may appear on CT and MRI as inflamed EOM[19] (Figure 6). Enlarged superior ophthalmic veins (SOVs) are typically seen in CCF. Transcranial doppler ultrasonography allows visualization of retrograde flow through the SOV, suggestive of CCF[20] and angiography can be used to best characterize the fistulous communication (Figure 6C).

Contrast-enhanced T1 MRI with fat suppression best visualizes inflammation of the muscles, tendons, and surrounding fat, which is seen as swelling of the tendon and belly of the EOM. While not diagnostic, involvement of the perimuscular tendon is a distinguishing finding of non-thyroid inflammatory disease[17]. In Figure 4C, a

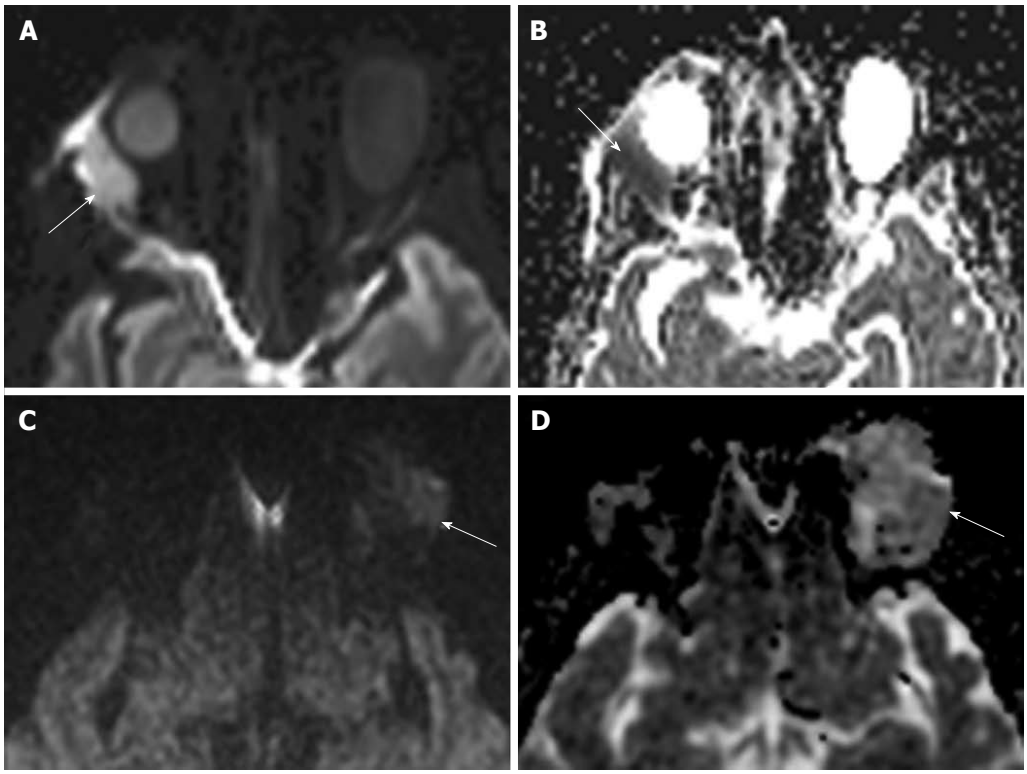

Figure 3 Lacrimal gland lymphoma (A and B) compared to inflammatory dacryoadenitis (C and D). A: DWI image in a patient with lacrimal gland lymphoma. Note the bright signal intensity (arrow) secondary to inhibition of water movement by the densely packed lymphoma cells; B: The corresponding ADC map of this patient shows an associated reduction in ADC, represented by the dark signal just lateral to the orbit (arrow); C: DWI image in a patient with inflammatory dacryocystadenitis. Note the dark signal compared to the patient with lymphoma (arrow); D: ADC map shows bright signal in the involved lacrimal gland (arrow) as compared to normal brain parenchyma. DWI: Diffusion-weighted imaging; ADC: Apparent diffusion coefficient.

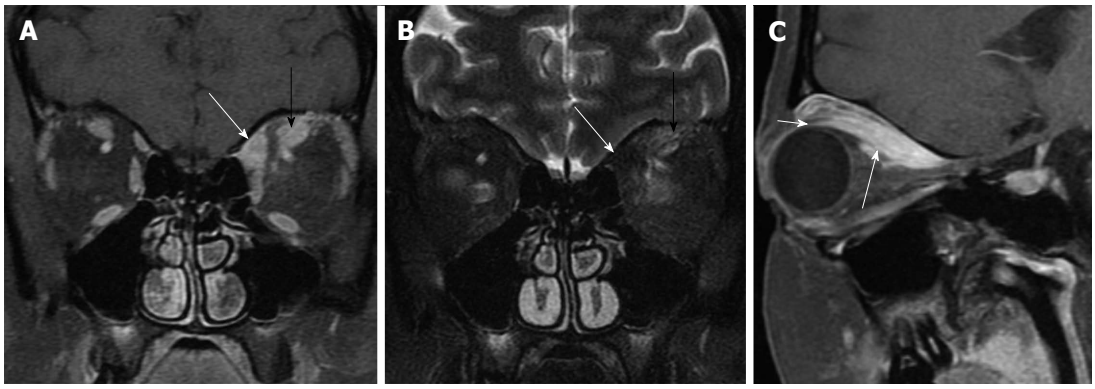

Figure 4 Myositic pseudotumor. A: Coronal fat-suppressed contrast-enhanced T1 shows enlarged left superior oblique (white arrow) and superior rectus (black arrow) muscles, and mild infiltration of the surrounding fat; B: Coronal fat-suppressed T2 shows low signal in the superior oblique muscle (white arrow), suggesting a more chronic, burned out process, whereas the superior rectus muscle (black arrow) shows brighter signal, indicative of a more acute process; C: Parasagittal oblique fat-suppressed contrast-enhanced T1 shows an enlarged superior rectus muscle belly (long arrow). The tendinous insertion (short arrow) is uncharacteristically spared by this process. Nevertheless, unilateral disease, infiltration of the surrounding fat, and early involvement of the superior oblique muscle indicate pseudotumor ahead of thyroid eye disease.

parasagittal oblique fat-suppressed contrast-enhanced T1 shows an enlarged superior rectus muscle belly with uncharacteristic sparing of the tendinous insertion. Nevertheless, unilateral disease, infiltration of the surrounding fat, and early involvement of the superior oblique muscle indicate pseudotumor ahead of thyroid eye disease. In cases where it is difficult to distinguish inflammation versus lymphoma, DWI can be used, as described above.

Cellulitis

Inflammatory orbital cellulitis describes inflammation of preseptal (peri-orbital) or postsetpal (orbital) fat[21]. Patients typically present with proptosis, chemosis, and painful diplopia[21]. Cellulitis of preseptal and orbital soft tissue is best evaluated on contrast-enhanced T1 MRI with fat suppression, where the most common finding is poorly-defined periorbital enhancement enveloping

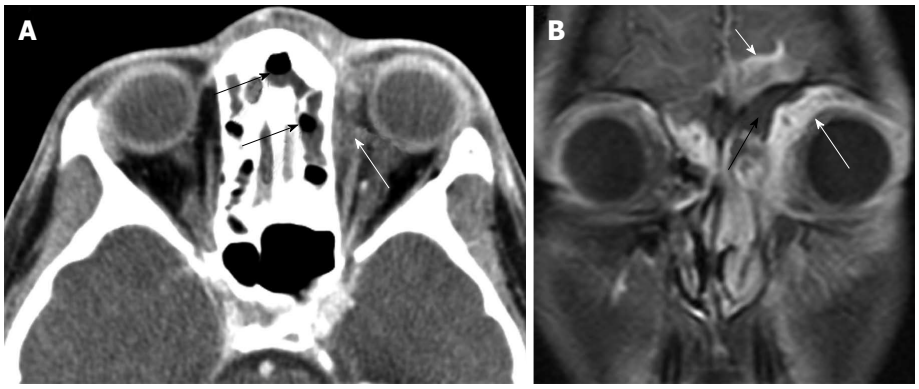

Figure 5 Infectious orbital cellulitis. A: Axial CT showing layering fluid in the ethmoid sinus and frontal recess on the left (black arrows), and infiltration of the orbital fat (white arrow); B: Coronal T1 fat saturated post-gadolinium MRI demonstrates orbitalfat infiltration (long white arrow). Fluid in the adjacent ethmoid sinus (black arrow) and intracranial extension of the process (short white arrow) are also features that indicate infection rather than orbital inflammatory disease. CT: Computed tomography; MRI: Magnetic resonance imaging.

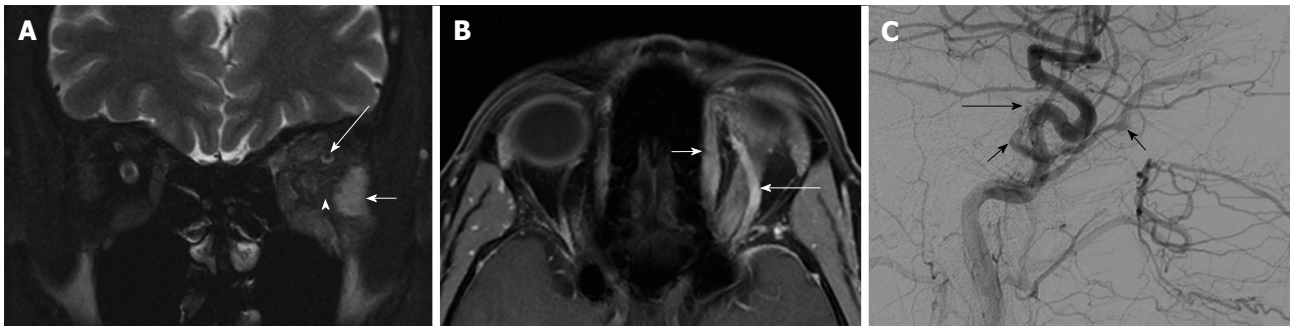

Figure 6 Indirect carotid-cavernous fistula. A: Coronal T2 MRI with fat saturation demonstrating mild infiltration of orbital fat (arrowhead) and thickening with high signal intensity in the EOMs. In this image, the lateral rectus muscle appears brightest (short white arrow). Note the enlarged SOV (long white arrow), suggesting CCF over myositis; B: Axial post-gadolinium T1 MRI with fat saturation. The SOV (long white arrow) is engorged secondary to retrograde flow from the cavernous sinus. The superior oblique muscle (short white arrow) is also enlarged; C: Angiogram with lateral projection common carotid artery injection (patient facing to the right) showing abnormal early filling in the cavernous sinus and SOV (short black arrows), as well as an abnormal tangle of vessels along dorsal surface of cavernous sinus (long black arrow), representing abnormally dilated intracavernous ICA branches. MRI: Magnetic resonance imaging; EOM: Extraocular muscles; SOV: Superior ophthalmic vein; CCF: Carotid cavernous fistula; ICA: Internal carotid artery.

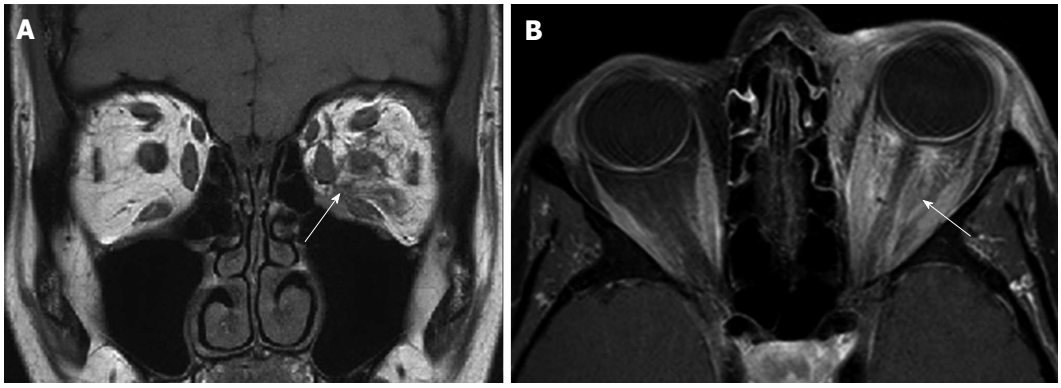

Figure 7 Diffuse cellulitic orbital inflammatory disease. A: Coronal T1-weighted image shows diffuse infiltration of the intraconal fat on the left (arrow); B: Axial fat-suppressed contrast-enhanced T1 shows diffuse enhancement throughout the intraconal fat. No well-defined focal mass or focal fluid collection is seen.

the globe and extending into post-septal fat[4]. Figure 7 is a T1-weighted MRI image showing diffuse infiltration of the intraconal fat. Infectious cellulitis shares similar imaging features, and it is important to obtain any clinical history of fever, sinusitis, or meningitis, as well as any evidence of leukocytosis[2,11]. Presence of an abscess is a clear indicator of an infectious process. On T2 MRI, infectious cellulitis typically presents as a hyperintense lesion, whereas OID lesions range from to hypo- to hyperintense[2]. Additional features suggesting inflammation of orbital and pre-septal fat include increased density and enhancement of periorbital soft tissues, eyelids, and orbital septum. Intraconal extension is a sign of advanced disease.

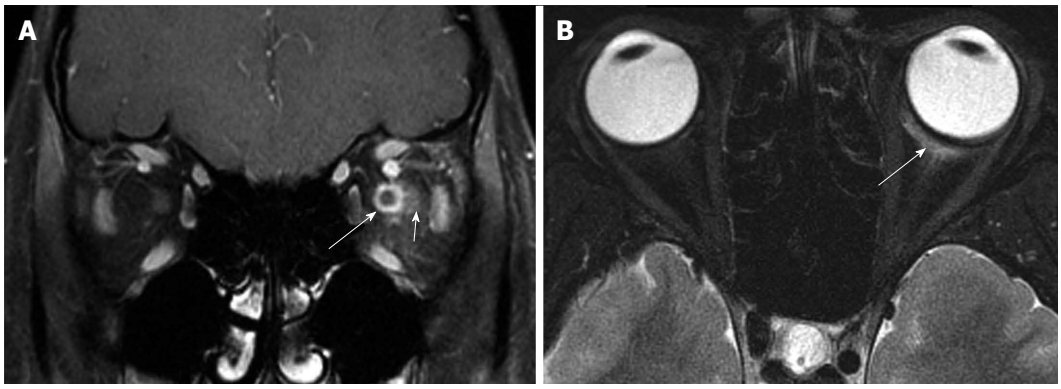

Figure 8 Perineuritic orbital inflammatory disease. A: Coronal fat-suppressed contrast-enhanced T1 shows circumferential enhancement about the left optic nerve (long arrow), with sparing of the nerve substance. There is also mild infiltration of the surrounding soft tissues (short arrow); B: Axial fat-suppressed T2 shows a small amount of edema about Tenon's capsule (arrow). This finding, along with clinical history of acute, painful presentation, help distinguish perineuritic pseudotumor from en plaque optic nerve sheath meningioma.

The differential diagnosis for inflammatory orbital cellulitis includes infection, CCF, cavernous sinus thrombosis, and Wegener's granulomatosis. Careful evaluation for any evidence of sinus disease is critical as infectious orbital cellulitis is a potentially life-threatening disease. Clinically, patients with infectious orbital cellulitis may have a history of diabetes or immunocompromise and a clinical history of sinus disease, recent dental procedures, or trauma. Due to the serious nature of infectious orbital cellulitis, a definitive diagnosis of OID may not be made until after a lack of response to empirical broad-spectrum antibiotic therapy[5]. A CCF may be distinguished from OID by presence of an enlarged SOV, abnormal fullness of the cavernous sinus, or, in larger fistulas, flow voids on T2 MRI. Similar to CCF, cavernous sinus thrombosis presents with an enlarged SOV. A non-enhancing filling defect in the cavernous sinus on CT venography or contrast-enhanced MRI differentiates cavernous sinus thrombosis from CCF or OID. Wegener's granulomatosis (*i.e.*, granulomatosis with polyangiitis) may also mimic OID but is often accompanied by surrounding sinonasal wall destruction, which is best appreciated on CT.

Optic perineuritis

When intraorbital inflammation extends along the optic nerve and nerve sheath, it is termed "perineuritis"[9]. Because inflammation affects the nerve sheath rather than the nerve itself, the primary presenting clinical feature is pain, while visual acuity, visual fields, and color vision are typically unaffected[22]. Because the abnormality involves a loosely organized inflammatory infiltrate around the optic nerve, the classic appearance is of increased signal intensity surrounding the optic nerve, and extending into adjacent fat on post-gadolinium T1 MRI with fat-suppression (Figure 8A)[9,22]. Enhancement of the optic nerve sheath is often poorly-defined[23], which, in addition to a history of pain, may serve as an important feature in distinguishing perineuritis from meningioma (Figure 8B). This finding, along with clinical history of acute, painful presentation, help distinguish perineuritic pseudotumor from en plaque optic nerve sheath meningioma. Features supporting a diagnosis of meningioma include a localized mass and calcifications on CT imaging[9].

The differential diagnosis also includes demyelinating optic neuritis, though demyelinating disease almost always spares the soft tissues around the nerve while involving the nerve substance diffusely[23]. It is important to distinguish perineuritis from optic neuritis, as the differential diagnosis and clinical course are quite different. Patients with optic neuritis (ON) are at high risk of developing multiple sclerosis and should be evaluated to rule out this disease. Diagnosis of optic perineuritis (OPN) is also critical, as prompt corticosteroid treatment may help prevent vision loss. Clinically, both OPN and ON typically present with eye pain and a swollen optic disc. While less commonly compared to ON, patients with OPN may also complain of vision impairment, though the vision impairment in OPN is often paracentral or arcuate[23]. MRI of perineuritis often shows a "tram-track" pattern of enhancement around the nerve, rather than involving the nerve itself. Additionally, syphilitic infection, sarcoidosis, and viral encephalitides should be considered in patients with perineuritis[24].

Periscleritis

Periscleritis may refer to inflammation of the sclera, uvea (iris, ciliary body, choroid), or tenon's capsule[9]. This condition may present as a uveitis or a scleritis/episcleritis. Clinically, features of this inflammatory condition may mimic infection or tumor and are characterized by orbital pain, exophthalmos, and eyelid edema. Periscleritis can be clearly seen on MR or CT as a heterogeneous thickening along the outer rim of the eye[25] (Figure 9), representing thickening of the sclera and/or uvea. Features of periscleritis can be best appreciated on axial T1 post-contrast MRI with fat saturation, which allows visualization of the enhancing vascular choroid as well as any extension into retrobulbar fat. A subchoroidal fluid collection displacing the retina may also be seen. Figure 9A shows an axial contrast-enhanced CT in an 87-year-old immunocompromised man with left eye pain and and ordering indication of "cellulitis". Note the mild infiltration of the

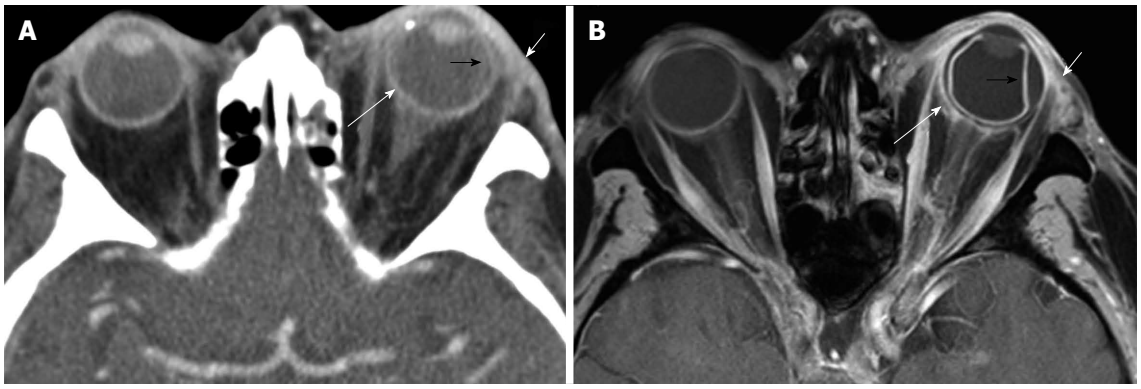

Figure 9 Periscleritic orbital inflammatory disease. Eighty-seven-year-old immunocompromised man with left eye pain and ordering indication of "cellulitis". A: Axial contrast-enhanced CT shows mild infiltration of the left periorbital fat (short white arrow). There is also periscleral edema (long white arrow), and subtle high density along the temporal surface of the globe that is suggestive of a subchoroidal fluid collection (black arrow); B: Axial fat-suppressed contrast-enhanced T1 shows these findings more conspicuously. Note that the elevated choroid layer (black arrow) extends anteriorly to the region of the ciliary body. Periscleral edema (long white arrow) extending to Tenon's capsule is better seen. CT: Computed tomography.

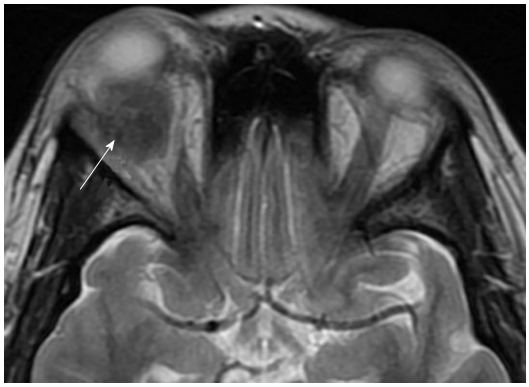

Figure 10 Orbital inflammatory disease producing a focal mass. Axial T2 shows a well-defined, T2 hypointense mass in the right orbit, discrete from adjacent extraocular muscles and from the lacrimal gland.

left periorbital fat, periscleral edema, and subtle high density along the temporal surface of the globe suggestive of a subchoroidal fluid collection. An axial fat-suppressed contrast-enhanced T1 MRI in this patient shows these findings more conspicuously (Figure 9B). Tenon's capsule (aka fascia bulbi or bulbar sheath) is a thin membrane that lies between the sclera and orbital fat[26]. Thickening is often seen in this area and may be accompanied by a periscleral fluid collection.

The differential diagnosis includes any systemic inflammatory disease that causes posterior scleritis, such as lupus or rheumatoid arthritis. Endophthalmitis may also have a similar imaging appearance, but clinical vitritis should be readily apparent in these cases. Infectious periscleritis often arises secondary to sinus infection and it is important to evaluate the paranasal sinuses, particularly the ethmoid sinus, in patients with uveoscleral thickening[4].

Focal mass

OID may also present as a focal inflammatory mass, which represents up to 9% of all orbital mass lesions and is the most common cause of painful orbital mass in adults[6,9]. Clinical presentation is highly variable as an inflammatory mass can be present anywhere in the orbit, with resulting symptoms related to mass effect and inflammation. A mass lesion in OID is best seen on axial T2 MRI, where it appears as a well-defined, T2 hypointense mass, discrete from adjacent EOM and from the lacrimal gland (Figure 10). The hypointensity appreciated in this image is secondary to fibrosis. On T1 MRI they appear slightly brighter, isointense to muscle, and show prominent post-gadolinium enhancement[27]. As lesions progress, fibrosis develops, resulting in retraction of adjacent structures. Infiltration of inflammation and fibrosis into the sclera and periorbital soft tissue may lead to globe deformity. In fact, the degree of fibrosis and traction on other tissues often suggests a greater chronicity of disease.

Inflammatory pseudotumors are often difficult to distinguish from a true neoplasm[28]. Lymphoma accounts for 20% of orbital mass lesions and is particularly difficult to distinguish from OID[27,28]. Clinically, lymphomatous lesions present more commonly with palpable mass, while OID may present with eyelid edema, optic nerve atrophy, and conjunctival congestion[27]. Imaging features of inflammatory pseudotumor that help distinguish it from lymphoma include marked T2 hypointensity and evidence of fibrosis. Lymphoma typically appears more lobular and, as described earlier, has greater diffusion restriction than OID on DWI. Metastases are usually brighter on T2 imaging. One exception to this is scirrhous breast cancer metastasis, which commonly produces a T2-hypointense, fibrotic mass with variable amount of traction on adjacent structures. Certain benign tumors, such as solitary fibrous tumor, can also show marked T2 hypointensity and overlap with OID in appearance[29].

Diffuse OID

Diffuse orbital inflammation is found in approximately 4%-11% of patients with OID[30]. Similar to focal mass, clinical presentation is highly variable as many sites of the orbit can be affected. Patients must be evaluated for systemic disease, including vasculitis and autoimmune conditions such as Churg-Strauss disease or Wegener's

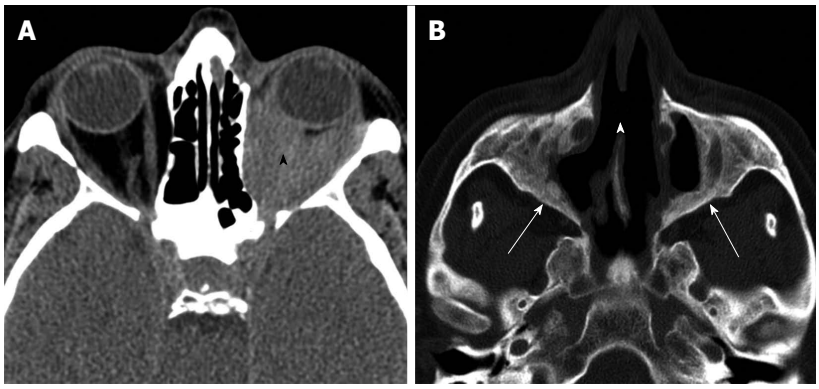

Figure 11 Wegener's granulomatosis. A: Non-enhanced axial CT through orbit demonstrating diffuse infiltration of orbital fat (black arrowhead); B: Axial CT in through sinuses in bone window shows destruction of medial maxillary sinus walls, perforation of nasal septum (white arrowhead), and chronic neo osteogenesis along sinus walls (white arrows). CT: Computed tomography.

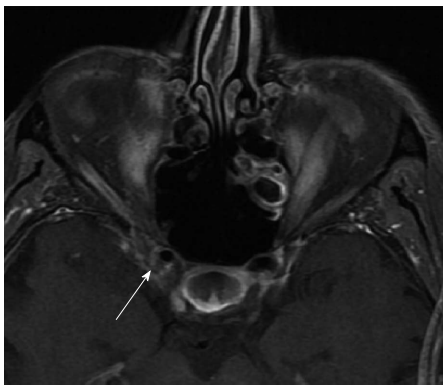

Figure 12 Orbital apicitis (Tolosa-Hunt). Axial fat-suppressed contrast-enhanced T1 shows ill-defined enhancement involving the right orbital apex, and extending into the middle cranial fossa along the margin of the cavernous sinus (arrow).

granulomatosis[31,32]. Common characteristics of orbital involvement in Wegener's include diffuse infiltration of orbital fat and sinonasal destructive changes (Figure 11). Chest imaging and an immunologic workup are suggested prior to biopsy of diffuse OID. Lymphoma may also mimic diffuse OID and, as described earlier, appears more lobular and may be best distinguished from OID using DWI MRI[3]. Chronic inflammation often contains regions with varying degrees of fibrosis, resulting in a heterogeneous appearance on MRI.

Orbital apicitis

Involvement of the orbital apex, while less common, is associated with the poorest outcome[4,9,33]. Inflammatory lesions of the orbital apex are at risk of invading the optic nerve or extending into the cavernous sinus. Tolosa-Hunt syndrome is a rare clinical condition caused by cavernous sinus inflammation presenting with relapsing/remitting acute orbital pain and paralysis of cranial nerves Ⅲ, Ⅳ, V_1, and Ⅵ[34]. Extension of OID into the cavernous sinus is a common cause of this clinical condition and, similar to other OID lesions, intravenous steroid treatment is the mainstay of care[11,34]. On T1 MRI, inflammation appears as an intermediate intensity lesion, as inflammatory tissue replaces the normal high-intensity fat at the orbital apex. Similar to other inflammatory pseudotumors, OID of the orbital apex appears hypointense on T2, with a darker signal indicating higher degrees of fibrosis[9,33]. In addition to the cavernous sinus, lesions of the orbital apex may also extend into the middle cranial fossa through the superior orbital fissure or optic canal, as well as the infratemporal fossa and pterygopalatine fossa through the inferior orbital fissure. Figure 12 shows an axial, fat-suppressed, contrast-enhanced T1 MRI in a patient with Tolosa-Hunt syndrome. Note the ill-defined enhancement involving the right orbital apex and extending into the middle cranial fossa along the margin of the cavernous sinus (arrow). Figure 13 shows bilateral cavernous sinus infiltration in a different patient, which resolved completely after treatment.

The differential diagnosis of orbital apex lesions includes meningioma, granulomatous disease, and local spread of central nervous system (CNS) pathology. Evidence of cystic foci likely represents necrotic lesions, which leads the diagnosis away from OID. Enhancement or fullness of the cavernous sinus can be appreciated on dynamic imaging and angiography may demonstrate narrowing of the cavernous sinus. Careful examination for disruption of the dural barrier and intracranial extension is critical. Common features of CNS involvement include abnormal soft tissue extending into the middle cranial fossa, expansion of the ipsilateral cavernous sinus walls, and post-gadolinium enhancement of the meninges or dura[9].

Sclerosing orbital inflammation

Sclerosing orbital inflammation is a rare condition representing 6%-8% of all inflammatory lesions of the orbit[35]. Previously thought to be along the spectrum of OID, it is now considered a distinct pathologic entity. Clinically, it is characterized by proptosis, mild external inflammatory signs, restricted motility, diplopia, and dull, chronic pain[5]. The natural history of the condition often involves a chronic, indolent, progressive process involving dense fibrosis and lymphocytic infiltrate. On CT or MRI, it is most commonly described as a homogenous, diffuse, ill-defined mass most frequently in the anterior orbit and mid-orbit.

Definitive diagnosis is by biopsy, revealing dense scarring and fibrosis. While no definitive treatment has been identified, early and aggressive steroid therapy is recommended as vision loss may occur in up to 30% of

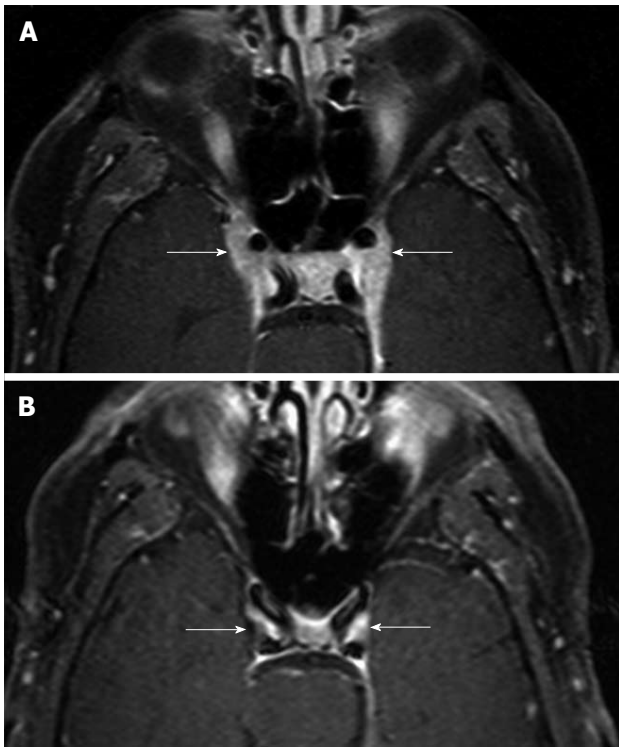

Figure 13 Tolosa-Hunt syndrome, before and after treatment. A: Axial fat-suppressed contrast-enhanced T1 showing bilateral cavernous sinus infiltration and enhancing tissue along the lateral margins of the cavernous sinus; B: Complete resolution after treatment.

affected patients[5].

CONCLUSION

OID or orbital pseudotumor, represents a group of heterogeneous inflammatory diseases, the exact etiology of which is unknown. The condition may involve a number of structures in the orbit, the clinical presentations and imaging findings of which are variable and overlapping. As OID is a diagnosis of exclusion, other pathologic conditions affecting the orbit must be ruled out. Imaging plays an important role in evaluation of OID, with proper identification of involved structures being a critical first step toward diagnosis. CT, MRI with fat suppression, and DWI all play a role in distinguishing OID from other pathologies affecting the orbit. Treatment for OID consists of pulsed corticosteroid therapy and the degree of response may often provide clues as to the diagnosis.

REFERENCES

1 **Swamy BN**, McCluskey P, Nemet A, Crouch R, Martin P, Benger R, Ghabriel R, Wakefield D. Idiopathic orbital inflammatory syndrome: clinical features and treatment outcomes. *Br J Ophthalmol* 2007; **91**: 1667-1670 [PMID: 17620331 DOI: 10.1136/bjo.2007.124156]

2 **Kapur R**, Sepahdari AR, Mafee MF, Putterman AM, Aakalu V, Wendel LJ, Setabutr P. MR imaging of orbital inflammatory syndrome, orbital cellulitis, and orbital lymphoid lesions: the role of diffusion-weighted imaging. *AJNR Am J Neuroradiol* 2009; **30**: 64-70 [PMID: 18842758 DOI: 10.3174/ajnr.A1315]

3 **Sepahdari AR**, Aakalu VK, Setabutr P, Shiehmorteza M, Naheedy JH, Mafee MF. Indeterminate orbital masses: restricted diffusion at MR imaging with echo-planar diffusion-weighted imaging predicts malignancy. *Radiology* 2010; **256**: 554-564 [PMID: 20656840 DOI: 10.1148/radiol.10091956]

4 **Yuen SJ**, Rubin PA. Idiopathic orbital inflammation: distribution, clinical features, and treatment outcome. *Arch Ophthalmol* 2003; **121**: 491-499 [PMID: 12695246 DOI: 10.1001/archopht.121.4.491]

5 **Gordon LK**. Orbital inflammatory disease: a diagnostic and therapeutic challenge. *Eye* (Lond) 2006; **20**: 1196-1206 [PMID: 17019419 DOI: 10.1038/sj.eye.6702383]

6 **Lee EJ**, Jung SL, Kim BS, Ahn KJ, Kim YJ, Jung AK, Park CS, Song SY, Park NH, Kim MS. MR imaging of orbital inflammatory pseudotumors with extraorbital extension. *Korean J Radiol* 2005; **6**: 82-88 [PMID: 15968146]

7 **Ferrero-Miliani L**, Nielsen OH, Andersen PS, Girardin SE. Chronic inflammation: importance of NOD2 and NALP3 in interleukin-1beta generation. *Clin Exp Immunol* 2007; **147**: 227-235 [PMID: 17223962 DOI: 10.1111/j.1365-2249.2006.03261.x]

8 **Narla LD**, Newman B, Spottswood SS, Narla S, Kolli R. Inflammatory pseudotumor. *Radiographics* 2003; **23**: 719-729 [PMID: 12740472 DOI: 10.1148/rg.233025073]

9 **Ding ZX**, Lip G, Chong V. Idiopathic orbital pseudotumour. *Clin Radiol* 2011; **66**: 886-892 [PMID: 21546008 DOI: 10.1016/j.crad.2011.03.018]

10 **Mafee MF**, Edward DP, Koeller KK, Dorodi S. Lacrimal gland tumors and simulating lesions. Clinicopathologic and MR imaging features. *Radiol Clin North Am* 1999; **37**: 219-39, xii [PMID: 10026740]

11 **Lutt JR**, Lim LL, Phal PM, Rosenbaum JT. Orbital inflammatory disease. *Semin Arthritis Rheum* 2008; **37**: 207-222 [PMID: 17765951 DOI: 10.1016/j.semarthrit.2007.06.003]

12 **Gündüz K**, Shields CL, Günalp I, Shields JA. Magnetic resonance imaging of unilateral lacrimal gland lesions. *Graefes Arch Clin Exp Ophthalmol* 2003; **241**: 907-913 [PMID: 14579116 DOI: 10.1007/s00417-003-0748-z]

13 **Politi LS**, Forghani R, Godi C, Resti AG, Ponzoni M, Bianchi S, Iadanza A, Ambrosi A, Falini A, Ferreri AJ, Curtin HD, Scotti G. Ocular adnexal lymphoma: diffusion-weighted mr imaging for differential diagnosis and therapeutic monitoring. *Radiology* 2010; **256**: 565-574 [PMID: 20656841 DOI: 10.1148/radiol.10100086]

14 **Lacrimal Gland Tumor Study Group**. An epidemiological survey of lacrimal fossa lesions in Japan: number of patients and their sex ratio by pathological diagnosis. *Jpn J Ophthalmol* 2005; **49**: 343-348 [PMID: 16187032 DOI: 10.1007/s10384-005-0224-x]

15 **Derr C**, Shah A. Bilateral dacryoadenitis. *J Emerg Trauma Shock* 2012; **5**: 92-94 [PMID: 22416166 DOI: 10.4103/0974-2700.93096]

16 **Kralik SF**, Kersten R, Glastonbury CM. Evaluation of orbital disorders and cranial nerve innervation of the extraocular muscles. *Magn Reson Imaging Clin N Am* 2012; **20**: 413-434 [PMID: 22877949 DOI: 10.1016/j.mric.2012.05.005]

17 **Costa RM**, Dumitrascu OM, Gordon LK. Orbital myositis: diagnosis and management. *Curr Allergy Asthma Rep* 2009; **9**: 316-323 [PMID: 19656480]

18 **Inaba H**, Hayakawa T, Miyamoto W, Takeshima K, Yamaoka H, Furukawa Y, Kawashima H, Ariyasu H, Wakasaki H, Furuta H, Nishi M, Nakao T, Sasaki H, Okada Y, Matsunaga K, Nakamura Y, Akamizu T. IgG4-related ocular adnexal disease mimicking thyroid-associated orbitopathy. *Intern Med* 2013; **52**: 2545-2551 [PMID: 24240795]

19 **Chapman PR**, Gaddamanugu S, Bag AK, Roth NT, Vattoth S. Vascular lesions of the central skull base region. *Semin Ultrasound CT MR* 2013; **34**: 459-475 [PMID: 24216454 DOI: 10.1053/j.sult.2013.09.003]

20 **Kiliç T**, Elmaci I, Bayri Y, Pamir MN, Erzen C. Value of

transcranial Doppler ultrasonography in the diagnosis and follow-up of carotid-cavernous fistulae. *Acta Neurochir* (Wien) 2001; **143**: 1257-1264, discussion 1264-1265 [PMID: 11810390 DOI: 10.1007/s007010100022]

21 **Danesh-Meyer HV**, Rosser PM. Orbital inflammatory disease. *Int Ophthalmol Clin* 2007; **47**: 79-92, ix [PMID: 18049282 DOI: 10.1097/IIO.0b013e3181571eee]

22 **Szatmáry G**. Imaging of the orbit. *Neurol Clin* 2009; **27**: 251-84, x [PMID: 19055983 DOI: 10.1016/j.ncl.2008.09.008]

23 **Purvin V**, Kawasaki A, Jacobson DM. Optic perineuritis: clinical and radiographic features. *Arch Ophthalmol* 2001; **119**: 1299-1306 [PMID: 11545635]

24 **Nakamura M**, Hara R, Kimura R, Ohgiya N, Yamamoto N, Morino I, Yamamoto M. Optic perineuritis not associated with syphilitic infection. *Neuro-Ophthalmology* 1999; **21**: 135-145 [DOI: 10.1076/noph.21.3.135.3900]

25 **Atlas SW**, Grossman RI, Savino PJ, Sergott RC, Schatz NJ, Bosley TM, Hackney DB, Goldberg HI, Bilaniuk LT, Zimmerman RA. Surface-coil MR of orbital pseudotumor. *AJR Am J Roentgenol* 1987; **148**: 803-808 [PMID: 3493667 DOI: 10.2214/ajr.148.4.803]

26 **Tenon JR**, Naus J, Blanken R. Anatomical observations on some parts of the eye and eyelids. 1805. *Strabismus* 2003; **11**: 63-68 [PMID: 12789585]

27 **Yan J**, Wu Z, Li Y. The differentiation of idiopathic inflammatory pseudotumor from lymphoid tumors of orbit: analysis of 319 cases. *Orbit* 2004; **23**: 245-254 [PMID: 15590527 DOI: 10.1080/01676830490487980]

28 **Kawakami K**, Ito R, Tono Y, Yazaki A, Murata T, Baba Y, Uchiyama T, Ito M. Orbital inflammatory lesion as an initial manifestation of systemic nasal type NK/T-cell lymphoma. *J Clin Exp Hematop* 2012; **52**: 137-139 [PMID: 23037631]

29 **Yang BT**, Wang YZ, Dong JY, Wang XY, Wang ZC. MRI study of solitary fibrous tumor in the orbit. *AJR Am J Roentgenol* 2012; **199**: W506-W511 [PMID: 22997401 DOI: 10.2214/AJR.11.8477]

30 **Yan J**, Qiu H, Wu Z, Li Y. Idiopathic orbital inflammatory pseudotumor in Chinese children. *Orbit* 2006; **25**: 1-4 [PMID: 16527767 DOI: 10.1080/01676830500505608]

31 **Takanashi T**, Uchida S, Arita M, Okada M, Kashii S. Orbital inflammatory pseudotumor and ischemic vasculitis in Churg-Strauss syndrome: report of two cases and review of the literature. *Ophthalmology* 2001; **108**: 1129-1133 [PMID: 11382641]

32 **Jordan N**, Verma H, Ekbote A, Sangle S, D'Cruz D. Dacryoadenitis and diffuse orbital inflammation: unusual first presentations of Churg-Strauss syndrome. *Orbit* 2011; **30**: 160-161 [PMID: 21574807 DOI: 10.3109/01676830.2011.569628]

33 **Kline LB**, Hoyt WF. The Tolosa-Hunt syndrome. *J Neurol Neurosurg Psychiatry* 2001; **71**: 577-582 [PMID: 11606665]

34 **Zurawski J**, Akhondi H. Tolosa-Hunt syndrome-a rare cause of headache and ophthalmoplegia. *Lancet* 2013; **382**: 912 [PMID: 24012271 DOI: 10.1016/S0140-6736(13)61442-7]

35 **Pemberton JD**, Fay A. Idiopathic sclerosing orbital inflammation: a review of demographics, clinical presentation, imaging, pathology, treatment, and outcome. *Ophthal Plast Reconstr Surg* 2012; **28**: 79-83 [PMID: 22262301 DOI: 10.1097/IOP.0b013e318238ecf7]

P- Reviewers: Rajabi MT, Sharma S **S- Editor**: Song XX
L- Editor: A **E- Editor**: Liu SQ

World Journal of Radiology

Online Submissions: http://www.wjgnet.com/esps/
bpgoffice@wjgnet.com
doi:10.4329/wjr.v6.i4.116

World J Radiol 2014 April 28; 6(4): 116-118
ISSN 1949-8470 (online)

MINIREVIEWS

Lung cancer screening-don't forget the chest radiograph

Johannes Gossner

Johannes Gossner, Department of Clinical Radiology, Evangelisches Krankenhaus Göttingen-Weende, 37074 Göttingen, Germany
Author contributions: Gossner J contributed solely to this work.
Correspondence to: Johannes Gossner, MD, Department of Clinical Radiology, Evangelisches Krankenhaus Göttingen-Weende, An der Lutter 24, 37074 Göttingen, Germany. johannesgossner@gmx.de
Telephone: +49-551-50341762 Fax: +49-551-50341127
Received: November 1, 2013 Revised: January 18, 2014
Accepted: April 11, 2014
Published online: April 28, 2014

Abstract

Lung cancer is a major health burden and early detection only bears the possibility of curative treatment. Screening with computed tomography (CT) recently demonstrated a mortality reduction in selected patients and has been incorporated in clinical guidelines. Problems of screening with CT are the excessive number of false positive findings, costs, radiation burden and from a global point of view shortage of CT capacity. In contrast, chest radiography could be an ideal screening tool in the early detection of lung cancer. It is widely available, easy to perform, cheap, the radiation burden is negligible and there is only a low rate of false positive findings. Large randomized controlled trials could not show a mortality reduction, but different large population-based cohort studies have shown a lung cancer mortality reduction. It has been argued that community-based cohort studies are more closely reflecting the "real world" of everyday medicine. Radiologists should be aware of the found mortality reduction and realize that early detection of lung cancer is possible when reading their daily chest radiographs. Offering a chest radiograph in selected scenarios for the early detection of lung cancer is therefore still justified.

Key words: Lung cancer; Screening; Mortality; Chest radiograph

Core tip: Screening with computed tomography (CT) recently demonstrated a mortality reduction in selected patients with lung cancer, but there are several shortcomings of screening with CT (false positive findings, high costs, radiation burden, shortage of capacity). In contrast, chest radiography could be an ideal screening tool in the early detection of lung cancer. It is widely available, its radiation burden is negligible and there is only a low rate of false positive findings. In contrast to randomized controlled trials different large population- based cohort studies have shown a lung cancer mortality reduction using chest radiography. In conclusion, early detection of lung cancer is also possible with chest radiography.

Gossner J. Lung cancer screening-don't forget the chest radiograph. *World J Radiol* 2014; 6(4): 116-118 Available from: URL: http://www.wjgnet.com/1949-8470/full/v6/i4/116.htm DOI: http://dx.doi.org/10.4329/wjr.v6.i4.116

Lung cancer is a major health burden and early detection only bears the possibility of curative treatment. Therefore a screening test would be desirable. A number of older studies have tested chest radiography and sputum cytology and most of them showed no reduction in mortality compared to randomized control groups[1]. The publication of the results of the National Lung Screening Trial (NLST), showing mortality reduction of 20% in patients undergoing screening with low-dose chest computed tomography (CT) in comparison to patients undergoing chest radiography, renewed the interest in screening for lung cancer[2]. Based on these results screening with CT for selected patient groups has recently been incorporated in different clinical guidelines. For example the American Association of Thoracic Surgery advocates screening with annual low-dose chest CT for smokers or former

smokers with a 30-pack year history beginning at the age of 55[3]. The main problem with CT screening is the excessive number of false positive findings. In the first two screening rounds of the NLST 27.3% and 27.8% of participants showed suspect findings (*i.e.,* a nodule measuring at least 4 mm). Of these nodules only 3.8% turned out to be lung cancers (230 out of 7731 positive results). This leads to high costs with further diagnostics and causes considerable anxiety in affected individuals with a suspect nodule. CT is also expensive *per se* and from a global point of view not readily available everywhere. Most health care systems will not be able to finance such a CT-based screening program. The radiation burden due to repeated CT scans should also be taken into account.

In contrast, chest radiography could be an ideal screening tool in the early detection of lung cancer. It is widely available, easy to perform, cheap, its radiation burden is negligible and there is only a low rate of false positive findings. As randomized controlled trials (RCT) have shown no reduction in lung cancer mortality compared to control groups it has been concluded by most investigators that screening with chest radiography is ineffective[1]. This view has been repeatedly challenged: most RCT have shown a survival advantage for screened individuals because of a stage shift in diagnosed cancers[4,5]. Because RCT are prone to selection bias (selection of highly motivated individuals and problem of generating two comparable groups) population based cohort studies may give a more realistic view of the situation in medical care[5,6]. Recently, a group of Italian investigators presented their follow-up data of a large population based cohort study[7]. Participation in this trial was offered to all patients at risk for lung cancer (smokers with more than 10 pack years between 45 and 75 years of age) by their general practitioner. The trial consisted of a baseline two view chest radiography and an annually repeated examination (single view) for the following four years. Five thousand eight hundred and fifteen subjects participated and follow up was 8 years. Compared to a statistical control population derived from the national health services data there was a lung cancer mortality reduction of 18% (172 deaths to lung cancer instead of 210 expected). Interestingly, there where only 3.4% false positive findings and only 0.16% unnecessary invasive procedures[7]. There are also several case-control studies from Japan showing a reduction of lung cancer mortality between 40% and 60% using screening with chest radiography and sputum cytology[8]. One population based case-control study from Japan used X-ray screening only and found a lung cancer mortality reduction of more than 20%[9]. Newer technologies like digital radiography, bone suppression or computer-aided nodule detection may further enhance the sensitivity of chest radiography in the detection of early lung cancer, but have not been adopted in the studies mentioned above[10]. Caro *et al*[11] calculated cost-effectiveness of lung cancer screening with chest radiography. They concluded that even an achieved mortality reduction of 6% could be cost-effective.

In conclusion, radiologists should realize that screening with chest radiography leads to reduced lung cancer mortality in population-based cohort studies. Radiologists should be aware that early detection of lung cancer is possible when reading their daily chest radiographs. And in the clinically common scenario of a worried middle aged smoker asking for lung cancer "screening" a chest radiograph is still justified.

Despite the exiting results of the NLST there are many unresolved issues with CT-based screening for lung cancer (how to reduce false-positive findings, optimal patient selection, long term outcome of screened patients, transferability of the results of the NLST to other populations)[12]. Until more data from ongoing trials is available, CT-based screening should therefore not be advocated and used cautiously only.

REFERENCES

1 **Humphrey LL**, Teutsch S, Johnson M. Lung cancer screening with sputum cytologic examination, chest radiography, and computed tomography: an update for the U.S. Preventive Services Task Force. *Ann Intern Med* 2004; **140**: 740-753 [PMID: 15126259 DOI: 10.7326/0003-4819-140-9-200405040-00015]

2 **Aberle DR**, Adams AM, Berg CD, Black WC, Clapp JD, Fagerstrom RM, Gareen IF, Gatsonis C, Marcus PM, Sicks JD. Reduced lung-cancer mortality with low-dose computed tomographic screening. *N Engl J Med* 2011; **365**: 395-409 [PMID: 21714641 DOI: 10.1056/NEJMoa1102873]

3 **Jaklitsch MT**, Jacobson FL, Austin JH, Field JK, Jett JR, Keshavjee S, MacMahon H, Mulshine JL, Munden RF, Salgia R, Strauss GM, Swanson SJ, Travis WD, Sugarbaker DJ. The American Association for Thoracic Surgery guidelines for lung cancer screening using low-dose computed tomography scans for lung cancer survivors and other high-risk groups. *J Thorac Cardiovasc Surg* 2012; **144**: 33-38 [PMID: 22710039 DOI: 10.1016/j.jtcvs.2012.05.060]

4 **Strauss GM**, Gleason RE, Sugarbaker DJ. Chest X-ray screening improves outcome in lung cancer. A reappraisal of randomized trials on lung cancer screening. *Chest* 1995; **107**: 270S-279S [PMID: 7781405 DOI: 10.1378/chest.107.6_Supplement.270S]

5 **Strauss GM**, Dominioni L. Chest X-ray screening for lung cancer: overdiagnosis, endpoints, and randomized population trials. *J Surg Oncol* 2013; **108**: 294-300 [PMID: 23982825]

6 **Dominioni L**, Rotolo N, Mantovani W, Poli A, Pisani S, Conti V, Paolucci M, Sessa F, Paddeu A, D'Ambrosio V, Imperatori A. A population-based cohort study of chest x-ray screening in smokers: lung cancer detection findings and follow-up. *BMC Cancer* 2012; **12**: 18 [PMID: 22251777 DOI: 10.1186/1471-2407-12-18]

7 **Dominioni L**, Poli A, Mantovani W, Pisani S, Rotolo N, Paolucci M, Sessa F, Conti V, D'Ambrosio V, Paddeu A, Imperatori A. Assessment of lung cancer mortality reduction after chest X-ray screening in smokers: a population-based cohort study in Varese, Italy. *Lung Cancer* 2013; **80**: 50-54 [PMID: 23294502 DOI: 10.1016/j.lungcan.2012.12.014]

8 **Sagawa M**, Nakayama T, Tsukada H, Nishii K, Baba T, Kurita Y, Saito Y, Kaneko M, Sakuma T, Suzuki T, Fujimura S. The efficacy of lung cancer screening conducted in 1990s: four case-control studies in Japan. *Lung Cancer* 2003; **41**: 29-36 [PMID: 12826309 DOI: 10.1016/S0169-5002(03)00197-1]

9 **Nakayama T**, Baba T, Suzuki T, Sagawa M, Kaneko M. An evaluation of chest X-ray screening for lung cancer in gunma prefecture, Japan: a population-based case-control study. *Eur J Cancer* 2002; **38**: 1380-1387 [PMID: 12091070]

10 **Freedman M**. State-of-the-art screening for lung cancer (part 1): the chest radiograph. *Thorac Surg Clin* 2004; **14**: 43-52

[PMID: 15382307 DOI: 10.1016/S1547-4127(04)00036-2]
11 **Caro JJ**, Klittich WS, Strauss G. Could chest X-ray screening for lung cancer be cost-effective? *Cancer* 2000; **89**: 2502-2505 [PMID: 11147636 DOI: 10.1002/1097-0142(20001201)89:11]
12 **Zompatori M**, Mascalchi M, Ciccarese F, Sverzellati N, Pastorino U. Screening for lung cancer using low-dose spiral CT: 10 years later, state of the art. *Radiol Med* 2013; **118**: 51-61 [PMID: 22744348 DOI: 10.1007/s11547-012-0843-5]

P- Reviewers: Ng SH, Razek AAKA, Sijens PE
S- Editor: Qi Y **L- Editor**: A **E- Editor**: Liu SQ

World Journal of Radiology

Online Submissions: http://www.wjgnet.com/esps/
bpgoffice@wjgnet.com
doi:10.4329/wjr.v6.i4.119

World J Radiol 2014 April 28; 6(4): 119-124
ISSN 1949-8470 (online)

MINIREVIEWS

Imaging of skeletal muscle in vitamin D deficiency

Bianca Bignotti, Angela Cadoni, Carlo Martinoli, Alberto Tagliafico

Bianca Bignotti, Carlo Martinoli, Radiology Department, University of Genoa, 16138 Genoa, Italy
Angela Cadoni, Alberto Tagliafico, Institute of Anatomy, Department of Experimental Medicine, University of Genoa, 16138 Genoa, Italy
Author contributions: Bignotti B, Cadoni A, Martinoli C and Tagliafico A entirely contributed to this paper.
Supported by Partially founded by the European Society of Musculoskeletal Radiology, Young Investigator Grant to Alberto Tagliafico; UNIGE, No. PRA 2012
Correspondence to: Alberto Tagliafico, MD, Institute of Anatomy, Department of Experimental Medicine, University of Genoa, Via de Toni 14, 16138 Genoa, Italy. albertotagliafico@gmail.com
Telephone: +39-347-9745122 Fax: +39-347-9745122
Received: December 27, 2013 Revised: February 28, 2014
Accepted: April 9, 2014
Published online: April 28, 2014

Key words: Muscle; Vitamin D; Vitamin D deficiency; Ultrasound; Computed tomography; Magnetic resonance imaging

Core tip: Elderly people are prone to accidental falls and many fractures sometimes due to vitamin D deficiency. In this narrative review we will discuss the role of skeletal muscle imaging in vitamin D-deficient individuals. The aim of this paper is to improve and encourage the role of radiologists in this field.

Bignotti B, Cadoni A, Martinoli C, Tagliafico A. Imaging of skeletal muscle in vitamin D deficiency. *World J Radiol* 2014; 6(4): 119-124 Available from: URL: http://www.wjgnet.com/1949-8470/full/v6/i4/119.htm DOI: http://dx.doi.org/10.4329/wjr.v6.i4.119

Abstract

Elderly people are prone to accidental falls and one of the main risk factor is considered muscle weakness. Several studies focused on muscle weakness and muscle morphology changes in the elderly that may be associated with vitamin D deficiency. The prevalence of vitamin D deficiency is higher than previously though representing an important issue for public health and prevention. There is an increased interest in vitamin D effects in skeletal muscle and imaging modalities are particularly involved in this field. In patients with vitamin D deficiency, ultrasound, computed tomography, densitometry and magnetic resonance imaging (MRI) can efficiently describe changes in muscle morphology and size. Moreover, new imaging modalities, such as MRI spectroscopy, may improve knowledge about the metabolic effects of vitamin D in skeletal muscle. In this narrative review we will discuss the role of skeletal muscle imaging in vitamin D-deficient individuals. The aim of this paper is to improve and encourage the role of radiologists in this field.

INTRODUCTION

Elderly people are prone to accidental falls. Many factors are involved in falls risks such as visual impairment, neurological disorders, orthopaedic disabilities, and drug effects. More than 33% of people aged over 65 fall each year and this issue is closely related to muscle weakness[1]. It has been suggested that reduced muscle strength and weakness may be associated with vitamin D deficiency, which is common among elderly people[2]. Vitamin D deficiency in adults primarily affects bone, up to osteomalacia in severe cases, due to the combination of bone mineralization defects and resorption, the latter of which is a result of secondary hyperparathyroidism[3]. Vitamin D deficiency has also been associated with a decline in physical performance and loss of muscle strength and decreased muscle mass. Symptomatic myopathy can occur in osteomalacia, and a more subtle muscular impairment is often present in patients with moderate or mild vitamin D deficiency[4].

Beside the vitamin D skeletal and extraskeletal effects[5], there is an increased interest on vitamin D effects in skeletal muscle. Imaging modalities are particularly in-

volved in this issue. Ultrasound (US), computed tomography (CT), densitometry and magnetic resonance imaging (MRI) can assess, with different physical principles the effects of vitamin D deficiency measuring changes in muscle morphology and size. Moreover, new imaging modalities, such as MRI spectroscopy, may improve knowledge about metabolic effects of vitamin D in skeletal muscle at a microscopical level. In this narrative review we will discuss recent developments in skeletal muscle imaging among elderly people with vitamin D deficiency.

VITAMIN D AND SKELETAL MUSCLE

The role of vitamin D in bone health and mineral homeostasis has been well established. There is growing evidence that vitamin D exerts several effects in skeletal muscle, including enhanced muscle strength, function and performance in general. Cell culture models suggested muscle vitamin D role in calcium handling, proliferation and differentiation, protection against insulin-resistance and arachidonic acid mobilization[6]. Vitamin D probably exerts its effects both indirectly, through calcium and phosphate pathways, and directly *via* binding of 1,25-dihydroxyvitamin D (1,25D) to the vitamin D receptor, that seems to be expressed in skeletal muscle cells, even if this topic is still under research[5,6].

It has been supposed that the vitamin D relationship with muscle strength may influence the increasing risk of accidental falls in the elderly[6]. Vitamin D deficiency is associated with proximal muscle weakness and reduction in performance speed, probably related to selective muscle atrophy of type Ⅱ muscle fibers[5,6]. Moreover, proximal muscle weakness in severe vitamin D deficiency may be caused by secondary hyperparathyroidism and consequent hypophosphatemia[5]. It has been reported that proximal myopathy and muscle pain in subjects with severe vitamin D deficiency resolve in most cases with vitamin D supplementation[7]. In addition, a recent systematic review focused on healthy adults reported that higher 25-hydroxyvitamin D levels may have a positive effect for increasing muscle strength and reducing the incidence of injuries, but further researches are needed to strengthen these hypotheses[8]. It has also been suggested an association between low levels of vitamin D and fibromyalgia, in particular among women, but more researches in this field are still needed[7].

Therefore, vitamin D role in skeletal muscle and its association with muscle weakness and falls are an active area of research supported by clinical, biochemical and imaging parameters.

SKELETAL MUSCLE IMAGING

Muscle imaging is complex and presents unique anatomical and morphological challenges, which require a continuous integration of dynamic, physiologic, and functional capabilities of modern imaging techniques. The optimal use of US and MRI in various muscle disorders, including muscle strains and tears, delayed onset muscle soreness, myositis ossificans, muscle hernia, acute and chronic exertion compartment syndromes, inflammatory and infectious diseases, tumours and non-neoplastic masses is crucial to obtain the best information clinically useful. The value of CT, US, MRI in each muscle disorder has to weighted up to take advantage of strengths and weaknesses of the each technique and to understand the appropriate place of modern imaging in the clinical management of patients with muscle disease[9,10].

It is known that US, MRI, and CT are widely used with different purposes to visualize the normal anatomy of the musculo-skeletal system. However, in recent years, new and technologically advanced imaging techniques have been introduced for both clinical and research purposes to study the muscular anatomy from a physiological and microscopical point of view. For example, elastography has been introduced to assess the elastic properties of tendons and muscles. Using MRI, diffusion tensor imaging (DTI) has been introduced to study the architecture of the skeletal muscle. The DTI technique is based on the measurement of the apparent diffusion of water in a (biological) tissue. It is concluded that DTI fiber directions resemble fascicle directions visible in high-resolution images very well. Indeed, on DTI images it is possible to observe and study specific features of the skeletal muscle such as the pennate insertion on the aponeuroses and the pennation angle[9,10]. DTI has the potential to be introduced in biomechanical research on skeletal muscle function. The imaging evaluation of skeletal muscle is often performed on US. The use of small-sized probes working in general at high frequencies (frequency band 7-15 MHz) is suitable for very superficial muscles. On the other hand, if a large and deep muscle should be evaluated, for example, at the level of the lower limb it should be better to use low-frequency probes with high penetration of the US-beam (frequency band 3.5-10 MHz). It is important to remember that to depict the normal anatomy of a large wide muscle, such as the biceps femoris and the sartorius, it is possible to use an extended field-of-view which is an option frequently available on the majority of US machines currently available. The advantage of US over MRI is that the muscle may be studied "*in vivo*" in a relaxed status and during contraction.

STUDYING THE RELATIONSHIP BETWEEN VITAMIN D AND MUSCLES WITH CLINICAL IMAGING

Changes in muscle morphology in patients with severe vitamin D deficiency have been reported in literature. In the elderly, muscular atrophy with fatty infiltration is associated with vitamin D deficiency. Muscle trophism can be evaluated with clinical imaging modalities. In particular, to study the skeletal muscle with diagnostic imaging several modalities may be used: US, CT, dual-energy X-ray absorptiometry (DEXA) and MRI. The cross-sectional area (CSA) of a muscle is normally used to evaluate mus-

Table 1 Percentage of selective atrophy of thigh muscle in patients with vitamin D deficiency: Our clinical records

Rectus femoris	Adductors	Semitendinosus	Semimembranosus	Biceps femoris	Gracilis	Sartorius
30%	23%	8%	30%	8%		

Note that the Gracilis muscle and the Sartorius muscle are spared.

cle size and volume. Moreover, CSA is directly related to muscle strength[11]. MRI and CT can both assess CSA and muscle composition with different physical principles. US has a limited field-of-view: this limitation hampers direct measurement of CSA of large muscles due to insufficient visualization of the whole muscle bulk[11]. US, MRI and CT can assess the presence of higher skeletal fat content than in normal muscles. Fatty replacement may present as a focal process or as a diffuse change involving one group of muscle of the entire skeletal muscle, as largely demonstrated for dystrophic muscle diseases[12]. Table 1 shows the prevalence of selective complete fatty degeneration and atrophy of the thigh muscles as recorded in our clinical practice and as demonstrated in literature[4]. This review has been focused on vitamin D deficiency and skeletal muscle, and it will not discuss the huge literature about skeletal muscle diseases.

We will discuss the role of each modality in assessing skeletal muscle in vitamin D-deficient patient. Research studies in literature frequently refers to skeletal muscle and sarcopenia, a syndrome with loss of skeletal muscle mass and strength that occurs in the elderly[13]. In severe vitamin D deficient patients imaging of skeletal muscle may overlap with that of sarcopenia.

US

Using US it has been shown that quantitative muscle US is a potential alternative for assessment of disease severity and progression in several muscular diseases. The main findings in muscular diseases are increased echo intensity, reflecting increased infiltration of fat or fibrous tissue in muscles, and decreased muscle thickness, indicative of atrophy. Additional advantages of US are high discriminating ability, low cost, fast execution, and non-X-ray dependent nature. Structural abnormalities quantified with US may reflect muscle function or strength[14-16]. Moreover, US has been proposed as a reliable method for monitoring the extent of sarcopenia measuring muscle thickness, especially of musculus vastus medialis and musculus intermedius[11].

However, muscular US has been shown to have several disadvantages regarding the reliability of the results in terms of intra- and inter-observer agreement (Tagliafico *et al*[9], personal communication).

US elastography assesses tissue stiffness before and after compression[17]. Until now, there are limited data about the use of elastography to assess normal and pathologic skeletal muscle. However, it is likely that fatty infiltration of a muscle determines global reduce stiffness, as suggested in studies on inflammatory myositis[17].

There are no significant radiological studies about US assessment of skeletal muscle in individuals with vitamin D deficiency. We encourage research studies using US because this modality has the advantage of being available even at bedside, cheap and easily repeatable.

CT and densitometry (DEXA)

Regarding CT it has been shown that radiological measures of bone health measured with quantitative CT were not affected by persisting low vitamin D levels[18]. Non-enhanced CT scan of the pelvis demonstrated that the fat content varied among the hip muscles, with an anteroposterior gradient from the hip flexors to the hip extensors. This gradient increased after fifty years of age. Higher fat content was associated with poorer performance on physical tests, even after adjustment for the CSA of the muscle. Figure 1 shows cross-sectional CT of thigh muscles in a patient with vitamin D deficiency. Higher fat content was also associated with greater age, higher body-mass index, and lower physical activity[19]. This data has been supported by the data on muscle of the thigh and vitamin D deficiency[4]. Using very sophisticated and new techniques it has been found that the characteristic increase in osteoid-covered surfaces in vitamin D-deficient bone hampers remodelling of the remaining mineralized bone tissue. Using spatially resolved synchrotron bone mineral density distribution analyses and spectroscopic techniques, the bone tissue within the osteoid frame has a higher mineral content with mature collagen and mineral constituents, which are characteristic of aged tissue[20]. A recent cross-sectional study demonstrated a positive correlation between 1,25D levels and total skeletal muscle mass as measured on DEXA among subjects younger than 65 years[21]. This was supported by greater isometric knee extension moment in women with higher 1,25D levels. However, no association was found between 25D levels and muscle mass or strength or in those over 65 years of age. Among 26 subjects with chronic kidney disease, thigh muscle CSA on MRI correlated significantly with a model including 1,25D levels, calcium levels, and daily physical activity. Functional parameters assessing gait and proximal musculature also independently correlated with 1,25D[7,21].

MRI

By our group it has been shown that fatty degeneration of thigh muscles detected on MRI was associated with vitamin D deficiency and impaired balance and gait. Selective complete fatty degeneration of single muscles was observed[4]. These data are also supported by previous studies on muscle biopsy specimens[4].

Fatty replacement and atrophy can be evaluated with MRI using a scoring system from 0 to 3 (grade 0 = normal appearance; grade 3 = severe changes)[4]. For illustra-

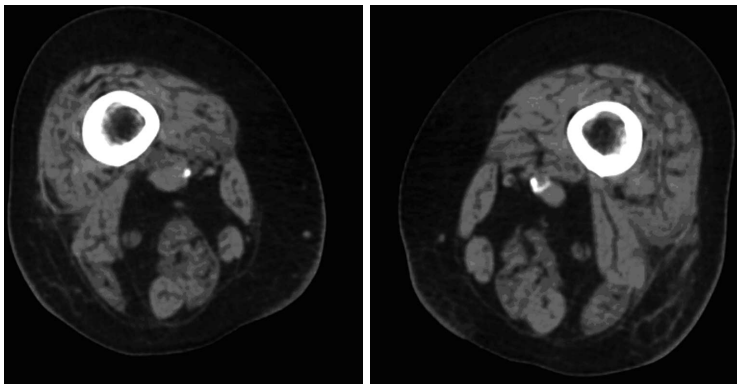

Figure 1 Cross-sectional computed tomography at the level of the middle thigh showing fatty degeneration and atrophy of skeletal muscles in a vitamin D-deficient patient.

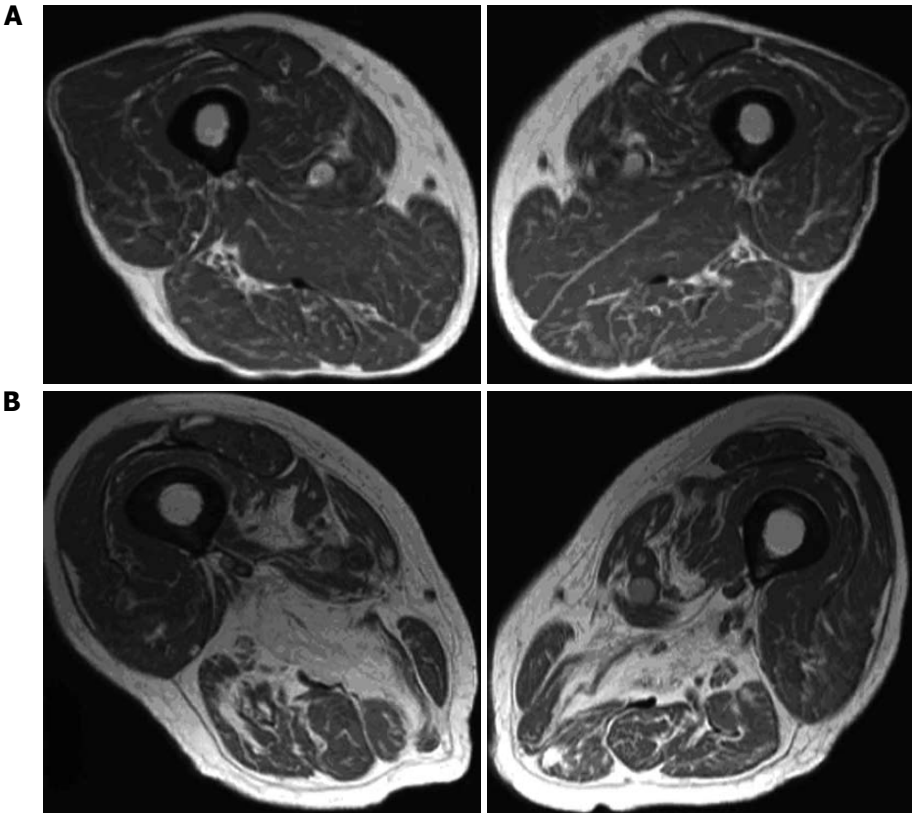

Figure 2 Magnetic resonance imaging of two different grades of fatty degeneration and atrophy involving thigh muscle in patients with vitamin D deficiency. A: Grade 1 (less than 30% of the volume of muscles involved); B: Grade 2 (30%-60% of the volume of muscles compromised).

tion, Figure 2 shows MRI of two different grade of fatty atrophy involving thigh muscle in patients with vitamin D deficiency. The hypothesis that arose was that atrophy of skeletal muscle fibers and their replacement by fat tissue are the anatomic basis for the impairment in muscular performance described in older vitamin D-deficient people[4]. It may supposed that fatty substitution related to vitamin D deficiency may be the result of the lack of the known trophic effects of vitamin D on skeletal muscle cells[4]. If the thigh muscles are affected, the lack of enough muscular bulk may hamper balance and gait. Clinical scores were concordant with this observation. Concerning technical MRI protocols we suppose that a standard, patient-friendly protocol, including T1 and T2 weighted sequences may be sufficient for the follow-up of elderly people with potential vitamin D deficiency. In another study of 366 older patients receiving MRI of one shoulder for the investigation of potential rotator cuff injury, a correlation between higher fatty infiltration of rotator cuff muscles and lower serum levels of 25D was reported[22]. After multivariate linear regression analysis, this association remained statistically significant in two muscle groups (*i.e.,* supraspinatus and infraspinatus muscles) but only among those whose MRI also demonstrated a full-thickness rotator cuff tear (228 patients).

Conventional MRI shows distribution pattern of fatty degeneration and it can be used for disease monitoring after treatment. Moreover, MRI allows standardize image protocols that can be useful to engage diagnostic or monitoring multi-centric trials.

New MRI sequences such as diffusion, perfusion and spectroscopy may improve the role of MRI in muscular evaluation of vitamin D role. In particular, spectroscopy magnetic resonance spectroscopy (MRS) may provide metabolic information on the musculoskeletal system. Phosphorus-31 MRS (31P-MRS) is a noninvasive technique that allows observation of mitochondrial function and oxidative phosphorylation *in vivo*. Based on the hy-

pothesis that a suboptimal mitochondrial function may lead to myopathy in vitamin D-defiecient subjects, a recent study used 31P-MRS to observe that cholecalciferol therapy in vitamin D-deficient subjects improved both mitochondrial oxidative function and symptoms of myopathy and fatigue[23]; this result represented a direct sign of a link between vitamin D and mitochondria in skeletal muscle. Therefore, MRS lead to improve knowledge about vitamin D effects on skeletal muscle.

CONCLUSION

Many studies examined the specific effects of vitamin D on muscle function and physical performance. However, a very important review stated that comparing these studies is made very difficult by the variety of outcome measures used to assess muscle function[7]. We believe that including the role of diagnostic imaging to study the anatomy of skeletal muscle and not only its function may add new insights into vitamin D and muscle relationships. It has been suggested an association between vitamin D deficiency and structural muscle changes such as atrophy and fatty infiltration, both of which can be detected with cross-sectional imaging[12]. However, there are several confounders as, for example, disuse, drug use and denervation. Moreover, skeletal muscle is a highly metabolic tissue that respond not only to vitamin D effects, but to a variety of hormones and factors including, but not limited to, IL-6, brain-derived neurotrophic factor, insulin, glucocorticoids, thyroid hormones[7]. Each factor and hormone contributes and influences muscle differentiation, metabolism and function, through well known and emerging mechanisms[7]. In addition, one of the main topic is that imaging modalities can't yet differ between extracellular fat and intracellular fat, of important pathophysiological significance[7].

On the other hand, imaging modalities permit to monitor muscle changes in size and tissue architecture. Moreover, new imaging modalities such as MRS may improve the knowledge about the direct effects of vitamin D on skeletal muscle.

In conclusion, we believe that the use of diagnostic imaging should be strongly encouraged to have radiological outcomes added to clinical and biochemical outcomes. Additional studies are needed to determine the exact role of imaging in the care of patients with vitamin D deficiency.

REFERENCES

1 **Venning G**. Recent developments in vitamin D deficiency and muscle weakness among elderly people. *BMJ* 2005; **330**: 524-526 [PMID: 15746134]

2 **Semba RD**, Garrett E, Johnson BA, Guralnik JM, Fried LP. Vitamin D deficiency among older women with and without disability. *Am J Clin Nutr* 2000; **72**: 1529-1534 [PMID: 11101482]

3 **Lips P**. Vitamin D deficiency and secondary hyperparathyroidism in the elderly: consequences for bone loss and fractures and therapeutic implications. *Endocr Rev* 2001; **22**: 477-501 [PMID: 11493580]

4 **Tagliafico AS**, Ameri P, Bovio M, Puntoni M, Capaccio E, Murialdo G, Martinoli C. Relationship between fatty degeneration of thigh muscles and vitamin D status in the elderly: a preliminary MRI study. *AJR Am J Roentgenol* 2010; **194**: 728-734 [PMID: 20173152 DOI: 10.2214/AJR.09.3130]

5 **Wacker M**, Holick MF. Vitamin D - effects on skeletal and extraskeletal health and the need for supplementation. *Nutrients* 2013; **5**: 111-148 [PMID: 23306192 DOI: 10.3390/nu5010111]

6 **Dirks-Naylor AJ**, Lennon-Edwards S. The effects of vitamin D on skeletal muscle function and cellular signaling. *J Steroid Biochem Mol Biol* 2011; **125**: 159-168 [PMID: 21397021 DOI: 10.1016/j.jsbmb.2011.03.003]

7 **Girgis CM**, Clifton-Bligh RJ, Hamrick MW, Holick MF, Gunton JE. The roles of vitamin D in skeletal muscle: form, function, and metabolism. *Endocr Rev* 2013; **34**: 33-83 [PMID: 23169676 DOI: 10.1210/er.2012-1012]

8 **Redzic M**, Lewis RM, Thomas DT. Relationship between 25-hydoxyvitamin D, muscle strength, and incidence of injury in healthy adults: a systematic review. *Nutr Res* 2013; **33**: 251-258 [PMID: 23602241 DOI: 10.1016/j.nutres.2013.02.007]

9 **Tagliafico A**, Bignotti B, Airaldi S, Martinoli C. Correlation of Skeletal Muscle Anatomy to MRI and US Findings. In: Weber MA. Magnetic Resonance Imaging of the Skeletal Musculature. Berlin Heidelberg: Springer, 2014: 27-39

10 **Martinoli C**, Airaldi A, Bignotti B, Tagliafico A. Imaging the Skeletal Muscle: When to Use MR imaging and When to Use Ultrasound. In: Weber MA. Magnetic Resonance Imaging of the Skeletal Musculature. Berlin Heidelberg: Springer, 2014: 41-52

11 **Strasser EM**, Draskovits T, Praschak M, Quittan M, Graf A. Association between ultrasound measurements of muscle thickness, pennation angle, echogenicity and skeletal muscle strength in the elderly. *Age* (Dordr) 2013; **35**: 2377-2388 [PMID: 23456136 DOI: 10.1007/s11357-013-9517-z]

12 **Fischer D**, Wattjes MP. MRI in Muscle Dystrophies and Primary Myopathies. In: Weber MA. Magnetic Resonance Imaging of the Skeletal Musculature. Berlin Heidelberg: Springer, 2014: 241-254

13 **Cruz-Jentoft AJ**, Baeyens JP, Bauer JM, Boirie Y, Cederholm T, Landi F, Martin FC, Michel JP, Rolland Y, Schneider SM, Topinková E, Vandewoude M, Zamboni M. Sarcopenia: European consensus on definition and diagnosis: Report of the European Working Group on Sarcopenia in Older People. *Age Ageing* 2010; **39**: 412-423 [PMID: 20392703 DOI: 10.1093/ageing/afq034]

14 **Heckmatt JZ**, Leeman S, Dubowitz V. Ultrasound imaging in the diagnosis of muscle disease. *J Pediatr* 1982; **101**: 656-660 [PMID: 7131136]

15 **Mayans D**, Cartwright MS, Walker FO. Neuromuscular ultrasonography: quantifying muscle and nerve measurements. *Phys Med Rehabil Clin N Am* 2012; **23**: 133-48, xii [PMID: 22239880 DOI: 10.1016/j.pmr.2011.11.009]

16 **Pillen S**, Tak RO, Zwarts MJ, Lammens MM, Verrijp KN, Arts IM, van der Laak JA, Hoogerbrugge PM, van Engelen BG, Verrips A. Skeletal muscle ultrasound: correlation between fibrous tissue and echo intensity. *Ultrasound Med Biol* 2009; **35**: 443-446 [PMID: 19081667 DOI: 10.1016/j.ultrasmedbio.2008.09.016]

17 **Drakonaki EE**, Allen GM, Wilson DJ. Ultrasound elastography for musculoskeletal applications. *Br J Radiol* 2012; **85**: 1435-1445 [PMID: 23091287 DOI: 10.1259/bjr/93042867]

18 **Dahlman I**, Gerdhem P, Bergström I. Vitamin D status and bone health in immigrant versus Swedish women during pregnancy and the post-partum period. *J Musculoskelet Neuronal Interact* 2013; **13**: 464-469 [PMID: 24292616]

19 **Daguet E**, Jolivet E, Bousson V, Boutron C, Dahmen N, Bergot C, Vicaut E, Laredo JD. Fat content of hip muscles: an anteroposterior gradient. *J Bone Joint Surg Am* 2011; **93**: 1897-1905 [PMID: 22012527 DOI: 10.2106/JBJS.J.00509]

20 **Busse B**, Bale HA, Zimmermann EA, Panganiban B, Barth

HD, Carriero A, Vettorazzi E, Zustin J, Hahn M, Ager JW, Püschel K, Amling M, Ritchie RO. Vitamin D deficiency induces early signs of aging in human bone, increasing the risk of fracture. *Sci Transl Med* 2013; **5**: 193ra88 [PMID: 23843449 DOI: 10.1126/scitranslmed.3006286]

21 **Marantes I**, Achenbach SJ, Atkinson EJ, Khosla S, Melton LJ, Amin S. Is vitamin D a determinant of muscle mass and strength? *J Bone Miner Res* 2011; **26**: 2860-2871 [PMID: 21915904 DOI: 10.1002/jbmr.510]

22 **Oh JH**, Kim SH, Kim JH, Shin YH, Yoon JP, Oh CH. The level of vitamin D in the serum correlates with fatty degeneration of the muscles of the rotator cuff. *J Bone Joint Surg Br* 2009; **91**: 1587-1593 [PMID: 19949122]

23 **Sinha A**, Hollingsworth KG, Ball S, Cheetham T. Improving the vitamin D status of vitamin D deficient adults is associated with improved mitochondrial oxidative function in skeletal muscle. *J Clin Endocrinol Metab* 2013; **98**: E509-E513 [PMID: 23393184 DOI: 10.1210/jc.2012-3592]

P- Reviewers: Arcangeli S, Shen J **S- Editor**: Gou SX
L- Editor: A **E- Editor**: Liu SQ

World Journal of Radiology

Online Submissions: http://www.wjgnet.com/esps/
bpgoffice@wjgnet.com
doi:10.4329/wjr.v6.i4.125

World J Radiol 2014 April 28; 6(4): 125-129
ISSN 1949-8470 (online)

CASE REPORT

Psoas muscle metastasis from cervical carcinoma: Correlation and comparison of diagnostic features on FDG-PET/CT and diffusion-weighted MRI

Sandip Basu, Abhishek Mahajan

Sandip Basu, Radiation Medicine Centre, Bhabha Atomic Research Centre, Tata Memorial Hospital Annexe, Parel, Mumbai 400012, India
Abhishek Mahajan, Department of Radiology, Tata Memorial Hospital, Mumbai 400012, India
Author contributions: Basu S and Mahajan A designed the study and wrote the manuscript.
Correspondence to: Dr. Sandip Basu, Radiation Medicine Centre, Bhabha Atomic Research Centre, Tata Memorial Hospital Annexe, Parel, Mumbai 400012, India drsanb@yahoo.com
Telephone: +91-22-24149428 Fax: +91-22-24157098
Received: November 30, 2013 Revised: March 10, 2014
Accepted: March 17, 2014
Published online: April 28, 2014

Abstract

Psoas muscle metastasis, though rare, is the commonest site of skeletal muscle involvement in cervical carcinoma. The appropriate clinical management of this condition, particularly of the pain related to malignant psoas syndrome, is still evolving and the diagnostic features on conventional morphological imaging modalities are often non specific, with the differential diagnosis lying between sarcoma, hematoma, and abscess. In this report, a comparison of various morphofunctional imaging modalities was made. Fluorodeoxyglucose-positron emission tomography (FDG-PET)/computed tomography (CT) was the first to suspect disease involvement of the psoas muscle, demonstrating intense FDG uptake (compared with the contralateral muscle), while ultrasound showed heterogeneous echotexture, and magnetic resonance imaging (MRI) showed subtle altered signal intensity in the right psoas muscle. Both anatomical imaging modalities and non contrast CT of the PET-CT examination demonstrated a bulky psoas muscle, without any focal abnormality. On diffusion-weighted imaging of MRI (DWI-MRI), restricted diffusion of the involved muscle was an important observation. The psoas muscle metastatic involvement was proven histopathologically. Thus, enhanced glucose metabolism and restricted diffusion in the newer non-invasive molecular imaging modalities (*e.g.*, PET/CT and DWI-MRI) could serve as valuable adjunctive parameters in diagnosing this entity in the absence of a focal abnormality in the anatomical modalities. In the treatment response monitoring scenario, FDG-PET/CT demonstrated near complete resolution following administration of 3 cycles of systemic chemotherapy and local external radiotherapy.

Key words: Psoas muscle metastasis; Carcinoma cervix; Fludeoxyglucose-positron emission tomography/Computed tomography; Diffusion weighted magnetic resonance imaging

Core tip: Psoas muscle metastasis, though unusual, forms the commonest site of skeletal muscle involvement in cervical carcinoma. The present communication describes the comparative diagnostic features of this relatively unusual but important entity on newer non-invasive molecular imaging modalities such as fluorodeoxyglucose-positron emission tomography/computed tomography (CT) and diffusion-weighted imaging of magnetic resonance imaging (MRI) as well as the conventional imaging modalities (*e.g.*, ultrasound, CT and MRI). Currently, there is a lack of characteristic diagnostic imaging features on conventional imaging modalities which have been nonspecific in this domain, and the differential diagnosis includes sarcoma, hematoma, and abscess, thus the newer molecular imaging approaches need critical exploration and comparison.

Basu S, Mahajan A. Psoas muscle metastasis from cervical

carcinoma: Correlation and comparison of diagnostic features on FDG-PET/CT and diffusion-weighted MRI. *World J Radiol* 2014; 6(4): 125-129 Available from: URL: http://www.wjgnet.com/1949-8470/full/v6/i4/125.htm DOI: http://dx.doi.org/10.4329/wjr.v6.i4.125

INTRODUCTION

Skeletal muscle metastasis from cervical carcinoma is a rare event (less than 1% incidence), the most common being the involvement of the psoas muscle. There is a lack of characteristic diagnostic imaging features on conventional imaging modalities which have been nonspecific in this domain and the differential diagnosis includes sarcoma, hematoma, and abscess[1-6]. Thus the features of this relatively unusual but important entity on newer non-invasive molecular imaging modalities [*e.g.*, positron emission tomography/computed tomography (PET/CT) and diffusion-weighted imaging of magnetic resonance imaging (DWI-MRI)] need critical exploration and comparison.

CASE REPORT

A 52-year-old female, who presented with bleeding per vaginum 2 years previously and was diagnosed with squamous cell cervical carcinoma grade ⅢB, had undergone external radiation therapy (40 Gy over 20 times) to the pelvis and cisplatinum-based chemotherapy (concluded in 2011). She recently complained of pain in both thighs which was not relieved by analgesics and was referred for fluorodeoxyglucose-PET (FDG-PET)/CT for evaluation of disease status. On the whole-body survey with a full-ring dedicated LYSO-based time of flight PET-CT scanner, intense FDG uptake (Figure 1) was noted in the right psoas muscle [maximal standardized uptake value (SUVmax): 13.79 g/mL], in addition to foci in the prevertebral (SUVmax: 4.26 g/mL), left paraaortic (SUVmax: 3.64 g/mL), peribronchial and hilar lymph nodes. Metabolically active lesions in the right psoas muscle were further correlated radiologically: transverse and longitudinal grey scale ultrasound images (Figure 2) revealed a bulky right psoas muscle showing heterogeneous echotexture. On MRI (Figure 3), axial T1W and coronal T2W sequences revealed a bulky right psoas muscle (arrowhead) and altered signal intensity. On axial DWI there was evidence of restricted diffusion in the involved muscle (Figure 3C and 3D). Ultrasound-guided fine needle aspiration cytology of the right psoas muscle confirmed the presence of squamous cell carcinoma in the described lesion. Follow-up FDG-PET/CT was undertaken for treatment response monitoring, where FDG-PET/CT (Figure 4) demonstrated near-complete resolution of FDG uptake in the psoas muscle as well as the other foci following administration of 3 cycles of systemic chemotherapy and palliative local external radiotherapy (20 Gy over 5 times in 1 wk).

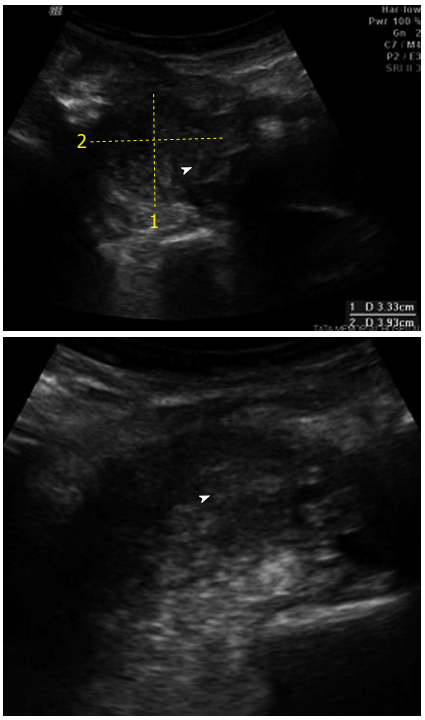

Figure 2 Ultrasound of the abdomen demonstrating a bulky right psoas muscle with heterogenous echotexture.

DISCUSSION

The various factors attributed to the relative rarity of skeletal muscle metastasis in a malignant process include: (1) contractility of muscles leading to turbulent blood flow; (2) unfavorable pH; and (3) the presence of protease inhibitors[2]. The peer-reviewed literature on psoas muscle metastasis in the context of carcinoma cervix is limited, primarily emphasizing the diagnostic dilemma in differentiating this entity mainly from post-irradiation abscess and sarcoma[1-6]. The challenges and refractoriness of the pain related to malignant psoas syndrome arising from a background of cervical carcinoma has been another aspect that has been described in the form of case reports[7-9] with one report describing a good outcome with combined surgical excision and adjuvant radiation therapy.

The psoas muscle involvement mimicking abscess and an aggressive course has been primarily described in the context of HIV-positive women, though recent reports have also demonstrated this in HIV-negative women as well[3-5]. Contrast-enhanced CT, MRI and ultrasound have all been utilized in this area with variable success and non-specific findings. In one report[3], contrast-enhanced CT demonstrated a well-defined hypo-dense lesion with peripheral enhancement, suggesting psoas abscess. MRI findings were also suggestive of abscess, though FDG-PET imaging was not undertaken in this case. In our case, FDG-PET/CT demonstrated intense FDG uptake corresponding to the lesion that was clearly distinctive in demonstrating the lesion (when compared with the

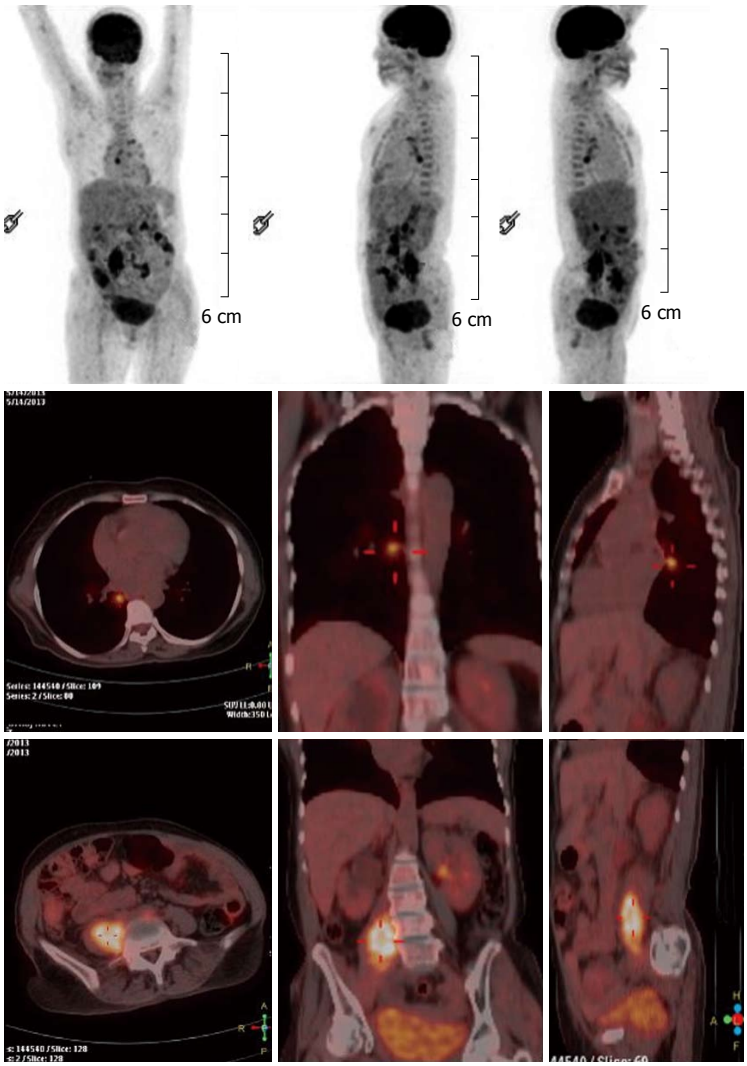

Figure 1 Whole body fluorodeoxyglucose-positron emission tomography/computed tomography. This first suggested disease involvement of the psoas muscle demonstrating intense FDG uptake (compared with the contralateral muscle). In addition, FDG foci are noted in the prevertebral, left paraaortic, peribronchial and hilar lymph nodes. FDG: Fluorodeoxyglucose.

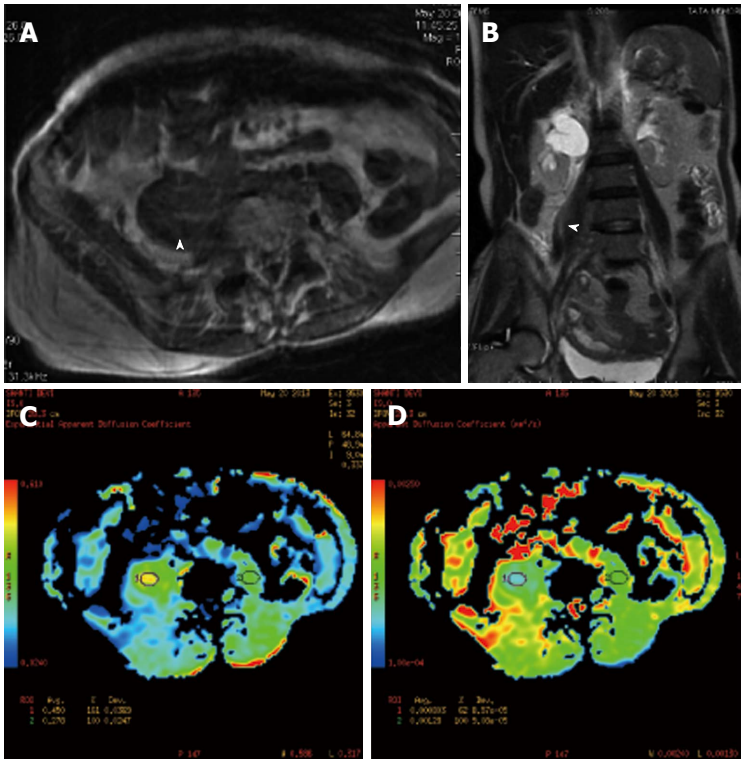

Figure 3 Magnetic resonance imaging. Axial T1W and coronal T2W equence (A and B) reveals a bulky right psoas muscle (arrowhead) and shows altered signal intensity. On axial diffusion weighted images (C and D) there is e/o restricted diffusion in the involved segment.

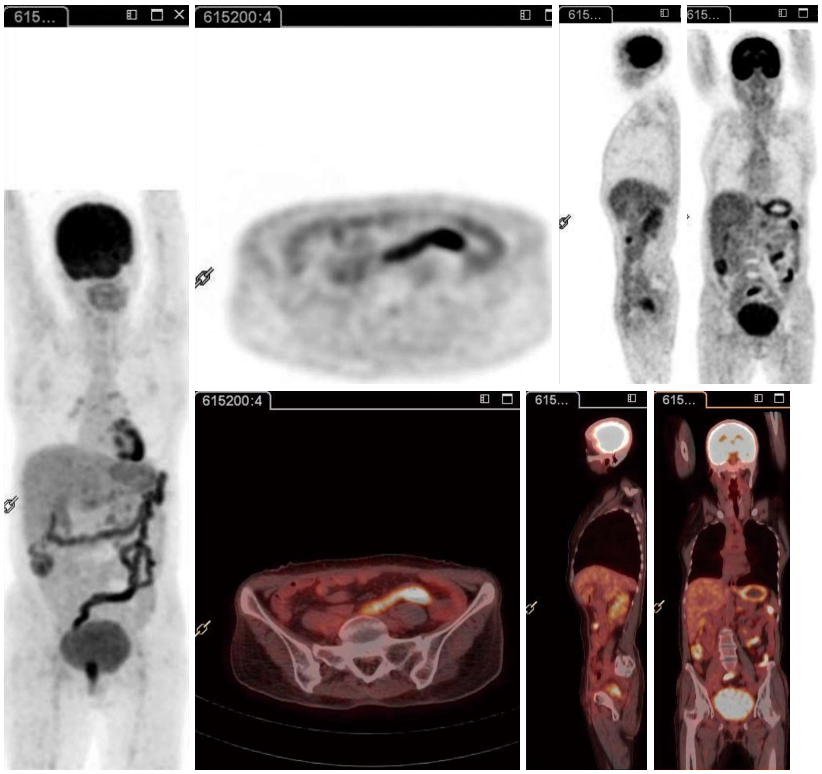

Figure 4 Follow-up fluorodeoxyglucose-positron emission tomography/computed tomography following administration of 3 cycles of systemic chemotherapy and local external radiotherapy demonstrating near-complete resolution of the fluorodeoxyglucose uptake in the psoas muscle as well as other foci.

contralateral muscle), while ultrasound showed heterogeneous echotexture and MRI showed subtle altered signal intensity in the right psoas muscle. Both the anatomical imaging modalities and the non contrast CT of the PET-CT examination demonstrated a bulky psoas muscle. Restricted diffusion of the involved segment on DWI-MRI was an important observation in addition to altered signal intensity on conventional MRI. Thus, in the absence of any focal abnormality on the anatomical modalities, enhanced glucose metabolism and restricted diffusion in the newer non-invasive molecular imaging modalities (*e.g.*, PET/CT and DWI-MRI) could serve as a valuable adjunct parameter in diagnosing this important entity.

COMMENTS

Clinical diagnosis

The patient presented with bleeding per vaginum 2 years previously and was diagnosed with squamous cell cervical carcinoma grade ⅢB. She had undergone radiation therapy and cisplatinum-based chemotherapy (concluded in 2011).

Differential diagnosis

Recurrence of cervical carcinoma.

Pathological diagnosis

Ultrasound-guided fine needle aspiration cytology of the right psoas muscle confirmed the presence of squamous cell carcinoma in the described psoas muscle lesion.

Treatment

The patient underwent 3 cycles of systemic chemotherapy following the diagnosis of disease recurrence in the psoas muscle.

Related reports

Follow-up fluorodeoxyglucose-positron emission tomography/computed tomography (FDG-PET/CT) demonstrated near-complete resolution of FDG uptake in the psoas muscle as well as the other foci following administration of 3 cycles of systemic chemotherapy and local external radiotherapy.

Experiences and lessons

In addition to demonstrating a relatively unusual site of metastasis, the present report illustrates the comparative diagnostic features of this relatively unusual but important entity on newer non-invasive molecular imaging modalities such as FDG-PET/CT and diffusion-weighted imaging of magnetic resonance imaging as well as the conventional imaging modalities (*e.g.*, ultrasound, CT and magnetic resonance imaging).

Peer review

This is an interesting case. Well written, and good length as a case report.

REFERENCES

1 **Hong JH**, Song SH, Lee JK, Lee NW, Lee KW. Metastatic cervical adenocarcinoma mimicking retroperitoneal sarcoma of the psoas muscle on imaging. *Eur J Gynaecol Oncol* 2011; **32**: 221-223 [PMID: 21614923]

2 **Kamal M**, Touiti D, Jouhadi H, Benider A. Iliopsoas Metastasis from Cervix Carcinoma Masquerading as Psoas Abscess. *J Cancer Sci Ther* 2012; **4**: 75-76 [DOI: 10.4172/1948-5956.1000114]

3 **Kalra N**, Aiyappan S, Nijhawan R, Sharma SC, Khandelwal N. Metastatic carcinoma of cervix mimicking psoas abscess on imaging: a case report. *J Gynecol Oncol* 2009; **20**: 129-131 [PMID: 19590727 DOI: 10.3802/jgo.2009.20.2.129]

4 **Devendra K**, Tay SK. Metastatic carcinoma of the cervix presenting as a psoas abscess in an HIV-negative woman. *Singapore Med J* 2003; **44**: 302-303 [PMID: 14560863]

5 **Bar-Dayan Y**, Fishman A, Levi Z, Rachmani R. Squamous cell carcinoma of the cervix with psoas abscess-like metastasis in an HIV-negative patient. *Isr J Med Sci* 1997; **33**: 674-676 [PMID: 9397142]

6 **Smith RW**, Gooneratne NS. Psoas bed gallium uptake in a patient with carcinoma of the cervix post irradiation--abscess

or metastasis. *Clin Nucl Med* 1978; **3**: 230 [PMID: 679578 DOI: 10.1097/00003072-197806000-00009]

7 **Stevens MJ**, Atkinson C, Broadbent AM. The malignant psoas syndrome revisited: case report, mechanisms, and current therapeutic options. *J Palliat Med* 2010; **13**: 211-216 [PMID: 20053159]

8 **Komatsu S**, Iseki M, Morita Y, Inada E. [A case of malignant psoas syndrome diagnosed while treating sciatica]. *Masui* 2013; **62**: 863-866 [PMID: 23905413]

9 **Strauss JB**, Shah AP, Chen SS, Gielda BT, Kim AW. Psoas muscle metastases in non-small cell lung cancer. *J Thorac Dis* 2012; **4**: 83-87 [PMID: 22295171]

P- Reviewers: Kim YS, Peitsidis P, Socea B **S- Editor**: Wen LL
L- Editor: Cant MR **E- Editor**: Liu SQ

World Journal of Radiology

Online Submissions: http://www.wjgnet.com/esps/
bpgoffice@wjgnet.com
www.wjgnet.com

World J Radiol 2014 April 28; 6(4): I-V
ISSN 1949-8470 (online)

INSTRUCTIONS TO AUTHORS

GENERAL INFORMATION

World Journal of Radiology (*World J Radiol*, *WJR*, online ISSN 1949-8470, DOI: 10.4329) is a peer-reviewed open access (OA) academic journal that aims to guide clinical practice and improve diagnostic and therapeutic skills of clinicians.

Aim and scope

WJR covers topics concerning diagnostic radiology, radiation oncology, radiologic physics, neuroradiology, nuclear radiology, pediatric radiology, vascular/interventional radiology, medical imaging achieved by various modalities and related methods analysis. The current columns of *WJR* include editorial, frontier, diagnostic advances, therapeutics advances, field of vision, mini-reviews, review, topic highlight, medical ethics, original articles, case report, clinical case conference (clinicopathological conference), and autobiography.

We encourage authors to submit their manuscripts to *WJR*. We will give priority to manuscripts that are supported by major national and international foundations and those that are of great basic and clinical significance.

WJR is edited and published by Baishideng Publishing Group (BPG). BPG has a strong professional editorial team composed of science editors, language editors and electronic editors. BPG currently publishes 41 OA clinical medical journals, and is one of the leading medical publishers, with the first-class editing and publishing capacity and production.

Columns

The columns in the issues of *WJR* will include: (1) Editorial: The editorial board members are invited to make comments on an important topic in their field in terms of its current research status and future directions to lead the development of this discipline; (2) Frontier: The editorial board members are invited to select a highly cited cutting-edge original paper of his/her own to summarize major findings, the problems that have been resolved and remain to be resolved, and future research directions to help readers understand his/her important academic point of view and future research directions in the field; (3) Diagnostic Advances: The editorial board members are invited to write high-quality diagnostic advances in their field to improve the diagnostic skills of readers. The topic covers general clinical diagnosis, differential diagnosis, pathological diagnosis, laboratory diagnosis, imaging diagnosis, endoscopic diagnosis, biotechnological diagnosis, functional diagnosis, and physical diagnosis; (4) Therapeutics Advances: The editorial board members are invited to write high-quality therapeutic advances in their field to help improve the therapeutic skills of readers. The topic covers medication therapy, psychotherapy, physical therapy, replacement therapy, interventional therapy, minimally invasive therapy, endoscopic therapy, transplantation therapy, and surgical therapy; (5) Field of Vision: The editorial board members are invited to write commentaries on classic articles, hot topic articles, or latest articles to keep readers at the forefront of research and increase their levels of clinical research. Classic articles refer to papers that are included in Web of Knowledge and have received a large number of citations (ranking in the top 1%) after being published for more than years, reflecting the quality and impact of papers. Hot topic articles refer to papers that are included in Web of Knowledge and have received a large number of citations after being published for no more than 2 years, reflecting cutting-edge trends in scientific research. Latest articles refer to the latest published high-quality papers that are included in PubMed, reflecting the latest research trends. These commentary articles should focus on the status quo of research, the most important research topics, the problems that have now been resolved and remain to be resolved, and future research directions. Basic information about the article to be commented (including authors, article title, journal name, year, volume, and inclusive page numbers); (6) Minireviews: The editorial board members are invited to write short reviews on recent advances and trends in research of molecular biology, genomics, and related cutting-edge technologies to provide readers with the latest knowledge and help improve their diagnostic and therapeutic skills; (7) Review: To make a systematic review to focus on the status quo of research, the most important research topics, the problems that have now been resolved and remain to be resolved, and future research directions; (8) Topic Highlight: The editorial board members are invited to write a series of articles (7-10 articles) to comment and discuss a hot topic to help improve the diagnostic and therapeutic skills of readers; (9) Medical Ethics: The editorial board members are invited to write articles about medical ethics to increase readers' knowledge of medical ethics. The topic covers international ethics guidelines, animal studies, clinical trials, organ transplantation, *etc.*; (10) Clinical Case Conference or Clinicopathological Conference: The editorial board members are invited to contribute high-quality clinical case conference; (11) Original Articles: To report innovative and original findings in radiology; (12) Brief Articles: To briefly report the novel and innovative findings in radiology; (13) Meta-Analysis: Covers the systematic review, mixedtreatment comparison, meta-regression, and overview of reviews, in order to summarize a given quantitative effect, *e.g.*, the clinical effectiveness and safety of clinical treatments by combining data from two or more randomized controlled trials, thereby providing more precise and externally valid estimates than those which would stem from each individual dataset if analyzed separately from the others; (15) Letters to the Editor: To discuss and make reply to the contributions published in *WJR*, or to introduce and comment on a controversial issue of general interest; (16) Book Reviews: To introduce and comment on quality monographs of radiology; and (17) Autobiography: The editorial board members are invited to write their autobiography to provide readers with stories of success or failure in their scientific research career. The topic covers their basic personal information and information about when they started doing research work, where and how they did research work, what they have achieved, and their lessons from success or failure.

Name of journal

World Journal of Radiology

ISSN

ISSN 1949-8470 (online)

Launch date

December 31, 2009

Frequency

Monthly

Editor-in-Chief

Kai U Juergens, MD, Associate Professor, MRT und PET/CT, Nuklearmedizin Bremen Mitte, ZEMODI - Zentrum für morpholo-

Editorial Office
Jian-Xia Cheng, Director
Jin-Lei Wang, Vice Director
World Journal of Radiology
Room 903, Building D, Ocean International Center,
No. 62 Dongsihuan Zhonglu, Chaoyang District,
Beijing 100025, China
Telephone: +86-10-85381891
Fax: +86-10-85381893
E-mail: bpgoffice@wjgnet.com
http://www.wjgnet.com

Publisher
Baishideng Publishing Group Co., Limited
Flat C, 23/F., Lucky Plaza, 315-321 Lockhart Road,
Wanchai, Hong Kong, China
Telephone: +852-31779906
Fax: +852-65557188
E-mail: bpgoffice@wjgnet.com
http://www.wjgnet.com

Production center
Beijing Baishideng BioMed Scientific Co., Limited
Room 903, Building D, Ocean International Center,
No. 62 Dongsihuan Zhonglu, Chaoyang District,
Beijing 100025, China
Telephone: +86-10-85381892
Fax: +86-10-85381893

Representative office
USA Office
8226 Regency Drive,
Pleasanton, CA 94588-3144, United States
Telephone: +1-925-2238242
Fax: +1-925-2238243

Instructions to authors
Full instructions are available online at http://www.wjgnet.com/1948-5204/g_info_20100312180518.htm.

Indexed and Abstracted in
PubMed Central, PubMed, Digital Object Identifier, and Directory of Open Access Journals.

SPECIAL STATEMENT

All articles published in this journal represent the viewpoints of the authors except where indicated otherwise.

Biostatistical editing
Statisital review is performed after peer review. We invite an expert in Biomedical Statistics to evaluate the statistical method used in the paper, including *t*-test (group or paired comparisons), chi-squared test, Ridit, probit, logit, regression (linear, curvilinear, or stepwise), correlation, analysis of variance, analysis of covariance, *etc*. The reviewing points include: (1) Statistical methods should be described when they are used to verify the results; (2) Whether the statistical techniques are suitable or correct; (3) Only homogeneous data can be averaged. Standard deviations are preferred to standard errors. Give the number of observations and subjects (*n*). Losses in observations, such as drop-outs from the study should be reported; (4) Values such as ED50, LD50, IC50 should have their 95% confidence limits calculated and compared by weighted probit analysis (Bliss and Finney); and (5) The word 'significantly' should be replaced by its synonyms (if it indicates extent) or the *P* value (if it indicates statistical significance).

Conflict-of-interest statement
In the interests of transparency and to help reviewers assess any potential bias, *WJR* requires authors of all papers to declare any competing commercial, personal, political, intellectual, or religious interests in relation to the submitted work. Referees are also asked to indicate any potential conflict they might have reviewing a particular paper. Before submitting, authors are suggested to read "Uniform Requirements for Manuscripts Submitted to Biomedical Journals: Ethical Considerations in the Conduct and Reporting of Research: Conflicts of Interest" from International Committee of Medical Journal Editors (ICMJE), which is available at: http://www.icmje.org/ethical_4conflicts.html.

Sample wording: [Name of individual] has received fees for serving as a speaker, a consultant and an advisory board member for [names of organizations], and has received research funding from [names of organization]. [Name of individual] is an employee of [name of organization]. [Name of individual] owns stocks and shares in [name of organization]. [Name of individual] owns patent [patent identification and brief description].

Statement of informed consent
Manuscripts should contain a statement to the effect that all human studies have been reviewed by the appropriate ethics committee or it should be stated clearly in the text that all persons gave their informed consent prior to their inclusion in the study. Details that might disclose the identity of the subjects under study should be omitted. Authors should also draw attention to the Code of Ethics of the World Medical Association (Declaration of Helsinki, 1964, as revised in 2004).

Statement of human and animal rights
When reporting the results from experiments, authors should follow the highest standards and the trial should conform to Good Clinical Practice (for example, US Food and Drug Administration Good Clinical Practice in FDA-Regulated Clinical Trials; UK Medicines Research Council Guidelines for Good Clinical Practice in Clinical Trials) and/or the World Medical Association Declaration of Helsinki. Generally, we suggest authors follow the lead investigator's national standard. If doubt exists whether the research was conducted in accordance with the above standards, the authors must explain the rationale for their approach and demonstrate that the institutional review body explicitly approved the doubtful aspects of the study.

Before submitting, authors should make their study approved by the relevant research ethics committee or institutional review board. If human participants were involved, manuscripts must be accompanied by a statement that the experiments were undertaken with the understanding and appropriate informed consent of each. Any personal item or information will not be published without explicit consents from the involved patients. If experimental animals were used, the materials and methods (experimental procedures) section must clearly indicate that appropriate measures were taken to minimize pain or discomfort, and details of animal care should be provided.

SUBMISSION OF MANUSCRIPTS

Manuscripts should be typed in 1.5 line spacing and 12 pt. Book Antiqua with ample margins. Number all pages consecutively, and start each of the following sections on a new page: Title Page, Abstract, Introduction, Materials and Methods, Results, Discussion, Acknowledgements, References, Tables, Figures, and Figure Legends. Neither the editors nor the publisher are responsible for the opinions expressed by contributors. Manuscripts formally accepted for publication become the permanent property of Baishideng Publishing Group Co., Limited, and may not be reproduced by any

means, in whole or in part, without the written permission of both the authors and the publisher. We reserve the right to copy-edit and put onto our website accepted manuscripts. Authors should follow the relevant guidelines for the care and use of laboratory animals of their institution or national animal welfare committee. For the sake of transparency in regard to the performance and reporting of clinical trials, we endorse the policy of the ICMJE to refuse to publish papers on clinical trial results if the trial was not recorded in a publicly-accessible registry at its outset. The only register now available, to our knowledge, is http://www.clinicaltrials.gov sponsored by the United States National Library of Medicine and we encourage all potential contributors to register with it. However, in the case that other registers become available you will be duly notified. A letter of recommendation from each author's organization should be provided with the contributed article to ensure the privacy and secrecy of research is protected.

Authors should retain one copy of the text, tables, photographs and illustrations because rejected manuscripts will not be returned to the author(s) and the editors will not be responsible for loss or damage to photographs and illustrations sustained during mailing.

Online submissions

Manuscripts should be submitted through the Online Submission System at: http://www.wjgnet.com/esps/. Authors are highly recommended to consult the ONLINE INSTRUCTIONS TO AUTHORS (http://www.wjgnet.com/1948-5204/g_info_20100312180518.htm) before attempting to submit online. For assistance, authors encountering problems with the Online Submission System may send an email describing the problem to bpgoffice@wjgnet.com, or by telephone: +86-10-85381891. If you submit your manuscript online, do not make a postal contribution. Repeated online submission for the same manuscript is strictly prohibited.

MANUSCRIPT PREPARATION

All contributions should be written in English. All articles must be submitted using word-processing software. All submissions must be typed in 1.5 line spacing and 12 pt. Book Antiqua with ample margins. Style should conform to our house format. Required information for each of the manuscript sections is as follows:

Title page

Title: Title should be less than 12 words.

Running title: A short running title of less than 6 words should be provided.

Authorship: Authorship credit should be in accordance with the standard proposed by International Committee of Medical Journal Editors, based on (1) substantial contributions to conception and design, acquisition of data, or analysis and interpretation of data; (2) drafting the article or revising it critically for important intellectual content; and (3) final approval of the version to be published. Authors should meet conditions 1, 2, and 3.

Institution: Author names should be given first, then the complete name of institution, city, province and postcode. For example, Xu-Chen Zhang, Li-Xin Mei, Department of Pathology, Chengde Medical College, Chengde 067000, Hebei Province, China. One author may be represented from two institutions, for example, George Sgourakis, Department of General, Visceral, and Transplantation Surgery, Essen 45122, Germany; George Sgourakis, 2nd Surgical Department, Korgialenio-Benakio Red Cross Hospital, Athens 15451, Greece

Author contributions: The format of this section should be: Author contributions: Wang CL and Liang L contributed equally to this work; Wang CL, Liang L, Fu JF, Zou CC, Hong F and Wu XM designed the research; Wang CL, Zou CC, Hong F and Wu XM performed the research; Xue JZ and Lu JR contributed new reagents/analytic tools; Wang CL, Liang L and Fu JF analyzed the data; and Wang CL, Liang L and Fu JF wrote the paper.

Supportive foundations: The complete name and number of supportive foundations should be provided, e.g. Supported by National Natural Science Foundation of China, No. 30224801

Correspondence to: Only one corresponding address should be provided. Author names should be given first, then author title, affiliation, the complete name of institution, city, postcode, province, country, and email. All the letters in the email should be in lower case. A space interval should be inserted between country name and email address. For example, Montgomery Bissell, MD, Professor of Medicine, Chief, Liver Center, Gastroenterology Division, University of California, Box 0538, San Francisco, CA 94143, United States. montgomery.bissell@ucsf.edu

Telephone and fax: Telephone and fax should consist of +, country number, district number and telephone or fax number, e.g. Telephone: +86-10-85381891 Fax: +86-10-85381893

Peer reviewers: All articles received are subject to peer review. Normally, three experts are invited for each article. Decision on acceptance is made only when at least two experts recommend publication of an article. All peer-reviewers are acknowledged on Express Submission and Peer-review System website.

Abstract

There are unstructured abstracts (no less than 200 words) and structured abstracts. The specific requirements for structured abstracts are as follows:

An informative, structured abstract should accompany each manuscript. Abstracts of original contributions should be structured into the following sections: AIM (no more than 20 words; Only the purpose of the study should be included. Please write the Aim in the form of "To investigate/study/…"), METHODS (no less than 140 words for Original Articles; and no less than 80 words for Brief Articles), RESULTS (no less than 150 words for Original Articles and no less than 120 words for Brief Articles; You should present *P* values where appropriate and must provide relevant data to illustrate how they were obtained, e.g. 6.92 ± 3.86 *vs* 3.61 ± 1.67, $P < 0.001$), and CONCLUSION (no more than 26 words).

Key words

Please list 5-10 key words, selected mainly from *Index Medicus*, which reflect the content of the study.

Core tip

Please write a summary of less than 100 words to outline the most innovative and important arguments and core contents in your paper to attract readers.

Text

For articles of these sections, original articles and brief articles, the main text should be structured into the following sections: INTRODUCTION, MATERIALS AND METHODS, RESULTS and DISCUSSION, and should include appropriate Figures and Tables. Data should be presented in the main text or in Figures and Tables, but not in both. The main text format of these sections, editorial, topic highlight, case report, letters to the editors, can be found at: http://www.wjgnet.com/1948-5204/g_info_list.htm.

Illustrations

Figures should be numbered as 1, 2, 3, *etc*., and mentioned clearly in the main text. Provide a brief title for each figure on a separate page. Detailed legends should not be provided under the figures. This part should be added into the text where the figures are applicable. Keeping all elements compiled is necessary in line-art image. Scale bars should be used rather than magnification factors, with the length of the bar defined in the legend rather than on the bar itself. File names should identify the figure and panel. Avoid layering type directly over shaded or textured areas. Please use uniform legends for the same

subjects. For example: Figure 1 Pathological changes in atrophic gastritis after treatment. A: ...; B: ...; C: ...; D: ...; E: ...; F: ...; G: …*etc*. It is our principle to publish high resolution-figures for the E-versions.

Tables

Three-line tables should be numbered 1, 2, 3, *etc*., and mentioned clearly in the main text. Provide a brief title for each table. Detailed legends should not be included under tables, but rather added into the text where applicable. The information should complement, but not duplicate the text. Use one horizontal line under the title, a second under column heads, and a third below the Table, above any footnotes. Vertical and italic lines should be omitted.

Notes in tables and illustrations

Data that are not statistically significant should not be noted. $^{a}P < 0.05$, $^{b}P < 0.01$ should be noted ($P > 0.05$ should not be noted). If there are other series of P values, $^{c}P < 0.05$ and $^{d}P < 0.01$ are used. A third series of P values can be expressed as $^{e}P < 0.05$ and $^{f}P < 0.01$. Other notes in tables or under illustrations should be expressed as ^{1}F, ^{2}F, ^{3}F; or sometimes as other symbols with a superscript (Arabic numerals) in the upper left corner. In a multi-curve illustration, each curve should be labeled with ●, ○, ■, □, ▲, △, *etc*., in a certain sequence.

Acknowledgments

Brief acknowledgments of persons who have made genuine contributions to the manuscript and who endorse the data and conclusions should be included. Authors are responsible for obtaining written permission to use any copyrighted text and/or illustrations.

REFERENCES

Coding system

The author should number the references in Arabic numerals according to the citation order in the text. Put reference numbers in square brackets in superscript at the end of citation content or after the cited author's name. For citation content which is part of the narration, the coding number and square brackets should be typeset normally. For example, "Crohn's disease (CD) is associated with increased intestinal permeability[1,2]". If references are cited directly in the text, they should be put together within the text, for example, "From references[19,22-24], we know that..."

When the authors write the references, please ensure that the order in text is the same as in the references section, and also ensure the spelling accuracy of the first author's name. Do not list the same citation twice.

PMID and DOI

Pleased provide PubMed citation numbers to the reference list, e.g. PMID and DOI, which can be found at http://www.ncbi.nlm.nih.gov/sites/entrez?db=pubmed and http://www.crossref.org/SimpleTextQuery/, respectively. The numbers will be used in E-version of this journal.

Style for journal references

Authors: the name of the first author should be typed in bold-faced letters. The family name of all authors should be typed with the initial letter capitalized, followed by their abbreviated first and middle initials. (For example, Lian-Sheng Ma is abbreviated as Ma LS, Bo-Rong Pan as Pan BR). The title of the cited article and italicized journal title (journal title should be in its abbreviated form as shown in PubMed), publication date, volume number (in black), start page, and end page [PMID: 11819634 DOI: 10.3748/wjg.13.5396].

Style for book references

Authors: the name of the first author should be typed in bold-faced letters. The surname of all authors should be typed with the initial letter capitalized, followed by their abbreviated middle and first initials. (For example, Lian-Sheng Ma is abbreviated as Ma LS, Bo-Rong Pan as Pan BR) Book title. Publication number. Publication place: Publication press, Year: start page and end page.

Format

Journals

English journal article (list all authors and include the PMID where applicable)

1 **Jung EM**, Clevert DA, Schreyer AG, Schmitt S, Rennert J, Kubale R, Feuerbach S, Jung F. Evaluation of quantitative contrast harmonic imaging to assess malignancy of liver tumors: A prospective controlled two-center study. *World J Gastroenterol* 2007; **13**: 6356-6364 [PMID: 18081224 DOI: 10.3748/wjg.13.6356]

Chinese journal article (list all authors and include the PMID where applicable)

2 **Lin GZ**, Wang XZ, Wang P, Lin J, Yang FD. Immunologic effect of Jianpi Yishen decoction in treatment of Pixu-diarrhoea. *Shijie Huaren Xiaohua Zazhi* 1999; **7**: 285-287

In press

3 **Tian D**, Araki H, Stahl E, Bergelson J, Kreitman M. Signature of balancing selection in Arabidopsis. *Proc Natl Acad Sci USA* 2006; In press

Organization as author

4 **Diabetes Prevention Program Research Group**. Hypertension, insulin, and proinsulin in participants with impaired glucose tolerance. *Hypertension* 2002; **40**: 679-686 [PMID: 12411462 DOI:10.1161/01.HYP.0000035706.28494.09]

Both personal authors and an organization as author

5 **Vallancien G**, Emberton M, Harving N, van Moorselaar RJ; Alf-One Study Group. Sexual dysfunction in 1, 274 European men suffering from lower urinary tract symptoms. *J Urol* 2003; **169**: 2257-2261 [PMID: 12771764 DOI:10.1097/01.ju.0000067940.76090.73]

No author given

6 21st century heart solution may have a sting in the tail. *BMJ* 2002; **325**: 184 [PMID: 12142303 DOI:10.1136/bmj.325.7357.184]

Volume with supplement

7 **Geraud G**, Spierings EL, Keywood C. Tolerability and safety of frovatriptan with short- and long-term use for treatment of migraine and in comparison with sumatriptan. *Headache* 2002; **42** Suppl 2: S93-99 [PMID: 12028325 DOI:10.1046/j.1526-4610.42.s2.7.x]

Issue with no volume

8 **Banit DM**, Kaufer H, Hartford JM. Intraoperative frozen section analysis in revision total joint arthroplasty. *Clin Orthop Relat Res* 2002; (**401**): 230-238 [PMID: 12151900 DOI:10.1097/00003086-200208000-00026]

No volume or issue

9 Outreach: Bringing HIV-positive individuals into care. *HRSA Careaction* 2002; 1-6 [PMID: 12154804]

Books

Personal author(s)

10 **Sherlock S**, Dooley J. Diseases of the liver and billiary system. 9th ed. Oxford: Blackwell Sci Pub, 1993: 258-296

Chapter in a book (list all authors)

11 **Lam SK**. Academic investigator's perspectives of medical treatment for peptic ulcer. In: Swabb EA, Azabo S. Ulcer disease: investigation and basis for therapy. New York: Marcel Dekker, 1991: 431-450

Author(s) and editor(s)

12 **Breedlove GK**, Schorfheide AM. Adolescent pregnancy. 2nd ed. Wieczorek RR, editor. White Plains (NY): March of Dimes Education Services, 2001: 20-34

Conference proceedings

13 **Harnden P**, Joffe JK, Jones WG, editors. Germ cell tumours V. Proceedings of the 5th Germ cell tumours Conference; 2001 Sep 13-15; Leeds, UK. New York: Springer, 2002: 30-56

Conference paper

14 **Christensen S**, Oppacher F. An analysis of Koza's computational effort statistic for genetic programming. In: Foster JA, Lutton E, Miller J, Ryan C, Tettamanzi AG, editors. Genetic programming. EuroGP 2002: Proceedings of the 5th European Conference on Genetic Programming; 2002 Apr 3-5; Kinsdale,

Ireland. Berlin: Springer, 2002: 182-191

Electronic journal (list all authors)

15 Morse SS. Factors in the emergence of infectious diseases. Emerg Infect Dis serial online, 1995-01-03, cited 1996-06-05; 1(1): 24 screens. Available from: URL: http://www.cdc.gov/ncidod/eid/index.htm

Patent (list all authors)

16 **Pagedas AC**, inventor; Ancel Surgical R&D Inc., assignee. Flexible endoscopic grasping and cutting device and positioning tool assembly. United States patent US 20020103498. 2002 Aug 1

Statistical data

Write as mean ± SD or mean ± SE.

Statistical expression

Express *t* test as *t* (in italics), *F* test as *F* (in italics), chi square test as χ^2 (in Greek), related coefficient as *r* (in italics), degree of freedom as υ (in Greek), sample number as *n* (in italics), and probability as *P* (in italics).

Units

Use SI units. For example: body mass, m (B) = 78 kg; blood pressure, p (B) = 16.2/12.3 kPa; incubation time, t (incubation) = 96 h, blood glucose concentration, c (glucose) 6.4 ± 2.1 mmol/L; blood CEA mass concentration, p (CEA) = 8.6 24.5 μg/L; CO_2 volume fraction, 50 mL/L CO_2, not 5% CO_2; likewise for 40 g/L formaldehyde, not 10% formalin; and mass fraction, 8 ng/g, *etc*. Arabic numerals such as 23, 243, 641 should be read 23243641.

The format for how to accurately write common units and quantums can be found at: http://www.wjgnet.com/1948-5204/g_info_20100312183048.htm.

Abbreviations

Standard abbreviations should be defined in the abstract and on first mention in the text. In general, terms should not be abbreviated unless they are used repeatedly and the abbreviation is helpful to the reader. Permissible abbreviations are listed in Units, Symbols and Abbreviations: A Guide for Biological and Medical Editors and Authors (Ed. Baron DN, 1988) published by The Royal Society of Medicine, London. Certain commonly used abbreviations, such as DNA, RNA, HIV, LD50, PCR, HBV, ECG, WBC, RBC, CT, ESR, CSF, IgG, ELISA, PBS, ATP, EDTA, mAb, can be used directly without further explanation.

Italics

Quantities: *t* time or temperature, *c* concentration, *A* area, *l* length, *m* mass, *V* volume.

Genotypes: *gyrA*, *arg* 1, *c myc*, *c fos*, *etc*.

Restriction enzymes: *Eco*RI, *Hin*dI, *Bam*HI, *Kbo* I, *Kpn* I, *etc*.

Biology: *H. pylori*, *E coli*, *etc*.

Examples for paper writing

All types of articles' writing style and requirement will be found in the link: http://www.wjgnet.com/esps/NavigationInfo.aspx?id=15

SUBMISSION OF THE REVISED MANUSCRIPTS AFTER ACCEPTED

Authors must revise their manuscript carefully according to the revision policies of Baishideng Publishing Group Co., Limited. The revised version, along with the signed copyright transfer agreement, responses to the reviewers, and English language Grade B certificate (for non-native speakers of English), should be submitted to the online system via the link contained in the e-mail sent by the editor. If you have any questions about the revision, please send e-mail to esps@wjgnet.com.

Language evaluation

The language of a manuscript will be graded before it is sent for revision. (1) Grade A: priority publishing; (2) Grade B: minor language polishing; (3) Grade C: a great deal of language polishing needed; and (4) Grade D: rejected. Revised articles should reach Grade A or B.

Copyright assignment form

Please download a Copyright assignment form from http://www.wjgnet.com/1948-5204/g_info_20100312182928.htm.

Responses to reviewers

Please revise your article according to the comments/suggestions provided by the reviewers. The format for responses to the reviewers' comments can be found at: http://www.wjgnet.com/1948-5204/g_info_20100312182841.htm.

Proof of financial support

For papers supported by a foundation, authors should provide a copy of the approval document and serial number of the foundation.

STATEMENT ABOUT ANONYMOUS PUBLICATION OF THE PEER REVIEWERS' COMMENTS

In order to increase the quality of peer review, push authors to carefully revise their manuscripts based on the peer reviewers' comments, and promote academic interactions among peer reviewers, authors and readers, we decide to anonymously publish the reviewers' comments and author's responses at the same time the manuscript is published online.

PUBLICATION FEE

WJR is an international, peer-reviewed, OA online journal. Articles published by this journal are distributed under the terms of the Creative Commons Attribution Non-commercial License, which permits use, distribution, and reproduction in any medium and format, provided the original work is properly cited. The use is non-commercial and is otherwise in compliance with the license. Authors of accepted articles must pay a publication fee. Publication fee: 698 USD per article. All invited articles are published free of charge.

百世登

Baishideng®

Published by **Baishideng Publishing Group Co., Limited**
Flat C, 23/F., Lucky Plaza,
315-321 Lockhart Road, Wan Chai,
Hong Kong, China
Fax: +852-65557188
Telephone: +852-31779906
E-mail: bpgoffice@wjgnet.com
http://www.wjgnet.com